

The role of phytoplasma effectors in plant development

Parisatcha Sangsuwan, MSc

Principal Supervisor: Professor Matthew Dickinson

Thesis submitted to University of Nottingham for the degree of Doctor of Philosophy

April 2020

Abstract

One of the problems that can cause yield losses in crops is infection with phytoplasmas. In monocots, phytoplasmas cause serious problems in economic plants such as rice yellow dwarf (RYD), napier grass stunt disease (NGSD), sugarcane white leaf (SCWL) and sugarcane grassy shoot (SCGS). This research aims to identify phytoplasma effector proteins causing these symptoms, which is potentially of benefit for future studies to prevent host plants from getting the symptoms associated with phytoplasma effector proteins. Furthermore, phytoplasmas of gramineous plants were classified using the MLST technique into new groups or subgroups, particularly focusing on sugarcane diseases, because the 16Sr gene cannot classify closely related strains.

First of all, ten genes were used to classify the phytoplasmas of gramineous plants such as NGSD, SCWL, SCGS and Bermuda grass white leaf (BGWL) and the results showed that the *lpd, gro, gryB, ser* and *sec* gene primers classified the SCWL from the SCGS based on geographic origin. Interestingly, the result showed that the NGSD and BGWL phytoplasmas were quite distinct from those of sugarcane. These results support that the BGWL are correctly classified into the 16Sr XIV group whilst the NGSD should be classified into a new group. Primers based on the *asp*, *50S*, *secA*, *EF2* and *EF7* genes were less useful for classification, especially the *EF2* and *EF7* primers, which are for putative effector genes, presumably because these genes require conserved regions to interact with plant hosts whilst *pep* primers could not

amplify any samples. For future studies, the MLST analysis should include the effector genes and analysis of environmental factors such as soil type, soil moisture and soil nutrients should also be undertaken to help identify the causes of the different sugarcane symptoms.

Secondly, the NGSD genomic sequence contigs were analysed for secretion signals using bioinformatics and the results identified fourteen proteins that had the signal peptide sequences required to make them putative effectors. Seven of the putative effector genes from NGSD and two from SCWL were cloned and transformed into *Arabidopsis*, and for controls, *SAP11* genes (which is a known effector) were cloned from a range of other phytoplasmas held in the University of Nottingham collection. The results identified five *SAP11* genes from the 16SrI Blackcurrant reversion disease (BCRD) phytoplasma, 16SrI Strawberry green petal (SGP), 16SrII Vinca coconut phytoplasma (VCP), 16SrII Cotton phyllody (CoP) and 16SrX Apple proliferation (AP_SQ). Interestingly, the $SAP11_{AP_SQ}$ sequence was different from that in the NCBI database for the whole genome sequenced strain of Apple proliferation, indicating difference within 16Sr groups.

In the screening step, symptoms and gene expression using absolute quantitative PCR were analysed in the 2nd generation of transformed *Arabidopsis*. The transformed plants showed various phenotypes; phyllotaxis defects for $SAP11_{AP_SQ}$, $SAP11_{BCRD}$, $SAP11_{CoP}$ and $SAP11_{VCP}$; branching for $SAP11_{AP_SQ}$, $SAP11_{CoP}$, $SAP11_{SGP}$, $EF2_{NGSD}$, $EF7_{NGSD}$, $EF2_{SCWL}$ and $EF7_{SCWL}$. Furthermore, $SAP11_{AP_SQ}$ and $SAP11_{VCP}$ transformed plants were shorter than

wild type and vector only plants. Moreover, *SAP11*$_{AP_SQ}$ transformed plants produced clustered cauline leaves on the primary inflorescence and the *SAP11*$_{AP_SQ}$ did not produce flowers, whilst the *SAP11*$_{VCP}$ transformed flowers were smaller than wild type and vector only, although they were still fertile. These phenotypes result from SAP11 interacting with plant genes such as *BRC1* and *PME5* which control branching and phyllotaxis patterns respectively, *BP* which controls internode elongation and *PNF* and *PNY* which maintains inflorescence architecture and floral meristem function. According to the transformation results, the effector genes from NGSD and SCWL were successfully transformed into *Arabidopsis*; however, the transformed plants did not show any symptoms related to stunting or white leaf. Therefore, transformation into monocot models such as rice, barley or *Brachypodium* needs to be undertaken to observe the symptoms that might be specific to the host range. However, attempts were also made to undertake transformation in the monocot *Brachypodium* BD21 for symptom observation, but no results were obtained due to the time taken to obtain transformed plants and the closure of labs due to Covid-19. So, future studies will repeat transformation into monocots and observe the symptoms including plant gene expression levels.

Acknowledgements

Firstly, and foremost, I wish to thank my supervisor Professor Matthew Dickinson for his help, guidance and his patience throughout my PhD. Without his supervision, suggestions and help this project would not have been successful. I would like to acknowledge my internal assessor Professor Zoe Wilson for the feedback that she has provided to this thesis over the years.

Secondly, I wish to greatly acknowledgements the Royal Thai Government, for the financial support of my PhD. The acknowledgement list would not be complete without all the staff of the Department of Plant and Crop Sciences, all member of the Lab A58 for their support and help including the great teamwork during my experimental work and Dr. Behzad Talle and Dr. Jose Fernandez for their advice over the years.

Finally, many thanks to my family and friends for the continuous encouragements and support throughout my PhD study.

Table of Contents

The role of phytoplasma effectors in plant development i

Abstract i

Acknowledgements iv

Table of Contents v

List of Abbreviations xi

List of Figures xiv

List of Tables xl

Chapter 1: General introduction 1

1.1 Description of Phytoplasmas 1

1.2 Taxonomic Information 8

1.3 Phytoplasma classification and detection 10

1.3.1 Classification 10

1.3.2 Molecular Detection 20

1.4 Phytoplasma effectors 24

1.5 Protein secretion pathway 32

Sec pathway 32

Research aims and objectives 35

Chapter 2: Multilocus Sequence Typing of sugarcane white leaf and sugarcane grassy shoot 37

2.1 Introduction 37

2.2 Materials and Methods 39

2.2.1 DNA extraction 39

2.2.2 Phytoplasma preliminary tests 43

2.2.3 Multilocus Sequence Typing analysis 44

2.2.4 Non ribosomal gene analysis 48

2.3 Results 48

2.3.1 Preliminary tests to confirm presence of phytoplasmas with 16Sr primers 48

2.3.2 Multilocus Sequence Typing (MLST) analysis 52

2.3.2.1. Analysis of *50S* gene sequences 54

2.3.2.2 Analysis of *asp* gene sequences 55

2.3.2.3 Analysis of *gro* gene sequences 57

2.3.2.4 Analysis of *gryB* gene sequences 58

2.3.2.5 Analysis of *lpd* gene sequences 60

2.3.2.6 Analysis of *sec* gene sequences 63

2.3.2.7 Analysis of *ser* gene sequences 64

2.3.2.8 Analysis of *EF2* gene sequences 65

2.3.2.9 Analysis of *EF7* gene sequences 66

2.4 Discussion 74

Chapter 3: Bioinformatics for NGSD and SCWL effector prediction 79

3.1 Introduction 79

3.2 Materials and Methods 89

3.2.1 Signal Peptide prediction 89

3.2.2 Signal Peptide and candidate effector gene amplification 91

3.2.4 The Nuclear Localization Signal Prediction 96

3.3 Results 97

Signal Peptide prediction 97

3.4 Discussion 107

Chapter 4: Cloning and Transformation 111

4.1 Introduction 111

4.1.1 Plant models 111

4.1.2 Phytoplasma effector transformation 117

4.2 Materials and Methods 120

4.2.1 DNA extraction 120

4.2.2 LAMP assay: Phytoplasma preliminary test 121

4.2.3 PCR of the *SAP11* gene 122

4.2.4 SAP11 PCR product sequencing 124

4.2.5 *SAP11* genes, hypothetical genes and candidate effector genes construction 125

4.2.6 Agrobacterium competent cell preparation 131

4.2.7 *Agrobacterium* transformation 132

4.2.8 *Arabidopsis* transformation: Floral dip method (Clough and Bent, 1998) 133

4.2.9 Transformed *Arabidopsis* selection 134

4.2.10 *Brachypodium* callus induction and transformation (Alves *et al*., 2009; Thole and Vain, 2012; Bragg *et al*., 2015) 135
4.2.10.1 Seed sterilization 135
4.2.10.2 Callus induction 136
4.2.10.3 *Brachypodium* callus *Agrobacterium* transformation 138
4.2.10.4 Regeneration of transformed plants 139
4.2.11 Transformed plant screening 140
4.3 Results 141
4.3.1 LAMP results 141
4.3.2 PCR results 143
4.4 Discussion 158
4.4.1 SAP11 conserved sequences 158
4.4.2 Plasmid construction and transformation 162
Chapter 5: Gene expression analysis 167
5.1 Introduction 167
5.1.1 The phyllotaxy pattern 168
5.1.2 Branching and apical dominance 169
5.2 Materials and Methods 176
5.2.1 T_2 transformant detection 176
5.2.1.1 *Arabidopsis* transformed plants 176
5.2.1.2 *Brachypodium* transformed plants 177
5.2.2 RNA extraction and reverse transcription 178

5.2.3 Relative quantitative PCR 178

5.3 Results 181

5.3.1 *SAP11* gene expression and plant developmental gene expression 181

5.3.1.1 *SAP11*$_{AP_SQ}$ transformed plants 181

5.3.1.2 *SAP11*$_{BCRD}$ transformed plants 187

5.3.1.3 *SAP11*$_{C0P}$ Transformed plants 191

5.3.1.4 *SAP11*$_{SGP}$ Transformed plants 196

5.3.1.5 *SAP11*$_{VCP}$ Transformed plants 200

5.3.1.6 *EF1*$_{NGSD}$ Transformed plants 206

5.3.1.7 *EF2*$_{NGSD}$ Transformed plants 208

5.3.1.8 *EF3*$_{NGSD}$ Transformed plants 212

5.3.1.9 *EF4*$_{NGSD}$ Transformed plants 215

5.3.1.10 *EF5*$_{NGSD}$ Transformed plants 217

5.3.1.11 *EF6*$_{NGSD}$ Transformed plants 218

5.3.1.12 *EF7*$_{NGSD}$ Transformed plants 221

5.3.1.13 *EF2*$_{SCWL}$ Transformed plants 225

5.3.1.15 *EF7*$_{SCWL}$ Transformed plants 229

5.4 Discussion 236

5.4.1 Plant Branching 237

5.4.2 Plant phyllotaxis patterns 239

Chapter 6 General discussion and conclusions 244

6.1 Geographic phytoplasma distribution and diversity 244

6.2 Classification of phytoplasmas of gramineous plants 245

6.3 SAP11 gene diversity 246

6.4 The effect of phytoplasma effectors on plant development 248

6.4.1 Transformation efficiency 248

6.4.2 Interaction of phytoplasma effectors with plant genes and development 249

6.5 Suggestions for future studies 252

Bibliography 255

Appendices 287

Chapter 2 287

List of Abbreviations

AFR	Auxin response factor
AP	Apple proliferation
AP1	APETALA1
att	Attachment site
AY-WB	Aster yellows witches' broom
BCRD	Black currant reversion disease
BGWL	Bermuda grass white leaf
BGWL	Bermuda grass white leaf from Malaysia
BGWLVN	Bermuda grass white leaf from Vietnam
BL	BLIND
BLH	BEL1-like
BLL	Brinjal Little leaf
BLR	*BELLINGER*
BP	*BREVIPEDICELLUS*
BRC1	*BRANCHED1*
Ca.	Candidatus
CaMV	Cauliflower mosaic virus
CCD	Coiled Coil Domain
CoP	Cotton phyllody
CPh	Clover phyllody
C-PMU	Circular- extrachromosomal form
Ct/Cq	Threshold cycle
EF	Effector protein
EY	Elm yellows
Ftsy	Membrane-associated SRP receptor
HG	Homogalacturonan

HGT	horizontal gene transfer
JA	Jasmonic acid
KNOX	KNOTTED-Like
LAMP	Loop-mediated isothermal amplification
LB	Left Border
L-PMU	Linear extrachromosomal form
LNI	Plum leptonecrosis
LY	Lethal yellows
MLO	Mycoplasma-like organisms
MLST	Multilocus Sequence Typing
MTF	MADS-domain transcription factor
NLS	Nuclear localization signal
NGSD	Napier grass stunt phytoplasma disease
NLS	Nuclear Localization Signal
ORF	Open reading frame
OY-M	Onion yellows phytoplasma mild strain
PCR	Polymerase Chain Reaction
PHYL1	*Phyllogen* gene
PiPs	Posttranslationally interaction proteins
PME5	*PECTINMETHYLTRANSFERASE5*
PMU	Potential Mobile Unit
PNF	*POUNDFOOLISH*
PNY	*Pennywise*
PnWB	Peanut witches' broom
PWB	Potato witches' broom
RAD23	*RADIATION SENSITIVE23*
RB	Right border
RG	Rehmannia glutinosa
RYD	Rice yellow dwarf

SAP	Secreted AY-WB phytoplasma protein
SAM	Shoot Apical Meristem
SCGS	Sugarcane grassy shoot
SCGSSLK	Sugarcane grassy shoot from Sri Lanka
SCGSVN	Sugarcane grassy shoot from Vietnam
SCWL	Sugarcane white leaf
SCWLHT	Sugarcane white leaf Heat Treated
SCWLSLK	Sugarcane white leaf from Sri Lanka
SCWLTh	Sugarcane white leaf from Thailand
SCWLVN	Sugarcane white leaf from Vietnam
SE	Standard errors
SEL	Size exclusion limit
SEP3	*SEPALLATA3*
SGP	Strawberry green petal
SP	Soybean phyllody
SP	Signal peptide
SRP	Signal recognition particle
SVM	Sequence-Variable Mosaics
T4SS	Type IV Secretion Pathway
TALE	Three-amino-acid-loop-extension
Tat	Twin-arginine translocation
TB1	*TEOSINE BRANCHED1*
TCP	*TEOSINE-BRANCHED CYCLOIDEA PROLIFERATION*
TE	Transformation efficiency
tengu	Tengu-su inducer
VCP	Vinca coconut phyllody
Vir gene	*Virulence* gene
WBD	Wheat blue dwarf
WT	Wild type

List of Figures

Chapter1

Figure 1.1 Electron micrograph of cross section of sieve tube showed phytoplasmas infecting in plant (cross section, Bar = 200 nm) (Duduk and Bertaccini, 2011). 2

Figure 1.2 Dual life cycle of phytoplasmas which live in insect vectors and plants, and each step of infection. When the leafhoppers feed on the phytoplasma infected plants, the phytoplasmas will move from the plant phloem into the leafhopper body for multiplication. Subsequently, when the leafhoppers feed on healthy plants, the phytoplasma will be transmitted back into plant phloem where it can reproduce and the plant will show the characteristic symptoms..... 3

Figure 1.3 Virescence symptoms on periwinkle flowers infected with phytoplasma (Duduk and Bertaccini, 2011). 6

Figure 1.4 Phyllody symptoms on hydrangea infected with phytoplasma on the right compared with a healthy hydrangea plant on the left (Maejima *et al*., 2014)..... 6

Figure 1.5 Witches' broom symptoms in almond infected with phytoplasma on the right compared with a healthy almond plant on the left (Yusuf *et al*., 2003) 7

Figure 1.6 Stunt symptoms on Napier grass infected with phytoplasma (Asudi *et al*., 2015)..... 7

Figure 1. 7 A phylogenetic tree showing wall-less bacteria groups and their relationship to Gram positive walled bacteria (Zhao and Davis., 2016). 9
Figure 1.8 Phylogenetic tree of Mollicutes indicating the genetic code on the right side (Labroussaa *et al*., 2016)..... 10
Figure 1.9 A tree topology reconstructed for the phytoplasma 16Sr groups; circles encompass group members (Wei *et al*., 2007). 14
Figure 1.10 Phytoplasma primer position diagram for the 16S-23S rRNA gene 21
Figure 1.11 Schematic diagram of primer position for phytoplasma detection by LAMP(Tomlinson *et al*., 2013)..... 23
Figure 1.12 A model for Tengu and SAP11 effectors inhibiting LOX2, JA and SA genes (Ma and Ma, 2016). 27
Figure 1.13 The mechanism of Tengu induced witches' broom via auxin down-regulation (Maejima *et al*., 2014)..... 28
Figure 1.14 A model for Tengu reduced levels of JA and auxin on each part of the floral maturation pathway (Minato *et al*., 2014). 28
Figure 1.15 A model for PHYLLOGEN effector destabilised MADS domain (Maejima *et al*., 2014). 29
Figure 1.16 Position of SAP11 (red arrow) on SAP11 PMU-like region in the AY-WB chromosome (Sugio and Hogenhout, 2012)..... 30
Figure 1.17 Homologous genes between PnWB PMU and AY-WB PMU1 (Ku *et al*., 2013). 31
Figure 1. 18 Two major Gram-positive bacterial export pathways; (a) the general Secretion (Sec) protein export pathway and (b) the twin-arginine translocation (Tat) protein export pathway (Freudl, 2018)..... 34

Chapter 2

Figure 2.1 Schematic diagram of primer positions for phytoplasma detection of the 16S rRNA by the PCR method (Mannan *et al*., 2010)..... 44
Figure 2.2 Phytoplasma infected plants showing PCR products from P1/P7 and R16mF2/R16mR1 primers. Lanes: (M) 1 Kb marker, (1) Napier grass, (2) Napier grass stunt disease infected leaves, (3) Sugarcane white leaf from Thailand 1, (4) Sugarcane white leaf from Thailand 2, (5) Sugarcane white leaf from Vietnam, (6) Sugarcane white leaf from India, (7) Sugarcane white leaf from Sri Lanka 1, (8) Sugarcane white leaf from Sri Lanka 2, (9) Sugarcane white leaf from Sri Lanka 3, (10) Sugarcane grassy shoot from Sri Lanka 1, (11) Sugarcane grassy shoot from Sri Lanka 2, (12) Sugarcane grassy shoot from Sri Lanka 3, (14) Sugarcane grassy shoot from Vietnam 1, (15) Sugarcane grassy from Vietnam 2, (16) Bermuda grass white leaf 1, (17) Bermuda grass white leaf 2 and (18) Bermuda grass white leaf 3. 49
Figure 2.3 Unrooted phylogenetic tree constructed with the neighbour-joining method based on sequences of the 16S rRNA gene with 1000 bootstrap value. The phylogenetic tree shows the relationship among the samples listed in Table 2.1; sugarcane disease, NGSD, BGWL and AY-WB as an outgroup. Branch lengths are proportional to the number of inferred character stated information, bar = 0.010 substitution per nucleotide position and the bootstrap values are expressed as percentages of 1000 replications. 51
Figure 2.4 Unrooted phylogenetic tree constructed with the neighbour-joining method based on sequences of the 50S gene with 1000 bootstrap value. The phylogenetic tree shows the relationship among the samples listed in Table

2.1; sugarcane disease, NGSD, BGWL and AY-WB as an outgroup. Branch lengths are proportional to the number of inferred character stated information, bar = 0.050 substitution per nucleotide position and the bootstrap values are expressed as percentages of 1000 replications. 55
Figure 2.5 Unrooted phylogenetic tree constructed by neighbour-joining method based on sequences of the asp gene with 1000 bootstrap value. The phylogenetic tree shows the relationship among the samples listed in Table 2.1; sugarcane disease, NGSD and AY-WB as an outgroup. Branch lengths are proportional to the number of inferred character stated information, bar = 2 substitution per nucleotide position and the bootstrap values are expressed as percentages of 1000 replications. 56
Figure 2.6 Unrooted phylogenetic tree constructed by neighbour-joining method based on sequences of the gro gene with 1000 bootstrap value. The phylogenetic tree shows the relationship among the samples listed in Table 2.1; sugarcane disease, NGSD, BGWL and AY-WB as an outgroup. Branch lengths are proportional to the number of inferred character stated information, bar = 0.050 substitution per nucleotide position and the bootstrap values are expressed as percentages of 1000 replications. 58
Figure 2.7 Unrooted phylogenetic tree constructed by neighbour-joining method based on sequences of the gryB gene with 1000 bootstrap value. The phylogenetic tree shows the relationship among the samples listed in Table 2.1; sugarcane disease, NGSD, BGWL and AY-WB as an outgroup. Branch lengths are proportional to the number of inferred character stated information, bar = 0.2 substitution per nucleotide position and the bootstrap values are expressed as percentages of 1000 replications. 60

Figure 2.8 Unrooted phylogenetic tree constructed by neighbour-joining method based on sequences of the lpd gene with 1000 bootstrap value. The phylogenetic tree shows the relationship among the samples listed in Table 2.1; sugarcane disease, NGSD, BGWL and AY-WB as an outgroup. Branch lengths are proportional to the number of inferred character stated information, bar = 0.050 substitution per nucleotide position and the bootstrap values are expressed as percentages of 1000 replications. 62
Figure 2.9 Unrooted phylogenetic tree constructed by neighbour-joining method based on sequences of the secA gene with 1000 bootstrap value. The phylogenetic tree shows the relationship among the samples listed in Table 2.1; sugarcane disease, and AY-WB as an outgroup. Branch lengths are proportional to the number of inferred character stated information, bar = 0.1 substitution per nucleotide position and the bootstrap values are expressed as percentages of 1000 replications. 63
Figure 2.10 Unrooted phylogenetic tree constructed by neighbour-joining based on sequences of the ser gene with 1000 bootstrap value. The phylogenetic tree shows the relationship among the samples listed in Table 2.1; sugarcane disease, NGSD, BGWL and AY-WB as an outgroup. Branch lengths are proportional to the number of inferred character stated information, bar = 0.050 substitution per nucleotide position and the bootstrap values are expressed as percentages of 1000 replications. 64
Figure 2.11 Unrooted phylogenetic tree constructed by neighbour-joining method based on sequences of the EF2 gene. with 1000 bootstrap value. The phylogenetic tree shows the relationship among the samples listed in Table 2.1; sugarcane disease, NGSD, BGWL and AY-WB as an outgroup. Branch

lengths are proportional to the number of inferred character stated information, bar = 0.1 substitution per nucleotide position and the bootstrap values are expressed as percentages of 1000 replications. 66
Figure 2.12 Unrooted phylogenetic tree constructed by neighbour-joining based on sequences of the EF7 gene with 1000 bootstrap value. The phylogenetic tree shows the relationship among the samples listed in Table 2.1; sugarcane disease, NGSD, BGWL and AY-WB as an outgroup. Branch lengths are proportional to the number of inferred character stated information, bar = 0.050 substitution per nucleotide position and the bootstrap values are expressed as percentages of 1000 replications. 67
Figure 2.13 Phylogenetic tree of the GryB, Sec, Gro, Lpd, Ser, 50S, Ser, EF2 and EF7 constructed by neighbour-joining method with 1000 bootstrap value. 73

Chapter 3

Figure 3.1 Diagram of effector transportation via plasmodesmata (Sugio *et al.*, 2011). The leafhoppers inoculate phytoplasmas into plant phloem of leaves and then phytoplasmas secrete effector proteins into plant cells and the effector proteins move to the nuclei of cells and sink tissues to cause symptoms of disease. 80
Figure 3.2 $SAP11_{AY\text{-}WB}$ diagram showing the location of the signal peptide (SP) and nuclear localisation signal (NLS) in the preprotein and SAP11 protein (Bai *et al*., 2009). 81
Figure 3.3 Comparison of phytoplasma effectors; Tengu, SAP11 and SAP54 protein sequence, alignments showed the SP, NLS and coiled coil domain

(CCD) in different groups of phytoplasma (Cho et al., 2019). The SAP11 has the SP, CCD and NLS that is present in phytoplasmas of 16SrI group. The SAP54 has the SP, CCD and Virulence Domain that it is not found in SAP11, and Tengu has the SP and Virulence Domain. 83
Figure 3.4 PMU diagram including gene regions on each PMU. A, PMU1-4 showing size and gene regions and B, SAP11 PMU-like region showing gene positions (Bai *et al*., 2006; Hogenhout *et al*., 2008). 85
Figure 3.5 Structure of a signal peptide comprised of three domains. 87
Figure 3.6 The phylogenetic tree showing the relationship between different groups of phytoplasmas, noting the ones used in this study and the groups they belong to (Nicolaisen and Horvath, 2008). 88
Figure 3.7 The Sanger Artemis program analysing ORFs of NGSD contigs. 90
Figure 3.8 The Predisi program analysing SP sequences from NGSD ORFs. 91
Figure 3.9 The PrediSi result of EF protein. A, the score of EF1 protein. B, EF1 protein peak. C, the score of EF2 protein and D, signal peptide sequence and cleavage position of EF2 protein. 99
Figure 3.10 NGSD effector PCR products from effector specific primers by PCR method. Lanes (1) 50 bp ladder, (2) PCR product from EF5 primer, (3) PCR product from EF4 primer, (4) PCR product from EF6 primer, (5) PCR product from EF3 primer, (6) PCR product from EF2 primer and (7) PCR product from EF1 primer. 100
Figure 3.11 NGSD effector and SCWL effector PCR products from effector specific primers by PCR method. Lanes (1) 50 bp ladder, (2) non-template

control, (3) PCR product from EF7 primers in NGSD, (4) PCR product from EF2 primers in SCWL and (5) PCR product from EF7 prime in SCWL. 100
Figure 3.12 EF1 PCR product without signal peptides comparing to EF1-SP PCR product. 101
Figure 3.13 Protein alignment of hypothetical protein of $SAP11_{PnWB}$ compared with group XI phytoplasmas. The $SAP11_{PnWB}$ is template to primer design for amplify to NGSD and SCWL. 104
Figure 3.14 EF2 Protein alignment of NGSD compared with SCWL phytoplasma..... 105
Figure 3. 15 SAP11 protein sequences of Peanut witches'-broom phytoplasma (PnWB), Napier grass stunt disease (NGSD) and Sugarcane white leaf (SCWL) were aligned using ClustalW omega program. Nuclear localization signal (NLS) is indicated in red font, and part of the coiled coil structure required for binding TCP is shown in grey colour..... 105
Figure 3.16 $EF7_{SCWL}$ protein showing NLS score and position. 106
Figure 3.17 $EF2_{NGSD}$ having no NLS position..... 107

Chapter 4

Figure 4.1 Phylogenetic relationship between Brachypodium and Pooideae (Draper *et al*.,2001). 113
Figure 4.2 Six stages of Brachypodium immature embryos. Scale bar = 5 mm (Vogel and Hill, 2008). 115
Figure 4.3 Flowchart of Brachypodium transformation by agrobacterium mediated procedure (Thole and Vain, 2012). There are 6 steps to regenerate transformed Brachypodium, the first step is sowing the Brachypodium seeds

to get immature seed and the second step is callus induction from immature embryos. This step takes 6 weeks to get 40 times callus for the next step and the third step is Agrobacterium transformation and the transformed callus are then moved to selective medium in the fourth step, which takes 5 weeks. The fifth step is regeneration of the transformed callus, which takes 4-6 weeks and the final step is seed production, which takes 12-14 weeks to get the next generation seeds. 116

Figure 4.4 The $SAP11_{AYWB}$ gene used as template for primer design. Grey-colour letters show the position of the forward and reverse primer and underline letters indicate the positions of the semi-nested primer..... 123

Figure 4.5 Map of the pCR8 plasmid. There are 2 sites of attL1 and attL2 which complement the attR1 and attR2 of pGWB5 and there is spectinomycin resistance for colony selection. Source: Invitrogen™ Gateway™ pCR™8/GW/TOPO™ TA Cloning Kit. 127

Figure 4.6 Map of the pGWb5 plasmid. There are 2 sites of attR1 and attR2 which complement the attL1 and attL2 of pCR8 and there are the CaMV 35S promoter and NOS terminator. There are also Kan^R encoding kanamycin resistance for bacterial colony selection in bacteria and Hyg^R encoding hygromycin resistance for plant selection. 129

Figure 4.7 Map of the pBRACT214 plasmid. There are 2 sites of attR1 and attR2 which complement the attL1 and attL2 of pCR8 and there are the Ubiquitin promoter and NOS terminator. There is Hyg^R encoding hygromycin resistance for plant selection (Viktorova *et al*., 2019)..... 130

Figure 4.8 Schematic diagram of Gateway™ LR Clonase™ II Enzyme mix kit procedure. Source: Invitrogen Gateway™ LR Clonase™ II Enzyme mix kit. 131
Figure 4.9 The structure of a Brachypodium spiklet and individual floret. .. 136
Figure 4.10 Immature Brachypodium embryo showed scutella side down (Betekhtin *et al*., 2016). 138
Figure 4.11 Candidate SAP11 PCR products from specific primers by PCR method. Lanes (1) 100 bp ladder, (2) PCR product from AP, (3) PCR product from BCRD, (4) PCR product from CoP, (5) PCR product from SGP and (6) PCR product from VCP. 143
Figure 4.12 Protein alignment of group 16SrI hypothetical protein. 146
Figure 4. 13 Protein alignment of SAP11 protein of group 16SrI phytoplasmas. 146
Figure 4.14 Protein alignment of SAP11 16SrI and 16SrX..... 147
Figure 4.15 Protein alignment of hypothetical protein of group II and X phytoplasmas. 147
Figure 4.16 Protein alignment of group II compared with group X and group XI phytoplasmas. 148
Figure 4.17 Blastn result showing our 16Sr AP to be similar to 16Sr AP strain SQ. 149
Figure 4.18 Protein alignment of group X compared between AP_CaPM and AP_SQ 149
Figure 4. 19 $SAP11_{AY\text{-}WB}$ protein compared with $SAP11_{PnWB}$ (Sugio et al., 2014 and Chang et al., 2018). The underlined sequence shows NLS sequences and the grey colour shows the TCP-Binding coiled coil structure. 150

Figure 4.20 Candidate effector protein $SAP11_{SGP}$ and $SAP11_{BCRD}$ were aligned with $SAP11_{AY\text{-}WB}$ and underlined region shows NLS, and the coiled coil structure is shown in grey colour..... 151
Figure 4.21 Candidate effector protein $SAP11_{AP_SQ}$, $SAP11_{CoP}$ and $SAP11_{VCP}$ were aligned with $SAP11_{PnWB}$ and underlining shows the NLS, and the coiled coil structure was shown in grey colour..... 152
Figure 4.22 SAP11 protein alignment between samples and Tengu. The sequences were aligned using ClustalW and dots represent amino acids identical to $SAP11_{AY\text{-}WB}$ consensus sequences; dash represents amino acid deletions in the protein..... 153
Figure 4.23 The phylogenetic tree was constructed from SAP11 proteins and candidate hypothetical proteins using neighbour-joining in MEGA X program used 1000 replicates for bootstrap analysis..... 154
Figure 4.24 T_1 transformed Arabidopsis screening on 0.8% of ½ MS agar with 50 µg/ml hygromycin. The red arrow shows transformed-resistant Arabidopsis. 155
Figure 4. 25 PCR product of $SAP11_{AP_SQ}$ T_1 transformed plants compared with wild type and pGWB5. Lanes (1) 100 bp ladder, (2) Arabidopsis wild type, (3) Arabidopsis transformed with Vector pGWB5 only, (4) Arabidopsis transformed with $SAP11_{AP_SQ}$ line 1, (5) Arabidopsis transformed with $SAP11_{AP_SQ}$ line 2, (6) pGWB5 with $SAP11_{AP_SQ}$ effector gene insert and (7) Non-template control..... 156
Figure 4.26T_0 transformed Brachypodium screened on MSMO adding 300 mg/L Timentin and 30 µg/ml hygromycin. A. The red arrow shows green

resistant transformed Brachypodium and the white arrow shows the albino transformed plant. B. Green shoot of transformed Brachypodium. 157

Figure 4.27 A. transformed Brachypodium in glasshouse. B. PCR product of $Ef2_{NGSD}$ T_0 transformed Brachypodium compared with wild type and positive control. Lanes (1) 100 bp ladder, (2) Brachypodium wild type, (3) $Ef2_{NGSD}$-pBRACT214 vector, (4) $Ef2_{NGSD}$ T_0 transformed Brachypodium, (5) Non-template control. 157

Figure 4.28 The phylogenetic tree showing the relationship between different groups of phytoplasmas (Nicolaisen and Harvath, 2001), noting the ones used in this study and the groups they belong to. 159

Chapter 5

Figure 5.1 A schematic of the common phyllotaxies. 168

Figure 5.2 A schematic of the role of BLR in PME5 expression in plants at the meristem and internode (Peaucelle *et al*., 2011)..... 169

Figure 5.3 A Schematic of witches' broom induced by the Tengu effector protein (Maejama *et al*., 2014). 172

Figure 5.4 Scheme of SWP1 function in inducing witches' broom symptoms by mediating the degradation of BRC1 through a proteasome system (Wang and Jiao 2018). 173

Figure 5.5 The SAP54 effector protein interacted with specific MADS-box transcription factors (MTFs) and degrades via the 26S proteasome, which leads to leaf-like flower structure (MacLean *et al*., 2011 and 2014). 174

Figure 5.6 Schematic of phyllody-like symptoms induced by the phyllogen effector protein (Maejima *et al.*, 2014). 175

Figure 5.7 Schematic of TENGU-induced reduction of jasmonic acid and auxin levels (Minato *et al*., 2014). 176
Figure 5.8 Relative gene expression of transgene compared to *PP2A* (actin) gene that were examined by relative quantitative RT-PCR with the gene expression level in wild type set to 1. The columns show gene expression levels of wild type, vector only and three transformed plants and standard errors (SEs) (bars) of relative quantitative RT-PCR from three biological replicates. The * above the columns indicates statistical difference ($p<0.05$) by student t-test. 181
Figure 5.9 *Arabidopsis* T_2 generation and $SAP11_{AP_SQ}$ transformed plants. A. T_2 $SAP11_{AP_SQ}$ transformed plant compared to wild type and vector only. B. $SAP11_{AP_SQ}$ transformed plant showing the clustered cauline leaves (aerial rosettes). C. Clustered cauline leaves (aerial rosettes) (white arrow) and terminated flower (red arrow) and D. Wild type leaf compared to $SAP11_{AP_SQ}$ transformed leaf. E, F, and G. The transformed plant showing secondary stems at the same point on the primary stem. 183
Figure 5.10 Relative gene expression of *BRC1* and *PME5* genes compared to *PP2A* (actin) gene that were examined by relative quantitative RT-PCR with the gene expression level in wild type set to 1. The columns show gene expression levels of wild type, vector only and three transformed plants and standard errors (SEs) (bars) of relative quantitative RT-PCR from three biological replicates. The * above the columns indicates statistical differences ($p<0.05$) by student t-test. 185
Figure 5.11 Relative gene expression of *PNF, PNY* and *BP/KNATT1* genes compared to *PP2A* (actin) gene that were examined by relative quantitative

RT-PCR with the gene expression level in wild type set to 1. The columns show gene expression levels of wild type, vector only and three transformed plants and standard errors (SEs) (bars) of relative quantitative RT-PCR from three biological replicates. The * above the columns indicates statistical differences ($p<0.05$) by student t-test..... 186

Figure 5.12 Relative gene expression of transgene compared to *PP2A* (actin) gene that were examined by relative quantitative RT-PCR with the gene expression level in wild type set to 1. The columns show gene expression levels of wild type, vector only and three transformed plants and standard errors (SEs) (bars) of relative quantitative RT-PCR from three biological replicates. The * above the columns indicates statistical differences ($p<0.05$) by student t-test. 187

Figure 5.13 *Arabidopsis* T_2 generation and *SAP11*$_{BCRD}$ transformed plants. A. T_2 *SAP11*$_{BCRD}$ transformed plant compared to wild type and vector only. B. *SAP11*$_{BCRD}$ transformed plant showing phyllotaxis symptom. 188

Figure 5.14 Relative gene expression of *BRC1* and *PME5* genes compared to *PP2A* (actin) gene that were examined by relative quantitative RT-PCR with the gene expression level in wild type set to 1. The columns show gene expression levels of wild type, vector only and three transformed plants and standard errors (SEs) (bars) of relative quantitative RT-PCR from three biological replicates. The * above the columns indicates statistical differences ($p<0.05$) by student t-test. 189

Figure 5.15 Relative gene expression of *PNF, PNY* and *BP/KNATT1* genes compared to *PP2A* (actin) gene that were examined by relative quantitative RT-PCR with the gene expression level in wild type set to 1. The columns

show gene expression levels of wild type, vector only and three transformed plants and standard errors (SEs) (bars) of relative quantitative RT-PCR from three biological replicates. The * above the columns indicates statistical differences ($p<0.05$) by student t-test..... 190
Figure 5.16 Photograph showing the flowers of wild type (A), vector only (B) and *SAP11*$_{BCRD}$ transformed plants (C) bar = 1mm. 191
Figure 5.17 Relative gene expression of transgene compared to *PP2A* (actin) gene that were examined by relative quantitative RT-PCR with the gene expression level in wild type set to 1. The columns show gene expression levels of wild type, vector only and three transformed plants and standard errors (SEs) (bars) of relative quantitative RT-PCR from three biological replicates. The * above the columns indicates statistical differences ($p<0.05$) by student t-test. 192
Figure 5.18 *Arabidopsis* T_2 generation and *SAP11*$_{CoP}$ transformed plants. A. T_2 *SAP11*$_{CoP}$ transformed plant compared to wild type and vector only. B. *SAP11*$_{CoP}$ transformed plant showing phyllotaxis symptom. 193
Figure 5.19 Relative gene expression of *BRC1* and *PME5* genes compared to *PP2A* (actin) gene that were examined by relative quantitative RT-PCR with the gene expression level in wild type set to 1. The columns show gene expression levels of wild type, vector only and three transformed plants and standard errors (SEs) (bars) of relative quantitative RT-PCR from three biological replicates. The * above the columns indicates statistical differences ($p<0.05$) by student t-test. 194
Figure 5.20 Relative gene expression of *PNF, PNY* and *BP/KNATT1* genes compared to *PP2A* (actin) gene that were examined by relative quantitative

RT-PCR with the gene expression level in wild type set to 1. The columns show gene expression levels of wild type, vector only and three transformed plants and standard errors (SEs) (bars) of relative quantitative RT-PCR from three biological replicates. The * above the columns indicates statistical differences ($p<0.05$) by student t-test..... 195

Figure 5.21. Photograph showing the flowers of wild type (A), vector only (B) and *SAP11$_{CoP}$* transformed plants (C) bar = 1mm. 196

Figure 5.22. Relative gene expression of transgene compared to *PP2A* (actin) gene that were examined by relative quantitative RT-PCR with the gene expression level in wild type set to 1. The columns show gene expression levels of wild type, vector only and three transformed plants and standard errors (SEs) (bars) of relative quantitative RT-PCR from three biological replicates. The * above the columns indicates statistical differences ($p<0.05$) by student t-test. 197

Figure 5.23 *Arabidopsis* T_2 generation and *SAP11$_{SGP}$* transformed plants. A. T_2 *SAP11$_{SGP}$* transformed plant compared to wild type and vector only. B. *SAP11$_{SGP}$* transformed plant showing more branching stem. 198

Figure 5.24 Relative gene expression of *BRC1* and *PME5* genes compared to *PP2A* (actin) gene that were examined by relative quantitative RT-PCR with the gene expression level in wild type set to 1. The columns show gene expression levels of wild type, vector only and three transformed plants and standard errors (SEs) (bars) of relative quantitative RT-PCR from three biological replicates. The * above the columns indicates statistical differences ($p<0.05$) by student t-test. 198

Figure 5.25 Relative gene expression of *PNF, PNY* and *BP/KNATT1* genes compared to *PP2A* (actin) gene that were examined by relative quantitative RT-PCR with the gene expression level in wild type set to 1. The columns show gene expression levels of wild type, vector only and three transformed plants and standard errors (SEs) (bars) of relative quantitative RT-PCR from three biological replicates. The * above the columns indicates statistical differences ($p<0.05$) by student t-test..... 199

Figure 5.26 Photograph showing the flowers of wild type (A), vector only (B) and $SAP11_{SGP}$ transformed plants (C) bar = 1mm. 200

Figure 5.27 Relative gene expression of transgene compared to *PP2A* (actin) gene that were examined by relative quantitative RT-PCR with the gene expression level in wild type set to 1. The columns show gene expression levels of wild type, vector only and three transformed plants and standard errors (SEs) (bars) of relative quantitative RT-PCR from three biological replicates. The * above the columns indicates statistical differences ($p<0.05$) by student t-test. 201

Figure 5.28 *Arabidopsis* T_2 generation and $SAP11_{VCP}$ transformed plants. A. T_2 $SAP11_{VCP}$ transformed plant compared to wild type and vector only. B. $SAP11_{VCP}$ transformed plant showed the height of transformed plant and phyllotaxis of secondary inflorescence meristems. C. A representative flower. D. Wild type flower. E. Transformed leaf. F. Wild type leaf G. Phyllotaxis symptom at siliques and H. Normal silique pattern (Wild type). I. Transformed plant showing the organ fusion. 203

Figure 5.29 Relative gene expression of *BRC1* and *PME5* genes compared to PP2A (actin) gene that were examined by relative quantitative RT-PCR with

the gene expression level in wild type set to 1. The columns show gene expression levels of wild type, vector only and three transformed plants and standard errors (SEs) (bars) of relative quantitative RT-PCR from three biological replicates. The * above the columns indicates statistical differences ($p<0.05$) by student t-test. 204

Figure 5.30 Relative gene expression of *PNF, PNY* and *BP/KNATT1* genes compared to *PP2A* (actin) gene that were examined by relative quantitative RT-PCR with the gene expression level in wild type set to 1. The columns show gene expression levels of wild type, vector only and three transformed plants and standard errors (SEs) (bars) of relative quantitative RT-PCR from three biological replicates. The * above the columns indicates statistical differences ($p<0.05$) by student t-test..... 205

Figure 5.31 Photograph showing the flowers of wild type (A), vector only (B) and $SAP11_{VCP}$ transformed plants (C) bar = 1mm. 206

Figure 5.32 Relative gene expression of transgene compared to *PP2A* (actin) gene that were examined by relative quantitative RT-PCR with the gene expression level in wild type set to 1. The columns show gene expression levels of wild type, vector only and three transformed plants and standard errors (SEs) (bars) of relative quantitative RT-PCR from three biological replicates. The * above the columns indicates statistical differences ($p<0.05$) by student t-test. 207

Figure 5.33 *Arabidopsis* T_2 generation and $EF1_{NGSD}$ transformed plants. A. T_2 $EF1_{NGSD}$ transformed plant compared to wild type and vector only. B. $EF1_{NGSD}$ transformed plant showing the normal morphology. 208

Figure 5.34 Photograph showing the flowers of wild type (A), vector only (B) and $EF1_{NGSD}$ transformed plants (C) bar = 1mm. 208
Figure 5.35 Relative gene expression of transgene compared to *PP2A* (actin) gene that were examined by relative quantitative RT-PCR with the gene expression level in wild type set to 1. The columns show gene expression levels of wild type, vector only and three transformed plants and standard errors (SEs) (bars) of relative quantitative RT-PCR from three biological replicates. The * above the columns indicates statistical differences ($p<0.05$) by student t-test. 209
Figure 5.36 Arabidopsis T_2 generation and $EF2_{NGSD}$ transformed plants. A. T_2 $EF2_{NGSD}$ transformed plant compared to wild type and vector only. B. $EF2_{NGSD}$ transformed plant showing the more branching stem. 210
Figure 5.37. Relative gene expression of *BRC1* and *PME5* genes compared to *PP2A* (actin) gene that were examined by relative quantitative RT-PCR with the gene expression level in wild type set to 1. The columns show gene expression levels of wild type, vector only and three transformed plants and standard errors (SEs) (bars) of relative quantitative RT-PCR from three biological replicates. The * above the columns indicates statistical differences ($p<0.05$) by student t-test. 210
Figure 5.38. Relative gene expression of *PNF, PNY* and *BP/KNATT1* genes compared to *PP2A* (actin) gene that were examined by relative quantitative RT-PCR with the gene expression level in wild type set to 1. The columns show gene expression levels of wild type, vector only and three transformed plants and standard errors (SEs) (bars) of relative quantitative RT-PCR from

three biological replicates. The * above the columns indicates statistical differences ($p<0.05$) by student t-test..... 211
Figure 5.39.Photograph showing the flowers of wild type (A), vector only (B) and *EF2*$_{NGSD}$ transformed plants (C) bar = 1mm..... 212
Figure 5.40. Relative gene expression of transgene compared to *PP2A* (actin) gene that were examined by relative quantitative RT-PCR with the gene expression level in wild type set to 1. The columns show gene expression levels of wild type, vector only and three transformed plants and standard errors (SEs) (bars) of relative quantitative RT-PCR from three biological replicates. The * above the columns indicates statistical differences ($p<0.05$) by student t-test. 213
Figure 5. 41.Arabidopsis T_2 generation and *EF3*$_{NGSD}$ transformed plants. A. T_2 *EF3*$_{NGSD}$ transformed plant compared to wild type and vector only. B. EF3$_{NGSD}$ transformed plant showing the normal morphology. 214
Figure 5.42. Photograph showing the flowers of wild type (A), vector only (B) and *EF3*$_{NGSD}$ transformed plants (C) bar = 1mm..... 214
Figure 5.43. Relative gene expression of transgene compared to *PP2A* (actin) gene that were examined by relative quantitative RT-PCR with the gene expression level in wild type set to 1. The columns show gene expression levels of wild type, vector only and three transformed plants and standard errors (SEs) (bars) of relative quantitative RT-PCR from three biological replicates. The * above the columns indicates statistical differences ($p<0.05$) by student t-test. 215

Figure 5.44. Arabidopsis T_2 generation and *EF4*$_{NGSD}$ transformed plants. A. T_2 *EF4*$_{NGSD}$ transformed plant compared to wild type and vector only. B. *EF4*$_{NGSD}$ transformed plant showing the normal morphology. 216
Figure 5.45. Photograph showing the flowers of wild type (A), vector only (B) and *EF4*$_{NGSD}$ transformed plants (C) bar = 1mm. 216
Figure 5.46.Relative gene expression of transgene compared to *PP2A* (actin) gene that were examined by relative quantitative RT-PCR with the gene expression level in wild type set to 1. The columns show gene expression levels of wild type, vector only and three transformed plants and standard errors (SEs) (bars) of relative quantitative RT-PCR from three biological replicates. The * above the columns indicates statistical differences ($p<0.05$) by student t-test. 217
Figure 5.47. Arabidopsis T_2 generation and *EF5*$_{NGSD}$ transformed plants. A. T_2 *EF5*$_{NGSD}$ transformed plant compared to wild type and vector only. B. *EF5*$_{NGSD}$ transformed plant showing the normal morphology. 218
Figure 5.48. Photograph showing the flowers of wild type (A), vector only (B) and EF5$_{NGSD}$ transformed plants (C) bar = 1mm. 218
Figure 5.49. Relative gene expression of transgene compared to *PP2A* (actin) gene that were examined by relative quantitative RT-PCR with the gene expression level in wild type set to 1. The columns show gene expression levels of wild type, vector only and transformed plants and standard errors (SEs) (bars) of relative quantitative RT-PCR from three biological replicates. The * above the columns indicates statistical differences ($p<0.05$) by student t-test. 219

Figure 5.50.*Arabidopsis* T_2 generation and *EF6*$_{NGSD}$ transformed plants. A. T_2 *EF6*$_{NGSD}$ transformed plant compared to wild type and vector only. B. *EF6*$_{NGSD}$ transformed plant showing the normal morphology. 220
Figure 5.51. Photograph showing the flowers of wild type (A), vector only (B) and *EF6*$_{NGSD}$ transformed plants (C) bar = 1mm. 220
Figure 5.52 Relative gene expression of transgene compared to *PP2A* (actin) gene that were examined by relative quantitative RT-PCR with the gene expression level in wild type set to 1. The columns show gene expression levels of wild type, vector only and three transformed plants and standard errors (SEs) (bars) of relative quantitative RT-PCR from three biological replicates. The * above the columns indicates statistical differences ($p<0.05$) by student t-test. 221
Figure 5.53. *Arabidopsis* T_2 generation and *EF7*$_{NGSD}$ transformed plants. A. T_2 *EF7*$_{NGSD}$ transformed plant compared to wild type and vector only. B. *EF7*$_{NGSD}$ transformed plant showing a more branched stem. 222
Figure 5.54. Relative gene expression of *BRC1* and *PME5* genes compared to *PP2A* (actin) gene that were examined by relative quantitative RT-PCR with the gene expression level in wild type set to 1. The columns show gene expression levels of wild type, vector only and three transformed plants and standard errors (SEs) (bars) of relative quantitative RT-PCR from three biological replicates. The * above the columns indicates statistical differences ($p<0.05$) by student t-test. 223
Figure 5.55 Relative gene expression of *PNF, PNY* and *BP/KNATT1* genes compared to *PP2A* (actin) gene that were examined by relative quantitative RT-PCR the gene expression level in wild type set to 1. The columns show

gene expression levels of wild type, vector only and three transformed plants and standard errors (SEs) (bars) of relative quantitative RT-PCR from three biological replicates. The * above the columns indicates statistical differences ($p<0.05$) by student t-test. 224
Figure 5.56. Photograph showing the flowers of wild type (A), vector only (B) and *EF7*$_{NGSD}$ transformed plants (C) bar = 1mm. 225
Figure 5.57. Relative gene expression of transgene compared to *PP2A* (actin) gene that were examined by relative quantitative RT-PCR with the gene expression level in wild type set to 1. The columns show gene expression levels of wild type, vector only and three transformed plants and standard errors (SEs) (bars) of relative quantitative RT-PCR from three biological replicates. The * above the columns indicates statistical differences ($p<0.05$) by student t-test. 225
Figure 5.58 *Arabidopsis* T_2 generation and *EF2*$_{SCWL}$ transformed plants. A. T_2 *EF2*$_{SCWL}$ transformed plant compared to wild type and vector only. B. *EF2*$_{SCWL}$ transformed plant showing a more branched stem. 226
Figure 5.59 Relative gene expression of *BRC1* and *PME5* genes compared to *PP2A* (actin) gene that were examined by relative quantitative RT-PCR with the gene expression level in wild type set to 1. The columns show gene expression levels of wild type, vector only and three transformed plants and standard errors (SEs) (bars) of relative quantitative RT-PCR from three biological replicates. The * above the columns indicates statistical differences ($p<0.05$) by student t-test. 227
Figure 5.60. Relative gene expression of *PNF, PNY* and *BP/KNATT1* genes compared to *PP2A* (actin) gene that were examined by relative quantitative

RT-PCR with the gene expression level in wild type set to 1. The columns show gene expression levels of wild type, vector only and three transformed plants and standard errors (SEs) (bars) of relative quantitative RT-PCR from three biological replicates. The * above the columns indicates statistical differences ($p<0.05$) by student t-test..... 228

Figure 5.61 Photograph showing the flowers of wild type (A), vector only (B) and *EF2*$_{SCWL}$ transformed plants (C) bar = 1mm..... 229

Figure 5.62. Relative gene expression of transgene compared to *PP2A* (actin) gene that were examined by relative quantitative RT-PCR with the gene expression level in wild type set to 1. The columns show gene expression levels of wild type, vector only and three transformed plants and standard errors (SEs) (bars) of relative quantitative RT-PCR from three biological replicates. The * above the columns indicates statistical differences ($p<0.05$) by student t-test. 230

Figure 5.63 *Arabidopsis* T_2 generation and *EF7*$_{SCWL}$ transformed plants. A. T_2 *EF7*$_{SCWL}$ transformed plant compared to wild type and vector only. B. *EF7*$_{SCWL}$ transformed plants showing more branched stems..... 231

Figure 5.64. Relative gene expression of *BRC1* and *PME5* genes compared to *PP2A* (actin) gene that were examined by relative quantitative RT-PCR with the gene expression level in wild type set to 1. The columns show gene expression levels of wild type, vector only and three transformed plants and standard errors (SEs) (bars) of relative quantitative RT-PCR from three biological replicates. The * above the columns indicates statistical differences ($p<0.05$) by student t-test. 232

Figure 5.65 Relative gene expression of *PNF, PNY* and *BP/KNATT1* genes compared to *PP2A* (actin) gene that were examined by relative quantitative RT-PCR with the gene expression level in wild type set to 1. The columns show gene expression levels of wild type, vector only and three transformed plants and standard errors (SEs) (bars) of relative quantitative RT-PCR from three biological replicates. The * above the columns indicates statistical differences ($p<0.05$) by student t-test..... 233

Figure 5.66. Photograph showing the flowers of wild type (A), vector only (B) and $EF7_{SCWL}$ transformed plants (C) bar = 1mm..... 234

Figure 5.67. SAP11 protein homologs interacted with different plant genes and showed various phenotypes and flowers and √ represents plant gene was affected by effect from effector proteins and X represents plant gene was not affected by effector proteins..... 242

Chapter 6

Figure 6.1The phylogenetic tree was constructed from *SAP11* sequences obtained in this thesis. A. The SAP11 phylogenetic tree between 16SrX, 16SrXI and 16SrXIV. B. The phylogenetic tree between 16SrI, 16SrII, 16SrX and 16SrXI..... 247

Figure 6.2 The effect of the *BRC1* gene by the SAP11 effector protein causing branching (Wang and Jiao, 2018)..... 249

Figure 6.3 Inhibition of the *BLR* and *PME5* genes in plant development by SAP11 (Peaucelle *et al.*, 2011)..... 250

Figure 6.4 Effect of inhibiting the *PME5* level to cause organ fusion (Andres-Robin *et a*l., 2018)..... 251

Figure 6.5 Inhibition of the *PNF/PNY* gene for flower development by SAP11 (Kanrar *et al*., 2008). 252

List of Tables

Chapter 1

Table 1.1 Phytoplasma classification based on the RFLP technique of 16S rRNA (Zhao and Davis, 2016). 12

Table 1.2 16S rRNA subgroup classification based on Lee *et al*. (1998) 14

Table 1.3 Conventional PCR primers for phytoplasma detection of the 16S rRNA (IPPC, 2016). 22

Table 1.4 Example LAMP primers and SecA gene primers for detection of phytoplasma 16S rRNA..... 23

Chapter 2

Table 2.1 Phytoplasma strains examined in this study 40

Table 2.2 Nucleotide primers for phytoplasma detection 43

Table 2.3 MLST analysis primers used in this study 47

Table 2.4 Summary of the PCR results for each gene in MLST analysis..... 52

Table 2.5 Summary of the classified samples for each gene 68

Chapter 3

Table 3.1 List of primers for NGSD effector amplification in NGSD and SCWL that included signal peptides. 94

Table 3.2 List of primers for NGSD effector amplification in NGSD and SCWL excluding signal peptides..... 95

Table 3.3 List of protein sequences. 102

Table 3.4 List of protein similarity and identity from NCBI database. 103

Chapter 4

Table 4.1 Comparison of Biological genomic traits among Arabidopsis thaliana, Oryza sativa and Brachypodium distachyon (Draper *et al*., 2001; Zhussupova *et al*., 2013)..... 114

Table 4.2 Phytoplasmas and 16Sr group samples used in the experiment 121

Table 4.3 List of SAP11 gene primers and M13 primers for colony PCR... 123

Table 4.4 Time to amplification and annealing temperature from LAMP experiments 142

Table 4.5 List of protein similarity and identity from NCBI database 144

Table 4.6 List of protein sequences 145

Chapter 5

Table 5.1 List of qPCR primers used for relative quantitative PCR 180

Table 5.2 Summary of the effect of the effector proteins on plant gene expression..... 235

Chapter 1: General introduction

Phytoplasmas are a group of bacteria that infect a broad variety of plants such as medicinal plants, flowering plants and fruiting plants. They have no cell wall and it is not possible to culture them on artificial medium. Moreover, they have small genomes lacking some metabolite genes such that it is presumed that they live by using many metabolites obtained from hosts. Phytoplasmas also live in insects for propagation and transmission into plants when the insects feed on a plant. Phytoplasmas produce effector proteins to inhibit plant developmental pathways such as flower development, auxin biosynthetic pathways etc. and as a result there is often a loss of yield in infected plants.

1.1 Description of Phytoplasmas

Phytoplasmas are unicellular organisms that were originally called mycoplasma-like organisms (MLO) because the morphology of phytoplasmas is similar to animal mycoplasmas. They were first identified in mulberry by Doi *et al*. (1967). Phytoplasmas are related to other bacteria, most closely the Gram-positive *Bacillus* spp. but they have no cell wall and they are sensitive to tetracyclin because the tetracyclin binds to the 30S ribosomal protein and inhibits protein synthesis (Namba, 2019); moreover, rifampicin also inhibits phytoplasmas growth (Tanno *et al*., 2018). Phytoplasmas are small in diameter and genome size with diameters between 200-800 nm (Figure 1.1) and

genome sizes of 550-1500 kb which are low in G+C content (Sugio and Hogenhout, 2012; Sugawara *et al*., 2013).

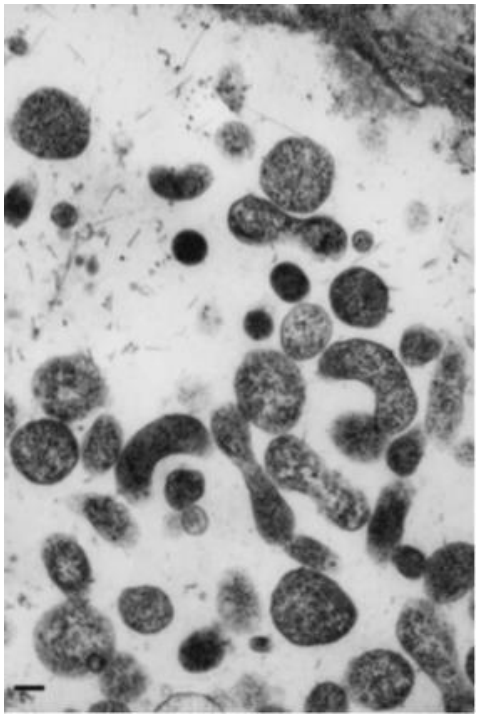


Figure 1.1 Electron micrograph of cross section of sieve tube showed phytoplasmas infecting in plant (cross section, Bar = 200 nm) (Duduk and Bertaccini, 2011).

Phytoplasmas are unique microorganism, having a dual life cycle in insect and plant hosts (Figure 1.2). They lack numerous metabolic functions such as amino acid or fatty acid biosynthesis, the TCA cycle or oxidative phosphorylation, which is related to the nutrient-rich environments of the hosts and consequently they acquire several metabolites and directly import metabolic compounds from their host (Sugawara *et al*., 2002). Their genomes have various structures and gene contents which are minimal metabolic gene sets (Duduk and Bertaccini, 2011). In addition, they have been found to be

restricted to the phloem cells of host plants and in the same way, they invade specific organs of insect vectors, including salivary glands, for transmission (Hogenhout *et al*., 2008; Rashid *et al*., 2018). Phytoplasmas have also been found in other cells than the phloem cells in parasitic plants, for example parenchyma cells. Siller *et al*. (1987) found phytoplasmas inside parenchyma cells of *Cuscuta*, whilst in 2003, Cordova *et al*. (2003) studied lethal yellow (LY) phytoplasma in Atlantic coconut palm and they were able to detect LY DNA in embryos of coconut palms.

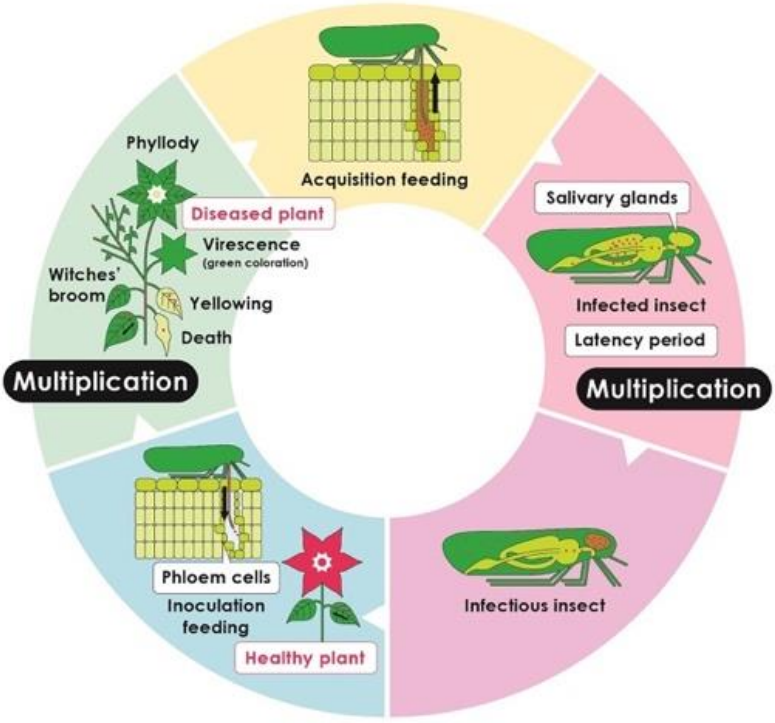


Figure 1.2 Dual life cycle of phytoplasmas which live in insect vectors and plants, and each step of infection. When the leafhoppers feed on the phytoplasma infected plants, the phytoplasmas will move from the plant phloem into the leafhopper body for multiplication. Subsequently, when the leafhoppers feed on healthy plants, the phytoplasma will be transmitted back

into plant phloem where it can reproduce and the plant will show the characteristic symptoms.

Source: https://www.u-tokyo.ac.jp/focus/en/features/f_00072.html

In addition, phytoplasma genome sequences have been completed for Aster yellows witches' broom (AY-WB), Onion yellows (OY-M), Australian grapevine yellows (AUSGY) and Apple proliferation (AP) strains and almost all phytoplasma genomes sequenced to date are circular (OY-M, AY-WB and AUSGY) although that of AP is linear. These phytoplasma genomes contain prophage sequences which are believed to have contributed to phytoplasma genome expansion. However, prophage sequences in phytoplasma genomes lack canonical genes such as integrases, terminases and prohead proteases as well as phage sequences which are found in the subclade of *Spiroplasmas* infecting plants and honeybees (Dickinson, 2010; Ku *et al*., 2013).

Phytoplasmas spread naturally from plant to plant via insect vectors such as leafhoppers (*Cicadellidae*), planthoppers (*Fulgoromorha*) and psyllids (*Psyllidae*). Phytoplasmas accumulate to high levels in gut cells and salivary glands and enter the intestine lumen; they are then released into plant phloem during feeding (Weintraub and Beanland, 2006). Remarkably, phytoplasma infection can have both positive and negative effects on the insect vectors. In some cases, as a positive effect, infected insects are able to live longer than uninfected insects, whilst in other cases infection has the negative effect of reducing the life span of the insect vectors (Weintraub and Beanland, 2006).

In addition, phytoplasma invasion can take 10 days or longer in insect organs, which depends on phytoplasma species, insect species and temperature (Dickinson, 2010).

In their plant hosts, phytoplasmas induce a range of symptoms, some of which, such as increasing branching and bushiness, can be used to make ornamental plants more attractive to consumers (Bertaccini, 2007). In addition, the symptoms in plants often make the plants more attractive to phytoplasma insect vectors to feed. In crop plants however, infections can result in significant yield losses with plants showing various symptoms such as stunting, yellowing, witches' broom (proliferation of stems, branches and leaves), virescence (loss of normal flower colour) and phyllody (development of floral parts into leaf-like structure) and altered production of volatiles (Figures 1.3 -1.6) (Sugio *et al*., 2011). These symptoms depend on host range and usually appear within one week of infection, although it can take longer to develop more severe symptoms depending on temperature, plant age and plant species. Most potential host plants are dicotyledonous, but there are a few host plants that are monocotyledonous and herbaceous (Sugio and Hogenhout, 2012).



Figure 1.3 Virescence symptoms on periwinkle flowers infected with phytoplasma (Duduk and Bertaccini, 2011).



Figure 1.4 Phyllody symptoms on hydrangea infected with phytoplasma on the right compared with a healthy hydrangea plant on the left (Maejima *et al*., 2014).



Figure 1.5 Witches' broom symptoms in almond infected with phytoplasma on the right compared with a healthy almond plant on the left (Yusuf *et al*., 2003)



Figure 1.6 Stunt symptoms on Napier grass infected with phytoplasma (Asudi *et al*., 2015)

1.2 Taxonomic Information

Superkingdom: Prokaryote

Kingdom: Monera

Domain: Bacteria

Phylum: Firmicutes (Gram positive bacteria and Low G+C content)

Class: Mollicutes

Order: Acholeplasmatales

Famlily: Acholeplasmataceae

Genus: Phytoplasma; *Candidatus*

Phytoplasmas are prokaryotes without cell walls and they are in the kingdom Monera in the Bacterial domain and belong to the phylum Firmicutes. The class genus; *Candidatus* (*Ca*.) Phytoplasma identifies them as having different biological characteristics from *mycoplasmas*, *ureaplasmas*, *spiroplasmas* and *acholeplasma* (Figure 1.7). However, the phytoplasma genome is different from other members in the class Mollicutes (Hogenhout *et al*., 2008) and interestingly, they are more closely related to the Gram-positive bacteria.

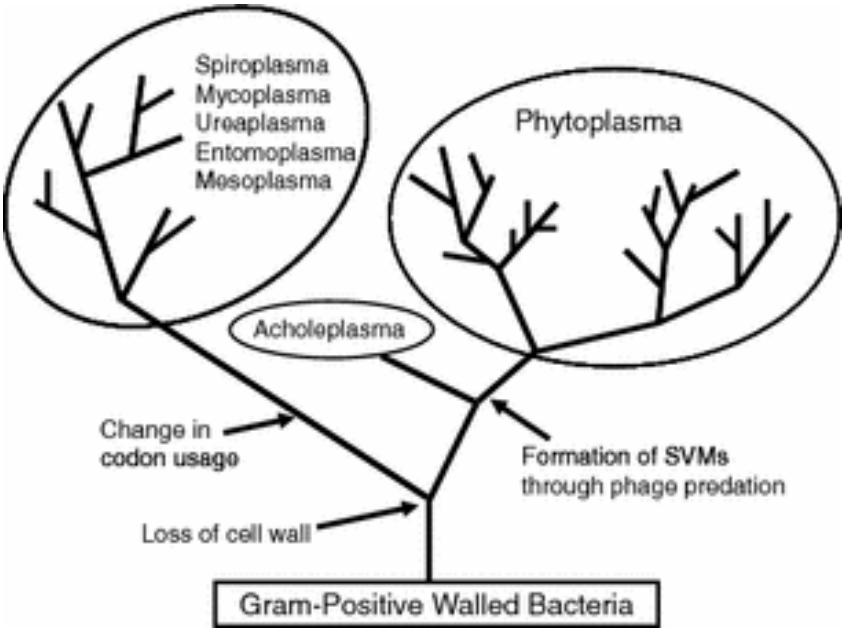


Figure 1. 7 A phylogenetic tree showing wall-less bacteria groups and their relationship to Gram positive walled bacteria (Zhao and Davis., 2016).

In addition, phytoplasmas and acholeplasmas have standard codon usage (Figure 1.8) whereas other wall-less bacteria appear to use the UGA codon for tryptophan and one stop codon (Razin *et al*., 1998). Furthermore, some *Spiroplasma* species share insect vectors with phytoplasmas, such as *Spiroplasma citri*, *S. kunkelli* and *S. phoeniceum*. At present, because they cannot be grown routinely in axenic culture, the International Research Programme on Comparative Mycoplasmology (IRPCM) has placed phytoplasmas within the novel genus '*Candidatus* (*Ca*.) phytoplasma' with '*Ca.* species' defined based on 16S ribosomal rRNA sequences. There are more than 900 sequences of 16S rRNA genes of phytoplasmas in GenBank that can be used to classify phytoplasma strains.

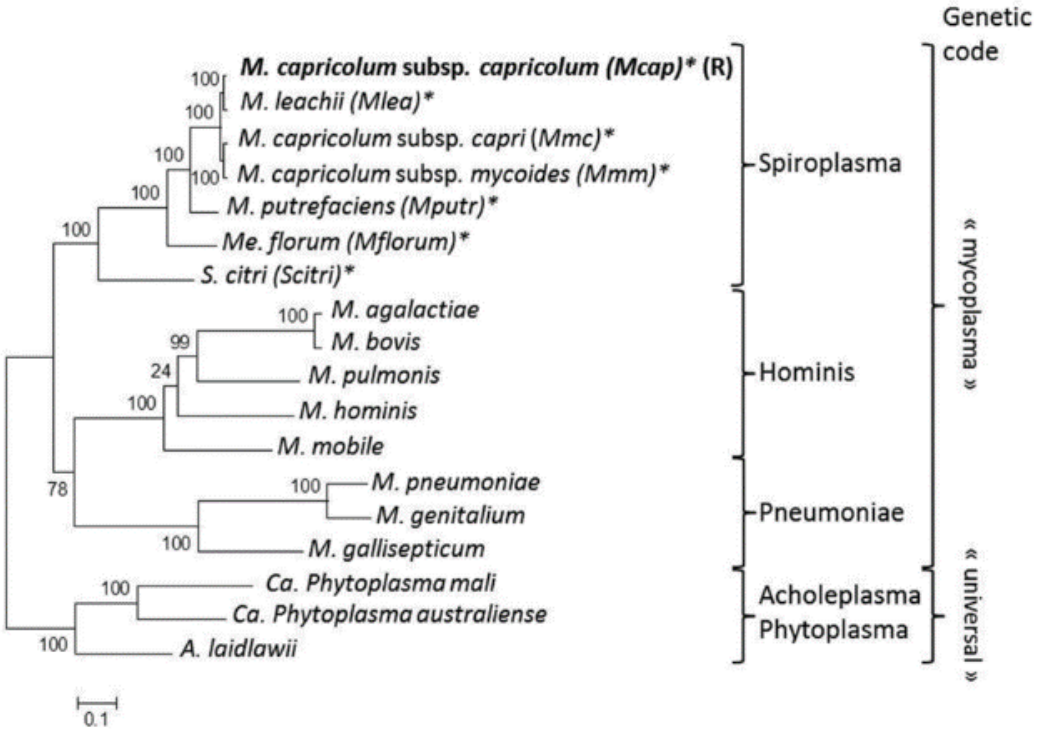


Figure 1.8 Phylogenetic tree of Mollicutes indicating the genetic code on the right side (Labroussaa *et al*., 2016).

1.3 Phytoplasma classification and detection

1.3.1 Classification

Phytoplasmas cannot be cultured in artificial media so they have to be maintained in host plants for research, and the Madagascan periwinkle, *Catharanthus rosea*, has proved to be a useful model plant in which to maintain many phytoplasma isolates. Prior to the 1990s, phytoplasma classification was based on by biophysical and biochemical techniques, but nucleic acid-based assay techniques such as PCR on the 16S rRNA region and PCR/RFLP have now superseded these to aid with classifying the diversity and genetic-relationships of phytoplasma groups.

Whilst sequencing of 16S rRNA genes gives the most accurate information of relationships between isolates for classification purposes, since it looks at variation in every nucleotide position across the gene, the RFLP technique is often used as a quicker and cheaper approach for looking at genetic relatedness, and RFLP patterns are used to define phytoplasma groups in the 16Sr grouping system that runs in parallel to the '*Ca.* species' system. When phytoplasmas associated with new disease outbreaks are being identified, the conventional approach is to amplify their 16S rRNA genes, undertake RFLP analysis and compare their RFLP patterns with RFLP patterns of known reference isolates. There are now over 30 groups and subgroups of phytoplasma based on the RFLP technique and there are subgroups in each group (Zhao and Davis, 2016). Figure 1.9 is a phylogenetic tree based on the 16Sr gene that shows the twenty-eight 16Sr groups of phytoplasma (Figure 1.9) based on the Zhao and Davis (2016) data and there are a lot of subgroups in each group as shown in Tables 1.1 and 1.2.

Additionally, there are other PCR primers based on conserved sequences such as the 23S RNA, *tuf* gene and *secY* gene etc for refining classifications and aiding detection and identification.

Table 1.1 Phytoplasma classification based on the RFLP technique of 16S rRNA (Zhao and Davis, 2016).

Group	Number of '*Ca*. Phytoplasma' species
16SrI: Aster yellows group	2 ('*Ca*. Phytoplasma asteris' and '*Ca*. Phytoplasma lycopersici')
16SrII: Peanut witches' broom group	2 ('*Ca*. Phytoplasma aurantifolia' and '*Ca*. Phytoplasma australasiae')
16SrIII: X-disease group	1 ('*Ca*. Phytoplasma pruni')
16SrIV: Coconut lethal yellows group	2 ('*Ca* Phytoplasma palmae' and '*Ca*. Phytoplasma cocostanzaniae')
16SrV: Elm yellows group	5 ('*Ca*. Phytoplasma ulmi', '*Ca*. Phytoplasma ziziphi', '*Ca*. Phytoplasma rubi', '*Ca*. Phytoplasma balanitae' and '*Ca*. Phytoplasma vitis')
16SrVI: Clover proliferation group	2 ('*Ca*. Phytoplasma trifolii' and '*Ca*. Phytoplasma sudamericanum')
16SrVII: Ash yellows group	1 ('*Ca*. Phytoplasma fraxini')
16SrVIII: Loofah witches' broom group	1 ('*Ca*. Phytoplasma luffae')
16SrIX: Pigeon pea witches'' broom group	1 ('*Ca*. Phytoplasma phoenicium')
16SrX: Apple proliferation group	4 ('*Ca*. Phytoplasma mali', '*Ca*. Phytoplasma pyri', '*Ca*. Phytoplasma prunorum' and '*Ca*. Phytoplasma spartii')
16SrXI: Rice yellow dwarf group	2 ('*Ca*. Phytoplasma oryzae' and '*Ca*. Phytoplasma cirsii')
16SrXII: Stolbur group	5 ('*Ca*. Phytoplasma australiense', '*Ca*. Phytoplasma japonicum', '*Ca*. Phytoplasma fragariae', '*Ca*. Phytoplasma solani' and '*Ca*. Phytoplasma convolvuli')
16SrXIII: Mexican periwinkle virescence group	1 (AF248960, '*Ca*. Phytoplasma hispanicum')
16SrXIV: Bermudagrass white leaf group	1 ('*Ca*. Phytoplasma cynodontis')
16SrXV: Hibiscus witches' broom group	1 ('*Ca*. Phytoplasma brasiliense')
16SrXVI: Sugar cane yellow leaf syndrome group	1 ('*Ca*. Phytoplasma graminis')

16SrXVII: Papaya bunchy top group	1 (‘*Ca*. Phytoplasma caricae’)
16SrXVIII: American potato purple top wilt group	1 (‘*Ca*. Phytoplasma americanum’)
16SrXIX: Japanese chestnut witches’ broom group	1 (‘*Ca*. Phytoplasma castaneae’)
16SrXX: Buckthorn witches’ broom group||	1 (‘*Ca*. Phytoplasma rhamni’)
16SrXXI: Pine shoot proliferation group	1 (‘*Ca*. Phytoplasma pini’)
16SrXXII: Nigerian coconut lethal decline (LDN) group	1 (‘*Ca*. Phytoplasma palmicola’)
16SrXXIII: Buckland Valley grapevine yellows group	1 (reference strain 16S rRNA gene GenBank accession no. AY083605)"
16SrXXIV: Sorghum bunchy shoot group	1 (reference strain 16S rRNA gene GenBank accession no. AF509322)"
16SrXXV: Weeping tea tree witches’ broom group	1 (reference strain 16S rRNA gene GenBank accession no. AF521672)"
16SrXXVI: Mauritius sugar cane yellows D3T1 group	1 (reference strain 16S rRNA gene GenBank accession no. AJ539179)"
16SrXXVII: Mauritius sugar cane yellows D3T2 group	1 (reference strain 16S rRNA gene GenBank accession no. AJ539180)"
16SrXXVIII: Havana derbid phytoplasma group	1 (reference strain 16S rRNA gene GenBank accession no. AY744945)"
16SrXXIX: Cassia witches’ broom group	1 (‘*Ca*. Phytoplasma omanense’)
16SrXXX: Salt cedar witches’ broom group	1 (‘*Ca*. Phytoplasma tamaricis’)
16SrXXXI: Soybean stunt phytoplasma group	1 (‘*Ca*. Phytoplasma costaricanum’)
16SrXXXII: Malaysian periwinkle virescence phytoplasma group	1 (‘*Ca*. Phytoplasma malaysianum’)
16SrXXXIII: Allocasuarina phytoplasma group	1 (‘*Ca*. Phytoplasma allocasuarinae’)

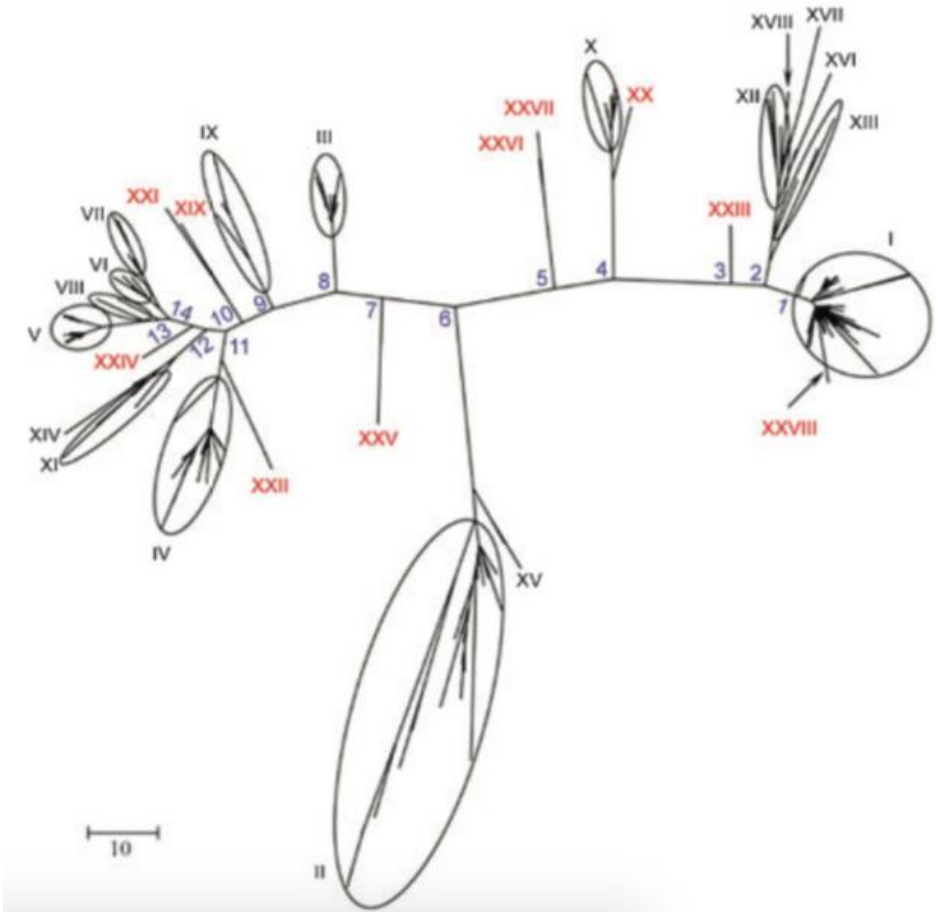


Figure 1.9 A tree topology reconstructed for the phytoplasma 16Sr groups; circles encompass group members (Wei *et al*., 2007).

Table 1.2 16S rRNA subgroup classification based on Lee *et al*. (1998)

16S rRNA group	Phytoplasma strain	GenBank acc. No.	Reference
16SrI: Aster yellows			
I-A	Aster yellows witches' broom (AY-WB)	NC_007716	Bai *et al*., 2006
	Tomato big bud (BB)	L33760	Lee *et al.*, 1992
I-B	Onion yellows mild strain (OY-M)	NC_005303	Oshima *et al*., 2004

	'*Ca.* P. asteris', aster yellows (MAY)	M30790	Lee *et al*., 2004a
I-C	Clover phyllody (CPh)	AF222065	Lee *et al*., 2004a
I-D	Paulownia witches' broom (PaWB)	AY265206	Lee *et al*., 2004a
I-E	Blueberry stunt (BBS3)	AY265213	Lee *et al*., 2004a
I-F	Aster yellows apricot - Spain (A-AY)	X68338 AY265211	Kison, 1992* Lee *et al*., 2004a
I-I	Strawberry witches' broom (STRAWB1)	U96614	Jomantiene *et al*., 1998
I-K	Strawberry witches' broom (STRAWB2)	U96616	Jomantiene *et al*., 1998
I-L	Aster yellows (AV2192)	AY180957	Lee *et al*., 2003
I-M	Aster yellows (AVUT)	AY265209	Lee *et al*., 2004a
I-N	Aster yellows (IoWB)	AY265205	Lee *et al*., 2004a
I-O	Soybean purple stem (SPS)	AF268405	Lee *et al*., 2004a
I-P	Aster yellows from *Populus* (PopAY)	AF503568	Šeruga *et al*., 2003
I-Q	Cherry little leaf (ChLL)	-	Valiunas *et al*., 2006
I-R	Strawberry phylloid fruit (StrawbPhF)	AY102275	Jomantiene *et al*., 2002a
16SrII: Peanut WB			
II-A	Peanut witches' broom (PnWB)	L33765	Gundersen *et al*., 1994
II-B	'*Ca.* P. aurantifolia', witches' broom of lime (WBDL)	U15442	Zreik *et al*., 1995
II-C	Faba bean phyllody (FBP)	X83432	Seemüller *et al*., 1998
II-D	Sweet potato little leaf (SPLL)	AJ289193	Gibb *et al*., 1995

II-E	*Pichris echioides* phyllody (PEY)	Y16393	Seemüller *et al*., 1998
II-F	Cotton phyllody (CoP)	EF186827	Martini *et al*., 2007
16SrIII: X-disease			
III-A	Western X-disease (WX)	AF533231	Liefting and Kirkpatrick, 2003
III-B	Clover yellow edge (CYE)	L33766 8	Gundersen *et al.*, 1994
III-C	Pecan bunch (PB)	EF186807	Martini *et al.*, 2007
III-D	Goldenrod yellows (GR1)	EF186810	Martini *et al.*, 2007
III-E	Spiraea stunt (SP1)	AF190228	Jomantiene *et al*, 1998
III-F	Milkweed yellows (MW1)	AF510724	Davis and Dally, 2002*
III-G	Walnut witches' broom (WWB)	AF190226 AF190227	Jomantiene *et al*, 1998
III-H	Poinsettia branch-inducing (PoiBI)	AF190223	Jomantiene *et al*, 1998
III-I	Virginia grapevine yellows (VGYIII)	AF060875	Davis *et al*., 1998
III-J	Chayote witches' broom (ChWBIII)	AF147706 AF1477067	Montano *et al*., 2000
III-K	Strawberry leafy fruit (SLF)	AF274876	Jomantiene *et al*, 2002
III-L	Cassava frog skin disease (CFSD)	EU346761	Alvarez *et al.*, 2009
III-P	Dandelion virescence (DanV)	AF370119 AF370120	Jomantiene and Davis, 2001*
III-Q	Black raspberry witches' broom (BRWB7)	AF302841	Davis *et al*., 2001
III-T	Sweet and sour cherry (ChD)	FJ231728	Valiunas *et al*., 2009
III-U	Cirsium white leaf (CWL)	AF373105 AF373106	Jomantiene *et al*., 2002b

16SrIV: Coconut lethal yellow			
IV-A	Coconut lethal yellowing (LYJ-C8)	AF498307	Harrison *et al*., 2002
IV-B	Yucatan coconut lethal decline (LDY)	U18753	Harrison *et al.*, 1994
IV-C	Tanzanian coconut lethal decline (LDT)	X80117	Harrison *et al.*, 1994
16SrV: Elm yellows			
V-A	'*Ca.* P. ulmi', elm yellows (EY)	AY197655	Lee *et al*., 2004b
V-B	'*Ca.* P. ziziphi', jujube witches' broom, (JWB-G1)	AB052876	Jung *et al*., 2003a
V-C	Alder yellows (ALY882)	AY197642	Lee *et al*., 2004b
V-C	Flavescence dorée (FD-C)	X76560	Daire *et al.*, 1992
V-D	Flavescence dorée (FD-D)	AJ548787	Torres *et al*., 2005
V-E	Rubus stunt (RuS)	Y16395	Seemüller *et al.*, 1998
16SrVI: clover proliferation			
VI-A	'*Ca.* P. trifolii', clover proliferation (CP)	AY390261	Hiruki and Wang, 2004
VI-B	Strawberry multiplier disease (SMPD)	AF036354	Jomantiene *et al.*, 1998
VI-C	Illinois elm yellows (ILEY)	AF268895 AF409069 AF409070	Jacobs *et al*., 2003
16SrVII: Ash yellow			
VII-A	'*Ca.* P. fraxini', ash yellows (AshY)	AF092209	Griffiths *et al*., 1999
VII-B	Erigeron witches' broom (ErWB)	AY034608	Barros *et al*., 2002
16SrVIII: Loofah witches' broom			
VIII-A	Loofah witches' broom (LufWB)	AF086621	Ho *et al.*, 2001
16SrIX: Pigeon pea withches'broom			
IX-A	Pigeon pea witches'-broom (PPWB)	AF248957	Davis *et al*, 2001

IX-B	'*Ca.* P. phoenicium', almond witches' broom (AlWB)	AF515636 AF515637	Verdin *et al*., 2003
IX-C	Naxos periwinkle virescence (NAXOS)	-	Duduk *et al*., 2008
16SrX: Apple proliferation			
X-A	'*Ca.* P. mali', apple proliferation (AP)	AJ542541	Seemüller and Schneider, 2004
X-B	'*Ca.* P. prunorum', European stone fruit yellows (ESFY)	AJ542544	Seemüller and Schneider, 2004
X-C	'*Ca.* P. pyri', pear decline (PD)	AJ542543	Seemüller and Schneider, 2004
X-D	'*Ca.* P. spartii', spartium witches' broom (SpaWB)	X92869	Marcone *et al*., 2004a
X-E	Black alder witches' broom (BAWB) or Buckthorn witches' broom (BWB)	X76431	Seemüller *et al.*, 1994
16SrXI: Rice yellow dwarf			
XI-A	'*Ca.* P. oryzae', rice yellow dwarf (RYD)	AB052873	Jung *et al*., 2003b
XI-B	Sugarcane white leaf (SCWL)	X76432	Lee *et al.*, 1997b
XI-C	Leafhopper-borne (BVK)	X76429	Seemüller *et al.*, 1994
16SrXII: Stolbur			
XII-A	Stolbur (STOL)	X76427	Seemüller *et al.*, 1994
XII-B	'*Ca.* P. australiense', Australian grapevine yellows (AUSGY)	L76865	Davis *et al*., 1997
16SrXIII: Mexican periwinkle virescence			
XIII-A	Mexican periwinkle virescence (MPV)	AF248960	Davis *et al*., 2016*
XIII-B	Strawberry green petal, Florida	U96616	Jomantiene *et al.*, 1998
16SrXIV: Bermudagrass white leaf			
XIV-A	'*Ca.* P. cynodontis' bermudagrass white leaf (BGWL)	AJ550984	Marcone *et al*., 2004b

16SrXV: Hibicus witches'broom			
XV-A	'*Ca*. P. brasiliense', hibiscus witches' broom (HibWB)	AF147708	Montano *et al.*, 2001
16SrXVI: Sugarcane yellow leaf syndrome			
XVI-A	'*Ca*. P. graminis'	AY725228	Arocha *et al.*, 2005
16SrXVII: Papaya bunchy top			
XVII-A	'*Ca*. P. caricae'	AY725234	Arocha *et al.*, 2005
16SrXVIII: American potato purple top wilt			
XVIII-A	'*Ca*. P. americanum'	DQ174122	Lee *et al.*, 2006b
16SrXIX: Cassia witches'-broom			
XIX-A	'*Ca*. P. omanense'	EF666051	Al-Saady *et al.*, 2008
	'*Ca*. P. castaneae'	AB054986	Jung *et al*., 2002
16SrXX: Buckthorn witches'-broom			
XX-A	'*Ca*. P. rhamni'	X76431	X76431 Marcone *et al*., 2004[a]
16SrXXI: Pine shoot proliferation			
XXI-A	*'Ca*. P. pini'	AJ632155	Schneider *et al*., 2005
16SrXXII: Nigerian coconut lethal decline (LDN)			
XXII-A	Phytoplasma sp. strain LDN	Y14175	Tymon *et al*., 1998
16SrXXIII: Buckland Valley grapevine yellow			
XXIII-A	Buckland valley grapevine yellows phytoplasma	AY083605	Constable *et al*., 1998
16SrXXIV: Sorghum bunchy shoot			
XXIV-A	Sorghum bunchy shoot phytoplasma	AF509322	Blanche *et al*., 2003
16SrXXV: Weeping tea tree witches'-broom			
XXV-A	Weeping tea witches'-broom phytoplasma	AF521672	2002*
16SrXXVI: Mauritius sugarcane yellow D3T1			
XXVI-A	Sugar cane phytoplasma D3T1	AJ539179	2003*

16SrXXVII: Mauritius sugarcane yellow D3T2			
XXVII-A	Sugar cane phytoplasma D3T2	AJ539180	2003*
16SrXXVIII: Havana derbid phyotplasma			
XXVIII-A	Derbid phytoplasma	AY744945	2004*

*, GenBank submission

1.3.2 Molecular Detection

Phytoplasmas have a broad range of plant hosts and insect vectors (Hogenhout *et al*., 2008) and whilst symptoms can develop after infection by insect vectors in about 7 days, this may often take longer depending on plants, phytoplasma species and environmental factors. Consequently, phytoplasma symptoms are often unpredictable, making it harder to control phytoplasma spread. Nevertheless, there are many techniques that have been developed to detect phytoplasmas such as immunodetection, PCR and Loop Mediated Isothermal Amplification (LAMP). These techniques have been used for both determination of infection in plants and for classification, especially PCR and LAMP assays.

There are universal primers that have been designed for amplification of the 16S rRNA region for analysis and detection of phytoplasmas, such as the P1/P7 primers for the first-stage PCR and R16F2n/R16R2 for second-stage nested PCR (Table 1.3) and the locations of these primers on the 16S rRNA region and sizes of products they produce are shown in Figure 1.10. Because the amount of phytoplasma genomic DNA in a plant DNA extract is generally lower than 1% of total genomic DNA, the nested-PCR assay is generally used

to increase the sensitivity and specificity for detection (Duduk and Bertaccini, 2011). However, conventional and nested PCR techniques for phytoplasma detection have higher risk of sample contamination than real-time PCR techniques (Christensen, 2004) and because of its better sensitivity and lower risk of contamination, real-time PCR is now the preferred technique for use in diagnostics testing facilities. Real-time PCR primers were originally designed based on 16S rRNA, although other sequences are now also being used, and there are also alternative sets of real-time primers developed for amplifying from plant DNA to avoid false negative results due to poor quality DNA samples, such as the plant COX assay based on the cytochrome oxidase gene or the plant 18S rRNA assay.

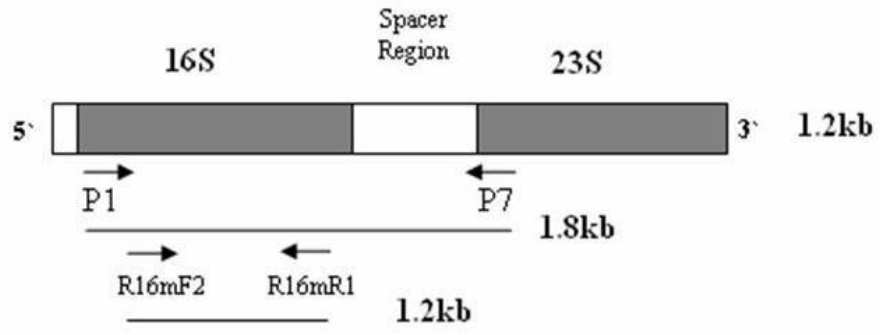


Figure 1.10 Phytoplasma primer position diagram for the 16S-23S rRNA gene (Mannan *et al*., 2010).

Table 1.3 Conventional PCR primers for phytoplasma detection of the 16S rRNA (IPPC, 2016).

Primers	Sequcences (5′–3′)	Developed by
P1 (Forward)	AAG AGT TTG ATC CTG GCT CAG GAT T	Deng and Hiruki, 1991
P7 (Reverse)	CGT CCT TCA TCG GCT CTT	Schuneider *et al*., 1995
R16F2n	GAA ACG ACT GCT AAG ACT GG	Gunderson and Lee, 1996
R16R2	TGA CGG GCG GTG TGT ACA AAC CCC G	Lee *et al*., 1993

Furthermore, Loop-mediated Isothermal Amplification (LAMP) assays have also been developed as simple, rapid, specific and cost-effective techniques for phytoplasma diagnostics. The LAMP technique requires 4 or 6 different primes for 6 specific regions on the target gene and the amplification process runs at a constant temperature of around 65°C for 20 min. For phytoplasmas, primer sets have been designed to target a number of genes such as the 16S rRNA, 23S rRNA and *SecA* gene (Figure 1.11 and Table 1.4). Primers have been designed that are specific for different 16Sr groups of phytoplasma, such as 16SrI, 16SrII, 16SrIII, 16SrV, 16SrX, 16SrXII and 16SrXXII (Bekele *et al*., 2011). LAMP can be done as a real-time assay, with the same low risks of sample contamination as for real-time PCR assays, and results can be easily visualised and presented as amplification time and annealing temperature compared to positive control.

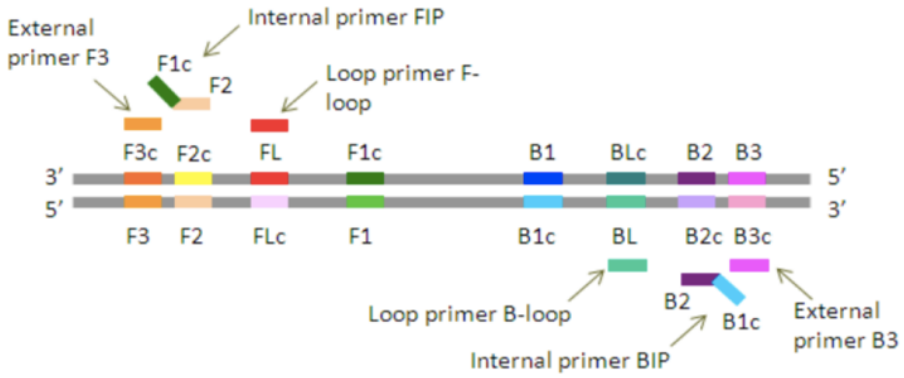


Figure 1.11 Schematic diagram of primer position for phytoplasma detection by LAMP(Tomlinson *et al*., 2013).

Table 1.4 Example LAMP primers and SecA gene primers for detection of phytoplasma 16S rRNA

Primers	Sequences (5′–3′)	Developed by
16S rRNA-FIP	GGT GTT CCT CCA TAT ATT TAC GCA TCT AGA GTA AGA TAG AGG CAA GTG	Lee *et al*., 1998
16S rRNA-BIP	CTG ACG CTG AGG CAC GAA AGA GTA CTC ATC GTT TAC GGC	
16S rRNA-F3	CAT TGT GAT GCT ATA AAA ACT GT	
16S rRNA-B3	CAA CAC TGG TTT TAC CCA AC	
secA-F3	TTCCACCAAATCTTTGAGCT	KogvŠek *et al*., 2015
secA-B3	ACAATAGCTACCAATATGGCAG	
secA-FIP	AATTAAGAGGACGTGCCGGTCGTTC GTCTTCGCTGGAAA	
secA-BIP	TCCTAAAACCGCCAAACCTCCGAAG AGGAACTGATATTCGCTT	
secA-LoopF	GAGATCCTGGTTATTCTCGCTT	
secA-LoopB	TTCAACAACGCCTTCACCT	

1.4 Phytoplasma effectors

Phytoplasmas replicate intracellularly in both hosts; insects and plants, and they release virulence effectors into host cells (Sugio *et al*., 2011). The word effector is often used to refer to elicitors, toxins, phytohormones and enzymes but for phytoplasmas it denotes a protein that is secreted from the phytoplasmas into the host cell to facilitate pathogen colonization (Rashid *et al.*, 2018). After infection, the pathogen effectors may also have a role in making the host plants more suitable for insect interactions such as by making them produce the sesquiterpene β-caryphyllene or changing the organic volatile compounds, or changing the colour of the plant to attract the psyllid for feeding and egg laying so that acquisition of the pathogen by the vector can be enhanced. Furthermore, phytoplasma effectors can change plant development to enhance proliferation of axillary meristems and delay the vegetative stage of flowering and in other cases the effectors induce increases in vegetative tissues and non-reproductive flower-like structure to extend the period for phytoplasma and insect vector fitness. In addition, effectors have been shown to suppress defences against herbivores (Maclean *et al*., 2011; Wei *et al*., 2013; Chang *et al*., 2019).

Effectors from phytoplasmas have been identified as SecA-secreted proteins, and this was initially done using whole genome sequences and prediction programs in aster yellows, where the effectors were given the name Secreted AY-WB Proteins (SAPs). The PIPELINE program was used for identifying secreted proteins in the AY-WB genome and the results showed that there

were 56 SAPs for secreted proteins and 20 SAPs for secreted membrane proteins (Bai *et al*., 2009). The expression of SAP genes are different in the plant compared to the insect; for example, SAP36 is only highly-expressed in insects whilst SAP27 is especially highly expressed in plants. Interestingly, there are two SAP genes which have been shown to change plant morphology; SAP11 and SAP54 (which is related to Tengu from the Onion yellows phytoplasma) (Sugio and Hogenhout, 2012).

The SAP effectors induce morphological and physiological changes; for example, some effectors induce witches' broom or affect leaf shapes whilst others modify plant-insect interaction. The Tengu effector protein from Onion yellows strain mild (OY-M) induces witches' broom symptom, whilst SAP11 and SAP54, found in AY-WB, induce witches' broom symptom, stunting and large numbers of axillary shoots. Meanwhile, PHYLLOGEN found in OY-M and PnWB induces phyllody by flower development destabilisation (Sugio *et al*., 2011b, Sugio and Hogenhout, 2012, Sugawara *et al.*, 2013; Oshima *et al*., 2013).

In the case of $SAP11_{AY\text{-}WB}$ -infected plants, it was found that SAP11 targets cell nuclei and that this effector has a NLS (Nuclear Localise Signal) region for this targeting and a TCP (TEOSINTE-BRANCHED, CYCLOIDEA, PROLIFRATION FACTOR1 AND 2), binding region (Bai *et al*., 2009). The TCP which is unique in kingdom Plantae is a family of transcription factors and there are two subgroups, which are the CIN and TB/CYC subgroups. In

Arabidopsis, CIN consists of eight genes (*TCP2, TCP3, TCP4, TCP5, TCP10, TCP13, TCP17* and *TCP24*) that regulate leaf development, leaf shape, spatial-temporal expression patterns in the leaf primordia, flower development including flowering time and moreover, this subclass control the *LOX2* gene (*LIPOXYGENASE2*) which is involved with jasmonic acid biosynthesis (*JA*) for plant maturation and senescence. Destabilisation of CIN-TPCs by SAP11 down-regulates *LOX2* and *JA* biosynthesis and then the infected plants exhibit senescence and changed leaf shape (Figure 1.12) (Sugio *et al.*, 2011a, Sugio *et al*., 2014b; Chang *et al*., 2018). In addition, JA controls plant pathogen infection against herbivores and tolerance to abiotic stresses including controlling plant development such as root growth, stamen and flower development and leaf senescence (Huang *et al*., 2017).

The TB/CYC subgroup of TCPs consists of three genes in *Arabidopsis* (*TCP1, TCP12* and *TCP18*) which are involved in axillary meristem development (Manassero *et al*., 2013, Chang *et al*., 2018, Suigo *et al*., 2014, Tan *et al.*, 2016, Janik *et al*., 2017; Sarvepalli and Nath, 2018)

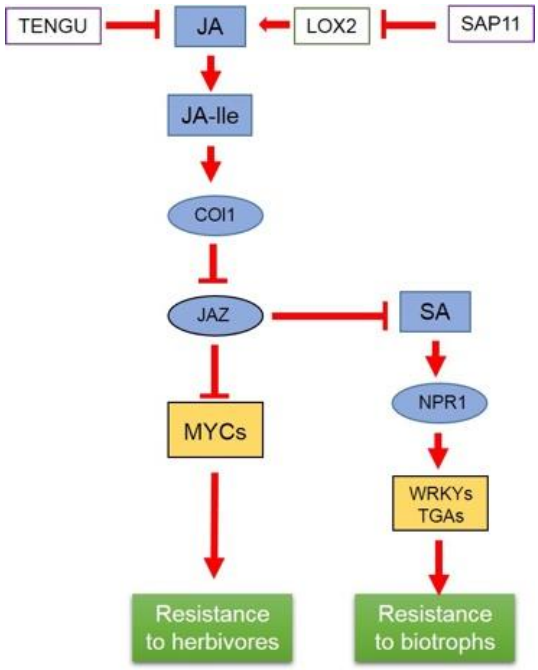


Figure 1.12 A model for Tengu and SAP11 effectors inhibiting LOX2, JA and SA genes (Ma and Ma, 2016).

In addition, Tengu (tengu-su inducer) virulence factors have been shown to cause witches' broom and dwarfism in onion yellows infected plants in Japan. This effector was identified from OY-M as a 4.5 kDa protein (Hoshi *et al*., 2009) and the *Tengu* gene was transformed into *Nicotiana benthamiana* to observe the effect of this gene. The result showed witches' broom and dwarfism, which was the same as occurred in transgenic *Arabidopsis thaliana*. Additionally, the results suggested that the Tengu effector inhibited auxin-related pathways for plant development (Figure 1.13). Multiple genes of auxin-related pathways responded to Tengu and were down regulated when plants were infected with the phytoplasmas (Figure 1.14) (Hoshi *et al*., 2009; Minato *et al*., 2014).

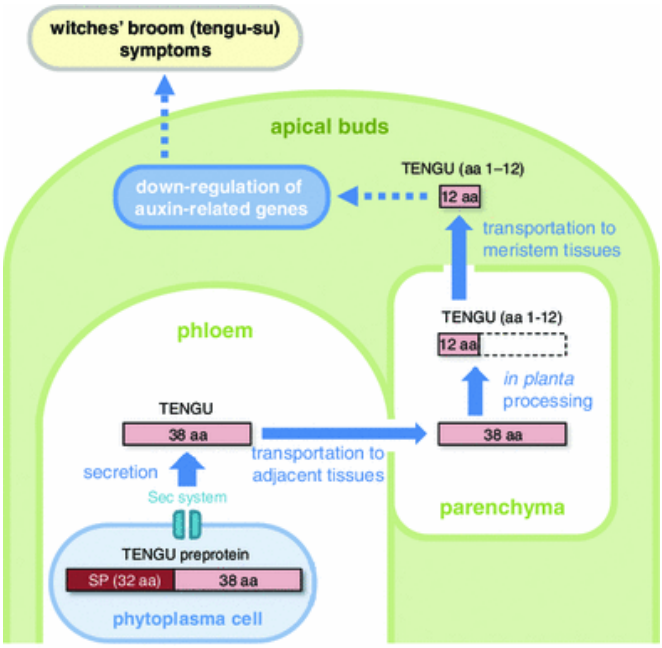


Figure 1.13 The mechanism of Tengu induced witches' broom via auxin down-regulation (Maejima *et al*., 2014).

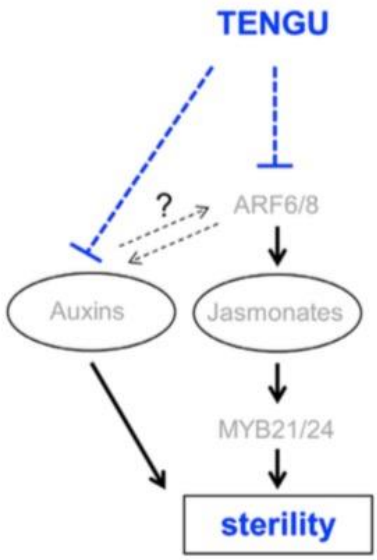


Figure 1.14 A model for Tengu reduced levels of JA and auxin on each part of the floral maturation pathway (Minato *et al*., 2014).

SAP54 is another effector causing malfunction of flower development. The floral organs are controlled by the MADS box homeotic transcription factor family. The $SAP54_{AY\text{-}WB}$ protein is 14 kDa and has a signal peptide for secretion and destabilises MADS box proteins so that infected plants have changes to green leaf-like flowers, form flowers within flowers and are sterile. SAP54 interacts with members of MTF (MADS-domain Transcription Factor) especially AP1 (APETALA1). AP1 regulates gene expression of flower meristems. SAP54 binds with the Keratin-like domain (K) of AP1 and destabilises this domain as a result of which MTF is degraded. Furthermore, it was found that insects lack the K domain so phytoplasmas can colonize many organs of insects (MacLean *et al*., 2011; 2014; Liu *et al.*, 2015; Yang *et al*., 2015). Furthermore, there is a *Phyllogen* gene (*PHYL1*) which is an ortholog gene of *SAP54* found in the OY-M and PnWB phytoplasmas. The *PHYL1* gene interacts with MADS domains and also results in malfunction of flower development (Figure 1.15) (Maejima *et al.*, 2014b; Hu *et al.*, 2015; Kitazawa *et al.*, 2017)

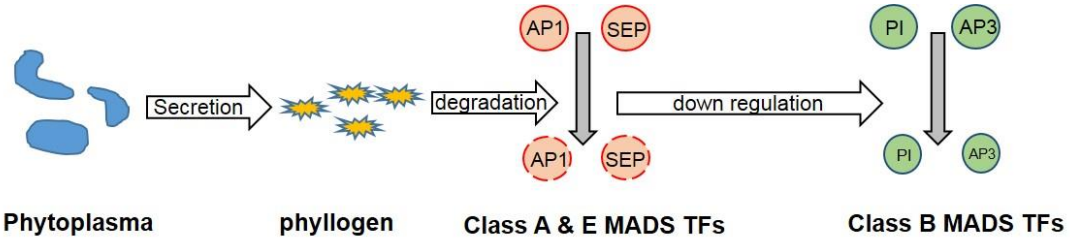


Figure 1.15 A model for PHYLLOGEN effector destabilised MADS domain (Maejima *et al*., 2014).

Phytoplasma effectors from the 16SrI type phytoplasmas have been shown to often lie on mobile elements called Potential Mobile Units (PMUs) or Sequence-Variable Mosaics (SVMs) within the phytoplasma genome, which are conserved-gene clusters with repeated sequences at the borders and several core genes such as DNA recombination and replication and transposases genes (Chung *et al*., 2013). For example, the AY-WB PMU1 is more than 20 Kb in size and consists of conserved sequences of DNA replication (*ssb, dnaB and dnaG*), recombination (*himA*) and synthesis protein (*tmk*), and includes the *tra5* gene which encodes for a putative transposase enzyme for horizontal mobilization (Dickinson, 2010, Toruño, 2010, Hogenhout *et al*., 2011). Moreover, PMUs contain the effectors genes such as *SAP36*, which lies on PMU1 or *SAP11* which lies on the SAP11 PMU-like region of AY-WB (Hogenhout and Loria, 2008) as shown in Figure 1.16. Interestingly, PMUs appear to be unique for phytoplasmas and are not found in other Mollicutes such as *Acholeplasmas* (Ku *et al*., 2013) and there are numerous copies of PMUs and PMU-like clusters in many phytoplasma genomes (Hogenhout and Loria, 2008), although how common these are in phytoplasmas outside the 16SrI and 16SrXII type sequenced so far, is unclear.



Figure 1.16 Position of SAP11 (red arrow) on SAP11 PMU-like region in the AY-WB chromosome (Sugio and Hogenhout, 2012).

In addition, PMUs appear to come in two forms; linear form (L-PMU) and circular extrachromosomal form (C-PMU), and the expression ratio of the two PMU forms depend on host type (Dickinson, 2010, Ku *et al*., 2013). In insects, the amount of the C-PMU is higher than the L-PMU in that C-PMU has self-replication and as a result, gene expression on the PMU in insect hosts is higher than plant hosts. Furthermore, PMUs appear to be able to re-integrate into phytoplasma genomes, since PMUs contain the *tra5* gene and PMUs may also be involved in horizontal gene transfer between phytoplasmas (Dickinson, 2010; Ku *et al*., 2013). The PMU re-insertion presumably rearranges gene clusters and contribute to genome instability (Figure 1.17) (Dickinson, 2010). Consequently, two characteristics of PMUs possibly relate to ecology and evolution of phytoplasma genomes (Chung *et al*., 2013).

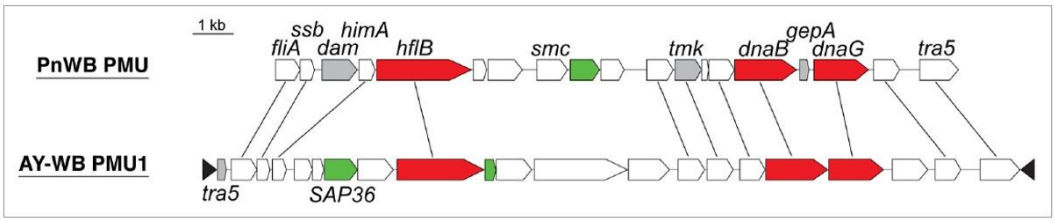


Figure 1.17 Homologous genes between PnWB PMU and AY-WB PMU1 (Ku *et al*., 2013).

As stated above, the effector genes often lie on PMUs for secretion into the host cell and these effectors are secreted via the SecA-dependent pathway (phytoplasmas lack genes for Type-III or Type-IV secretory systems), which

requires an N-terminal signal peptide for recognition, which is taken off before secretion (Kakizawa *et al*., 2004; Sugio *et al*., 2011). The genome of phytoplasmas have the minimal set of genes that are necessary for the function of a Sec-dependent protein translocation pathway such as SecA, SecE and SecY (Maejima, 2014).

1.5 Protein secretion pathway

Sec pathway

The Sec protein translocation pathway is essential for Gram positive bacteria to secrete various proteins for example toxic proteins, adhesins and hydrolytic enzymes. Additionally, phytoplasmas have the YidC system for membrane-protein synthesis. The *YidC* gene works together with Sec translocase to insert sec-dependent substrate proteins into hydrophobic bilayer (Dalbey and Kuhn, 2000; Serek *et al*., 2004).

The two systems of the Sec pathway require N-terminal signal peptide (SP) for secretion of proteins and the Sec system recognizes the signal peptide sequence and cleaves them using a signal peptidase before translocation via the SecYEG translocon into host cells (Kakizawa *et al*., 2004). The two systems are the cotranslational export mode and posttranslational mode. In the cotranslational mode, the pre-protein is a highly hydrophobic signal peptide that is recognised by the signal recognition particle (SRP), and SRP is synthesised by the ribosome. Then, there is a membrane-associated SRP

receptor (FtsY) that attaches with the pre-protein and subsequently takes SRP and SP off by signal peptidase before secretion via the SecYEG translocon.

In the posttranslational mode, the pre-protein is a less hydrophobic signal peptide than the other mode. In this mode, there are posttranslationally interacting proteins (PiPs) such as SecB binding pre-protein to maintain them in unfolded form and then SecB delivers the protein to SecA attaching to the SecYEG translocon. The protein passes through a pore of SecA requiring ATPase activity to transfer the protein to the periplasm via SecYEG translocation pore and after that the signal peptide is taken off by signal peptidase and the mature protein is released into the periplasm (Figure 1.18) (Tsirigotaki *et al*., 2017).

Furthermore, there is the twin-arginine translocation (Tat) pathway found in Gram-positive bacteria as well as Gram-negative bacteria. This pathway requires the twin-arginine pair, which is present in signal peptides. In the Tat system, the pre-protein is folded in the cytoplasm and binds to TatB and TatC. After that, TatA loads the protein to the periplasm and signal peptidase snips the signal protein off (Figure 1.18) (Freudl, 2018).

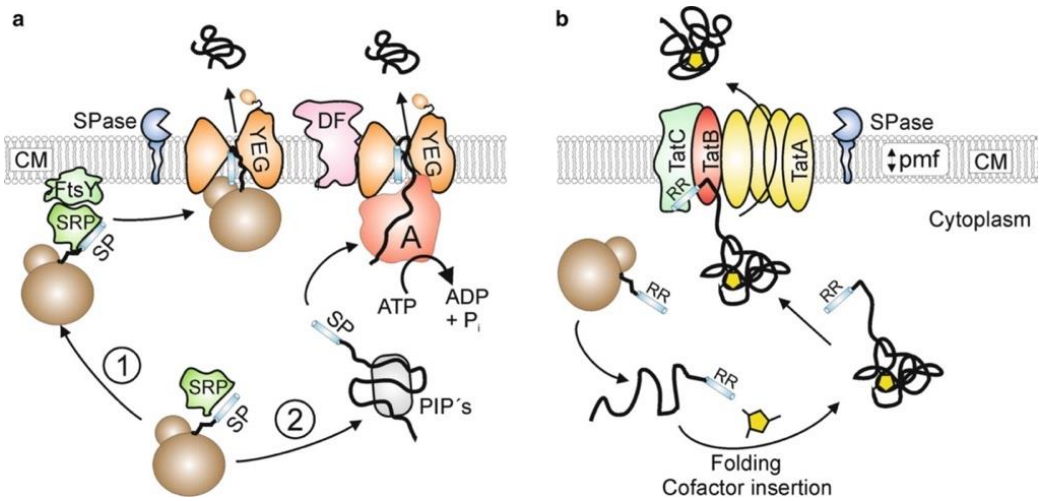


Figure 1. 18 Two major Gram-positive bacterial export pathways; (a) the general Secretion (Sec) protein export pathway and (b) the twin-arginine translocation (Tat) protein export pathway (Freudl, 2018).

Research aims and objectives

The Aims of this thesis focus on two areas of phytoplasma study.

The first aim, covered in chapter 2, involves the classification of the phytoplasmas infecting gramineous plants, especially sugarcane white leaf and sugarcane grassy shoot and aims to determine whether the phytoplasmas causing the two types of symptoms are the same or different phytoplasmas in order to classify the group or subgroup of sugarcane phytoplasma. The analysis method used the MLST technique that required non-ribosomal primers for classification.

The second aim, covered in subsequent chapters is to focus on the cloning and identification of specific effectors from a range of phytoplasmas, and in particular those from gramineous hosts including Napier grass stunt disease (NGSD) and sugarcane white leaf (SCWL) phytoplasmas, using bioinformatics techniques and identification of signal peptide sequences from Napier grass stunt genomic sequences to analyse secreted proteins that the phytoplasmas may use to affect the plant host.

The third aim was then to focus on amplification and cloning these effector genes from NGSD and SCWL and those obtained from other host plants that are held in the University of Nottingham collection and transformation of these

genes into model plants including *Arabidopsis* and *Brachypodium*, The aim was then to determine which effectors from NGSD and SCWL are responsible for the typical Napier grass and sugarcane phytoplasma symptoms of dwarfism and white leaf and other symptoms whilst the other effectors were studied to determine other effects on plant development. Work has been undertaken to examine the effect of these effector proteins in plant development, plant morphology and plant gene expression.

Chapter 2: Multilocus Sequence Typing of sugarcane white leaf and sugarcane grassy shoot

2.1 Introduction

Phytoplasma taxonomy has been based on nucleic acid-based assays since the 1990s, with techniques developed to detect and identify phytoplasmas based on the 16S rRNA gene, such as nested-PCR and PCR/RFLP (Arnaud *et al*., 2007; Li *et al*., 2013). However, the 16S rRNA is often inadequate for closely related phytoplasma strains because it is a highly conserved sequence; for example, it would classify phytoplasma strains sharing 16S rRNA sequence similarity of more than 97.5% into the same group (Li *et al*., 2014).

Fine tuning of strain classifications has therefore been achieved by combining 16S rRNA sequences with others, such as *rp*, *tuf*, *secY* and *secA* gene fragments (Duduk and Bertaccini, 2011; Li *et al*., 2014). This technique, defined as Multilocus Sequence Typing (MLST) has been widely used in prokaryotes and uses various genes which are non-ribosomal DNA for classification and each gene has a different level of evolution. In phytoplasmas it has been used in particular within the 16SrI, 16SrII, 16SrV and 16SrXI groups (Arnaud *et al.*, 2007, Li *et al.*, 2014, Abeysinghe *et al.,* 2016)

Phytoplasmas of gramineous plants have mainly been classified into the 16SrXI '*Candidatus* Phytoplasma *oryzae*' group, which includes Rice yellow dwarf (RYD) and phytoplasmas infecting sugarcane and napier grass. The closely related Bermuda grass white leaf strains have been classified into the 16SrXIV group.

Sugarcane diseases caused by phytoplasmas are a major problem in Asia and Australia. Significant sugarcane phytoplasma diseases in south and south-east Asia are sugarcane white leaf (SCWL), sugarcane grassy shoot (SCGS) and sugarcane yellow leaf (YLS) (Abeysinghe *et al*., 2016). The SCWL symptoms are leaf chlorosis and leaves that are smaller and narrower than wild type, whilst SCGS produces large numbers of tillers and develops into witches' broom symptoms. YLS shows yellow leaves and yellow midribs but the lamina is still green (Gaura *et al*., 2008). To date, there have been different results in the classifications of SCWL and SCGS. In Thailand, the two diseases were classified into two different phytoplasmas based on 16S rRNA (Wongkaew *et al*., 1997), whilst in India and China they were shown to belong to the same group based on the 16S-23S intergenic region (Nasare *et al*., 2007, Li *et al*., 2014; Wang *et al*., 2014). However, In 2017 SCGS phytoplasma strain SC-Phy38 found in India was classified into the 16SrXI-F subgroup based on 16S rRNA (Yadav *et al*., 2016).

The aim of this chapter has been to fine-tune the classification of the gramineous phytoplasmas, especially sugarcane white leaf and sugarcane grassy shoot, using the MLST technique and phylogenetic analysis by neighbour-joining in MEGA X program (www.megasoftware.net), to determine whether the phytoplasmas causing the two types of symptoms are the same or different phytoplasmas.

2.2 Materials and Methods

2.2.1 DNA extraction

Bermuda grass white leaf (BGWL) from Malaysia, sugarcane white leaf (SCWL) from Thailand, Vietnam, India and Sri Lanka, sugarcane grassy shoot (SCGS) from Vietnam and Sri Lanka (Table 2.1) were used for genomic DNA extraction by the 2 x CTAB method (20 ml 1 M Tris-HCl pH 8.0, 56 ml 5 M NaCl, 16 ml 0.5 M EDTA, 4.0 g CTAB powder, 4.0 g PVP40 and 0.2% β-mercaptoethanol). Each sample of phytoplasma infected leaves was extracted with 2 ml CTAB extraction buffer and homogenized at room temperature. After that, 800 μl of supernatant was transfer into a 1.5 ml new tube and incubated at 65°C for 30 min after which 500 μl of phenol: chloroform (Sigma-Aldrich Co., UK) was added into each tube and vortexed vigorously and centrifuged at 6000 x g for 10 min at 4°C. The supernatant was transfer into a new tube and 600 μl of isopropanol was added and mixed gently and then samples were incubated at -20°C for at least 2 hours. Tubes were then centrifuged at 16,000 x g for 15 min at 4°C, the supernatant was discarded and the pellet was

washed with 500 μl of 70% ethanol (V/V) and centrifuged for 1 min. The supernatant was discarded and the pellet was dried at room temperature for 1.5-2 hours. Subsequently, the pellet was dissolved with TE buffer (Sigma-Aldrich Co., UK) and then the concentrations of the genomic DNAs were measured by NanoDrop2000 Spectrophotometer (ThermoFisher Scientific Inc., UK), making the dilution to 50 ng/μl and stored at -20°C until required.

Table 2.1 Phytoplasma strains examined in this study

Phytoplasma strain	Abbreviation	Geographic origin	Notes on origin of sample
Napier Grass stunt Disease	NGSD	Kenya	*Pennisetum purpureum* plant in UoN collection; original isolation from Kenya
Sugarcane white leaf 1	SCWLTh1	Thailand	Plant material sampled from Lopburi, Thailand, 2019
Sugarcane white leaf 2	SCWLTh2	Thailand	Plant material sampled from Lopburi, Thailand, 2019
Sugarcane white leaf 1	SCWLVN1	Vietnam	Plant material sampled from near Ho Chi Minh City, 2018
Sugarcane white leaf 2	SCWLVN2	Vietnam	Plant material sampled from near Pleiku, 2018
Sugarcane white leaf 3	SCWLVN3	Vietnam	Plant material sampled from near Pleiku, 2018
Sugarcane white leaf 4	SCWLVN4	Vietnam	Plant material sampled from near Pleiku, 2018

Sugarcane white leaf 5	SCWLVN5	Vietnam	Plant material sampled from near Pleiku, 2018
Sugarcane white leaf 6	SCWLVN6	Vietnam	Plant material sampled from near Pleiku, 2018
Sugarcane white leaf 7	SCWLVN7	Vietnam	Plant material sampled from near Pleiku, 2018
Sugarcane white leaf 8	SCWLVN8	Vietnam	Plant material sampled from near Pleiku, 2018
Sugarcane white leaf 9	SCWLVN9	Vietnam	Plant material sampled from near Pleiku, 2018
Sugarcane white leaf 15	SCWLVN15	Vietnam	Plant material sampled from near Pleiku, 2018
Sugarcane white leaf 21	SCWLVN21	Vietnam	Plant material sampled from near Pleiku, 2018
Sugarcane white leaf Heat Treated	SCWLVN	Vietnam	Plant material sampled from near Nghe An, 2018
Sugarcane white leaf	SCWLIndia	India	Sample provided by Dr Govind Rao, 2019
Sugarcane white leaf 1	SCWLSLK1	Sri Lanka	Plant material sampled from Uva Province, Sri Lanka, 2011
Sugarcane white leaf 2	SCWLSLK2	Sri Lanka	Plant material sampled from Udawalawe, Sri Lanka, 2013
Sugarcane white leaf 3	SCWLSLK3	Sri Lanka	Plant material sampled from Udawalawe, Sri Lanka, 2013
Sugarcane grassy shoot 1	SCGSSLK1	Sri Lanka	Plant material sampled from Eastern Province, Sri Lanka, 2011

Sugarcane grassy shoot 2	SCGSSLK2	Sri Lanka	Plant material sampled from Udawalawe, Sri Lanka, 2013
Sugarcane grassy shoot 3	SCGSSLK3	Sri Lanka	Plant material sampled from Udawalawe, Sri Lanka, 2013
Sugarcane grassy shoot 1	SCGSVN1	Vietnam	Plant material sampled from Nghe An Province, 2018
Sugarcane grassy shoot 2	SCGSVN2	Vietnam	Plant material sampled from Nghe An Province, 2018
Bermudagrass white leaf 1	BGWL1	Malaysia	Plant material sampled from Putrajaya, 2008
Bermudagrass white leaf 2	BGWL2	Malaysia	Plant material sampled from Putrajaya, 2008
Bermudagrass white leaf 3	BGWL3	Malaysia	Plant material sampled from Putrajaya, 2008
Bermudagrass white leaf 1	BGWLVN1	Vietnam	Plant material sampled from near Ho Chi Minh City, 2019
Bermudagrass white leaf 2	BGWLVN2	Vietnam	Plant material sampled from near Ho Chi Minh City, 2019
Bermudagrass white leaf 9	BGWLVN9	Vietnam	Plant material sampled from near Ho Chi Minh City, 2019
Periwinkle			*Catharanthus rosea* plant in UoN collection
Napeir Grass			*Pennisetum purpureum* plant in UoN collection

2.2.2 Phytoplasma preliminary tests

The genomic DNAs from phytoplasma infected leaves and uninfected Napier grass plants were screened in a preliminary study by PCR with primers P1/P7 in the first round, and the PCR product was diluted 1/40 for second round PCR with primers R16mF2/ R16mR1 (Figure 2.1 and Table 2.2). The PCR reactions were performed using 1 x concentration of MangoMix® (Bioline, UK), 1 μl of genomic DNA, 1 μl of 10 mM of each primer and the total volume was 25 μl. The PCR thermal cycling program was: denaturation at 95°C for 5 min for 1 cycle and the denaturation at 95°C for 40 sec, annealing at 50°C for 40 sec, extension at 72°C for 1 min for 30 cycles and extension at 72°C for 10 min for one cycle. After PCR, 5 μl of PCR samples were electrophoresed on 1.5% agarose gels containing gel red stain (Biotium, USA).

Table 2.2 Nucleotide primers for phytoplasma detection

Primer name	Primer sequences (5′-3′)	references
P1 forward	GTCGTAACAAGGTATCCCTACCGG	Hanboonsong *et al.,*2002
P7 reverse	CGTCCTTCATCGGCTCTT	Smart *et al.,* 1996
R16mF2 forward	GAACGACTGTAAGACTGG	Lee *et al.,* 1993
R16mR1 reverse	TGACGGGCGGTGTGAVAAACCCCG	

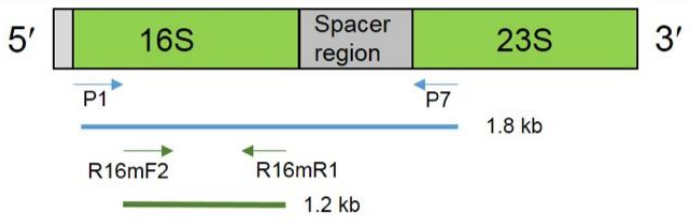


Figure 2.1 Schematic diagram of primer positions for phytoplasma detection of the 16S rRNA by the PCR method (Mannan *et al*., 2010).

2.2.3 Multilocus Sequence Typing analysis

To undertake the MLST analysis, a number of different sets of primers were designed. The strategy used was to take the napier grass stunt draft genomic sequence and identify a number of genes of >1 kb in length and then find the sequences of the equivalent genes in the Aster yellows witches' broom and apple proliferation phytoplasmas. Regions of close similarity were then identified and used to design primers in the hope that these would also work on phytoplasmas from other phylogenetic groups, including the Sugarcane white leaf and Bermuda grass white leaf groups. This strategy was used to obtain primers for the *ser* (serine tRNA ligase), *50S* (50S ribosomal protein), *pep* (peptide chain release factor 1), *gro* (chaperonin GroEL), *lpd* (dihydrolipoamide dehydrogenase), *gyrB* (DNA gyrase B subunit) and *asp* (aspartate tRNA ligase) genes. For *secA,* the primers published in Hodgetts *et al.* (2008) were used, whilst for the *EF2* and *EF7* sequences, the primers identified for the effector sequences discussed in Chapter 3 were used.

Phytoplasma genomic DNAs were subsequently amplified with primers for these non-ribosomal genes (Table 2.3). The PCR reactions were performed using 1 x concentration of MangoMix®, 1 μl of genomic DNA, 1 μl of 10 mM of each primer and the total volume was 25 μl. For the sec primers, the PCR thermal cycling program was: denature at 95°C for 10 min for 1 cycle and then denature at 95°C for 30 sec, annealing at 38°C for 45 sec, extension at 72°C for 1.30 min for 30 cycles and extension at 72°C for 10 min for one cycle. For the other primers, the cycle condition were as above but the annealing was 55°C for *EF2*, 50°C for *EF7*, 45°C for *50S* gene, 42°C for *lpd* gene, 40°C for *ser*, *gro* and *gryB* genes and 35°C for the *asp* and *pep* genes.

For the *ser* primer conditions, Serfor1 and SerRev2 were used for the first round PCR and a 1/40 μl dilution made for the second-round template and the second-round primers were Serfor2 and SerRev2. For the 50S gene, 50Sfor1 and 50Srev1 were used for the first round and a 1/40 μl dilution made for the second-round template and the second-round primers were 50Sfor2 and 50Srev1; a similar approach was used for *asp*. For the *gro* primers, the Grorev2 was the main primer for the first to the third round PCR and was used with Grofor1 for the first round PCR, Grofor2 for the second round PCR and Grofor3 for the third round PCR and the primer combinations were done likewise for the *lpd*, *gryB* and *sec* primers. LpdFor2 was the forward primer used for the first round PCR with LpdRev1 and then LpdFor2 was used with LPDRev2 and LpdRev3 for the second round and third round, respectively. For the *GryB* gene, GrybFor2 was the forward primer for the first round PCR

with GrybRev1 and then GrybFor2 was used with Grybrev2 and Grybrev3 for the second round and third round, respectively. SecAfor5 was the forward primer for PCR with SecArev3 and for the second round PCR SecAfor5 was used with SecArev2. For the *pep* primers, these primers were used in two rounds of PCR before gel electrophoresis.

After that, the PCR products were analysed on 1% agarose gels containing 10 μg/μl gel red stain. Subsequently, the PCR products were purified with GenElute™Gel Extraction Kit (Sigma-Aldrich Co., UK) following the manufacturer's instruction and then purified PCR products were sent for sequencing with specific forward and reverse primers for each gene by Eurofins Company (Ebersberg, UK).

Table 2.3 MLST analysis primers used in this study

Gene	Primer	Sequences (5'-3')
Ser	Serfor1	TACCKAATWTACCWCATG
	Serrev1	GTTCTKCCTAYAGCTAAAGC
	Serfor2	TGAAASARATGGGAGC
	Serrev2	CMGMATTACTAATAGARGC
50S	50Sfor1	CCTACATCWAAYGGRCATCG
	50Srev1	TACCCCAMGGMGTCATAGG
	50Sfor2	AGACATCGYGGMGGWGG
Pep	pepfor	TTAAAGGWGCSGCTGGAGG
	peprev	CGCTTCTTTCKCCTYTKCCG
Gro	Grofor1	ACWTTAGGWCCWAARGG
	Grofor2	ACTACWGCAACTGTTTTAGC
	Grorev2	AGMTTTWCCWCCACCWAC
	Grofor3	GCTCCAGGWTTCGGWGAT
Lpd	Lpdrev1	GGAAAACCATAAACACAAGAAGG
	Lpdfor2	CARTTAGGWGCTAAAGTAGC
	Lpdrev2	CRCCAATAGCATAAACTCC
	Lpdfor3	GCTACTGGTTCTAGTGC
GryB	Grybrev1	GTTCTGGATTCATTCWGG
	Grybfor2	AGATGAAGCWTTAGCTGG
	Grybrev2	CGTCCATCAACATCTGATC
	Grybfor3	AYACTTTRCACGCAGGAGG
Asp	Aspfor1	GCTTTACCTCAATCACC
	Asprev1	CGATCTAACCCTAAAGC
	Aspfor2	TGCTCGTTGTTTTAGAG
Sec	SecAfor5	ASTCGTGAAGCTGAAGG + AGCTAAAAGAGAATTTGAAGG
	SecArev3	GTTTTRGCAGTTCCTGTCATNCC
	SecArev2	CCNTCRCTAAATTGNCGTCC
EF2 gene (Chapter3)	EF2_F	AAGTCAACAATTGGAGTTATGGACGCTTA
	EF2_R	TGTTTTAGTTTTTTGATGTTCTTTTTTTTCTTTTCTT
EF7 gene (Chapter3)	EF7_F	ATGATGCAAATAAAAAATAAATTAT
	EF7_R	TTATTTTTTAGAATCATCAGGCTTTTT

2.2.4 Non ribosomal gene analysis

Nucleotide sequences from PCR products were analysed online using the www.ncbi.nlm.nih.gov/blastx website for primary checking of similarity and then reverse nucleotide sequences from each gene were converted to reverse-complementary strand with the http://reverse-complement.com/ online program and then forward nucleotide sequences and reverse nucleotide sequences were assembled together via CAP3 program (http://www.insilico.uni-duesseldorf.de/Cap3.html). Sequences were then aligned by ClustalW program (Bioedit program). Subsequently, phylogenetic trees were constructed using neighbour-joining in MEGA X program (www.megasoftware.net). The bootstrap value was performed with 1000 replicates to estimate the stability of nodes and to support the inferred clusters and clusters such the bootstrap values of 50-74% represent weak support, 75-84% moderate support and 85-100% strong support (Richardson *et al*., 2000)

2.3 Results

2.3.1 Preliminary tests to confirm presence of phytoplasmas with 16Sr primers

The preliminary result confirm that the thirty phytoplasma infected plants in Table 2.1 were infected and showed PCR products of 1.2 kb (Figure 2.2), and confirm that the non-infected Napier grass and healthy periwinkle did not generate phytoplasma PCR products (negative control).

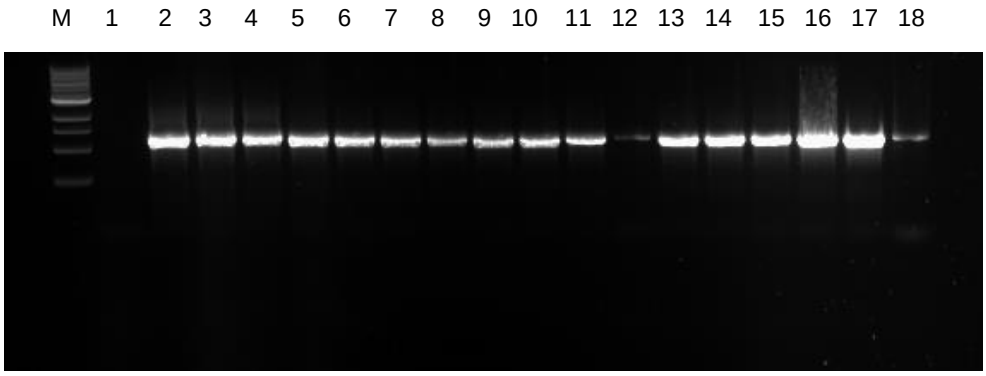


Figure 2.2 Phytoplasma infected plants showing PCR products from P1/P7 and R16mF2/R16mR1 primers. Lanes: (M) 1 Kb marker, (1) Napier grass, (2) Napier grass stunt disease infected leaves, (3) Sugarcane white leaf from Thailand 1, (4) Sugarcane white leaf from Thailand 2, (5) Sugarcane white leaf from Vietnam, (6) Sugarcane white leaf from India, (7) Sugarcane white leaf from Sri Lanka 1, (8) Sugarcane white leaf from Sri Lanka 2, (9) Sugarcane white leaf from Sri Lanka 3, (10) Sugarcane grassy shoot from Sri Lanka 1, (11) Sugarcane grassy shoot from Sri Lanka 2, (12) Sugarcane grassy shoot from Sri Lanka 3, (14) Sugarcane grassy shoot from Vietnam 1, (15) Sugarcane grassy from Vietnam 2, (16) Bermuda grass white leaf 1, (17) Bermuda grass white leaf 2 and (18) Bermuda grass white leaf 3.

The thirty PCR products with the 16Sr primers were used to construct a phylogenetic tree using the neighbour-joining method and 1000 bootstrap value. The phylogenetic tree (Figure 2.3) showed two clusters for the phytoplasmas causing sugarcane symptoms and BGWLs, whilst NGSD and AY-WB were an outlier and outgroup, respectively. The first sugarcane cluster consisted of sugarcane symptoms; sugarcane white leaf and grassy shoot

samples whilst the second cluster was Bermuda grass white leaf from Malaysia grouped with Vietnam. Since this primer combination could not separate the phytoplasmas that cause sugarcane symptoms, the MLST techniques was used to classify the sugarcane phytoplasmas.

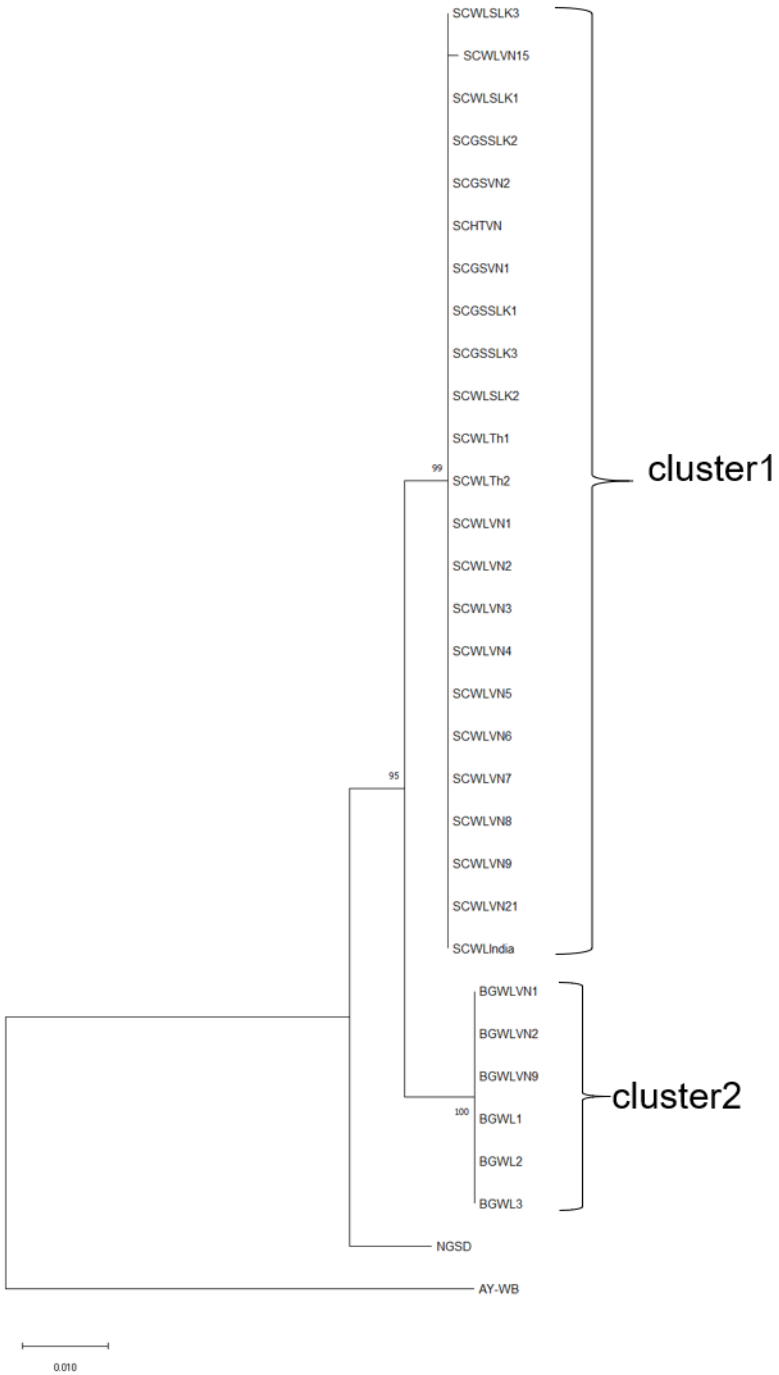


Figure 2.3 Unrooted phylogenetic tree constructed with the neighbour-joining method based on sequences of the 16S rRNA gene with 1000 bootstrap value. The phylogenetic tree shows the relationship among the samples listed in Table 2.1; sugarcane disease, NGSD, BGWL and AY-WB as an outgroup. Branch lengths are proportional to the number of inferred character stated

information, bar = 0.010 substitution per nucleotide position and the bootstrap values are expressed as percentages of 1000 replications.

2.3.2 Multilocus Sequence Typing (MLST) analysis

To determine the relationships between the phytoplasmas, in particular the sugarcane diseases, MLST was performed using the *ser*, *50S*, *pep*, *gro*, *lpd*, *gyrB*, *asp*, *secA*, *EF2* and *EF7* sequences. The result showed genetic variation within the 16SrXI phytoplasma group and between this group and 16SrXIV (Table 2.4).

Table 2.4 Summary of the PCR results for each gene in MLST analysis

Samples	16Sr	50S	asp	gro	gryB	lpd	ser	sec	EF2	EF7	pep
NGSD	√	√	√	√	√	√	√	-	√	√	-
SCWLTh1	√	√	-	-	-	-	-	-	√	√	-
SCWLTh2	√	√	-	-	-	-	-	-	√	-	-
SCWLVN1	√	-	-	-	-	-	-	-	-	-	-
SCWLVN2	√	√	-	-	-	√	-	-	-	-	-
SCWLVN3	√	-	-	-	-	√	-	-	-	-	-
SCWLVN4	√	-	-	√	-	√	-	-	-	-	-
SCWLVN5	√	√	-	√	-	√	-	-	√	-	-
SCWLVN6	√	-	--	√	-	√	-	-	-	√	-
SCWLVN7	√	-	-	√	-	√	-	-	-	-	-
SCWLVN8	√	-	-	√	-	√	√	-	√	√	-

SCWLVN9	√	√	-	√	√	√	√	-		√	-
SCWLVN15	√	-	√	-	√	√	√	-	√	√	-
SCWLVN21	√	-	-	√	√	√	-	-	--	-	-
SCHTVN	√	-	-	√	-	√	-	-	√	-	-
SCWLIndia	√	-	-	-	√	√	-	-	-	√	-
SCWLSLK1	√	√	-	√	-	-	√	-	-	√	-
SCWLSLK2	√	-	-	√	-	√	√	-	√	-	-
SCWLSLK3	√	√	--	√	-	√	√	-	-	-	-
SCGSSLK1	√	-	-	√	√	√	√	√	-	-	-
SCGSSLK2	√	√	√	-	-	-	-	√	-	-	-
SCGSSLK3	√	√	√	√	√	√	√	√	-	√	-
SCGSVN1	√	√	√	√	√	√	√	-	-	-	-
SCGSVN2	√	√	√	-	√	√	-	-	√	-	-
BGWLML1	√	-	-	√	√	√	√	-	√	√	-
BGWLML2	√	-	-	-	√	√	-	-	-	-	-
BGWLML3	√	-	-	-	-	√	√	-	√	-	-
BGWLVN1	√	√	-	-	-	-	-	-	-	-	-
BGWLVN2	√	√	-	-	-	-	-	-	-	-	-
BGWLVN9	√	-	-	√	√	√	√	-	√	√	-
Periwinkle	-	-	-	-	-	-	-	-	-	-	-
Napier grass	-	-	-	-	-	-	-	-	-	-	-

√: PCR product

-: no PCR product

2.3.2.1. Analysis of *50S* gene sequences

Thirty-two samples in Table 2.1 were tested but only seventeen samples gave PCR products. The phylogenetic tree was constructed using Aster yellows witches' broom (AY-WB) as the outgroup (Figure 2.4) and shows NGSD to be an outlier from the other samples and that the BGWLs (cluster2) grouped apart from the sugarcane diseases with a bootstrap value of 67 and the BGWLVN9 clustered with the BGWL strains from Malaysia with a bootstrap value of 98.

For the sugarcane diseases, the samples were grouped into one cluster (cluster1), although three of the SCWL samples from Vietnam formed a subcluster within this. However, the other SCWL from the same region in Vietnam grouped with the other SCWLs from Sri Lanka and Thailand, and with the SCGS samples from all regions, suggesting there is no consistent difference associated with region or symptoms.

The nucleotide and protein sequences (Appendices) showed nucleotide substitutions and deletions in the *50S* region. In particular, the NGSD sequences were shorter than the others.

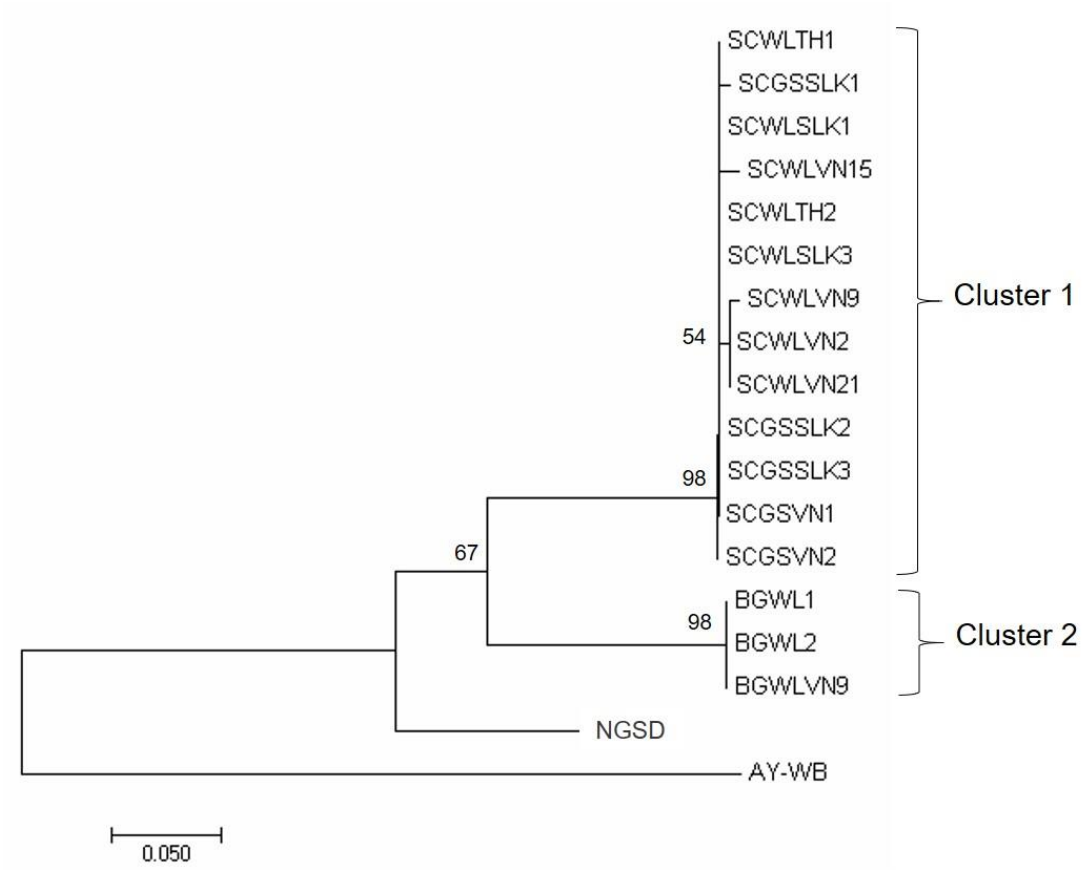


Figure 2.4 Unrooted phylogenetic tree constructed with the neighbour-joining method based on sequences of the 50S gene with 1000 bootstrap value. The phylogenetic tree shows the relationship among the samples listed in Table 2.1; sugarcane disease, NGSD, BGWL and AY-WB as an outgroup. Branch lengths are proportional to the number of inferred character stated information, bar = 0.050 substitution per nucleotide position and the bootstrap values are expressed as percentages of 1000 replications.

2.3.2.2 Analysis of *asp* gene sequences

Thirty-two samples including periwinkle and napier grass healthy plants listed in Table 2.1 were tested with the *asp* primers, but only six gave PCR products

of the expected size. Moreover, the primers could not amplify any BGWL samples. The phylogenetic tree was constructed (Figure 2.5) and the results again show that the NGSD sample was an outlier from the others. Because of the limited number of sugarcane isolates that gave positive PCR products, it was not possible to draw any conclusions about diversity between SCGS and SCWL, or on regional variation, and all the isolates essentially grouped together.

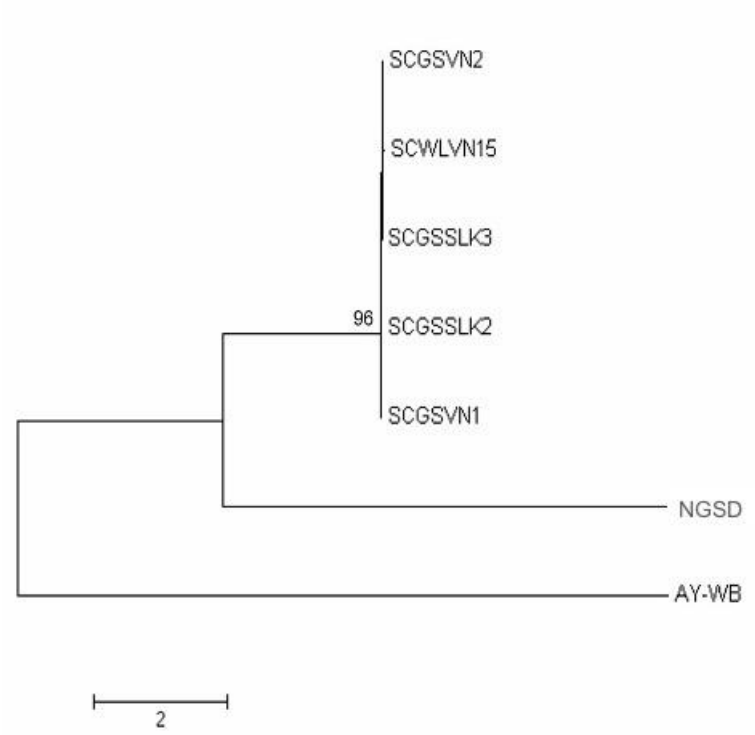


Figure 2.5 Unrooted phylogenetic tree constructed by neighbour-joining method based on sequences of the asp gene with 1000 bootstrap value. The phylogenetic tree shows the relationship among the samples listed in Table 2.1; sugarcane disease, NGSD and AY-WB as an outgroup. Branch lengths are proportional to the number of inferred character stated information, bar = 2 substitution per nucleotide position and the bootstrap values are expressed as percentages of 1000 replications.

2.3.2.3 Analysis of *gro* gene sequences

The primers amplified eighteen samples from thirty-two samples tested in Table 2.1 although there was no PCR product from the Thai SCWLs. The phylogenetic tree was constructed and AY-WB was used as an outgroup (Figure 2.6). The phylogenetic tree separated NGSD as an outlier and there was strong branch support to separate BGWLs (cluster2) from sugarcane samples with a bootstrap value of 95. In terms of sugarcane samples, SCWLIndia (cluster1.4) was distinct from the others with strong branch support (100 bootstrap value). The other cluster consisted of sugarcane diseases broadly grouped by region rather than symptoms, with the Vietnamese samples tending to group together and the Sri Lankan samples grouping together (cluster1.1-1.3). There were however, some exceptions such as SCGSVN1 grouping with the Sri Lankan SCWL samples (cluster1.3). Moreover, the cluster 1.2 containing SCGS from Sri Lanka was closely related to cluster 1.1 with a 68 bootstrap value and was distinct from SCWLSLKs (cluster1.3) with a 60 bootstrap value whilst the SCGSVN1 in cluster 1.3 was distinct from SCWLVNs (cluster1.1) with a 60 bootstrap value.

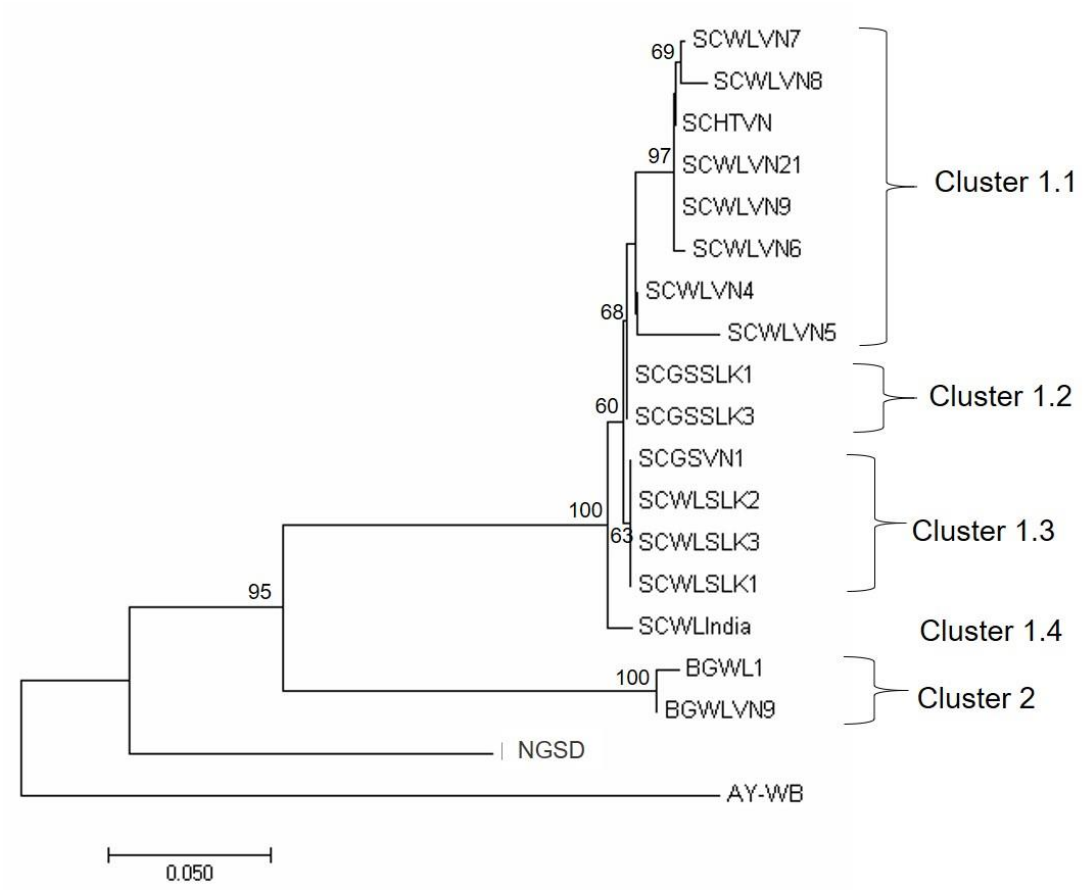


Figure 2.6 Unrooted phylogenetic tree constructed by neighbour-joining method based on sequences of the gro gene with 1000 bootstrap value. The phylogenetic tree shows the relationship among the samples listed in Table 2.1; sugarcane disease, NGSD, BGWL and AY-WB as an outgroup. Branch lengths are proportional to the number of inferred character stated information, bar = 0.050 substitution per nucleotide position and the bootstrap values are expressed as percentages of 1000 replications.

2.3.2.4 Analysis of *gryB* gene sequences

The *gryB* primers amplified twelve samples from the thirty-two tested samples in Table 2.1 but did not amplify the SCWLTh and SCWLSLK samples. The

phylogenetic tree was constructed using AY-WB as an outgroup (Figure 2.7) and again shows NGSD as an outlier and the BGWLs (cluster2) separate from the sugarcane disease samples with strong bootstrap support (85). It is interesting to note that the BGWL samples showed some separation from each other, and as a group, these sequences were a few bases longer than the sugarcane and napier grass sequences. The sugarcane disease samples separated into two clusters (cluster1.1 and 1.2) with 93 bootstrap value. The first cluster (cluster1.1) consisted of the SCGS samples from Sri Lanka and Vietnam along with the SCWL sample from India, whilst the SCWL samples from Vietnam formed the second cluster (cluster1.2). So, this primer might classify sugarcane diseases based on symptoms even though there was SCWLIndia in the cluster.

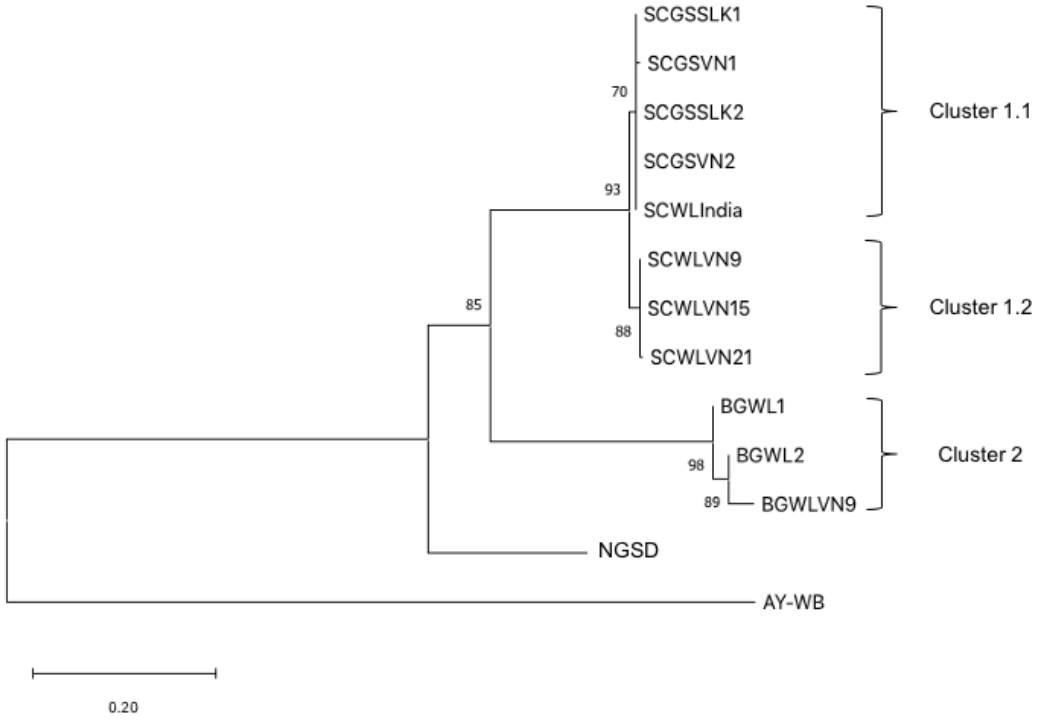


Figure 2.7 Unrooted phylogenetic tree constructed by neighbour-joining method based on sequences of the gryB gene with 1000 bootstrap value. The phylogenetic tree shows the relationship among the samples listed in Table 2.1; sugarcane disease, NGSD, BGWL and AY-WB as an outgroup. Branch lengths are proportional to the number of inferred character stated information, bar = 0.2 substitution per nucleotide position and the bootstrap values are expressed as percentages of 1000 replications.

2.3.2.5 Analysis of *lpd* gene sequences

These primers amplified twenty-five samples from thirty-two samples tested including periwinkle and napier grass healthy plants in Table 2.1 although the SCWLThs did not amplify. The phylogenetic was constructed with AY-WB as

an outgroup and the NGSD sample was an outlier (Figure 2.8). The primers classified the sugarcane symptoms from Vietnam based on symptoms into two clusters; 1.1 and 1.2 even though there were a few SCWLVNs grouped into cluster1.1. For the Sri Lanka samples, SCGSSLKs (red block) grouped together with SCWLSLK and SCWLVN samples in cluster1.1, whilst SCWLSLK1 was in cluster1.2 so there was no consistent organization based on either symptoms or region in sugarcane samples from Sri Lanka. The BGWL samples formed a separate cluster in which the BGWL1 (cluster2.1) was separated from the others (cluster2.2) with a 54 bootstrap value whilst the other BGWLs were grouped in the same subcluster with strong bootstrap value of 98.

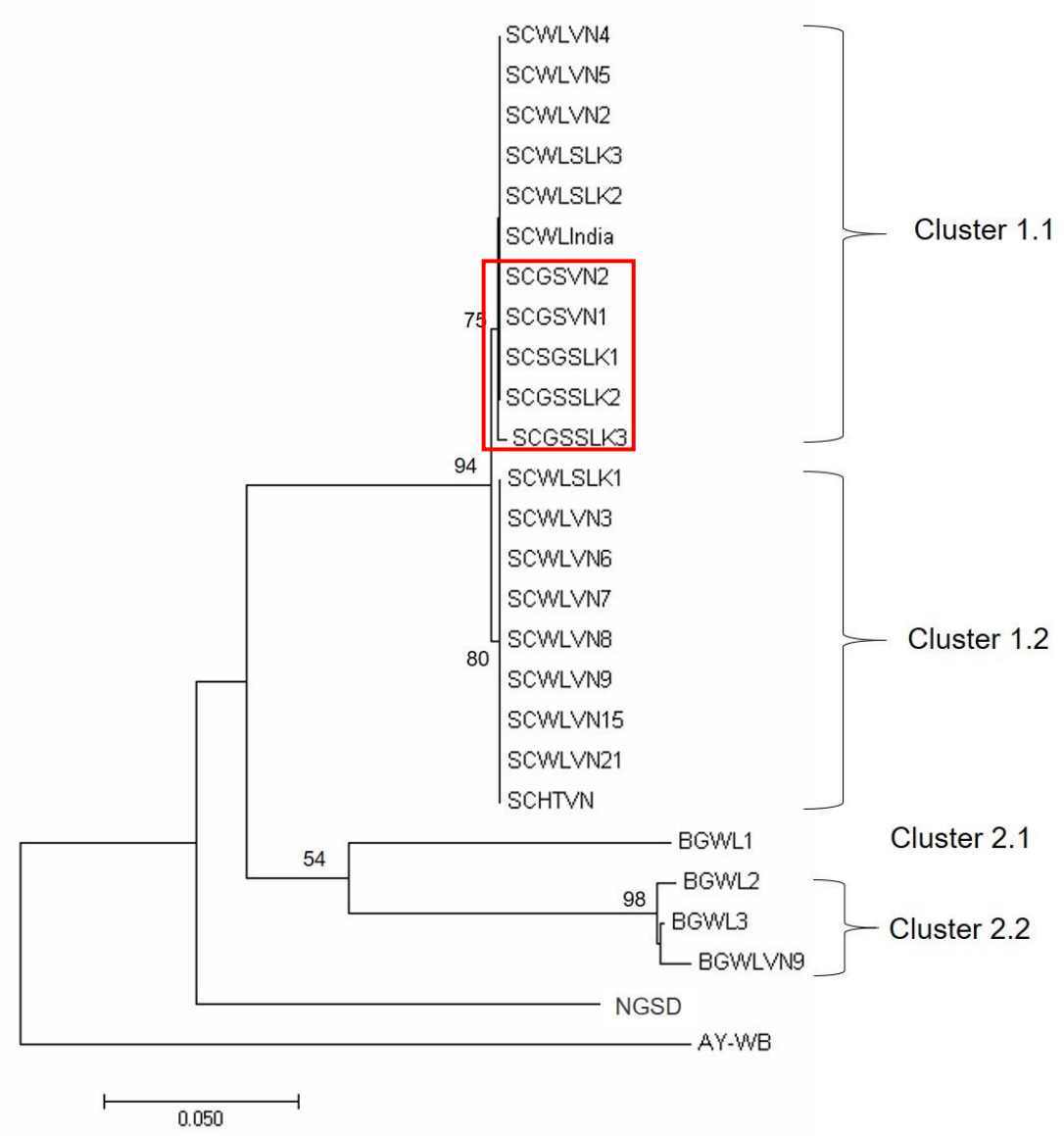


Figure 2.8 Unrooted phylogenetic tree constructed by neighbour-joining method based on sequences of the lpd gene with 1000 bootstrap value. The phylogenetic tree shows the relationship among the samples listed in Table 2.1; sugarcane disease, NGSD, BGWL and AY-WB as an outgroup. Branch lengths are proportional to the number of inferred character stated information, bar = 0.050 substitution per nucleotide position and the bootstrap values are expressed as percentages of 1000 replications.

2.3.2.6 Analysis of *sec* gene sequences

Only three Sri Lanka samples from the thirty-two samples tested in Table 2.1 gave PCR products and the phylogenetic tree was constructed to compare these with previous samples in the NCBI database from the study of Abeysinghe *et al.* (2016) (Figure 2.9). This grouped all the sugarcane samples together and separate from the napier grass stunt and Bermuda grass white leaf samples.

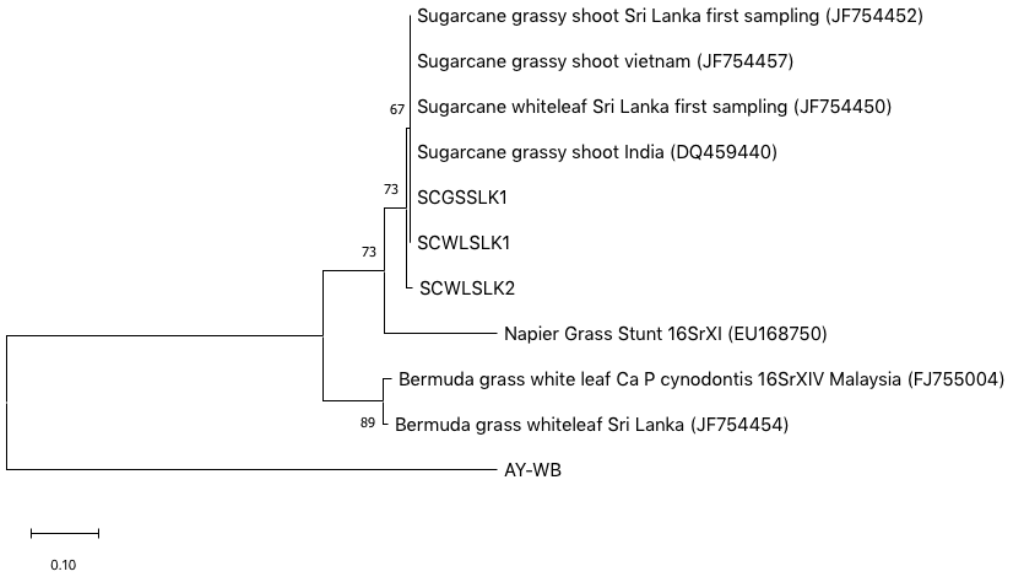


Figure 2.9 Unrooted phylogenetic tree constructed by neighbour-joining method based on sequences of the secA gene with 1000 bootstrap value. The phylogenetic tree shows the relationship among the samples listed in Table 2.1; sugarcane disease, and AY-WB as an outgroup. Branch lengths are proportional to the number of inferred character stated information, bar = 0.1 substitution per nucleotide position and the bootstrap values are expressed as percentages of 1000 replications.

2.3.2.7 Analysis of *ser* gene sequences

The *ser* primers amplified from thirteen out of the thirty-two samples in Table 2.1 although no amplification was obtained from the SCWLTh samples. The phylogenetic tree (Figure 2.10) again classified NGSD as an outlier and separated the BGWLs to cluster2 distinct from the sugarcane samples. For the sugarcane samples, the SCWL samples from Vietnam formed a distinct cluster1.3, whilst the SCGS from Vietnam clustered with the SCWL samples from Sri Lanka (cluster1.1) and with slight separation from the SCGS samples from Sri Lanka (cluster1.2). Based on this region, the Ser primers could classify the symptoms from Sri Lanka and Vietnam with moderate and strong bootstrap values, respectively.

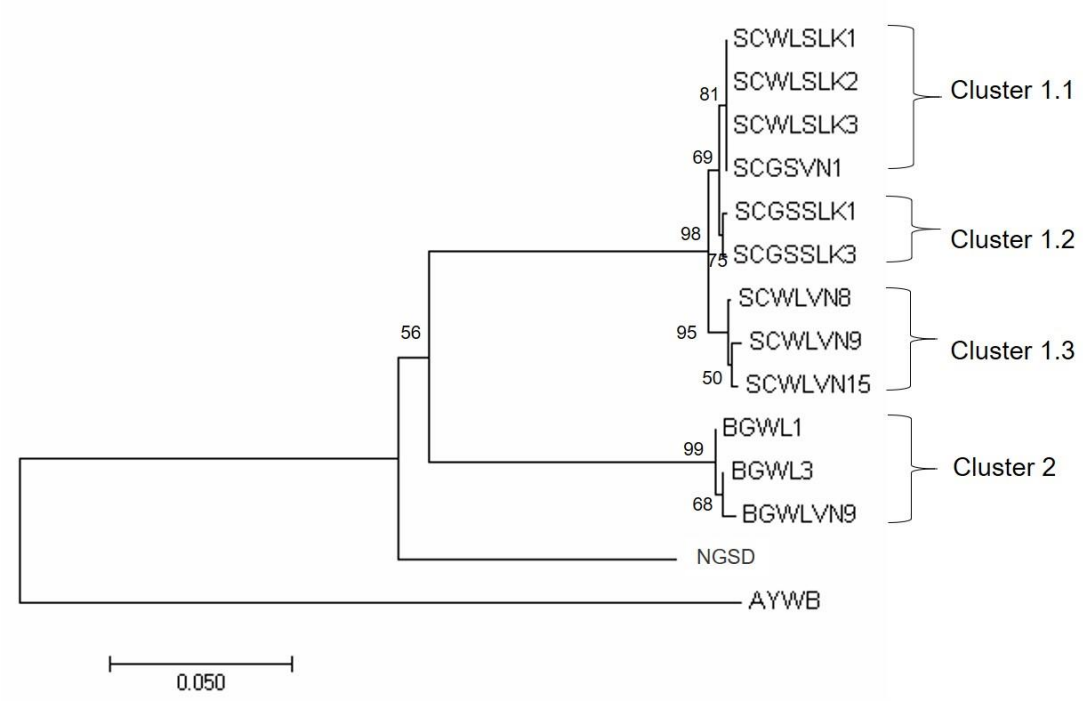


Figure 2.10 Unrooted phylogenetic tree constructed by neighbour-joining based on sequences of the ser gene with 1000 bootstrap value. The phylogenetic tree shows the relationship among the samples listed in Table

2.1; sugarcane disease, NGSD, BGWL and AY-WB as an outgroup. Branch lengths are proportional to the number of inferred character stated information, bar = 0.050 substitution per nucleotide position and the bootstrap values are expressed as percentages of 1000 replications.

2.3.2.8 Analysis of *EF2* gene sequences

With reference to chapter 3, bioinformatics was used to identify effector proteins from NGSD and SCWL that cause different symptoms in host plants. Moreover, the result in chapter 5 show that there were two effector proteins, EF2 and EF7 from NGSD and SCWL that affect plant morphology so the two effector proteins might be useful to classify the phytoplasmas causing sugarcane symptoms.

The *EF2* primers (from chapter 3) amplified from 12 samples out of the thirty-two samples tested in Table 2.1. The phylogenetic tree (Figure 2.11), with AY-WB as an outgroup, shows no separation between the sugarcane, Bermuda grass or napier grass samples for this effector gene.

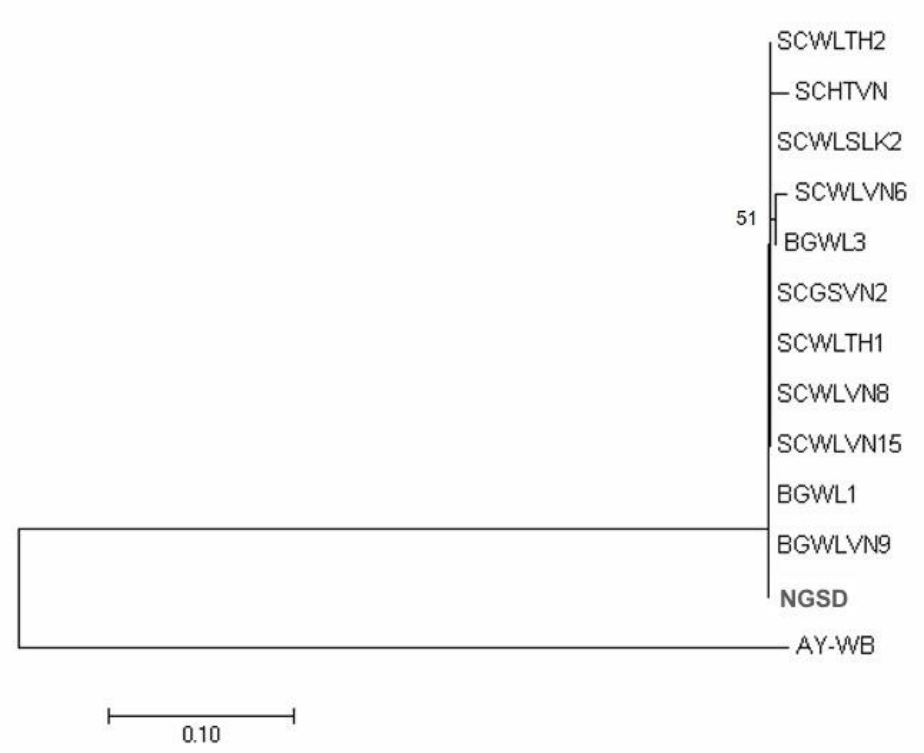


Figure 2.11 Unrooted phylogenetic tree constructed by neighbour-joining method based on sequences of the EF2 gene. with 1000 bootstrap value. The phylogenetic tree shows the relationship among the samples listed in Table 2.1; sugarcane disease, NGSD, BGWL and AY-WB as an outgroup. Branch lengths are proportional to the number of inferred character stated information, bar = 0.1 substitution per nucleotide position and the bootstrap values are expressed as percentages of 1000 replications.

2.3.2.9 Analysis of *EF7* gene sequences

The *EF7* primers from chapter 3 amplified eleven from the thirty-two samples tested in Table 2.1 and the phylogenetic tree was constructed and AY-WB the outgroup (Figure 2.12). The sequences showed some separation, but not consistent with either host, symptoms or geographic region. There were 4

clusters and the NGSD and BGWL were grouped to SCWLs (cluster1.1-1.3) however, it is interesting to note that SCGSSLK3 (cluster1.4) was separated from other SCWLs especially SCWLSLK1.

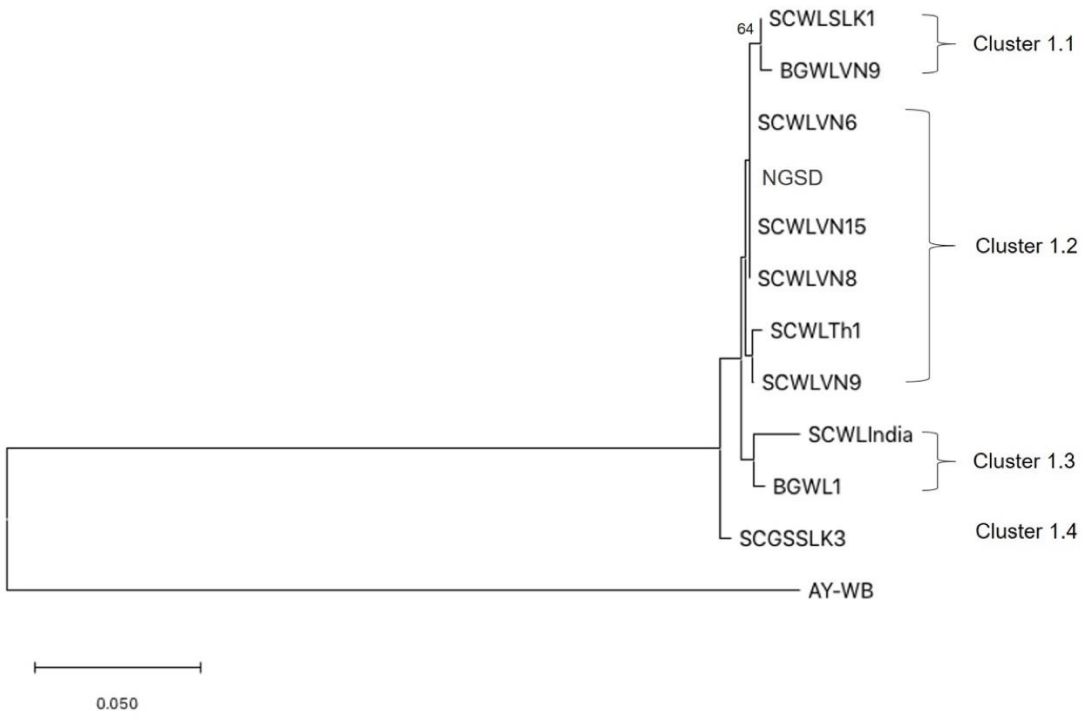


Figure 2.12 Unrooted phylogenetic tree constructed by neighbour-joining based on sequences of the EF7 gene with 1000 bootstrap value. The phylogenetic tree shows the relationship among the samples listed in Table 2.1; sugarcane disease, NGSD, BGWL and AY-WB as an outgroup. Branch lengths are proportional to the number of inferred character stated information, bar = 0.050 substitution per nucleotide position and the bootstrap values are expressed as percentages of 1000 replications.

All samples used to construct the phylogenetic trees and which were amplified with MLST primers are summarised into the Table 2.5 that separates into each cluster, outlier and outgroup.

Table 2.5 Summary of the classified samples for each gene

Primer	Samples						
	Cluster1.1	**Cluster1.2**	**Cluster1.3**	**Cluster1.4**	**Cluster 2**	**Outlier**	**Outgroup**
16S	SCWLTh1, SCWLTh2 SCWLVN1, SCWLVN2, SCWLVN3, SCWLVN4, SCWLVN5, SCWLVN6, SCWLVN7, SCWLVN8, SCWLVN9, SCWLVN15, SCWLVN21, SCHTVN SCWLIndia SCWLSLK1, SCWLSLK2, SCWLSLK3 SCGSVN1, SCGSVN2 SCGSSLK1, SCGSSLK2, SCGSSLK3				BGWL1 BGWL2 BGWL3 BGWLVN1 BGWLVN2 BGWLVN9	NGSD	AY-WB
50S	SCWLTh1, SCWLTh2 SCGSSLK1, SCGSSLK2, SCGSSLK3 SCGSVN1, SCGSVN2 SCWLSLK1, SCWLSLK3 SCWLVN2, SCWLVN5, SCWLVN9, SCWLVN15, SCWLVN21				BGWL1 BGWL2 BGWLVN9	NGSD	AY-WB
asp	SCGSVN2, SCWLVN15 SCGSSLK2, SCGSSLK3, SCGSVN1 SCWLTh1, SCWLTh2				No PCR product	NGSD	AY-WB

gro	SCWLVN 7, SCWLVN 8, SCHTN, SCWLVN 9, SCWLVN 6, SCWLVN 15, SCHTVN	SCGSSL K1 SCGSSL K3	SCGSVN 1 SCWLVN 1 SCWLVN 2 SCWLVN 3	SCWLIndia	BGWL1 BGWLV N9	NGSD	AY-WB
gryB	SCGSSL K1, SCGSSL K2 SCGSVN 1 SCGSVN 2 SCWLIndia	SCWLVN 9 SCWLVN 15 SCWLVN 21			BGWL1 BGWL2 BGWLV N9	NGSD	AY-WB
lpd	SCWLVN 2, SCWLVN 4, SCWLVN 5 SCWLSL K2	SCWLSL K1 SCWLVN 3 SCWLVN 6 SCWLVN 7			BGWL1 BGWL2 BGWL3 BGWLV N9	NGSD	AY-WB

	ScWLSLK3 SCWLIndia SCGSVN1 SCGSVN2 SCGSSLK1 SCGSSLK2 SCGSSLK3	SCWLVN8 SCWLVN9 SCWLVN15 SCWLVN21 SCHTVN					
sec	SCGSSLK2, SCGSSLK3, SCWLSLK2						AY-WB
ser	SCWLSLK1 SCWLSLK2 SCWLSLK3 SCGSVN1	SCGSSLK2 SCGSSLK3 SCWLVN8 SCWLVN9 SCWLVN15			BGWL1, BGWL3, BGWLVN9	NGSD	AY-WB
EF2	SCWLTH1, SCWLTh2, SCHTVN, SCWLSLK2, SCWLVN6, SCWLVN8, SCHTVN BGWL3, BGWLVN8, SCGSVN2, NGSD						AY-WB
EF7	SCWLSLK1	SCWLVN6, SCWLVN	SCWLIndia BGWL1	SCGSSLK3			AY-WB

	BGWLVN 9	8, SCWLVN 9, SCWLVN 15, SCWLTH 1 NGSD					

Sample = Sugarcane white leaf from Vietnam

Sample = Sugarcane white leaf from India

Sample = Sugarcane white leaf from Sri Lanka

Sample = Sugarcane white leaf from Thailand

Sample = Sugarcane grassy shoot from Sri Lanka

Sample = Sugarcane grassy shoot from Vietnam

Sample = Bermuda grass from Malaysia

Sample = Bermuda grass from Vietnam

Sample = Napier grass stunt disease from Kanya

Sample = Aster Yellow Witch'es Broom

Combining the data with all primers and the phylogenetic tree construction, the results showed there were two clusters (Figure 2.13). The first cluster (cluster1) consists of *GryB* grouped with *Sec*, *Gro*, *Lpd* and *Ser* so the individual results showed the genes in this cluster could classify the sugarcane symptoms based on region and symptoms even though there were some SCWL grouped with SCGS samples and vice versa. The other cluster

(cluster2) consists of *EF2* grouped with *asp EF7* and *50S* was an outlier of the cluster so the genes in this clade could not classify the sugarcane symptoms. Therefore, the concatenated phylogenetic results could classify the primers used for classification of the phytoplasmas causing sugarcane symptoms into two groups; classifying primers and non-classifying primers.

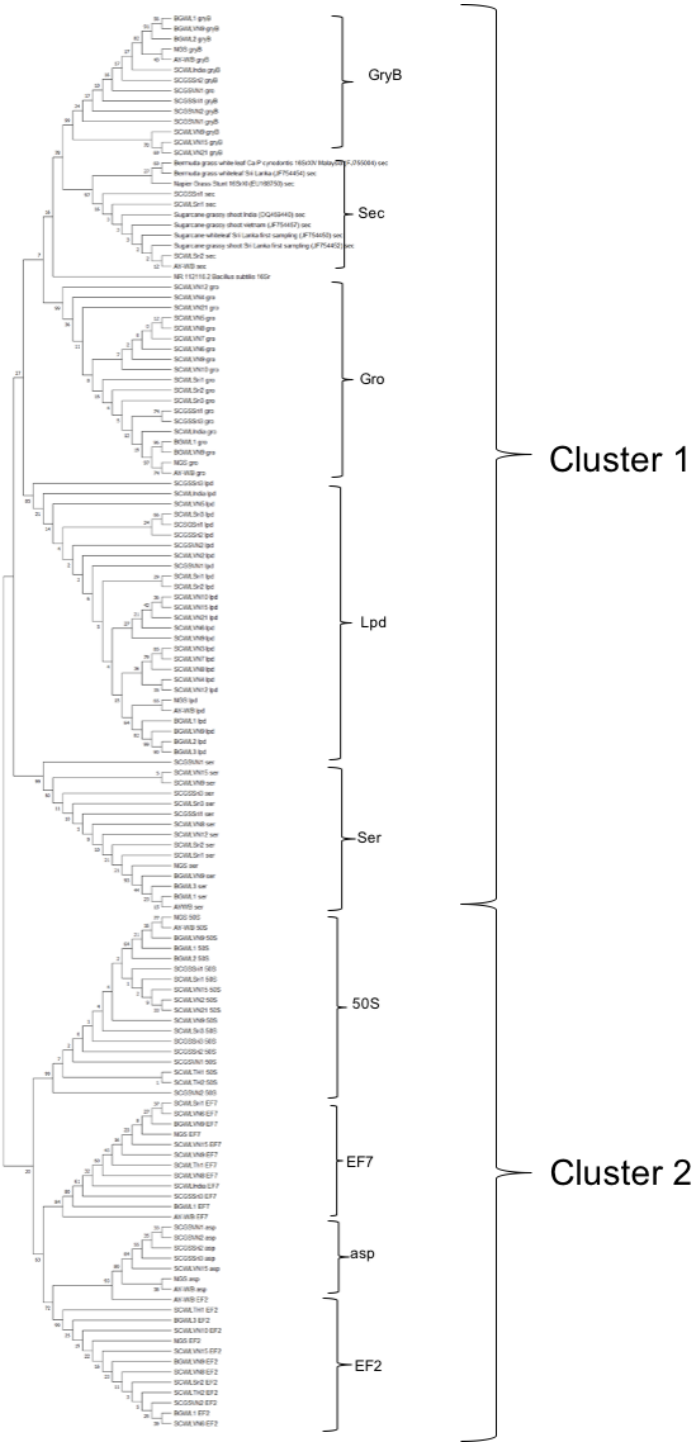


Figure 2.13 Phylogenetic tree of the GryB, Sec, Gro, Lpd, Ser, 50S, Ser, EF2 and EF7 constructed by neighbour-joining method with 1000 bootstrap value.

2.4 Discussion

Phytoplasmas are classified into based on the 16S rRNA sequences, which is a highly conserved sequence (Yadav *et.al*., 2016). To improve classification of closely related phytoplasma strains, the MLST technique has been developed and other genes have been used which are less conserved, such as *tuf, secA* and *rp* gene (Lee *et al*., 2006; Hodgetts *et al*., 2008).

This chapter aimed to determine whether the phytoplasmas causing the sugarcane white leaf (SCWL) and sugarcane grassy shoot (SCGS) are the same or different phytoplasmas and also compared these with NGSD and BGWL samples which are in the 16SrXI and 16SrXIV groups respectively. SCGS has been reported in India, Taiwan, Sri Lanka, Thailand and Vietnam (Rao *et al*., 2008; Viswanathan *et al*., 2011) whilst SCWL has been reported in Bangladesh, India, Malaysia, Thailand, Vietnam, Nepal and Pakistan (Viswanathan *et al*., 2011; Rao *et al*., 2008). Previous studies reported that SCWL and SCGS are closely related and they were classified to the 16SrXI-B subgroup of Rice yellow dwarf group (RYD, 16SrXI group) (Nasare *et al*., 2007) with NGSD placed in the same group whilst BGWL was classified to 16SrXIV. In this study, thirty samples, including sugarcane samples from India, Sri Lanka, Thailand and Vietnam were amplified with primers for ten non-ribosomal RNA genes. The PCR results showed that some primers could not amplify from certain samples. However, where PCR products and sequences

were obtained, the sequences were shown to encode the same protein using the BlastX online program.

Phylogenetic trees were constructed and the sample similarity analysed via bootstrap analysis. The results from all the primers except *asp* (which did not amplify from any of the Bermuda grass samples), *EF2* and *EF7* showed that the BGWLs were classified in a separate cluster from the sugarcane diseases, which is expected, since these are in 16SrXIV rather than 16SrXI. However, the results also showed that NGSD was consistently grouped separately from either the sugarcane or Bermuda grass samples, adding further support to the argument that this should not be classified as a 16SrXI phytoplasma, but should be in its own group, distinct from the 16SrXI and 16SrXIV groups.

In term of sugarcane diseases, *lpd, gro, gryB* and *ser* tended to separate SCGS from SCWL with strong branch support, confirming previous studies which suggest different strains may be responsible for the different symptoms (Wongkeaw *et al*., 1997). However, even within these separations, there were sometimes SCWL samples that grouped with SCGS samples, or vice versa, suggesting that other factors are also involved. Previous studies have also suggested that SCWL and SCGS are caused by the same phytoplasma strain (Nasare *et al*., 2007, Li *et al*., 2014; Wang *et al*., 2014) and in the MLST analysis conducted in this chapter the *asp*, *lpd* and *secA* sequences could not separate the SCWL from the SCGS samples, so it is possible that one strain causes both symptoms based on factors such as environmental conditions,

virulence strain, micronutrients in soil and vectors/hosts (Abeysinghe *et al*., 2016 and Cho *et al*., 2019). The environment is potentially an important factor that controls the symptoms and strain virulence. For example, SCWL from two areas in China, Lincang and Baoshan, was classified into two different cluster (100 bootstrap value) (Zhang *et al*., 2016) but gave the same symptoms, whilst SCGS in various states of India showed phenotypic variation depending on regions and time, but there was no genetic variation found between the phytoplasmas and they were in the same cluster (Viswanathan *et al*., 2011).

From a geographic perspective, the primers showed some separation of SCGS samples from SCWL samples apart from *asp*, *50S* and *secA*. Furthermore, the nucleotide and protein alignments showed non-conserved sequences including deletions and substitutions affecting the protein sequences between SCWL and SCGS. However, these results did not show a consistent pattern and there was no clear separation between samples from Vietnam and Sri Lanka, with as much variation occurring within a country as between countries. This suggests that whilst there are clear differences between individual specimens of the two sugarcane diseases within and between countries, these do not correlate with symptom development, nor with location.

As shown in Figure 2.13, the concatenated tree classified primers into two clusters based on their ability to separate the phytoplasmas from sugarcane. Similar results have been found previously by others, such as with the ability

of MLST to reclassify the 16SrI subgroups found in China based on host plants and geographic areas (Shaoshuai *et al*., 2017). Some of the individual phylogenetic trees, such as those based on the *gro*, *lpd* and *gryB* primers are presumably more discriminatory because of evolutionary rates, structural and functional constraints and substitution patterns etc (Gadagkar *et al*., 2005; Thiergart *et al*., 2014). Furthermore, the reliability of the concatenated tree depended on the bootstrap value and tree congruence (Thiergart *et al.,* 2014). Additionally, the concatenated tree of multiple genes increased the powerful of distinction and quality of the phylogenetic tree (Devulder *et al.,* 2005).

In summary, the results suggest that NGSD is an outlier that is not related to BGWL samples or sugarcane diseases, such that NGSD should be a new group as suggested by previous *leuS* results (Abeysinghe *et al*., 2016). Furthermore, whilst different phytoplasma strains may be associated with SCWL and SCGS, these are fundamental reason for the different symptoms, since it is also the case that the same phytoplasma (based on the MLST analysis) can be associated with the different symptoms. Whilst this does not rule out the possibility that it is the presence or absence of specific effectors in the strains that results in the distinction between SCWL and SCGS symptoms, and these differences could not be detected by the MLST analysis conducted, it is also the case that no consistent differences were found in the two effectors that were included in this study. Further studies should therefore be conducted on additional effector genes, to determine whether these are

responsible for the different symptoms, or whether the different symptoms are due to other factors such as the environment.

Chapter 3: Bioinformatics for NGSD and SCWL effector prediction

3.1 Introduction

Phytoplasmas cause significant symptoms, such as witches' broom, phyllody and virescence, in hundreds of plant species worldwide. Recent studies have shown that they produce several secreted proteins and of these there are some that have been shown to change plant morphology and these have been named effectors. Examples of such effectors are SAP11, SAP54, Tengu and PHYL1 (Phyllody1 effector). Phytoplasmas are related to Gram-positive bacteria and they have a single membrane, such that these effectors are secreted via the Sec-dependent pathway. The Sec-dependent pathway, furthermore, requires signal peptide (SP) sequences for targeting proteins for secretion through the outer membrane (Hogenhout and Boss, 2011).

When it comes to movement between plant cells, proteins can move from cell to cell via plasmodesmata. However, there is a size limit for protein transport known as the size exclusion limit (SEL) (Figure 3.1). The SEL depends on tissue type; for example, the SEL of sieve cells and companion cells is larger than 67 kDa, whilst in the source tissue, which produces carbohydrates for transport in the phloem to sink tissue, it is approximately 10 kDa, and in the phloem of sink tissue where carbohydrates are required for growth such as in the shoot apical meristem and flowers, it is around 50 kDa (Rashid *et al*.,

2018). According to work that has been conducted to date on phytoplasma effectors, the phytoplasmas colonise the phloem but the effectors are secreted via Sec dependent pathways into the phloem and then move to the nuclei of other cells by passing through sieve pores of phloem and into surrounding cells because the effector size is smaller than 40 kDa (Hogenhout and Loria, 2008; Bai *et al*., 2009; Sugio *et al*., 2011).

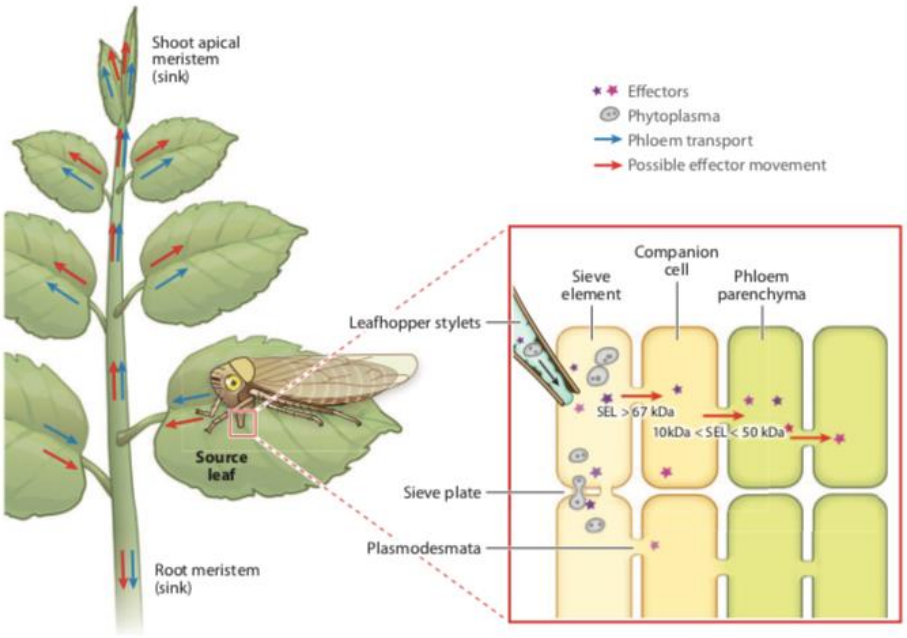


Figure 3.1 Diagram of effector transportation via plasmodesmata (Sugio *et al*., 2011). The leafhoppers inoculate phytoplasmas into plant phloem of leaves and then phytoplasmas secrete effector proteins into plant cells and the effector proteins move to the nuclei of cells and sink tissues to cause symptoms of disease.

In 2007, Bai and colleagues developed use of the SignalP program to predict N-terminal signal peptide sequences in phytoplasma genome sequences, and

to predict phytoplasma effector genes in AY-WB. Their results found 76 proteins that had signal peptide sequences in the AY-WB genome, and in addition, four of these proteins were predicted to have Nuclear Localization Signals (NLS), which are important for effectors to translocate to nuclei of cells; SAP11, SAP22, SAP30 and SAP42 (Figure 3.2). Subsequently, Sugio *et al*. (2014) studied the NLS and the results showed that a C-terminal deletion of proteins that had the NLS did not affect plant morphology, but deletion of the SAP11 NLS could destabilise TCPs and resulted in slightly changed leaf morphology and no accumulation of SAP11 in plant cell nuclei.

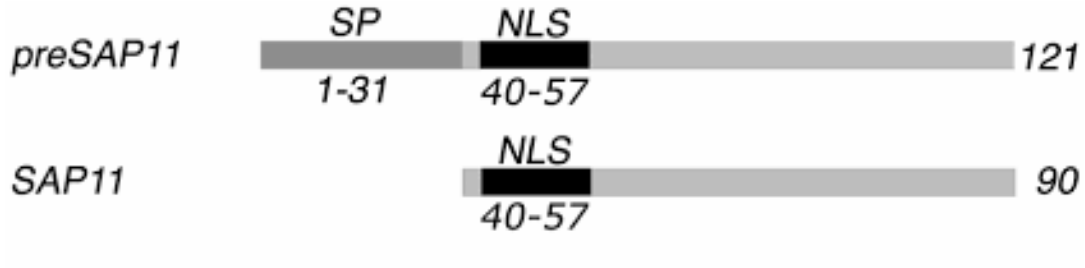


Figure 3.2 $SAP11_{AY\text{-}WB}$ diagram showing the location of the signal peptide (SP) and nuclear localisation signal (NLS) in the preprotein and SAP11 protein (Bai *et al*., 2009).

Furthermore, it is interesting to note that two other effectors, SAP54 and Tengu, have no NLS for translocation to plant cell nuclei and are different from SAP11 as shown in Figure 3.3. However, SAP54 can target to plant cell nuclei because SAP54 has a Coiled Coil Domain (CCD) to interact with plant genes, whilst Tengu was not found in the nuclei of cells. However, Tengu reduced the

levels of JA and Auxin to change plant morphology (Bai *et al*., 2006; Hoshi *et al*., 2009; Chen *et al*., 2011; Manato *et al*., 2014; Rashid *et al*., 2018).

Where it exists, the NLS consists of one or more short protein sequences that are lysine or arginine rich, although there are two type of NLS. The first type is monopartite, which is a single stretch of basic amino acid; for example, the monopartite NLS of SV40 is PKKKRKV. The second type is bipartite, which consists of two stretches of basic amino acids that are separated by a linker region or spacer sequences such as in *Xenopus laevis* which has a bipartite KR[PAATKKAGRA]KKKK NLS sequence. SAP11 has bipartite NLS sequences and there are approximately 18 amino acids in the NLS region (Bai *et al*., 2006; Sugio *et al*., 2014).

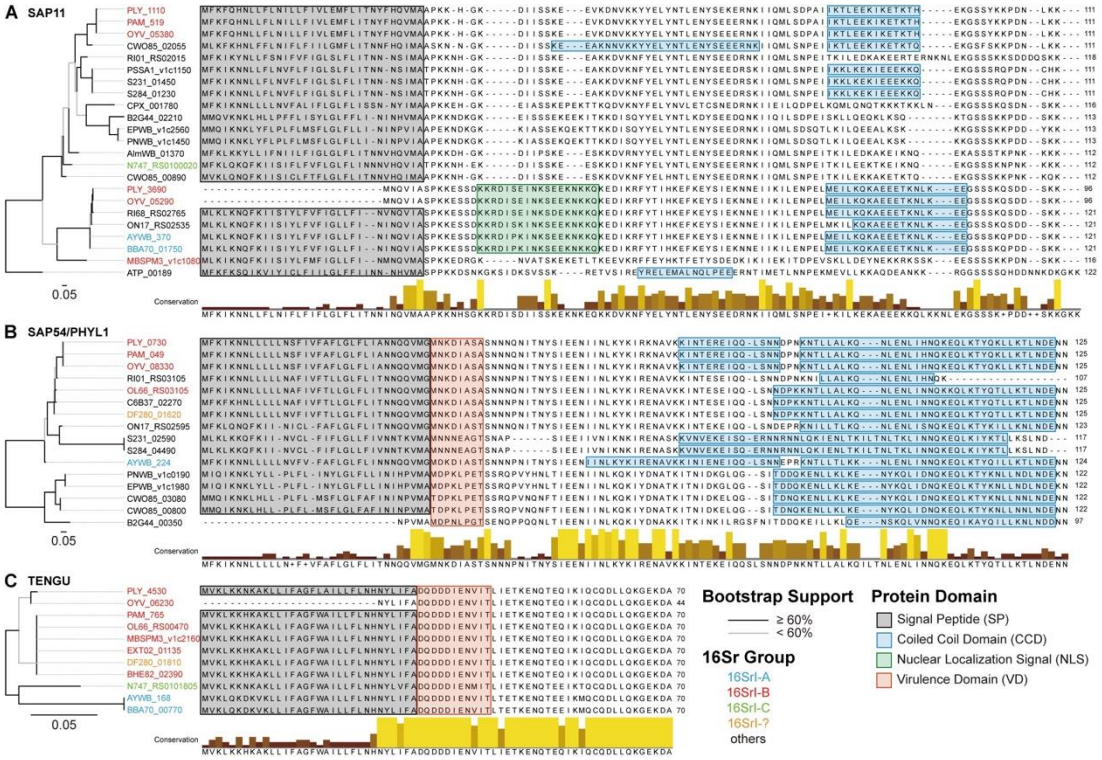
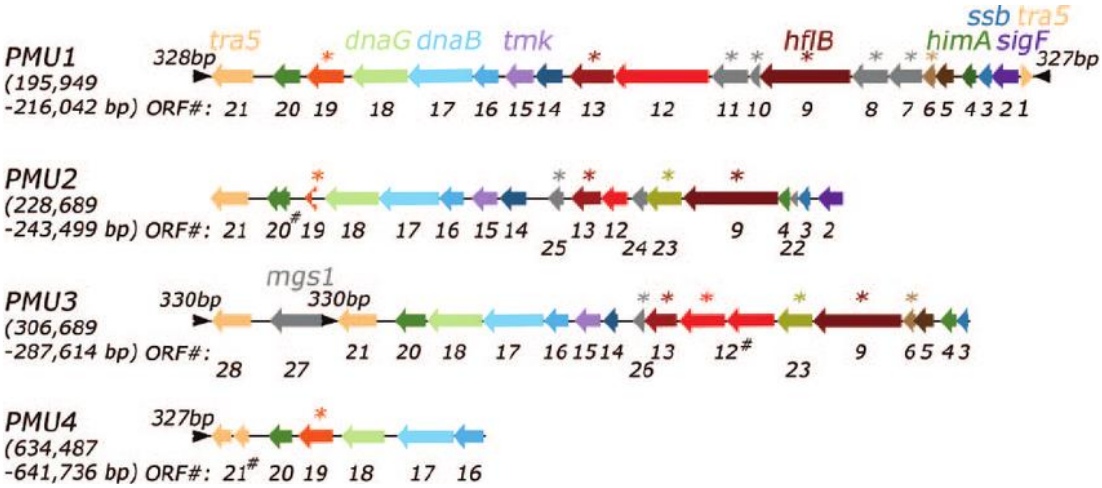


Figure 3.3 Comparison of phytoplasma effectors; Tengu, SAP11 and SAP54 protein sequence, alignments showed the SP, NLS and coiled coil domain (CCD) in different groups of phytoplasma (Cho *et al*., 2019). The SAP11 has the SP, CCD and NLS that is present in phytoplasmas of 16SrI group. The SAP54 has the SP, CCD and Virulence Domain that it is not found in SAP11, and Tengu has the SP and Virulence Domain.

The phytoplasma genome size is small and lacks some metabolic genes such as for amino acid and fatty acid biosynthesis etc (Oshima *et al*., 2004). Moreover, the genome contains various AT-rich repeated regions and there are insertion sequences, such as the IS3 unit. This unit is found in many bacterial genomes and is termed a Putative Mobile Unit (PMU) in AY-WB, or a sequence variable motif (SVM) in clover phyllody (CPh). In AY-WB, the

PMU1 is the largest and most complete repeat among the PMUs and is 20 kb containing 21 ORFs (Figure 3.4A). The PMU1 excises from the phytoplasma chromosome and is able to self-replicate and PMU1 has a number of predicted ORFs for DNA replication that consist of *ssb*, *dnaB* and *dnaG*. Furthermore, there are the synthesis protein (*tmk*), recombination proteins (*himA*), putative transposon (*tra5*) and flanking regions of 327 bp repeats at the border. Often, other PMUs are not complete and may lack some of the ORFs such as *tra5*, the 327 bp repeated region and may have lost the insertion sequences. Additionally, there are other PMUs that are smaller than the PMU1, such as PMU2, 3 and 4, which have parallel gene arrangements to PMU1 but may also lack the 327 bp repeated region, such as in the case of PMU2 (Figure 3.4A).

A



B



Figure 3.4 PMU diagram including gene regions on each PMU. A, PMU1-4 showing size and gene regions and B, SAP11 PMU-like region showing gene positions (Bai et al., 2006; Hogenhout *et al*., 2008).

Interestingly, all of these PMUs contain one gene with an N-terminal secretion signal peptide and other genes encoding proteins that localize to phytoplasma membranes, such that these are believed to be the key virulence regions in phytoplasmas. For example, SAP36 lies on the PMU1, SAP54 lies on PMU2

whilst SAP11 lies on a different PMU-like region (Figure 3.4B) (Hogenhout *et al*., 2008).

The signal peptide sequence is a short amino acid fragment located at the N-terminal end of the protein. The signal peptide controls and directs the protein to cellular and extracellular locations (Hiller *et al*., 2004; Plewczynsli *et al*., 2008). After protein translocation across cell membrane, the signal peptide is cleaved off from the protein by a signal peptidase. Signal peptides for the Sec-dependent pathway consists of three domains. The first domain is the n-region, which is a positive charged amino acid terminal; the second is the h-region, which is the central hydrophobic part of the peptide and the third domain is the c-region, which is the uncharged but polar part of the peptide and this region consists of the cleavage site for the signal peptidase to cut the signal peptide off after mature protein translocation (Figure 3.5).

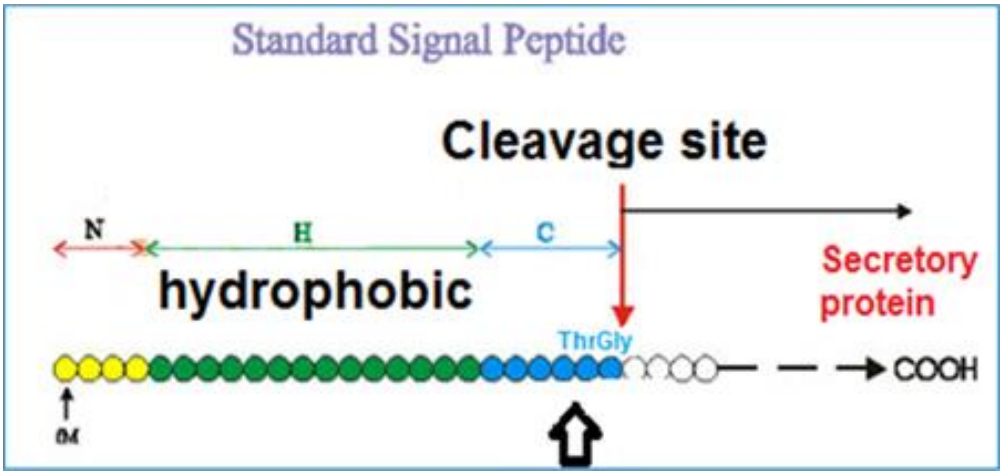


Figure 3.5 Structure of a signal peptide comprised of three domains.

Source: https://www.sigmaaldrich.com/technical-documents/articles/biology/signal-peptide-optimization.html

In this chapter, each of the Napier Grass Stunt Disease (NGSD) genome contigs, obtained in a previous whole genome sequencing project in the laboratory was searched for candidate effector proteins by the PrediSi program, which is an online program to predict the signal peptide sequences and cleavage sites, and can be used for large NCBI database analysis. Once identified, primers were designed for candidate effector genes and used to amplify the sequences from NGSD DNA and also from Sugar cane white leaf (SCWL) DNA, since NGSD was previously reported to be in the same 16SrXI phytoplasma group as SCWL, although the data presented in Chapter 2 suggests this may not hold true. However, it was anticipated that at least some effectors might be similar and amplifiable with the same sets of primers.

Moreover, phylogenetic trees have shown that the 16SrXI phytoplasmas are relatively closely related to 16SrII (PnWB) when compared with 16SrI (AY-WB) so the *SAP11*$_{PnWB}$ gene was used as a template for design of primers that might be able to amplify SAP11 like sequences from NGSD and SCWL (Figure 3.6). For this, the SAP11$_{PnWB}$ protein sequences were retrieved from the NCBI database (www.ncbi.nlm.nih.gov).

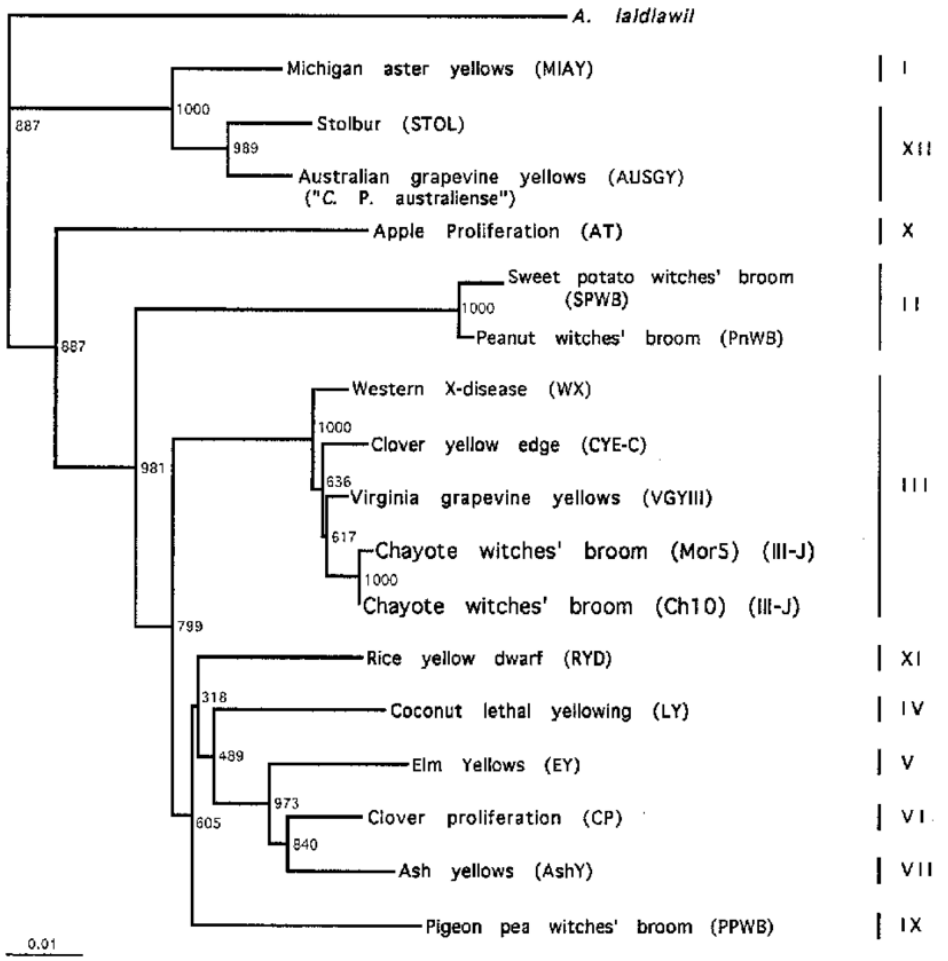


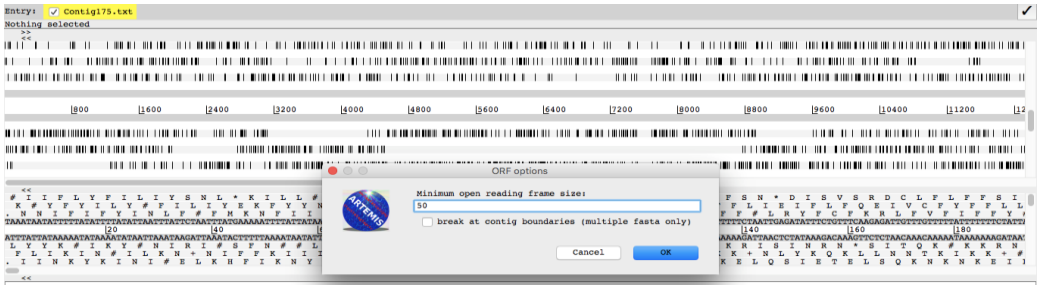
Figure 3.6 The phylogenetic tree showing the relationship between different groups of phytoplasmas, noting the ones used in this study and the groups they belong to (Nicolaisen and Horvath, 2008).

3.2 Materials and Methods

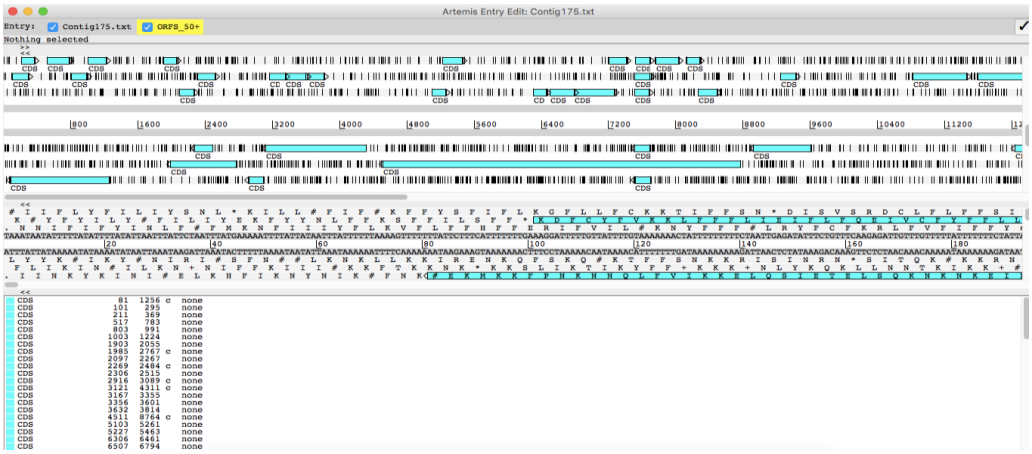
3.2.1 Signal Peptide prediction

Twenty contigs of the Napier grass stunt phytoplasma genome obtained from a previous PhD student study (Kawicha *et al*., 2014) which is believed to represent close to the full-length sequence, were analysed for Open Reading Frames (ORF) with the Sanger Artemis program (Figure 3.7A, B) and then each of the ORFs was translated to protein (Figure 3.7C) and analysed for signal peptide sequences with the PrediSi (Prediction of Signal peptides) program (Figure 3.8). Fourteen sets of primers were then designed for PCR by the Primer3 program to amplify potential effector sequences identified from the NGSD sequences.

A



B



C



Figure 3.7 The Sanger Artemis program analysing ORFs of NGSD contigs.

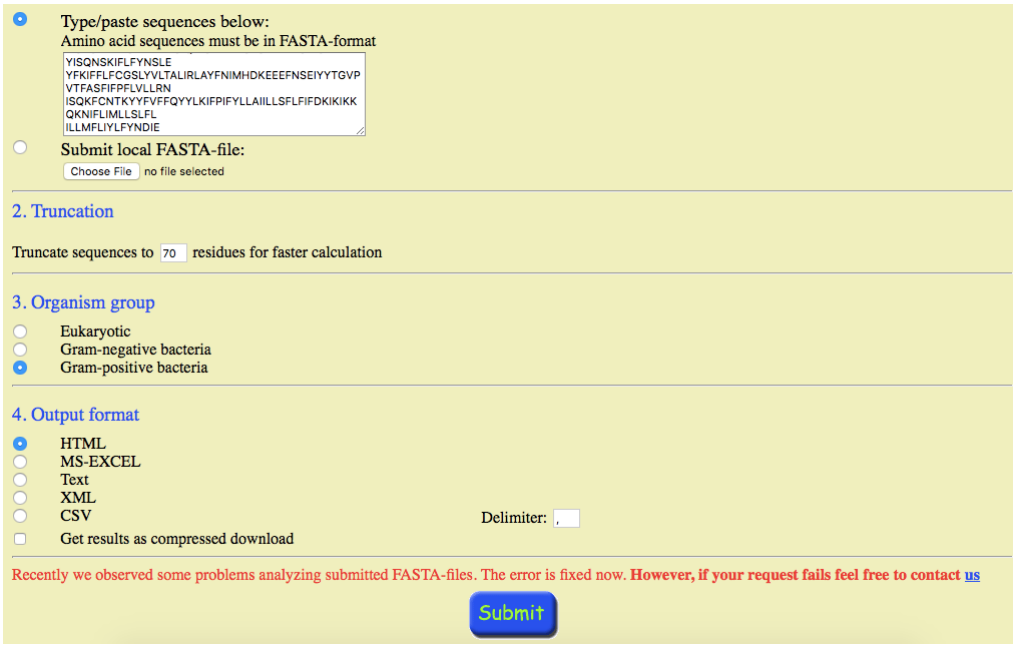


Figure 3.8 The Predisi program analysing SP sequences from NGSD ORFs.

3.2.2 Signal Peptide and candidate effector gene amplification

Napier grass stunt genomic DNA were amplified with the fourteen Ef-SP primers (Table 3.1). The PCR reactions were performed using 1x concentration of MangoMix® (Bioline, UK), 1 μl of genomic DNA, 1 μl of 10 mM of each primer and the total volume was 25 μl. The PCR thermal cycling program was: denaturation at 95°C for 5 min for 1 cycle and then denaturation at 95°C for 40 sec, annealing at 50°C for 40 sec, extension at 72°C for 1 min for 30 cycles and extension at 72°C for 10 min for one cycle. After that, PCR products were examined on 1.5% agarose gels containing 1 μg/ml gel red stain and then, PCR products were purified with QiAquick PCR purification kit (Qiagen, UK) following the manufacturer's instructions. The purified PCR

products were then inserted into pGEM®-T easy (Promega, UK) for blue-white colony selection. The ligation condition was 1x Rapid ligation buffer, 1 μl of 50 ng pGEM®-T easy vector, 2 μl of PCR product, 1 μl of T4 DNA ligase and total volume is 10 μl and mixed gently before incubation at 4°C overnight. For the next step, 5 μl of ligation reaction was added into 50 μl of JM109 competent cells (Promega, UK) and incubated on ice for 30 min after which the tube was heat shocked at 42°C for 1.30 min in a heated block and returned immediately onto ice and incubated for 5 min, before 300 μl of LB medium was added and the tube was incubated at 37°C for 3 hours with shaking (220 rpm). Subsequently, 100 μl of transformation culture was plated on LB agar containing 100 μg/ml ampicillin, 0.5 mM IPTG and 80 μg/ml X-gal and then the plates were incubated at 37°C for 16-24 hours.

White colonies were selected and amplified with M13 primers by PCR. The PCR conditions were as above and the PCR thermal cycling program was: denaturation at 95°C for 5 min for 1 cycle and the denaturation at 95°C for 40 sec, annealing at 55°C for 40 sec, extension at 72°C for 1.30 min for 35 cycles and extension at 72°C for 10 min for one cycle. Five microliters of PCR samples were analysed by 1% agarose gel containing gel red. The positive colonies were inoculated into LB broth adding 100 μg/ml ampicillin and incubated overnight by shaking at 37°C.

Plasmid extraction was performed for sequencing using the GeneElute™Plasmid Miniprep Kit (Sigma-Aldrich Co.). The plasmid extraction procedure followed the manufacturer's instruction. After sequencing, all nucleotide sequences including signal peptides sequences were compared with signal peptide sequence-template by ClustalW online program. Subsequently, the new primer sets for six PCR products were designed for NGSD and SCWL that had been positively identified as the right PCR products from the original 14 products, but with removal of the signal peptides, and PCR products were amplified with the new primers for each effector (Table 3.2). Moreover, Ef7 primers were designed from *SAP11*$_{PnWB}$ which were then used to amplify the *SAP11* genes from NGSD and SCWL genomes.

The PCR conditions were as above and the amplification cycle was: denaturation at 95°C for 5 min for 1 cycle and then denaturation at 95°C for 30 sec, annealing at X°C for 45 sec, extension at 72°C for 1 min for 30 cycles and extension at 72°C for 10 min for one cycle. After that, 5 μl of PCR samples were analysed on 1.5% agarose gel containing gel red.

Table 3.1 List of primers for NGSD effector amplification in NGSD and SCWL that included signal peptides.

Primer name	Primer sequences (5′-3′)	Annealing Temperature (°C)
Ef-SP-1 Fw	GAA TAA ATA AGT CTG AAA AAA CCA AC	50
Ef-SP-1 rev	GGC AAT ATC TTT GAA TAT GAT CCT C	50
Ef-SP-2 Fw	AAG TCA ACA ATT GGA GTT ATG GAC GCT TA	55
Ef--SP2 rev	TGT TTT AGT TTT TTG ATG TTC TTT TTT TTC TTT TCT T	55
Ef-SP-3 Fw	ACC TGT ACC TGG CGG ACC ATA TAA CAA AAC ACC	50
Ef-SP-3 rev	CGT TTG CAA GAA CAA GAA AGC GAA ATT AAT CAA	50
Ef-SP-4 Fw	CAT AGT ACC TAA ATC TTG TAT AGA ATA TAA AC	55
Ef-SP-4 rev	AAC TGG AGA AAA TGA ACC AAT AGA AAA A	55
Ef-SP-5 Fw	CTT TTT TTT TAT TAA TTT TAA TTA ATT TTT TAG	48
Ef-SP-5 rev	ATT TAG GTA CTA TGA ATT TAT TAT TT	48
Ef-SP-6 Fw	CCG TTG CCA GGG CGC CGA ATT TGA A	60
Ef-SP-6 rev	CCA TGA ACG TAT AAA TGA GGC CAT TGC G	60
Ef-SP-7 Fw	GAC AAA ACA CCA ACT GCA GGA ACT AAT AAA CTA GAA	60
Ef-SP-7 rev	GCG AGT TAT CAA AGA GTT TTA GAA GAA CC	60
Ef-SP-8 Fw	TTA TTT TTC CTC GCG CTG TTT TTT TTT TTT T	50
Ef-SP-8 rev	AGG AGC AAC TAA TAA AAA CAA TCA A	50
Ef-SP-9 Fw	TTG TTT AGT GTT TTG GAG GAT AGT T	50
Ef-SP-9 rev	CGG CGA TAA TCA GGC TGC GAA A	50
Ef-SP-10 Fw	GAT TTT TTA TTT TAT TAT GTG TT	45
Ef-SP-10 rev	ATA TAA AAA AAA AGA AAA ATA A	45
Ef-SP-11 Fw	GAC GAA AAT AAT TAA GAT AGT AAT AAT AAA A	60
Ef-SP-11 rev	TTT GCT ATC ATC ATT TTA TAT TTA TT	60
Ef-SP-12 Fw	TTT TTT ATG AAT ATC TTT ATA TGC	48
Ef-SP-12 rev	GAT TTA GGT ACT ATG AAT TTA TTA TTT	48
Ef-SP-13 Fw	CGA TAT AAA GCT ATA TAA GAC A	50
Ef-SP-13 rev	AGA ACA ATA CGC ACA AAA AGC AA	50
Ef-SP-14 Fw	AAA AAA ATA AAA TAA AGA TAG GAT AAT AAA AGA A	55
Ef-SP-14 rev	TTC TTT TTA TAG GTG ATA TTT GTG GTA TTC C	55

Table 3.2 List of primers for NGSD effector amplification in NGSD and SCWL excluding signal peptides

Primer name	Primer sequences	Annealing Temperature (°C)	Remark
Ef-1 Fw	ACAAA AAG CAG GCT GGG GGG ATA TCC CAT TTC TTC TAA TTC TG	60	
Ef-1 rev	ACA AGA AAG CTG GGT GGC AAT ATC TTT GAA TAT GAT C	60	
Ef-2 Fw	AAG TCA ACA ATT GGA GTT ATG GAC GCT TA	55	
Ef-2 rev	TGT TTT AGT TTT TTG ATG TTC TTT TTT TTC TTT TCT T	55	
Ef-3 Fw	AC AAA AAG CAG GCT GGG CAA TAA CAT CTT CAA AAG TAG GA	55	
Ef-3 rev	ACA AGA AAG CTG GGT CGT TTG CAA GAA CAA GAA AGC GAA ATT AAT CAA	55	
Ef-4 Fw	AC AAA AAG CAG GCT GGG GAG TCA TTC CTA AAA TAA TAG TT	55	
Ef-4 rev	ACA AGA AAG CTG GGT AAC TGG AGA AAA TGA ACC AAT AGA AAA A	55	
Ef-5 Fw	ACA AAA AGC AGG CTG GGC TCC TTT ACT GAT TAC TTT TGT A	40	
Ef-5 rev	ACA AGA AAG CTG GGT ATT TAG GTA CTA TGA ATT TAT TAT TT	40	
Ef-6 Fw	ACA AAA AGC AGG CTT GTA TTT ATT ATC TAA TTT TCG TTC	40	
Ef-6 rev	ACA AGA AAG CTG GGT CCA TGA ACG TAT AAA TGA GGC CAT TG	40	
Ef-7 Fw	ATG ATG CAA ATA AAA AAT AAA TTA T	50	WP_004994795
Ef-7 rev	TTA TTT TTT AGA ATC ATC AGG CTT TTT	50	

The PCR products were purified with QiAquick PCR purification kit (Qiagen, UK) following the manufacturer's instruction and ligated into pGEM®-T easy (Promega, UK). The ligation composition was then transformed into JM109 (Promega, UK) competent cells by heat shock procedure as described previously. White colonies were selected for PCR using M13 primers and then PCR products were analysed on 1% agarose gels containing gel red. The positive colonies were inoculated in LB broth adding 100 µg/ml ampicillin and incubated at 37°C overnight. For the next step, plasmid was extracted using the GeneElute™Plasmid Miniprep Kit (Sigma-Aldrich Co.) following the manufacturer's instruction for sequencing.

The nucleotide sequences were aligned to previous sequences that include signal peptide sequences and then the new nucleotide sequences were analysed by blastx using online tools (www.ncbi.nlm.nih.gov) to find the protein region similarity to NCBI databases. Subsequently, all PCR products were ligated into pGWB5 and pBRAC214 for transformation into plants as detailed in the next chapter.

3.2.4 The Nuclear Localization Signal Prediction

The nucleotide sequences from all PCR products were translated to protein and then each protein sequence was analysed for NLS position using the NLS mapper program (http://nls-mapper.iab.keio.ac.jp/cgi-bin/NLS_Mapper_form.cgi).

3.3 Results

Signal Peptide prediction

Each of the NGSD contigs was analysed for its ORFs by the Sanger Artemis program. This program was set to give the minimum ORF of 50 amino acids for ORF reading. The program then showed all the ORFs in the 6 possible reading frames from both strands as shown in Figure 3.7B. Subsequently, each of the protein sequences the ORFs were viewed in FASTA format and the protein sequences copies into the signal peptide prediction program, PrediSi. According to the PrediSi program, the FASTA protein format was filled in and chosen for Gram-positive bacteria to predict the signal peptide sequences (Figure 3.8). There are two possible results for signal peptide prediction and examples of both are shown in Figure 3.9. An N indicates that there is no signal peptide sequence and the table detail shows an example where the score was 0.378 which was lower than 0.5 (Figure 3.9A and B) whilst Y indicates that there was a signal peptide sequence and the score was 0.567 (>0.5) and the signal peptide peak and the cleavage position are also shown in Figure 3.9 C and D.

A

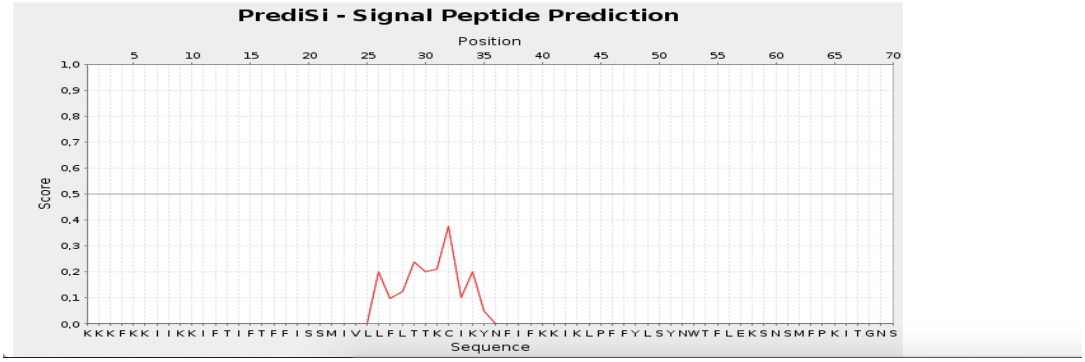
Settings:

Matrix:	null
Truncation:	70 residues
Output:	null

FASTA-ID	Score	Cleavage Position	Signal Peptide ?	Chart
unknown	0.3738	32	N	Details

B

Matrix:	Eukarya
Truncation:	70 residues
Cleavage position:	32
Score:	0.3738
Secreted protein:	**not predicted for secretion**



C

Matrix:	null
Truncation:	70 residues
Output:	null

FASTA-ID	Score	Cleavage Position	Signal Peptide ?	Chart
unknown	0.5657	36	Y	Details

D

Matrix:	Eukarya
Truncation:	70 residues
Cleavage position:	36
Score:	0.5657
Secreted protein:	predicted for secretion

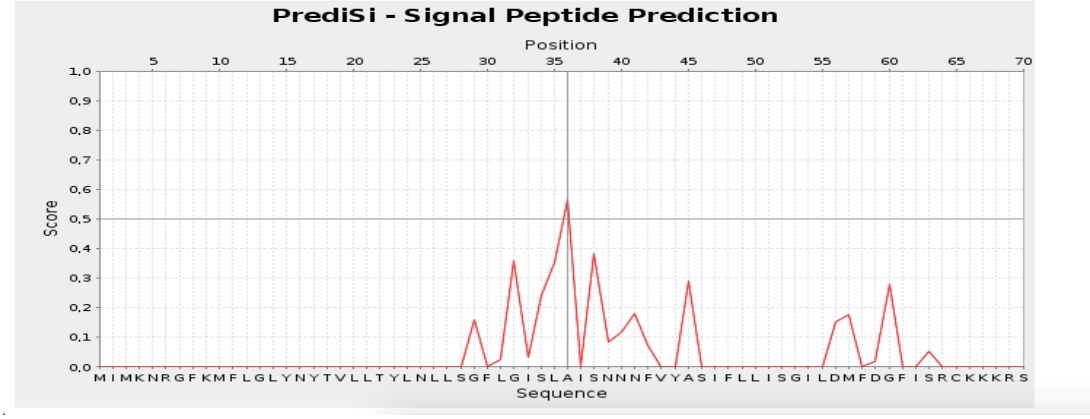


Figure 3.9 The PrediSi result of EF protein. A, the score of EF1 protein. B, EF1 protein peak. C, the score of EF2 protein and D, signal peptide sequence and cleavage position of EF2 protein.

The PrediSi result from the 20 NGSD contigs showed 14 proteins having signal peptide sequences and then primers were designed for each of these ORFs that included the signal peptide sequences (Table 3.1). The NGSD extracted DNA was then tested with fourteen primer pairs, and from these six PCR products were obtained. After that, PCR nucleotide sequences were compared with previous sequences and the result showed that the sequences completely matched. The Ef1 to Ef6 primers were then designed to amplify the same sequences but with SP signal removed, and at the same time the Ef7 primer set was designed from *SAP11*$_{PnWB}$. Subsequently, all these new primers were tested on NGSD and SCWL DNA. From this, the NGSD genome

gave seven PCR products (Figure 3.10), whilst when the SCWL genome was amplified with Ef2 to Ef7 the results showed two PCR products (Figure 3.11) including the SAP11 gene.

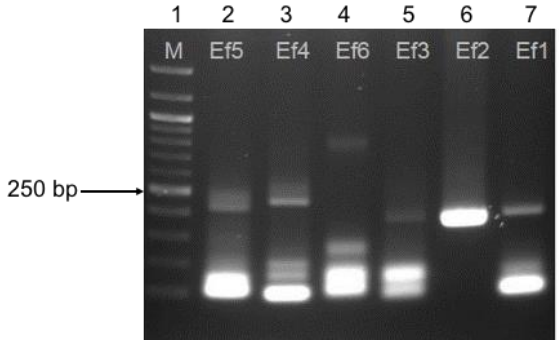


Figure 3.10 NGSD effector PCR products from effector specific primers by PCR method. Lanes (1) 50 bp ladder, (2) PCR product from EF5 primer, (3) PCR product from EF4 primer, (4) PCR product from EF6 primer, (5) PCR product from EF3 primer, (6) PCR product from EF2 primer and (7) PCR product from EF1 primer.

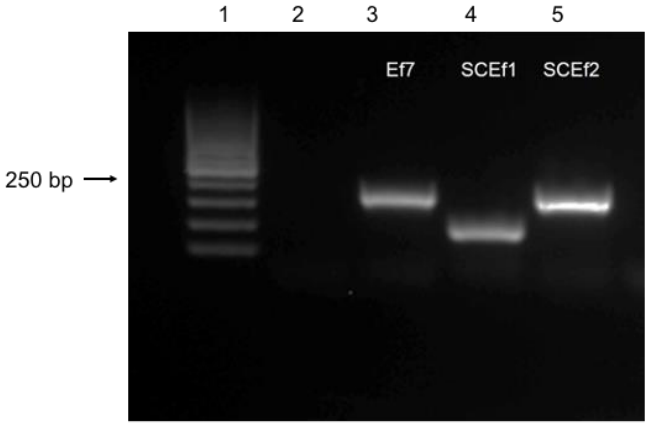


Figure 3.11 NGSD effector and SCWL effector PCR products from effector specific primers by PCR method. Lanes (1) 50 bp ladder, (2) non-template control, (3) PCR product from EF7 primers in NGSD, (4) PCR product from EF2 primers in SCWL and (5) PCR product from EF7 prime in SCWL.

Figure 3.12 shows alignment results between the *EF1* PCR products with and without SP which were completely matched apart from the absence of the SP.

```
EF1         ------------------------------------------------------------
EF1-SP      TTTATTAATCGATCTAAAATATCTTTTAATTGTTGTTTTTCTTTTTTTTTCCCAATAACA

EF1         ----------TTTATTAATCGATCTAAAATATCTTTTAATTGTTGTTTTTCTTTTTTTTT
EF1-SP      TCTTCAAAAGTTTATTAATCGATCTAAAATATCTTTTAATTGTTGTTTTTCTTTTTTTTT
                      **************************************************

EF1         CCCAATAACATCTTCAAAAGTAGGAAAATCTTTTGAATCTCTAAAATATTTATTAGCTGC
EF1-SP      CCCAATAACATCTTCAAAAGTAGGAAAATCTTTTGAATCTCTAAAATATTTATTAGCTGC
            ************************************************************

EF1         TAAATTATTATTTTCTTTTTCTATTCTTGCTTTGCTTTCTATTTTTACTTCTTTTAAAGT
EF1-SP      TAAATTATTATTTTCTTTTTCTATTCTTGCTTTGCTTTCTATTTTTACTTCTTTTAAAGT
            ************************************************************

EF1         GTTTAAAGCTTCACGAAAAGAAACGACAGCTTCGCTAAAAATCTTTCTATCTTGTTCTAA
EF1-SP      GTTTAAAGCTTCACGAAAAGAAACGACAGCTTCGCTAAAAATCTTTCTATCTTGTTCTAA
            ************************************************************

EF1         CTCTTCATTATTACTTTTTAACTCTGTTATTTCGCGTTTATATCTCCCAATTTCATTATT
EF1-SP      CTCTTCATTATTACTTTTTAACTCTGTTATTTCGCGTTTATATCTCCCAATTTCATTATT
            ************************************************************

EF1         CAAATATTCTTTTTTTTCTATTTCTAATTGCTTATCATTATTAATTTTTCGTTCAAGAAA
EF1-SP      CAAATATTCTTTTTTTTCTATTTCTAATTGCTTATCATTATTAATTTTTCGTTCAAGAAA
            ************************************************************

EF1         ATCAAATTTTTCATTAATCCTTCGGAACTCTTCCTTCAAATCATTATATTTGGTGATTTC
EF1-SP      ATCAAATTTTTCATTAATCCTTCGGAACTCTTCCTTCAAATCATTATATTTGGTGATTTC
            ************************************************************

EF1         TTGTTGGAGACTACTTGTTAATTTCTCAATACCTTTTGTTAAAATATCTATTTCTTTTTT
EF1-SP      TTGTTGGAGACTACTTGTTAATTTCTCAATACCTTTTGTTAAAATATCTATTTCTTTTTT
            ************************************************************

EF1         TAATTGA
EF1-SP      TAATTGA
            *******
```

Figure 3.12 EF1 PCR product without signal peptides comparing to EF1-SP PCR product.

Following PCR, the various products were sequenced to confirm their identity and to check with similarities to known effectors from 16SrII phytoplasmas and the results are shown in Tables 3.3 and 3.4.

Table 3.3 List of protein sequences.

No.	Sample	group	Protein translation
1	*EF1*$_{NGSD}$	XI	KYSKIIPYSFKSLILYPISSNSEKVKLHSFIFFIFVLGIFLANTQFPFFSVIL*
2	*EF2*$_{NGSD}$	XI	MFKLQNQFKIIRVFLFTFLGFLIINNNQVMAMGNKNSNNNSEISNDKEYALYIQAEIAIKSELTNLQLNNAKKSELLHKQQFITTEIEKYNKRQNNNQLSTTYGEQPESSRRNISSAINDDDENELSDDELQPMNLIKNNSKCPIDQ*
3	*EF3*$_{NGSD}$	XI	FINRSKISFNCCFSFFFPITSSKVGKSFESLKYLLAAKLLFSFSILALLSIFTSFKVFKASRKETTASLKIFLSCSNSSLLLFNSVISRLYLPISLFKYSFFSISNCLSLLIFRSRKSNFSLILRNSSFKSLYLVISCWRLLVNFSIPFVKISISFFN*
4	*EF4*$_{NGSD}$	XI	KKDNVVINGNISGVIPKIIVNDNKKIFKKSKSDGFLNQLIIKIKGNINKVEIINNLDIELISF*
5	*EF5*$_{NGSD}$	XI	KKDNVVINGNISGVIPKIIVNDNKKIFKKSKSDGFLNQLIIKIKGNINKVEIINNLDIELISF*
6	*EF6*$_{NGSD}$	XI	LFEIIFFILNLFLNLGFFKHFLYVLFLLTILNLCYNKSVKHSISSDYLEKKLYYA*
7	*EF7*$_{NGSD}$	XI	MMQIKNKLYFLPLFLMSFLGLFLLINTNPVIAAPEKNDKGKKIASSEKQEKTTKKDISQYYELYNTLENYSEEDRNKIIQMLSDSQTLKILQEEALKSKKKGSSSKKPDDSKK*
8	*EF2*$_{SCWL}$	XI	MFKLQNQFKIIRVFLFTFLGFLIINNNQVMAMGNKNSNNNSEISNDKEYALYIQAEIAIKSELTNLQLNNAKKSELLHKQQFITTEIEKYNKRQNNNQLSTTYGEQPESSRRNISSAINDDDENELSDDELQPMNLIKNNSKCPIDQ*
9	*EF7*$_{SCWL}$	XI	MMQIKNKLYFLPLFLMSFLGLFLLINTNPVIAAPEKNDKGKKIASSEKQEKTTKKDISQYYELYNTLENYSEEDRNKIIQMLSDSQTLKILQEEALKSKKKGSSSKKPDDSKK*

Table 3.4 List of protein similarity and identity from NCBI database.

No.	Sample (group)	Protein similarity	Identity (%)
1	*EF1*$_{NGSD}$	hypothetical protein [‘*Candidatus* Phytoplasma oryzae’]	100
2	*EF2*$_{NGSD}$	effector, AY-WB SAP67-like protein [Chrysanthemum yellows phytoplasma]	77
3	*EF3*$_{NGSD}$	hypothetical protein [‘*Candidatus* Phytoplasma oryzae’]	99
4	*EF4*$_{NGSD}$	magnesium-translocating P-type ATPase [‘*Candidatus* Phytoplasma oryzae’]	100
5	*EF5*$_{NGSD}$	magnesium-translocating P-type ATPase [‘*Candidatus* Phytoplasma oryzae’]	100
6	*EF6*$_{NGSD}$	-	-
7	*EF7*$_{NGSD}$	effector, AY-WB SAP11-like protein [Peanut witches'-broom phytoplasma]	95
8	*EF2*$_{SCWL}$	effector, AY-WB SAP67-like protein [Chrysanthemum yellows phytoplasma]	77
13	*EF7*$_{SCWL}$	effector, AY-WB SAP11-like protein [Peanut witches'-broom phytoplasma]	95

The protein result showed that effector 2 from NGSD and SCWL had similarity to the SAP67 effector protein of aster yellows type phytoplasmas, with 77% match to the Chrysanthemum yellows phytoplasma SAP67. Moreover, there are two hypothetical proteins from NGSD that showed 100% and 99% similarity with hypothetical proteins of ‘*Candidatus* Phytoplasma oryzae’ and also 100% to the magnesium-translocating P-type ATPase. However, there is

one protein from NGSD that cannot be identified. As for the SAP11 effector, the nucleotide sequences of NGSD and SCWL revealed 95% similarity when compared with Peanut witches'-broom phytoplasma (Table 3.4).

For the SAP11 protein, the protein sequences were compared to PnWB (group II) and the results show only one amino acid difference which is T (Threonine) instead of I (Isoleucine) (Figure 3.13)

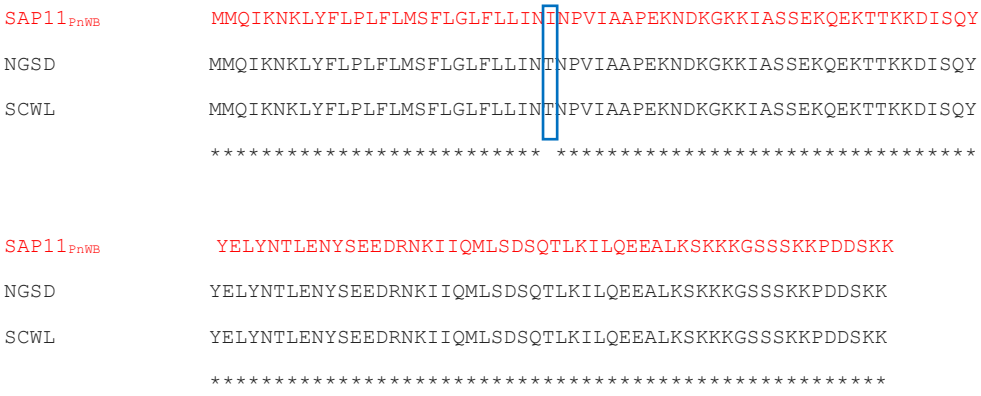


Figure 3.13 Protein alignment of hypothetical protein of $SAP11_{PnWB}$ compared with group XI phytoplasmas. The $SAP11_{PnWB}$ is template to primer design for amplify to NGSD and SCWL.

For the other potential effector protein sequences from NGSD, effector 2 appears to be the same as $EF2_{SCWL}$ with no mismatches; and appears to be related to the uncharacterised SAP67 protein from Chrysanthemum yellow phytoplasma (Figure 3.14).

```
Ef2NGSD         MFKLQNQFKIIRVFLFTFLGFLIINNNQVMAMGNKNSNNNSEISNDKEYALYIQAEIAIK   60
EF2SCWL         MFKLQNQFKIIRVFLFTFLGFLIINNNQVMAMGNKNSNNNSEISNDKEYALYIQAEIAIK   60
                ************************************************************

Ef2NGSD         SELTNLQLNNAKKSELLHKQQFITTEIEKYNKRQNNNQLSTTYGEQPESSRRNISSAIND   120
EF2SCWL         SELTNLQLNNAKKSELLHKQQFITTEIEKYNKRQNNNQLSTTYGEQPESSRRNISSAIND   120
                ************************************************************

Ef2NGSD         DDENELSDDELQPMNLIKNNSKCPIDQ      147
EF2SCWL         DDENELSDDELQPMNLIKNNSKCPIDQ      147
                ***************************
```

Figure 3.14 EF2 Protein alignment of NGSD compared with SCWL phytoplasma.

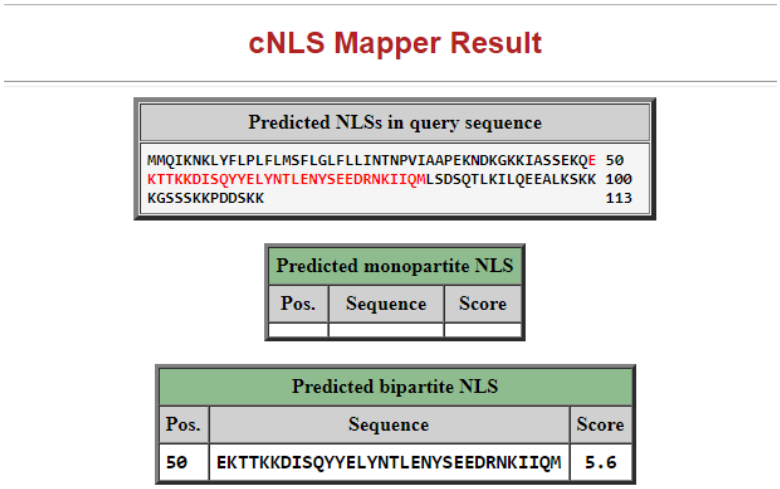
Furthermore, $SAP11_{NGSD}$ and $SAP11_{SCWL}$ were analysed for NLS and TCP-binding position by alignment to $SAP11_{PnWB}$ and the result showed that they have two positions and the protein sequences were similar (Figure 3.15).

```
                                                          NLS
PnWB        MMQIKNKLYFLPLFLMSFLGLFLLININPVIAAPEKNDKGKKIASSEKQEKTTKKDISQY
NGSD        MMQIKNKLYFLPLFLMSFLGLFLLINTNPVIAAPEKNDKGKKIASSEKQEKTTKKDISQY
SCWL        MMQIKNKLYFLPLFLMSFLGLFLLINTNPVIAAPEKNDKGKKIASSEKQEKTTKKDISQY
            ************************* ********************************

PnWB        YELYNTLENYSEEDRNKIIQMLSDSQTLKILQEEALKSKKKGSSSKKPDDSKK
NGSD        YELYNTLENYSEEDRNKIIQMLSDSQTLKILQEEALKSKKKGSSSKKPDDSKK
SCWL        YELYNTLENYSEEDRNKIIQMLSDSQTLKILQEEALKSKKKGSSSKKPDDSKK
            ****************************************************
                                    TCP-Binding
```

Figure 3. 15 SAP11 protein sequences of Peanut witches'-broom phytoplasma (PnWB), Napier grass stunt disease (NGSD) and Sugarcane white leaf (SCWL) were aligned using ClustalW omega program. Nuclear localization signal (NLS) is indicated in red font, and part of the coiled coil structure required for binding TCP is shown in grey colour.

According to NLS mapper, the SAP11 effector protein of SCWL was predicted by the NLS mapper program (http://nls-mapper.iab.keio.ac.jp/cgi-bin/NLS_Mapper_form.cgi) and the result showed the NLS sequences were longer than protein alignment with $SAP11_{PnWB}$. However, the NLS was in the same position and this program cannot predict the TCP-binding site (Figure 3.16). Moreover, the table showed a score for NLS of 5.6. This is above the cut-off score for nuclear localisation. If the score is higher than 5 it means a stronger NLS capacity to localize to the nucleus, whilst if the score is lower than 5 indicates localisation to the cytoplasm Furthermore, this program predicted that the NLS of SCWL which was bipartite.



cNLS Mapper Result

Predicted NLSs in query sequence
MMQIKNKLYFLPLFLMSFLGLFLLINTNPVIAAPEKNDKGKKIASSEKQE 50 KTTKKDISQYYELYNTLENYSEEDRNKIIQMLSDSQTLKILQEEALKSKK 100 KGSSSKKPDDSKK 113

Predicted monopartite NLS		
Pos.	Sequence	Score

Predicted bipartite NLS		
Pos.	Sequence	Score
50	EKTTKKDISQYYELYNTLENYSEEDRNKIIQM	5.6

Figure 3.16 $EF7_{SCWL}$ protein showing NLS score and position.

In addition, the other protein sequences were analysed for NLS position using the NLS mapper and the result didn't show an NLS for any of them (Figure 3.17) because the score was lower than 5.

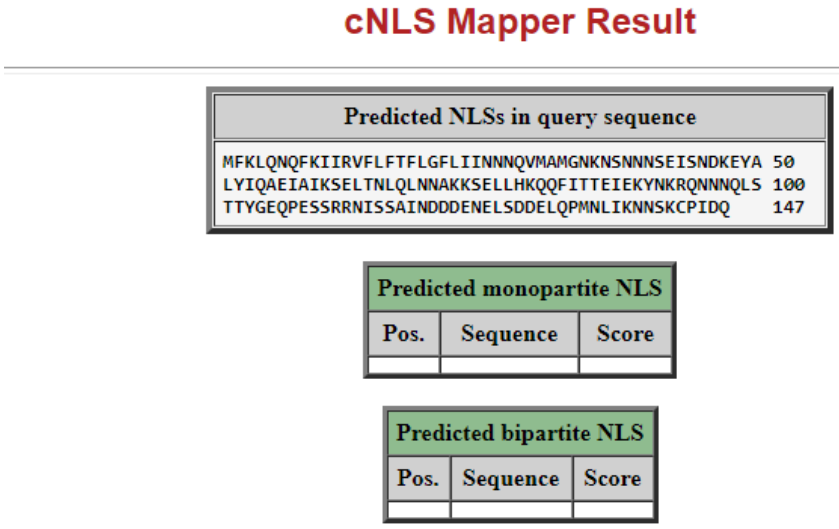


Figure 3.17 $EF2_{NGSD}$ having no NLS position.

All putative effector proteins were ligated into pGWB5 and pBRACT214 for transformation into plants and the symptoms observed are described in the next chapter.

3.4 Discussion

The NGSD contigs from a previous PhD student were retrieved from the NCBI Database (www.ncbi.nlm.nih.gov). Furthermore, although the SCWL genome has not been sequenced, it was predicted that this was likely to be relatively similar to NGSD (compared with any other currently sequenced phytoplasma genomes) because both the NGSD and SCWL belong to 16SrXI group (which also contains the Rice Yellow Dwarf (RYD) phytoplasma), although these are all in different 16SrXI subgroups.

Bioinformatics approaches, using the Sanger Artemis program, were used to analyse the sequence of the napier grass stunt genome to identify genes encoding small peptides with secretion signals that might be the equivalent to effector genes, since phytoplasmas are known to secrete effector proteins via the Sec-dependent pathway which requires signal peptides (SP) to transport the proteins to host cell (Bai *et al*., 2009). Kakizawa *et al*. (2001) identified the Sec proteins in OY phytoplasma to be SecA, SecE and SecY, and they found *secA* in plant phloem which was infected with phytoplasma, confirming the importance of the Sec system in phytoplasma-infected plants. It is also the case that phytoplasmas do not have the bacterial TypeIII or TypeIV secretion systems that are the typical secretion systems used by the main bacterial pathogens of plants (ie *Pseudomonas, Xanthomonas, Pectobacteria, Agrobacteria* etc.) for secreting effectors into plant cells. From the NGSD genome, fourteen potential effector genes were identified and amplified with the primers designed from this study, and following initial sequencing of these PCR products, six were subsequently identified for further study and primers were used to amplify these sequences (minus the secretion signals) (Figure 3.10 and 3.11). When these primers were tested on SCWL, two PCR products were amplified with *EF2* and *EF7* primers (Figure 3.11).

The other effector primers could not amplify from the SCWL genome, presumably because NGSD and SCWL are in different subgroups (Yadav *et al*., 2016), or even different groups (see Chapter 2) and there is presumably

significant sequence variation between them. Furthermore, Abeysinghe *et al*. (2016) studied NGSD and SCWL relationships and their result showed NGSD and SCWL were closely related (97%) when classified by the 16S rRNA and 85% similar which classified by the *SecA* gene. So it is probable that some parts of the NGSD and SCWL genomic DNAs are different and other parts are alike as shown for the SAP67 gene.

Indeed in whole genome analysis of the 16SrI-A Aster yellows witches' broom (AY-WB) phytoplasma with the 16SrI-B Onion yellows (OY) phytoplasma including Wheat Blue Dwarf (WBD) showed genome rearrangement and different genome sizes (Chen *et al*., 2014), which has analogies to the NGSD/SCWL situation, since these are different subgroups. Moreover, genes are unique; for example such as AY-WB has 671 genes but of these 79 genes are not found in OY (Bai *et al*., 2009; Chen *et al*., 2014). In addition, there are large sections of the genome that show inversions and chromosomal rearrangements with poor synteny between AY-WB and OY, particularly in the PMU/putative effector-rich regions, so some candidate effector genes in NGSD may not be found in SCWL because of evolution that phytoplasmas adapt to plant and insect hosts for multiplying and living (Kube *et al*, 2020).

The phytoplasma effectors require NLS for translocation to plant cell nuclei to destabilise plant development. In this chapter, $SAP11_{PnWB}$ was retrieved from the NCBI databases as a template for primer design and SAP11 protein sequences of NGSD and SCWL which were aligned to $SAP11_{PnWB}$ for

checking and the results showed there was an amino acid position mismatched not in the NLS and TCP-binding position. The $SAP11_{NGSD}$ and $SAP11_{SCWL}$ are also NLS and TCP-binding proteins and the proteins appear similar to $SAP11_{PnWB}$ so, the $SAP11_{NGSD}$ and $SAP11_{SCWL}$ probably translocate to plant cell nuclei. Using the NLS mapper online tools, $SAP11_{SCWL}$ was analysed for the NLS position and the result showed the score was 5.6 and the NLS sequence was longer than that of $SAP11_{PnWB}$. Moreover, the program showed the SAP11 NLS to be bipartite as is the case for $SAP11_{AYWB}$ and $SAP11_{PnWB}$ (Bai *et al*., 2009; Sugio *et al*., 2014). The result of analysis of the other putative effectors showed no NLS sites, suggesting that these proteins are secreted into the cytoplasm and do not translocate to the nuclei of cells. It is however likely that some of these putative effector proteins that showed hypothetical protein similarity to effectors even though they possessed no NLS sequences are indeed effectors, since the SAP54 effector and Tengu also have no NLS but have been shown to affect plant development (Bai *et al*., 2009; Hoshi *et al*., 2009; Chen *et al*., 2014; Rashid *et al*., 2018; Cho *et al*., 2019).

Chapter 4: Cloning and Transformation

4.1 Introduction

The detail of this chapter includes the cloning of each of the effector genes identified in chapter 3 and those from the other phytoplasma groups that are held in the University of Nottingham collection. It also includes the transformation of these into two model plants; a monocot, dicot, in order to observe whether the symptoms between monocot and dicot plants were broad or specific to the host range, and to determine whether classified the effector genes identified in NGSD and SCWL are responsible for stunt and white leaf.

4.1.1 Plant models

Arabidopsis thaliana is a dicot model plant belonging to the Crucifer (*Brassicaceae*), which is small, herbaceous, quick and easy to grow, has a small diploid genome (2n=10 and 125 Mb), is self-compatible and easy to transform. Furthermore, this plant can be grown on Petri plates under fluorescent lights and in a greenhouse, using pots or hydroponic systems (Meinke *et al*., 1998). Arabidopsis is suitable for studying the genetic, physiological and molecular biology of flowering plants and was the first plant to have a complete genome sequenced with around 27,000 genes that encode for about 35,000 proteins.

In terms of transformation, the simplest method to get the T_1 generation from a plant is the floral dip; however, the transformation efficiency is relatively low at around 0.76-1.57% for example in *A. thaliana* strain Col-0 (Ghedira *et al*., 2013).

As a monocot, *Brachypodium distachyon* (purple false brome) is a useful model, being an annual grass that is closely related to cereals such as wheat, barley, oat, perennial ryegrass and forage grasses. *Brachypodium distachyon* is a relatively new model plant with a small genome, estimated at 160 Mbp (26,000 coding genes) many of which are highly similar to wheat genes. Furthermore, it is a rapid growing plant and self-fertile, with simple growth requirements and diploidy in some genotypes. Additionally, molecular phylogenetic tree analysis (Figure 4.1) has revealed that *Brachypodium* is the ancestor of Pooidea, being more related to these crops than rice (Draper, 2001). Furthermore, whilst rice is beneficial for research studies as an alternative monocot, it has a much larger genome size and longer generation time (Vogel and Hill, 2008) (Table 4.1).

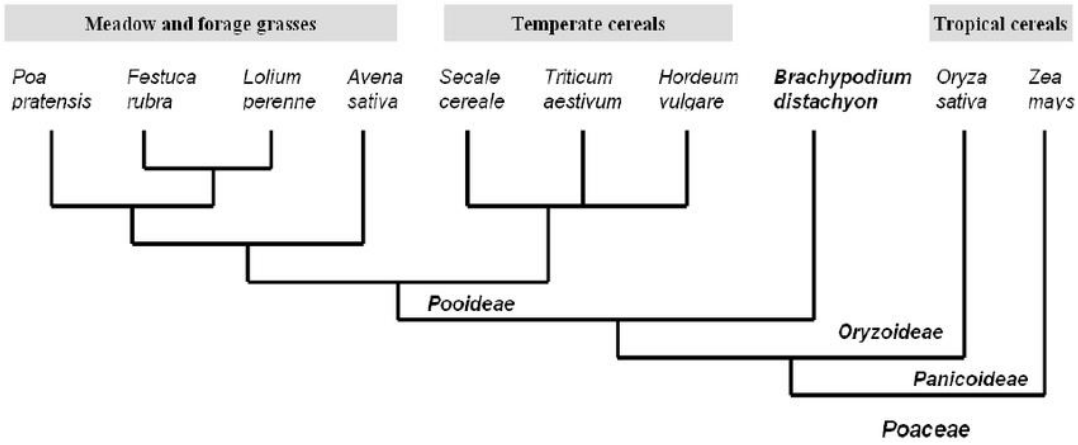


Figure 4.1 Phylogenetic relationship between Brachypodium and Pooideae (Draper *et al*.,2001).

Table 4.1 Comparison of Biological genomic traits among *Arabidopsis thaliana*, *Oryza sativa* and *Brachypodium distachyon* (Draper *et al*., 2001; Zhussupova *et al*., 2013).

Traits	***A.thaliana***	***B.distachyon***	***O.sativa***
Plant family	Crucifereae	Pooideae	Oryzodieae
Chromosome no. (2n)	10	10	24
Genome size (1C)	164 Mbp	160 Mbp	441 Mbp
Amount of repetitive DNA (%)	16%	12-15%	~20%
Breeding strategy	Self-fertile	Self-fertile	outbreeder
Life cycle (weeks)	8-10	11-18	20-30
Height at maturity (m)	~0.2	~0.2	1-1.2
Seed yield plant^{-1}	>1000	80-200	>1000
Growth requirements	Simple	Simple	Relatively specialized
Transformation efficiency (%)	0.5-4	~5	3-8

The transformation of *Brachypodium* requires embryogenic callus from immature embryos and was developed by Bablak *et al*. (1995). The embryogenic callus efficiency of *Brachypodium* depends on species and immature embryo age (Figure 4.2). There are two methods of transformation for *Brachypodium*. The first is biolistic transformation or particle bombardment in which transformed plants may contain many inserted gene copies as a result of rearrangement of the native DNA, and this method has been shown to be unsuitable for gene silencing studies because the expression level decreases in subsequent generations (Taylor and Fauquet, 2002). Another procedure is Agrobacterium-mediated transformation (Figure 4.3) which shows one or a few loci per each transformed *Brachypodium*; in comparison *Arabidopsis* and rice show on average 1.5 and 1.4 loci per transformed plant respectively (Scholthof *et al*., 2018).



Figure 4.2 Six stages of Brachypodium immature embryos. Scale bar = 5 mm (Vogel and Hill, 2008).

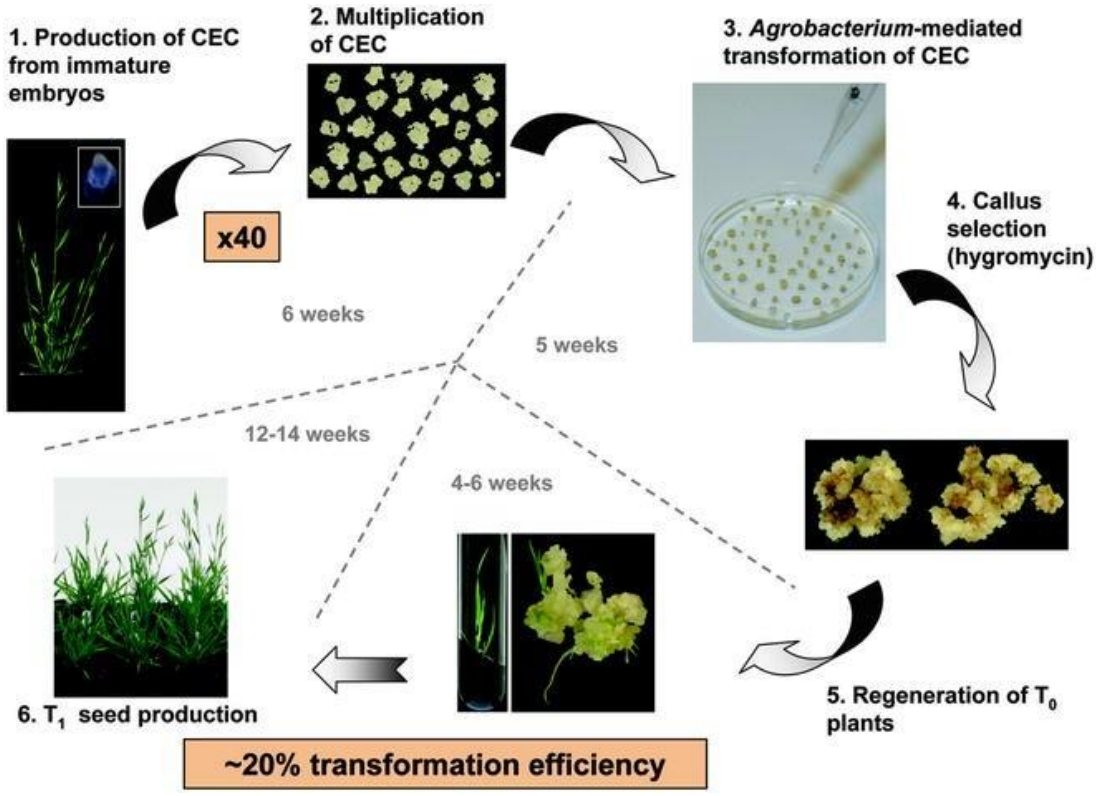


Figure 4.3 Flowchart of Brachypodium transformation by agrobacterium mediated procedure (Thole and Vain, 2012). There are 6 steps to regenerate transformed Brachypodium, the first step is sowing the Brachypodium seeds to get immature seed and the second step is callus induction from immature embryos. This step takes 6 weeks to get 40 times callus for the next step and the third step is Agrobacterium transformation and the transformed callus are then moved to selective medium in the fourth step, which takes 5 weeks. The fifth step is regeneration of the transformed callus, which takes 4-6 weeks and the final step is seed production, which takes 12-14 weeks to get the next generation seeds.

4.1.2 Phytoplasma effector transformation

In 2009, Hoshi *et al*. (2009) predicted secreted proteins from the OY genomic sequence using a bioinformatics program and they found a predicted virulence protein called PAM765 (Tengu). Tengu is a small peptide of about 38 residues so it is below the size exclusion limits in plant cells and can pass between them through the plasmodesmata. Additionally, when transformed into *A. thaliana* and also *Nicotiana benthamiana* Tengu caused witches' broom and dwarfism symptoms (Hoshi *et al*., 2009; Sugawara *et al*., 2013; Maejima *et al*., 2014a) because Tengu repressed *AFR6* and *ARF8*, regulating floral development. Consequently, flower maturation was impaired (Minato *et al*., 2014). The dwarfism and witches' broom phenotype are due to Tengu suppressing levels of phytohormones such as jasmonic acid and auxin in buds (Hoshi *et al*., 2009; Maejima *et al*., 2014).

In the case of AY-WB, a number of virulence proteins were also predicted from genome sequencing, which include the two secreted proteins, SAP11 and SAP54 which were shown to have different functions in plant hosts. These two virulence effectors were also discovered using a bioinformatics program to predict signal peptide sequences and nuclear localization signals (Bai *et al*., 2009). In the case of SAP11, this effector causes the host plant to show dwarfism and witches' broom in a similar way to Tengu and destabilises TCP transcription factors controlling cell proliferation in leaf morphogenesis. Moreover, SAP11 also directly decreases jasmonic acid levels (Sugio *et al*., 2011; Lu *et al*., 2014; Janik *et al*., 2017; Chang *et al*., 2018). SAP54 influences a different pathway to change the plant host. This effector affects flower

development and results in abnormal flowers, leaf-like flowers, sterile flowers and promotes attraction to flowers by leafhopper vectors (MacLean *et al*., 2011; Yang *et al.*, 2015; Orlovskis and Hogenhout, 2016).

Additionally, there is another effector gene, *PHYL1*, which is an ortholog of *SAP54* that is found in Peanut witches' broom (PnWB) phytoplasma (Hu *et al*., 2015). SAP54 and PHYL1 interact with a MADS domain protein and then the domain is degraded via the ubiquitin-proteasome pathway to cause flower malfunction (Maejima *et al*., 2014; Hu *et al*., 2015; Maejima *et al*., 2015).

Interestingly, there is an interlink between phytoplasmas and plant hosts including insect vectors. Some phytoplasmas are highly specific to plant and insect hosts, whilst others have broad host ranges. For example, aster yellows, '*Ca*. P. asteris' subgroup16SrI-B can be transmitted by insect vectors of more than 24 species and the phytoplasmas cause more than 70 diseases in numerous plant species (Weintraub and Beanland, 2006). Conversely, the 16SrI Maize Bunchy phytoplasma (MBSP) is specific to its plant host and when $SAP11_{MBSP}$ was transformed into *Arabidopsis* the transformed *Arabidopsis* showed branching instead of the leaf chlorosis that is found in infected Maize. It is therefore of interest to study whether the phytoplasma proteins have broad effects or are specific to particular plant hosts (Pecher *et al*., 2019).

Previous studies showed that effector proteins are conserved sequences in phytoplasma groups (Sugio *et al*., 2014; Cho *et al*., 2019). For example, *SAP11* gene in 16SrII-B in Oman was conserved even though the samples

were collected from different areas whilst the sequences was different from 16SrII-D (Alfafa witches' broom) even though they are in the same group (Al-Ghaithi *et al*., 2018). Furthermore, the SAP11 protein has two important regions to interact with plant genes; NLS and Coiled coil Domain (CCD) or TCP binding region. The NLS is important for translocation to the nucleus whilst the coiled coil domain is important to interact with plant genes to modify infected plants and make them suitable for phytoplasma colonisation and insect vector attraction (Bertaccini, 2007). Furthermore, the NLS and CCD regions are the least conserved (Sugio *et al*. 2014) and the CCD region shows some variation among SAP11 homologs (Figure 3.3) (Cho *et al*., 2019) so it makes the *SAP11* gene specific to plant hosts such as *SAP11*$_{\text{MBSP}}$ which shows the different symptoms between *Arabidopsis* and Maize (Pecher *et al*., 2019).

This chapter describes the cloning of the SAP11 like-putative effector genes from various phytoplasma, using bioinformatics for primer design and transformation procedures, into *A. thaliana* Col-0 and *B. distachyon* BD21 to observe the symptoms between dicot and monocot plants. It also describes transformation with other candidate effector genes from NGSD and SCWL.

4.2 Materials and Methods

4.2.1 DNA extraction

Eight isolates of phytoplasmas infecting periwinkle plants and uninfected plants (controls) were selected and used for genomic DNA extraction by the 2 X CTAB method (20 ml 1 M Tris-HCl pH 8.0, 56 ml 5 M NaCl, 16 ml 0.5 M EDTA, 4.0 g CTAB powder, 4.0 g PVP40 and 0.2% β-mercaptoethanol) (Table 4.2). Each sample of phytoplasma-infected periwinkle plant was extracted with 2 ml CTAB extraction buffer and homogenized at room temperature. After that, 800 μl of supernatant was transferred into a 1.5 ml new tube and incubated at 65°C for 30 min after which 500 μl of phenol (Sigma-Aldrich Co., UK) was added into each tube and vortexed vigorously and centrifuged at 3000 x g for 10 min at 4°C. The supernatant was transferred into a new tube and 600 μl of isopropanol was added and mixed gently and then samples were incubated at -20°C for at least 2 hours. Tubes were then centrifuged at 5000 x g for 15 min at 4°C, the supernatant was discarded and the pellet was washed with 500 μl of 70% ethanol (V/V) and centrifuged for 1 min. The supernatant was discarded and the pellet was dried at room temperature for 1.5-2 hours. Subsequently, the pellet was dissolved with TE buffer (Sigma-Aldrich Co., UK) and then the concentrations of genomic DNAs were measured by NanoDrop2000 Spectrophotometer (Thermo Fisher Scientific Inc.) and the concentration was diluted to 50 ng/μl and stored at -20°C until required.

Table 4.2 Phytoplasmas and 16Sr group samples used in the experiment

No.	Phytoplasma	16Sr group
1	RG (Rehmannia glutinosa)	I
2	SP (Soybean Phyllody)	II
3	VCP (Vinca Coconut Phyllody)	II
4	LNI (Plum Leptonecrosis)	II-B
5	PWB (Potato Witches' Broom)	IV
6	BLL (Brinjal Little Leaf)	V
7	EY (Elm Yellows)	V
8	AP (Apple Proliferation)	X
9	Periwinkle (Control)	-

4.2.2 LAMP assay: Phytoplasma preliminary test

Eight genomic DNAs from phytoplasma infected plants and one from a control plant were preliminary tested with LAMP assays with specific primers for each group of phytoplasma to confirm the presence of phytoplasmas. The Loop-Mediated Isothermal Amplification (LAMP) assay is a simple, rapid, specific and cost-effective diagnostic technique that was developed by Eiken Chemical Co.,Ltd and requires 4 or 6 different primes to 6 specific regions on the target gene and the amplification process runs at a constant temperature of 65°C for 20-30 min. For different phytoplasmas, specific primer sets have been developed targeting either the 16S rRNA or *SecA* gene. The primers are group specific for each group of phytoplasma such as 16SrI, 16SrII, 16SrIII, 16SrV,

16SrX, 16SrXII and 16SrXXII and do not amplify from other phytoplasma groups (Bekele *et al*., 2011).

For each set of eight LAMP 1x reactions a mastermix was made consisting of 46 μl water, 23 μl 10X primer mix and 115 μl Enzyme master mix (Optigene, UK). The 10x Primer Mix contained 16 μM FIP primer, 16 μM BIP, 2 μM F3, 2 μM B3, 4 μM LoopF, 4 μM LoopB in TE or water. Aliquots of 20 μl were then placed into each reaction tube and subsequently 1 μl of genomic DNA was added into each tube and then put into the LAMP machine with the following program: 63°C for 30 min and then anneal in which the DNA is heated to 94°C and allowed to cool back down to 72°C.

4.2.3 PCR of the *SAP11* gene

The *SAP11* nucleotide sequences of AYWB was used to design *SAP11* primers (Figure 4.4). The *SAP11* primers used are shown in Table 4.3. Nine genomic DNA samples were tested in PCR reactions using MangomixTaq™ DNA polymerase (Bioline Ltd.) and *SAP11* specific primers, including those extracted from infected plants noted in Table 4.2 and the SGP (16Sr I), BCRD (16Sr I) and CoP (16Sr II) from a DNA sample held in the University of Nottingham collection. The PCR reactions were performed using 1x concentration of MangoMix®, 1 μl of genomic DNA, 1 μl of 10 mM of each primer and the total volume was 25 μl. For amplification of *SAP11* from group 16SrII and group 16SrXI, the cycle condition was: denaturation at 95°C for 5 min for 1 cycle and then denaturation at 95°C for 40 sec, annealing at 50°C

for 40 sec, extension at 72°C for 1 min for 30 cycles and extension at 72°C for 10 min for one cycle. Subsequently, 5 μl of each PCR sample was electrophoresed on 1.5% agarose gels containing gel red™ (Biotium, USA).

Table 4.3 List of SAP11 gene primers and M13 primers for colony PCR

Primer Name	Primer sequences 5´-3´	Reference
SAP11F (For 16SrI)	ATG TTA AAA CTA AAA AAT CAA TTT AAA ATA AT	*SAP11*$_{AYWB}$ gene (Figure 4.4)
SAP11R (For 16SrI)	TTA TTT TTT AGA ATC ATC AGG TTG TTT TG	
SAP11nested R (For 16SrI and 16SrX)	ATG TCA CCT AAA AAA GAA TCT AAT GAT AAA AAA AG	
SAP11F (For 16SrII and 16SrX)	ATGATGCAAATAAAAAATAAATTAT	Anabestani *et al.* (2017)
SAP11R (For 16SrII and 16SrX)	TTATTTTTTAGAATCATCAGGC	
M13Fw	GTTTTCCCAGTCACGAC	Commercial Primers
M13Rev	CAGGAAACAGCTATGAC	

SAP11$_{AYWB}$ gene

ATGTTAAAACTAAAAAATCAATTTAAAATAATTAGTATTTATTTATTTGTATTTATA
GGTTTATTATTTATTAATATAAATCAAGTAATAGCTTCACCTAAAAAAGAATCTAG
TGATAAAAAAAGAGATATTCCGAAAATTAATAAATCAGAAGAAAAAAACAAAAAA
CAAAAAGAAGATATAAAAAGATTTTATACAATACATAAAGAATTTAAAGAATATT
CAATTGAAAAAAATAATGAAATTATAAAAATTTTAGAAAACCCTGAATTAATGGA
AATATTAAAACAAAAAGCCGAAGAGGAAACGAAAAATTTAAAAGAAGAAGGTTC
TTCTTCAAAACAACCTGATGATTCTAAAAAATAA

Figure 4.4 The *SAP11*$_{AYWB}$ gene used as template for primer design. Grey-colour letters show the position of the forward and reverse primer and underline letters indicate the positions of the semi-nested primer.

4.2.4 SAP11 PCR product sequencing

SAP11 PCR products were purified with the QiAqicuk PCR purification kit (Qiagen Ltd., UK) following the manufacturer's instructions and subsequently each PCR product was inserted into pGEM®-T easy (Promega, UK) for blue-white colony selection. The ligation conditions were 1x Rapid ligation buffer, 1 μl of 50 ng pGEM®-T easy vector, 2 μl of PCR product, 1 μl of T4 DNA ligase and total volume was 10 μl and mixed gently before incubation at 4°C overnight. In the next step, 5 μl of ligation reaction was added into 50 μl of JM109 competent cells (Promega, UK) and incubated on ice for 30 min after which the tubes were heat shocked at 42°C for 1.30 min in a heated block and returned immediately onto the ice and incubated for 5 min before 300 μl of LB medium was added. The tubes were then incubated at 37°C for 3 hours with shaking (220 rpm). Subsequently, 100 μl of transformation culture was plated on LB agar containing 100 μg/ml ampicillin, 0.5 mM IPTG and 80 μg/ml X-gal and then the plates were incubated at 37°C for 16-24 hours for blue-white colony selection. White colonies were selected and confirmed by the PCR method with M13 primers, which are specific primers for blue-white colony selection. Cycling conditions for colony PCR were as follows: denaturation at 95°C for 10 min for 1 cycle and then denaturation at 95°C for 40 sec, annealing at 50°C for 45 sec, extension at 72°C for 1 min for 30 cycles and extension at 72°C for 10 min for one cycle.

After that, 10 μl of PCR samples were analysed on 1% agarose gels containing gel red. Positive colonies were cultured in LB medium broth supplemented with 100 μg/ml ampicillin and then the effector inserted-plasmids were extracted with GeneElute™Plasmid Miniprep Kit (Sigma-Aldrich Co., UK), following the manufacturer's instructions for sequencing. Nucleotide sequences were analysed using the nucleotide Blastx (Basic Local Alignment Search Tool) program on the website www.ncbi.nlm.nih.gov and were aligned with full sequences of the *SAP11*$_{AY\text{-}WB}$ and *SAP11*$_{PnWB}$ gene.

4.2.5 *SAP11* genes, hypothetical genes and candidate effector genes construction

Following confirmation that the PCR products represented the full-length sequences, an A residue was added to these PCR products of the *SAP11* genes and hypothetical gene fragments from NGSD and SCWL (Chapter 3) at the 3′ end with an A-tailing kit (NEB, UK). The reaction was X μl of PCR-amplified DNA (50 ng), 5 μl of 1 X ThermoPol® Buffer, 10 μl of 1 mM dATP, 0.2 μl *Taq* DNA Polymerase, X μl H_2O and the total volume was 50 μl and then reaction tubes were incubated at 72°C for 20 min.

For the next step, PCR products with added A nucleotides were ligated into the pCR8 vector (pCR8 vector/TA cloning kit, Invitrogen UK) (Figure 4.5). The reaction set up was 1 μl A-tailing PCR product from previous step, 1 μl Salt solution, 1 μl pCR8 vector and 3 μl H_2O. Subsequently, the reaction tubes

were incubated at room temperature for 5 min and then 2 μl of ligated-vector were added into TOP10F′ *E.coli* competent cells (Invitrogen UK). The tubes were incubated on ice for 30 min, then heat shocked for 45 seconds at 42°C and immediately returned onto the ice box and incubated for 2 min. Subsequently, 350 μl of LB medium was added into the transformation tube with shaking at 37°C for 1 hour and after that, the LB solution was plated on LB agar containing 50 μg/ml spectinomycin and incubated at 37°C for 16-18 hours. Positive colonies were determined by PCR with gene specific primers and inoculated in LB broth containing 50 μg/ml spectinomycin and incubated overnight at 37°C with shaking. Plasmids were extracted using GeneElute™Plasmid Miniprep Kit (Sigma-Aldrich Co., UK), following the manufacturer's instructions for sequencing and then nucleotide sequences were compared with the previous sequences by the ClustalW online program (https://www.ebi.ac.uk/Tools/msa/clustalo/).

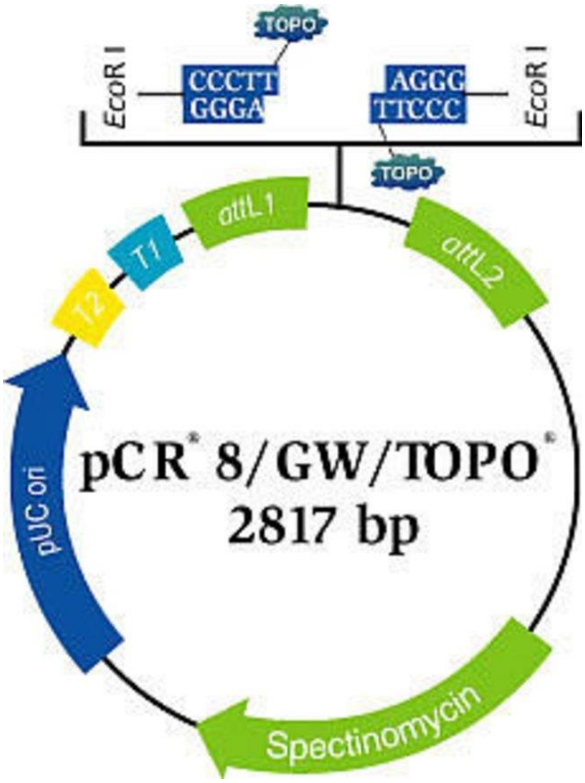


Figure 4.5 Map of the pCR8 plasmid. There are 2 sites of attL1 and attL2 which complement the attR1 and attR2 of pGWB5 and there is spectinomycin resistance for colony selection. Source: Invitrogen™ Gateway™ pCR™8/GW/TOPO™ TA Cloning Kit.

After that, the positive plasmids were combined with the Gateway pDestination vector. In this experiment, there were two types of vector; the pGWB5 vector has the CaMV 35S promoter (Figure 4.6) that is suitable for dicotyledon plants and the pBRACT214 vector has the Ubiquitin promoter which is suitable for monocot plants (Figure 4.7). Each of the pDestination vectors were combined with each of the effector-pCR8 vectors at attL1 and attL2 positions by Gateway™ LR Clonase™ II Enzyme mix kit (Invitrogen, UK) (Figure 4.8). The LR reaction was 1 μl Effector-pCR8 plasmid (100 ng), 1 μl pGWB5 (150

ng), 6 μl TE buffer pH 8.0 and 2 μl LR Clonase II enzyme mix. The reaction tubes were incubated at 25°C for 3 hours and then 1 μl of proteinase K was added to stop the reaction at 37°C for 10 min. Three microlitres of LR reaction solution was transformed into TOP10F′ *E.coli* competent cells with heat shocked using the procedure as described in the previous step. Three hundred microlitres of LB medium was added into the tube with shaking at 37°C for 3 hours and the solution was plated on LB agar containing 50 μg/ml kanamycin and incubated at 37°C for 16-18 hours. Colonies were determined for the correct direction of the insert with specific reverse primer and attB1 adapter forward primer by PCR. The positive colonies were inoculated in LB broth medium with 50 μg/ml kanamycin overnight with shaking and then plasmids were extracted using GeneElute™Plasmid Miniprep Kit (Sigma-Aldrich Co., UK) following the manufacturer's instructions for sequencing. Nucleotide sequences were compared with ClustalW online program.

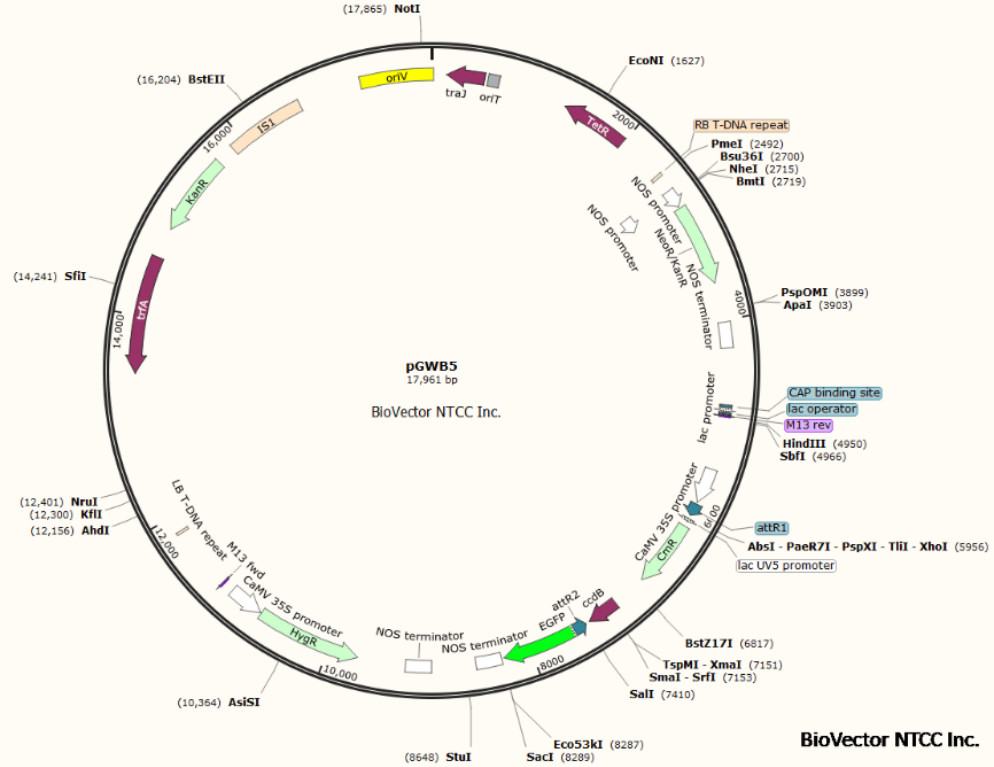


Figure 4.6 Map of the pGWb5 plasmid. There are 2 sites of attR1 and attR2 which complement the attL1 and attL2 of pCR8 and there are the CaMV 35S promoter and NOS terminator. There are also Kan^R encoding kanamycin resistance for bacterial colony selection in bacteria and Hyg^R encoding hygromycin resistance for plant selection.

Source: http://www.biovector.net/product/420631.html

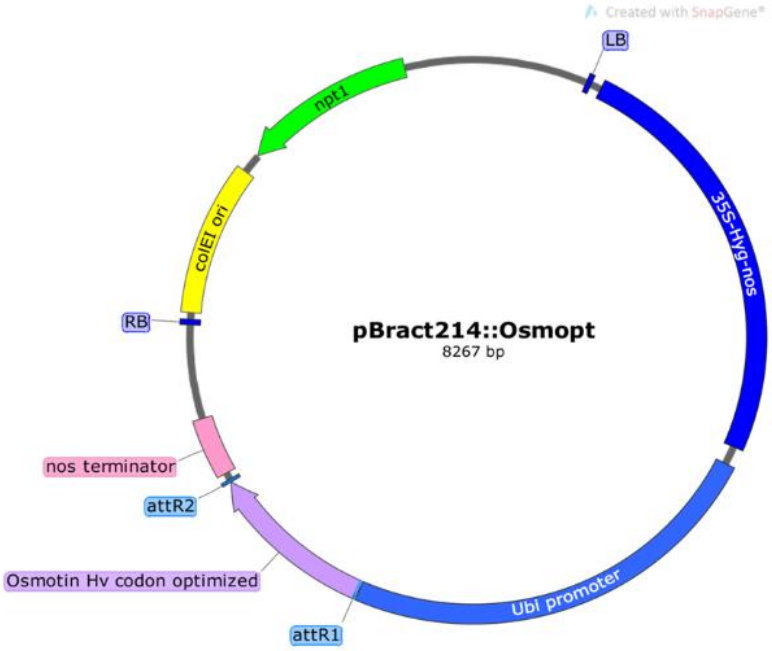


Figure 4.7 Map of the pBRACT214 plasmid. There are 2 sites of attR1 and attR2 which complement the attL1 and attL2 of pCR8 and there are the Ubiquitin promoter and NOS terminator. There is Hyg^R encoding hygromycin resistance for plant selection (Viktorova et al., 2019).

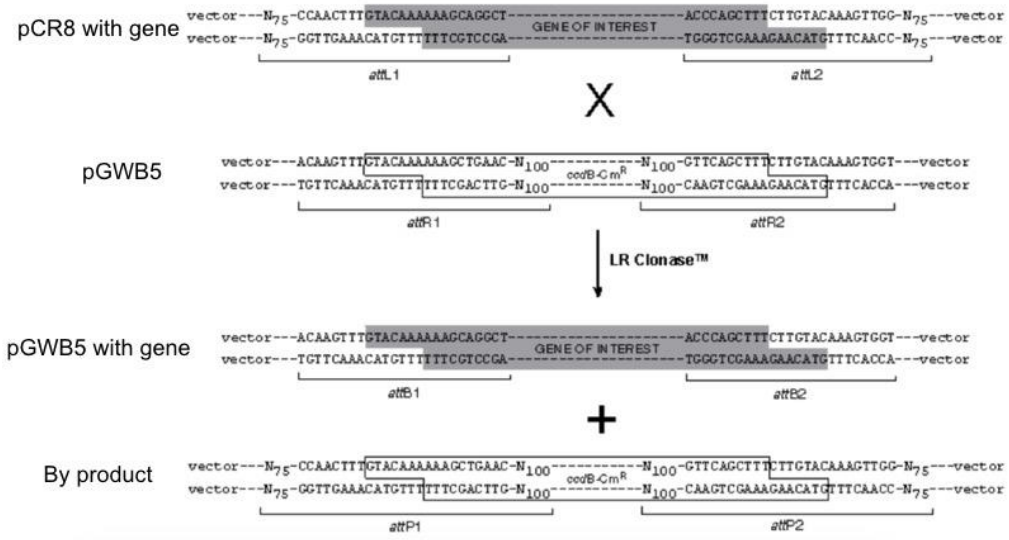


Figure 4.8 Schematic diagram of Gateway™ LR Clonase™ II Enzyme mix kit procedure. Source: Invitrogen Gateway™ LR Clonase™ II Enzyme mix kit.

4.2.6 *Agrobacterium* competent cell preparation

In this step, the effector gene vectors were transformed into *Arabidopsis* and *Brachypodium* using different methods for transformation. For *Arabidopsis*, the effector gene vectors were transformed into flowers by the floral dip method and *Agrobacterium tumefaciens* strain GV3101 was appropriate for this method. On the other hand, *Agrobacterium tumefaciens* strain AGL1 was used for *Brachypodium* callus transformation because this strain is a more super-virulent strain than GV3101.

Agrobacterium tumefaciens strain GV3101 and AGL1 were streaked on LB agar containing 30 μg/ml rifampicin for Ti plasmid selection and allowed to grow for 2-3 days at 28°C. *Agrobacterium* colonies were picked and

transferred into 100 ml LB broth supplemented with 30 μg/ml rifampicin and grown overnight with shaking at 28°C. Fifty millilitres of *Agrobacterium* solution was added into 500 ml LB medium and grown until the OD_{600} was approximately 1-1.5. The *Agrobacterium* solution was then transferred into 50 ml cold centrifuge tubes and transferred immediately onto ice for 20 min before centrifugation at 4000 x g for 15 min at 4°C. The supernatant was discarded and then 25 ml 10% cold glycerol was added and gently resuspended and then centrifuged at 4000 x g for 15 min at 4°C, after which the supernatant was decanted and repeatedly resuspended with 25 ml 10% cold glycerol before centrifugation. Afterwards, the supernatant was discarded and 10 ml of 10% cold glycerol was added and centrifuged at 4000 x g for 15 min at 4°C. In the last step, the supernatant was discarded and the pellet was gently resuspended with 2 ml 10% cold glycerol and aliquoted into 40 μl in pre-chilled 0.5 ml tubes in liquid nitrogen and stored at -80°C.

4.2.7 *Agrobacterium* transformation

The positive plasmids of effector-pGWB5 and effector-pBRACT214 were transformed into *A. tumefaciens* GV3101 and AGL1 strain respectively by electroporation. One microlitre of effector-pGWB5 or effector-pBRACT214 (100 ng) was added into 40 μl of *A. tumefaciens* competent cells and mixed gently and placed on ice. After that, the solution was transferred to an electroporation cuvette and moved into the electroporation arm and set up to pulse for *Agrobacterium* cells (Biorad, UK). After pulsing, the cuvette was removed and 300 μl of LB medium was added into the cuvette after which the

solution was transferred to a microcentrifuge tube with shaking at 28°C for 3 hours. Subsequently, 50 μl of the solution was plated on LB agar containing 50 μg/ml kanamycin and 30 μg/ml rifampicin and then the plates were incubated at 28°C for 2-3 days. Colonies were checked with specific primers by PCR. Positive colonies were inoculated into LB broth, which contained 50 μg/ml kanamycin and 30 μg/ml rifampicin and shaken at 28°C for 2-3 days before collecting in 30% glycerol and storing at -80°C for the next step.

4.2.8 *Arabidopsis* transformation: Floral dip method

(Clough and Bent, 1998)

Arabidopsis thaliana Col-0 was grown at a density of 2-3 plants per small pot (9 cm diameter) until they had formed inflorescence shoots. *Agrobacterium tumefaciens* strain GV3101, with the effector-plasmid vector, was grown up in 3 ml LB medium including 30 μg/ml rifampicin and 50 μg/ml kanamycin and shaken at 200 rpm at 28°C overnight. The next day, the 3 ml LB starter was transferred into 300 ml LB (for 3 pots) after which 30 μg/ml rifampicin and 50 μg/ml kanamycin were added and shaken at 28°C overnight until OD_{600nm} was approximately 0.8-1.0. Subsequently, *Agrobacterium* solution was centrifuged at 4000 x g for 10 min for antibiotic removal and then the *Agrobacterium* pellet was resuspended with resuspension solution which contained 0.654 g ½ MS salt (Sigma-Aldrich Co., UK), 15 g sucrose, 150 μl Tween20 and 300 ml water.

The solution was mixed gently until completely dispersed. After that, the solution was poured into a dipping tray and then *Arabidopsis* flowers were dipped into the solution for 1.30 min. The dipped plant was then covered with clear-plastic wrap to maintain humidity for 24 h and laid on the tray overnight; moreover, the dipped plant was not exposed to excessive light. The next day, the dipped plant was placed back to vertical. The floral dip method was repeated one week later on the same plants. Subsequently, dipped plants were watered until seeds become yellow (mature), then watering was stopped and dried seeds were harvested.

4.2.9 Transformed *Arabidopsis* selection

Selection-Petri dishes were prepared with 0.8% of ½ MS (Murashigi and Skoog) (Sigma-Aldrich Co., UK) agar plus 50 μg/ml hygromycin without sugar. Subsequently, T_1 Arabidopsis seeds were sterilised with 5% bleach and 0.05% Tween20 and mixed occasionally over 5 min and then the solution was decanted. Seeds were rinsed with sterile water 5 times. In the next step, sterile seeds were added into 1 ml sterile water for 500-800 seeds and then the seeds were poured into the selection-Petri dishes and gently mixed to disperse the seeds. The selection-Petri dishes were dried in the laminar flow hood for about 15 min and then the selected Petri dishes were sealed with surgical tape and incubated in the cold room or 4°C for 2-3 nights. The selection-Petri dishes were then transferred to the growth room with a controlled environment at 24°C under 16 hours light for 14 days. After 14 days, transformed plants should have green cotyledons in the selection-Petri dishes and the resistant plants

were transferred into moist soil and grown under plastic wrap for 1 week to keep moist. The T_1 transformed *Arabidopsis* grew until they formed siliques.

4.2.10 *Brachypodium* callus induction and transformation (Alves *et al*., 2009; Thole and Vain, 2012; Bragg *et al*., 2015)

4.2.10.1 Seed sterilization

In the case of *Brachypodium*, callus induction is different from other plants because it is successful in immature embryos whilst for other plants such as rice, corn etc, it is successful in mature embryos. First of all, mature seeds of *Brachypodium* wild type Bd21 were sown in soil and the pots were vernalized for 2 weeks at 4ºC and moved to a glasshouse at 23ºC for 4-6 weeks under 20 hours light. During this stage, plants formed spikelets approximately 7-16 days after this stage, and the immature embryos were harvested when they were very small and translucent (<0.5 mm). The individual immature seeds were harvested and kept in a small amount of water in a 50 ml Falcon tube to keep seeds moist and these could be stored for a few hours. Before sterilization, the lemma was peeled (Figure 4.9) and the seeds were then washed in 70% ethanol for 30 sec and the supernatant decanted. For the next step, 5% bleach (NaOCL) and 0.05% Tween-20 solution was added into the tubes and gently shaken for 4 min and the supernatant was discarded and then rinsed with sterile water for 3 times. Subsequently, the seeds were poured into a Petri dish for immature embryo dissection.

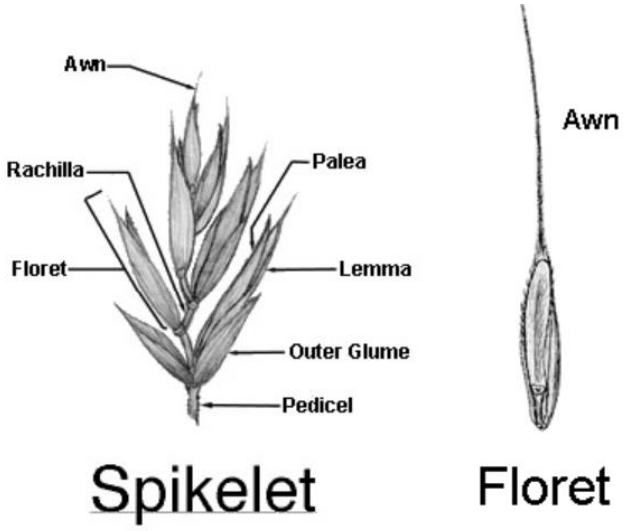


Figure 4.9 The structure of a Brachypodium spiklet and individual floret.

Source: http://www.csdl.tamu.edu/FLORA/ta es/tracy/610/brachypodium.html

4.2.10.2 Callus induction

Basic solid medium for callus culture or MSB3 consists of 4.1 g/L of MS powder (Sigma-Aldrich Co., UK), 25 μg/ml of 2,4-D (Sigma-Aldrich Co., UK), 30 g/L of sucrose and 2 g phytagel (Sigma-Aldrich Co., UK), adjusted to pH 5.8 with KOH and autoclaved. When the MSB3 cooled down, 10 ml of M5 vitamin was added and aliquoted into the Petri-dish plates. For callus induction medium, 0.6 mg/ml of $CuSO_4.5H_2O$ was added to the MSB3 before sterilization.

The 100x M5 vitamin consists of 0.04 g nicotinic acid, 0.05 g thiamine-HCl, 4 g cysteine, 0.2 g glycine, and 0.04 g pyridoxine-HCl in a final volume of 1 L

deionised H_2O with pH adjusted to 5.8 by adding KOH. Following filter-sterilisation, the solution was stored in aliquots of 50 ml at −20°C in the dark.

After sterilization, the palea was removed from seeds to reveal the translucent immature embryo inside. The immature embryo is opposite the pollen and near the tip of the seed. The immature embryo was dissected out of the immature seed using forceps to anchor the seed by stabbing and another set of fine forceps was used to take the immature embryo out of the seed and placed on MSB3 medium with the scutellar side down (Figure 4.10). The plates were sealed with surgical tape and incubated at 28°C in the dark for 3 weeks and then the subculture period was reduced to 2 weeks and 1 weeks, respectively. During the first period of callus induction, yellow callus and amorphous callus would arise at the 2nd or 3rd week. For subculture, yellow callus was only selected for transformation and the callus was broken into a few pieces and transferred onto fresh MSB3 containing 0.6 mg/ml of $CuSO_4.5H_2O$. At the 5th week, the yellow callus was suitable for transformation; however, they were subcultured for an additional week before transformation and one plate contained 50 calli.



Figure 4.10 Immature Brachypodium embryo showed scutella side down (Betekhtin *et al*., 2016).

4.2.10.3 *Brachypodium* callus *Agrobacterium* transformation

Two days prior to transformation, *Agrobacterium* sp. strain AGL1 containing plasmid vector was streaked on MGL medium (5 g tryptone, 2.5 g yeast extract, 5 g NaCl, 5 g mannitol, 0.1 g $MgSO_4$, 0.25 g K_2HPO_4 and 1.2 g glutamic acid with the volume adjusted to 1 L and pH 7.2) containing 30 μg/ml of rifampicin and 50 μg/ml of kanamycin for Ti plasmid and plasmid vector selection, respectively. The plates were then incubated at 28°C for two nights after which the *Agrobacterium* was scraped from half of the plate and suspended in 10 ml MSB3 medium solution containing 45 μg/ml of acetosyringone (Sigma-Aldrich Co., UK) and 0.1% Synperonic PE/F68 (Sigma-Aldrich Co., UK) and then vortexed for dispersion. The suspension was measured at $OD_{600\ nm}$ = 0.6. Subsequently, the callus was moved into

sterile 50 ml Falcon tubes and the callus was flooded with the 10 ml of *Agrobacterium* suspension for 5 min at room temperature and mixed gently.

Subsequently, the *Agrobacterium* suspension was removed with a 1 ml micropipette until there were no bubbles and the callus was poured into the Petri-dish plate contained 2 sterilized filter papers for liquid removal in order to limit overgrowth of *Agrobacterium* under laminar flow hood until dry. The callus was then transferred to a new Petri-dish plate prepared with 1 piece of sterile filter paper by hand-pickup and the callus were spread around the plate. In this step, the callus was divided into multiple plates and sealed with surgical tape. Subsequently, the transformed callus plates were incubated at 23°C in the dark for 48 hours and an empty plate was put on the top of the callus stack for moisture limitation. In the next step, the transformed callus was transferred into selective medium which was MSB3 containing 50 μg/ml of hygromycin and 300 mg/L of Timentin for 2 weeks at 28°C in dark conditions.

4.2.10.4 Regeneration of transformed plants

Two weeks after selection, the transformed plants were transferred onto MSMO medium which is Murashige and Skooge minimal organic (MSMO, Sigma-Aldrich Co., UK) containing 30 g/L of maltose, 300 mg/L Timentin and 30 μg/μl hygromycin, 0.1 mg/ml of kinetin and 2.5 g/L phytagel and then the transformed callus was incubated for 3-5 weeks at 28°C under 16 hours photoperiod. Subsequently, individual shoots were transferred to MS medium boxes containing 30 g/L of sucrose with 150 mg/L of Timentin after which the

transformed plants were cultured for 3 weeks at 28°C under 16 hours photoperiod. Subsequently, the plants were transferred to MS medium containing 30 g/L sucrose, 5 g/L phytagel, 4 g/L charcoal, 150 mg/L Timentin and 10 ml 100x B5 vitamin solution until the transformed plants were fully rooted and then they were moved into pots and grown at 23°C under 20 hours photoperiod, covered with a lid for a week and then the lid was opened for growing in normal conditions until they formed the spiklet (T_1 seeds).

The 100x B5 vitamin consists of 100 mg nicotinic acid, 1 g thiamine-HCl, 10 g mo-inositol and 100 mg pyridoxine-HCl in a final volume of 1 L deionised H_2O; with the pH was adjusted to 5.8 by adding KOH and filter-sterilised and stored in aliquots of 50 ml at −20°C in the dark.

4.2.11 Transformed plant screening

The T_1 transformed *Arabidopsis* and T_0 transformed *Brachypodium* were grown in the glasshouse at 23°C. The transformed plants that had effector genes were compared to wild type and plants transformed with vector only by PCR with specific primers to confirm effector gene insertion into host plant genomic DNA. The positive-transformed plants continued growing until seed formation. The next generation seeds were selected on ½ MS agar containing 50 μg/ml hygromycin. The resistant plants were sown in soil until the next step.

For PCR screening, genomic DNA extractions from transformed plants and wild types were done using Thermo Scientific Phire Plant Direct PCR master Mix (ThermoFisher Scientific, UK). The small piece of leaf was placed into 20 µl dilution buffer and then the leaf was crushed with a pipette tip by pressing briefly against the tube wall. The tube was then spun down and 1 µl of supernatant was used as a template in PCR with specific primers for effector genes. The PCR conditions were as above and the amplification cycle was: denaturation at 95°C for 5 min for 1 cycle and then denaturation at 95°C for 30 sec, annealing at 50°C for 45 sec, extension at 72°C for 1 min for 30 cycles and extension at 72°C for 10 min for one cycle. After that, 5 µl of PCR samples were analysed on 1.5% agarose gels containing gel red™ (Biotium, USA).

4.3 Results

4.3.1 LAMP results

The LAMP technique is a relatively new method for gene amplification and is simple and rapid to use for diagnostics (Bekele *et al*., 2011). In this study, the LAMP technique was the first step to confirm the presence of phytoplasmas in the plants, using group specific primers and universal primers. LAMP results showed each sample was within the expected 16Sr group of phytoplasma and the negative controls of periwinkle plants and non-template control showed no amplification and annealing temperature. The LAMP results (Table 4.4) showed the time/annealing temperature from the samples was the same as the positive control in each specific group. For example, the RG sample in

16SrI showed 22/83.76 whist the 16SrI positive control showed 22.3/83.62 etc. Based on the LAMP results, 16SrI, 16SrII and 16SrX group samples were chosen for SAP11 amplification with specific primers (Table 4.4) along with frozen DNA stock samples of BCRD, CoP and SGP in groups 16SrI and 16SrII.

Table 4.4 Time to amplification and annealing temperature from LAMP experiments

Group / Sample	I	II	III	V	VI	X
RG	22.00/ 83.76	-	-	-	-	-
SP	-	16.15/ 80.92	-	-	-	-
VCP	-	11.00/ 80.15	-	-	-	-
EY	-	-	-	20.00/ 87.08	-	-
LNI	-	-	11.45/ 84.05	-	-	-
BLL	-	-	-	14.30/ 87.03	-	-
PWB	-	-	-	-	13.15/ 85.56	-
AP	-	-	-	-	-	12.45/ 85.97
NGSD	-	-	-	-	-	9.30/ 82.68
periwinkle	-	-	-	-	-	-
Non template control	-	-	-	-	-	-
Positive	22.30/ 83.62	12.15/ 80.76	6.45/ 84.10	15.15/ 87.38	11.30/ 86.74	16.45/ 80.40

4.3.2 PCR results

PCR products of the *SAP11* genes of AP, BCRD, CoP, SGP and VCP are shown in Figure 4.11. The PCR products were purified and ligated into pGEMT-easy and the ligated-vectors were transformed into competent cells for blue-white colony selection. The white colonies were screened by PCR with M13 forward and reverse primers and white colonies that showed PCR products of the correct size were inoculated into LB with 50 µg/ml of ampicillin and then extracted for sequencing.

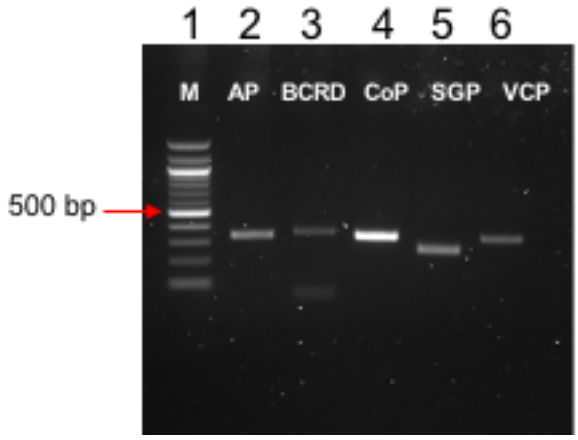


Figure 4.11 Candidate SAP11 PCR products from specific primers by PCR method. Lanes (1) 100 bp ladder, (2) PCR product from AP, (3) PCR product from BCRD, (4) PCR product from CoP, (5) PCR product from SGP and (6) PCR product from VCP.

Following sequencing, samples were analysed with the Blastx and ClustalW programs and compared with SAP11 protein sequences from NCBI

databases. Based on the Blastx program, the sequences for AP, CoP and VCP were similar to $SAP11_{PnWB}$, whilst BRCD and SGP were similar with a hypothetical phytoplasma protein (Table 4.5 and Figure 4.12). Furthermore, the ClustalW program showed conserved sequences between samples and SAP11 proteins.

Table 4.5 List of protein similarity and identity from NCBI database

Sample (group)	Protein similarity	Identity (%)
AP(X)	effector, AYWB SAP11-like protein [Peanut witches'-broom phytoplasma]	98
BCRD (I)	hypothetical protein [Vaccinium witches'-broom phytoplasma]	99
CoP (II)	effector, AYWB SAP11-like protein [Peanut witches'-broom phytoplasma]	100
SGP (I)	hypothetical protein [Poinsettia branch-inducing phytoplasma]	97
VCP (II)	effector, AYWB SAP11-like protein [Peanut witches'-broom phytoplasma]	100

Table 4.6 List of protein sequences

Sample	group	Protein translation
AP	X	MMQIKNKLYFLPLFLMSFLGLFLLINTNPVIAAPEKNDKGKKIASS EKQEKTTKKDISQYYELYNTLENYSEEDRNKIIQMLSDSQTLKIL QEEALKSKKKGSSSKKPDDSKK*
BCRD	I	MLKLKNQFKIISIYLFVFIGLLFINVNQVIASPKKESSDKKRDISEIN KSEEKNKKQKEDIKRFYTIHKEFKEYSIEKNNEIIKILENPELMEIL KQKAEEETKNLKEEGSSSKQPDDSKK*
SGP	I	MSPKKESNDKKRDISEINKSEEKNKKQKEDIKRFYTIHKEFKEYS IEKNNEIIKILENPELMKILKQKAEEETKNLKEEGSSSKQPDDSKK *
CoP	II	MMQIKNKLYFLPLFLMSFLGLFLLININPVIAAPEKNDKGKKIASS EKQEKTTKKDISQYYELYNTLENYSEEDRNKIIQMLSDSQTLKIL QEEALKSKKKGSSSKKPDDSKK*
VCP	II	MMQIKNKLYFLPLFLMSFLGLFLLININPVIAAPEKNDKGKKIASS EKQEKTTKKDISQYYELYNTLENYSEEDRNKIIQMLSDSQTLKIL QEEALKSKKKGSSSKKPDDSKK*

From the 16SrI phytoplasmas, SGP and BCRD, two protein sequence were obtained and compared with the reference sequence of $SAP11_{AY\text{-}WB}$, and the protein sequences showed that there are three positions in which the proteins varied from $SAP11_{AY\text{-}WB}$ (Figure 4.13). At these positions, the changes are from I (Isoleucine) to V (Valine), P (Proline) to S (Serine) and K (Lysine) to E (Glutamic acid). Additionally, the hypothetical protein from SGP lacked some amino acids; however, the others were the same amino acid sequences as for the BCRD hypothetical protein (Figure 4.12).

```
BCRP      MLKLKNQFKIISIYLFVFIGLLFINVNQVIASPKKESSDKKRDISEINKSEEKNKKQKED
SGP       ------------------------------MSPKKESNDKKRDISEINKSEEKNKKQKED
                                        ******.**********************

BCRP      IKRFYTIHKEFKEYSIEKNNEIIKILENPELMEILKQKAEEETKNLKEEGSSSKQPDDSK
SGP       IKRFYTIHKEFKEYSIEKNNEIIKILENPELMKILKQKAEEETKNLKEEGSSSKQPDDSK
          ********************************:****************************

BCRP      K*
SGP       K*
          **
```

Figure 4.12 Protein alignment of group 16SrI hypothetical protein.

```
BCRD      MLKLKNQFKIISIYLFVFIGLLFINVNQVIASPKKESSDKKRDISEINKSEEKNKKQKED     60
SGP                                   MSPKKESSDKKRDISEINKSEEKNKKQKED     60
AY-WB     MLKLKNQFKIISIYLFVFIGLLFININQVIASPKKESSDKKRDIPKINKSEEKNKKQKED     60
                                  :    :************* :**************

BCRD      IKRFYTIHKEFKEYSIEKNNEIIKILENPELMEILKQKAEEETKNLKEEGSSSKQPDDSK     120
SGP       IKRFYTIHKEFKEYSIEKNNEIIKILENPELMEILKQKAEEETKNLKEEGSSSKQPDDSK     120
AY-WB     IKRFYTIHKEFKEYSIEKNNEIIKILENPELMEILKQKAEEETKNLKEEGSSSKQPDDSK     120
          ************************************************************

BCRD      K       121
SGP       K       121
AY-WB     K       121
          *
```

Figure 4. 13 Protein alignment of SAP11 protein of group 16SrI phytoplasmas.

For the 16SrII and 16SrX phytoplasmas, the SAP11s from CoP and VCP (16SrII) and AP (16SrX) were compared with the previously identified SAP11 from Peanut witches' broom (16SrII) (Figure 4.14). The protein sequences of $SAP11_{CoP}$ and $SAP11_{VCP}$ are identical to the $SAP11_{PnWB}$, and the $SAP11_{AP}$-effector protein is also well conserved with $SAP11_{PnWB}$, despite this being from a different 16Sr group. Only one amino acid position is different in $SAP11_{AP}$ from the others, which is T (Threonine) instead of I (Isoleucine) (Figure 4.15).

```
AP        MMQIKNKLYFLPLFLMSFLGLFLLINTNPVIAAPEKNDKGKKIASSEKQEKTTKKDISQY
CoP       MMQIKNKLYFLPLFLMSFLGLFLLININPVIAAPEKNDKGKKIASSEKQEKTTKKDISQY
VCP       MMQIKNKLYFLPLFLMSFLGLFLLININPVIAAPEKNDKGKKIASSEKQEKTTKKDISQY
          ************************ ***********************************

AP        YELYNTLENYSEEDRNKIIQMLSDSQTLKILQEEALKSKKKGSSSKKPDDSKK*
CoP       YELYNTLENYSEEDRNKIIQMLSDSQTLKILQEEALKSKKKGSSSKKPDDSKK*
VCP       YELYNTLENYSEEDRNKIIQMLSDSQTLKILQEEALKSKKKGSSSKKPDDSKK*
          ******************************************************
```

Figure 4.14 Protein alignment of SAP11 16SrI and 16SrX.

```
AP        MMQIKNKLYFLPLFLMSFLGLFLLINTNPVIAAPEKNDKGKKIASSEKQEKTTKKDISQY
PnWB      MMQIKNKLYFLPLFLMSFLGLFLLININPVIAAPEKNDKGKKIASSEKQEKTTKKDISQY
CoP       MMQIKNKLYFLPLFLMSFLGLFLLININPVIAAPEKNDKGKKIASSEKQEKTTKKDISQY
VCP       MMQIKNKLYFLPLFLMSFLGLFLLININPVIAAPEKNDKGKKIASSEKQEKTTKKDISQY
          ************************ ***********************************

AP          YELYNTLENYSEEDRNKIIQMLSDSQTLKILQEEALKSKKKGSSSKKPDDSKK     113
PnWB        YELYNTLENYSEEDRNKIIQMLSDSQTLKILQEEALKSKKKGSSSKKPDDSKK     113
CoP         YELYNTLENYSEEDRNKIIQMLSDSQTLKILQEEALKSKKKGSSSKKPDDSKK     112
VCP         YELYNTLENYSEEDRNKIIQMLSDSQTLKILQEEALKSKKKGSSSKKPDDSKK     113
            ************************************************
```

Figure 4.15 Protein alignment of hypothetical protein of group II and X phytoplasmas.

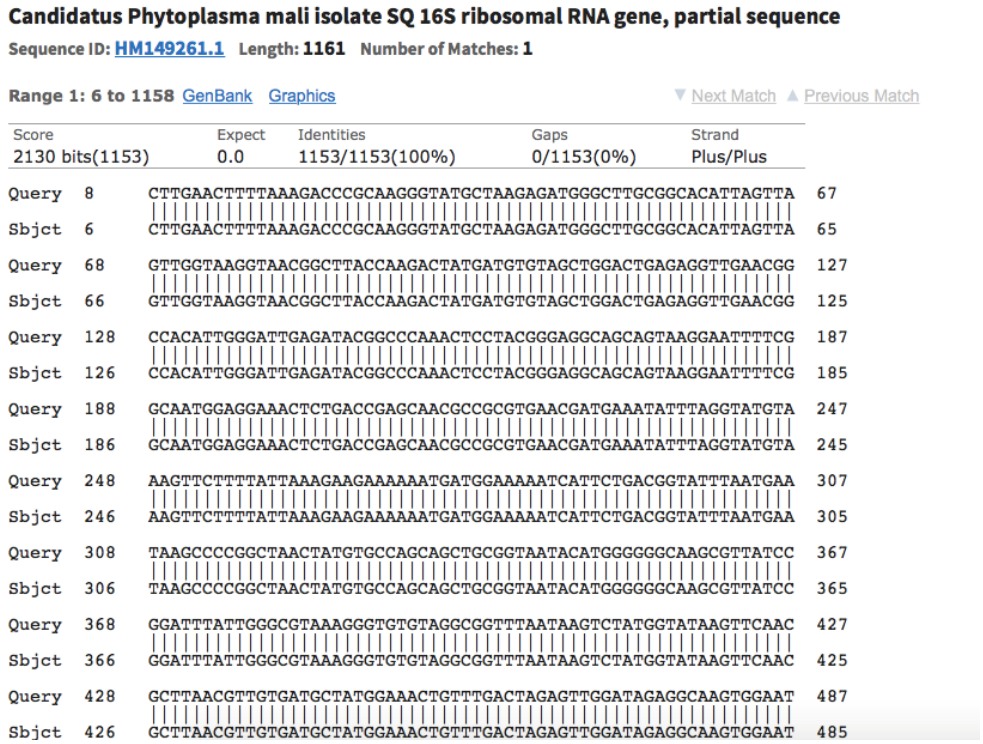
Interestingly, the protein sequence of the group 16SrX phytoplasma is the same as group XI (see chapter 3), with the same change of I to T (Figure 4.16) at the same position, with the other positions being completely conserved and also conserved to $SAP11_{PnWB}$.

```
PnWB_SAP11          MMQIKNKLYFLPLFLMSFLGLFLLININPVIAAPEKNDKGKKIASSEKQEKTTKKDISQY
CoP                 MMQIKNKLYFLPLFLMSFLGLFLLININPVIAAPEKNDKGKKIASSEKQEKTTKKDISQY
VCP                 MMQIKNKLYFLPLFLMSFLGLFLLININPVIAAPEKNDKGKKIASSEKQEKTTKKDISQY
AP                  MMQIKNKLYFLPLFLMSFLGLFLLINTNPVIAAPEKNDKGKKIASSEKQEKTTKKDISQY
NGSD                MMQIKNKLYFLPLFLMSFLGLFLLINTNPVIAAPEKNDKGKKIASSEKQEKTTKKDISQY
SCWL                MMQIKNKLYFLPLFLMSFLGLFLLINTNPVIAAPEKNDKGKKIASSEKQEKTTKKDISQY
                    ************************* *********************************

PnWB_SAP11          YELYNTLENYSEEDRNKIIQMLSDSQTLKILQEEALKSKKKGSSSKKPDDSKK    113
CoP                 YELYNTLENYSEEDRNKIIQMLSDSQTLKILQEEALKSKKKGSSSKKPDDSKK    112
VCP                 YELYNTLENYSEEDRNKIIQMLSDSQTLKILQEEALKSKKKGSSSKKPDDSKK    113
AP                  YELYNTLENYSEEDRNKIIQMLSDSQTLKILQEEALKSKKKGSSSKKPDDSKK    113
NGSD                YELYNTLENYSEEDRNKIIQMLSDSQTLKILQEEALKSKKKGSSSKKPDDSKK    113
SCWL                YELYNTLENYSEEDRNKIIQMLSDSQTLKILQEEALKSKKKGSSSKKPDDSKK    113
                    ***************************************************
```

Figure 4.16 Protein alignment of group II compared with group X and group XI phytoplasmas.

In the case of *SAP11*$_{AP}$, the sequence is different from that for the full genome sequence of AP in the NCBI database, so the 16S rRNA sequences were blastn with the NCBI database. The result showed that the sequence of the phytoplasma in our collection was 100% identical to '*Ca.* Phytoplasma *mali*' strain SQ that was first detected in Poland (Cies'linska and Morgas, 2011) (Figure 4.17). However, the *SAP11* gene and complete genome sequence in the NCBI database is from '*Ca*. Phytoplasma *mali*' strain AT (*SAP11*$_{CaPM}$). This suggests that the *SAP11* effector gene from strain SQ is different to that in strain AT, as shown in Figure 4.18. The protein alignment showed some amino acids of SAP11$_{AP_SQ}$ were deleted in the NLS and TCP-binding region (Figure 4.22).



Candidatus Phytoplasma mali isolate SQ 16S ribosomal RNA gene, partial sequence

Sequence ID: HM149261.1 Length: 1161 Number of Matches: 1

Range 1: 6 to 1158 GenBank Graphics ▼ Next Match ▲ Previous Match

Score	Expect	Identities	Gaps	Strand
2130 bits(1153)	0.0	1153/1153(100%)	0/1153(0%)	Plus/Plus

```
Query  8     CTTGAACTTTTAAAGACCCGCAAGGGTATGCTAAGAGATGGGCTTGCGGCACATTAGTTA  67
             ||||||||||||||||||||||||||||||||||||||||||||||||||||||||||||
Sbjct  6     CTTGAACTTTTAAAGACCCGCAAGGGTATGCTAAGAGATGGGCTTGCGGCACATTAGTTA  65

Query  68    GTTGGTAAGGTAACGGCTTACCAAGACTATGATGTGTAGCTGGACTGAGAGGTTGAACGG  127
             ||||||||||||||||||||||||||||||||||||||||||||||||||||||||||||
Sbjct  66    GTTGGTAAGGTAACGGCTTACCAAGACTATGATGTGTAGCTGGACTGAGAGGTTGAACGG  125

Query  128   CCACATTGGGATTGAGATACGGCCCAAACTCCTACGGGAGGCAGCAGTAAGGAATTTTCG  187
             ||||||||||||||||||||||||||||||||||||||||||||||||||||||||||||
Sbjct  126   CCACATTGGGATTGAGATACGGCCCAAACTCCTACGGGAGGCAGCAGTAAGGAATTTTCG  185

Query  188   GCAATGGAGGAAACTCTGACCGAGCAACGCCGCGTGAACGATGAAATATTTAGGTATGTA  247
             ||||||||||||||||||||||||||||||||||||||||||||||||||||||||||||
Sbjct  186   GCAATGGAGGAAACTCTGACCGAGCAACGCCGCGTGAACGATGAAATATTTAGGTATGTA  245

Query  248   AAGTTCTTTTATTAAAGAAGAAAAAATGATGGAAAAATCATTCTGACGGTATTTAATGAA  307
             ||||||||||||||||||||||||||||||||||||||||||||||||||||||||||||
Sbjct  246   AAGTTCTTTTATTAAAGAAGAAAAAATGATGGAAAAATCATTCTGACGGTATTTAATGAA  305

Query  308   TAAGCCCCGGCTAACTATGTGCCAGCAGCTGCGGTAATACATGGGGGGCAAGCGTTATCC  367
             ||||||||||||||||||||||||||||||||||||||||||||||||||||||||||||
Sbjct  306   TAAGCCCCGGCTAACTATGTGCCAGCAGCTGCGGTAATACATGGGGGGCAAGCGTTATCC  365

Query  368   GGATTTATTGGGCGTAAAGGGTGTGTAGGCGGTTTAATAAGTCTATGGTATAAGTTCAAC  427
             ||||||||||||||||||||||||||||||||||||||||||||||||||||||||||||
Sbjct  366   GGATTTATTGGGCGTAAAGGGTGTGTAGGCGGTTTAATAAGTCTATGGTATAAGTTCAAC  425

Query  428   GCTTAACGTTGTGATGCTATGGAAACTGTTTGACTAGAGTTGGATAGAGGCAAGTGGAAT  487
             ||||||||||||||||||||||||||||||||||||||||||||||||||||||||||||
Sbjct  426   GCTTAACGTTGTGATGCTATGGAAACTGTTTGACTAGAGTTGGATAGAGGCAAGTGGAAT  485
```

Figure 4.17 Blastn result showing our 16Sr AP to be similar to 16Sr AP strain SQ.

```
AP_CaPM      MFKFKSQIKLIYICLFIILGLFFIINNNYVMASPPKKDSNKGKSIDKSVSSKRETVSIRE   60
AP_SQ        MMQIKNKLYFLPLFLMSFLGLFLLINTNPVIAAPE--KNDKGKKIASSEKQEKTTKKDIS   58
             *   *         *   ****  ** * * * *      *** *  *      *

AP_ CaPM      YRELEMALNQLPEEERNTIMETLNNPEKMEVLLKKAQDEANKKRGGSSSSQHDDNNKDKG  120
AP_SQ         QYYELYNTLENYSEE-DRNKIIQMLSDSQTLKILQEEALKSKKKGSSSKKPDD-SKK---  113
                     **                            ** * **    *   *

AP_ CaPM      KK   122
AP_SQ         --   113
```

Figure 4.18 Protein alignment of group X compared between AP_CaPM and AP_SQ

Additionally, the SAP11$_{PnWB}$ and SAP11$_{AY\text{-}WB}$ protein sequences that were the templates for primer design, were aligned together and the result showed that

there are three different amino acid positions and the SAP11$_{AY\text{-}WB}$ protein sequence is longer than SAP11$_{PnWB}$ (Figure 4.19). However, they have both been shown to encode SAP11 proteins that induce plant morphology alterations. Moreover, these alignments reveal two positions that have been identified as important conserved sequences for SAP11 interactions with plant cells. These positions are the NLS (nuclear localization signal) which is required for subcellular localization in plant cells, and the TCP-binding region which interacts with CIN-TCP for altering plant morphology (Sugio *et al*., 2014).

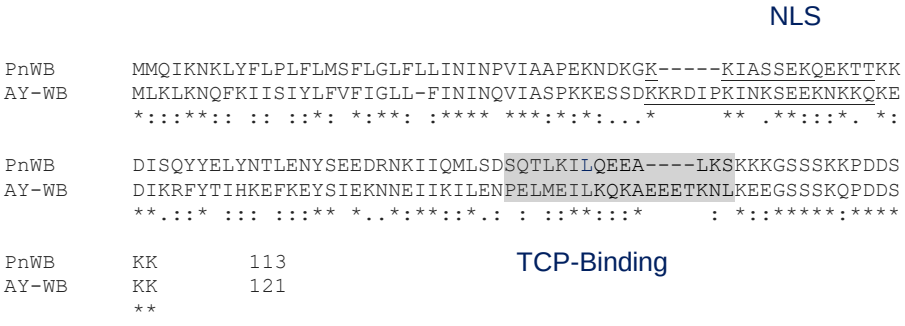


Figure 4. 19 SAP11$_{AY\text{-}WB}$ protein compared with SAP11$_{PnWB}$ (Sugio *et al*., 2014 and Chang *et al*., 2018). The underlined sequence shows NLS sequences and the grey colour shows the TCP-Binding coiled coil structure.

Figure 4.20 showed NLS and TCP-binding protein positions for the 16SrI-C isolates used in this study (SAP11$_{BCRD}$ and SAP11$_{SGP}$) compared with the previous sequenced 16SrI-A SAP11$_{AY\text{-}WB}$, and the protein sequences were matched except for in the NLS sequences, where there are the amino acids P and K in SAP11$_{AY\text{-}WB}$ that are not matched in the others (S and E).

```
BCRD       MLKLKNQFKIISIYLFVFIGLLFINVNQVIASPKKESSDKKRDISEINKSEEKNKKQKED      60
SGP                                    MSPKKESSDKKRDISEINKSEEKNKKQKED      60
AY-WB      MLKLKNQFKIISIYLFVFIGLLFININQVIASPKKESSDKKRDIPKINKSEEKNKKQKED      60
                                       :************ .:**************

BCRD       IKRFYTIHKEFKEYSIEKNNEIIKILENPELMEILKQKAEEETKNLKEEGSSSKQPDDSK      120
SGP        IKRFYTIHKEFKEYSIEKNNEIIKILENPELMEILKQKAEEETKNLKEEGSSSKQPDDSK      120
AY-WB      IKRFYTIHKEFKEYSIEKNNEIIKILENPELMEILKQKAEEETKNLKEEGSSSKQPDDSK      120
           ************************************************************

BCRD       K       121
SGP        K       121
AY-WB      K       121
           *
```

Figure 4.20 Candidate effector protein $SAP11_{SGP}$ and $SAP11_{BCRD}$ were aligned with $SAP11_{AY\text{-}WB}$ and underlined region shows NLS, and the coiled coil structure is shown in grey colour.

SAP11$_{PnWB,}$ which is in the 16SrII group and was a template for *SAP11* candidate effector gene primers, was aligned with $SAP11_{AP_SQ}$ $SAP11_{CoP}$ and $SAP11_{VCP}$ proteins and the result showed there are NLS and coiled coil (TCP-binding) structures at the same positions of $SAP11_{PnWB}$ (Figure 4.21). Furthermore, $SAP11_{AP_SQ}$ is the 16SrX group but protein sequences are similar to the others (16SrII) because $SAP11_{AP_SQ}$ was closely related to 16SrII (Nicolaisen and Harvath, 2008) and the alignment results showed there was only one amino acid different to 16SrII group, which is T instead of I, and there are no differences in the NLS position.

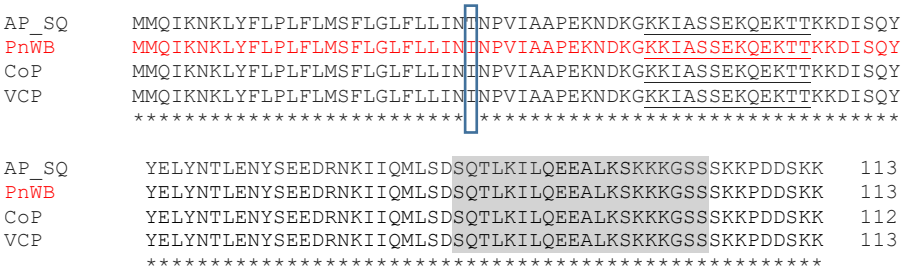


Figure 4.21 Candidate effector protein $SAP11_{AP_SQ}$, $SAP11_{CoP}$ and $SAP11_{VCP}$ were aligned with $SAP11_{PnWB}$ and underlining shows the NLS, and the coiled coil structure was shown in grey colour.

All of the candidate effector protein sequences with signal peptides were aligned and compared with the Teugu protein and the result showed some amino acids were conserved in each group (Figure 4.22). Furthermore, the NLS region of the 16SrII, 16SrX and 16SrXI phytoplasmas lacked some nucleotides and there are also nucleotide substitution including in the TCP-binding protein region. Interestingly, Tengu lacked the NLS region and the TCP- binding region was different from SAP11 effectors.

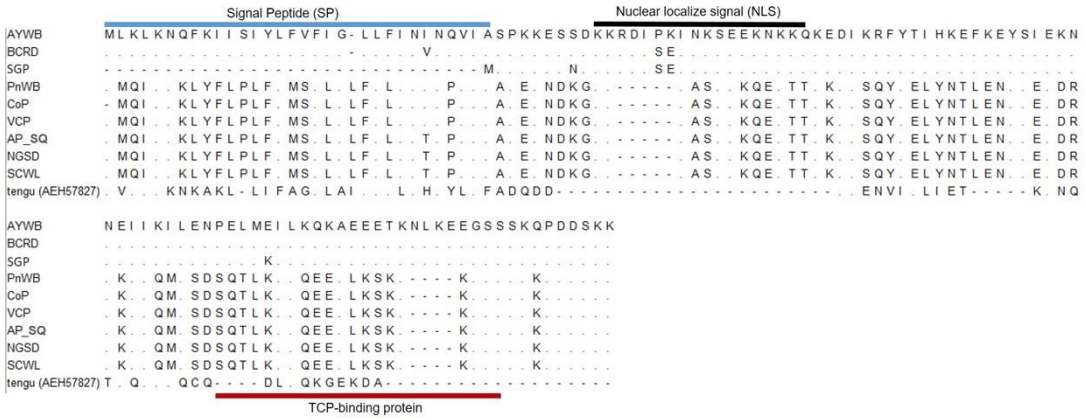


Figure 4.22 SAP11 protein alignment between samples and Tengu. The sequences were aligned using ClustalW and dots represent amino acids identical to $SAP11_{AY\text{-}WB}$ consensus sequences; dash represents amino acid deletions in the protein.

A phylogenetic tree was constructed using the neighbour-joining method with a bootstrap of 1000 replicates for SAP11 protein alignments of each phytoplasma and with Tengu (AEH57827) as the outgroup. This method used MEGA X software. The phylogenetic tree showed three clusters, including the Teugu outgroup, and the 16SrI group was distinct from the other clusters and included $SAP11_{AY\text{-}WB}$ and $SAP11_{BCRD}$ with strong branch support, whilst $SAP11_{SGP}$ was in a sister clade and the branch was moderately supported. The last cluster consisted of 16SrII, 16SrX and 16SrXI phytoplasmas. Moreover, the 16SrX grouped in the same clade as 16SrXI whilst 16SrII was separated but much more closely related than to 16SrI (Figure 4.23). These results were in line with the phylogenetic tree based on 16S rRNA RFLP (Figure 4.28) (Nicolaisen and Harvath, 2008).

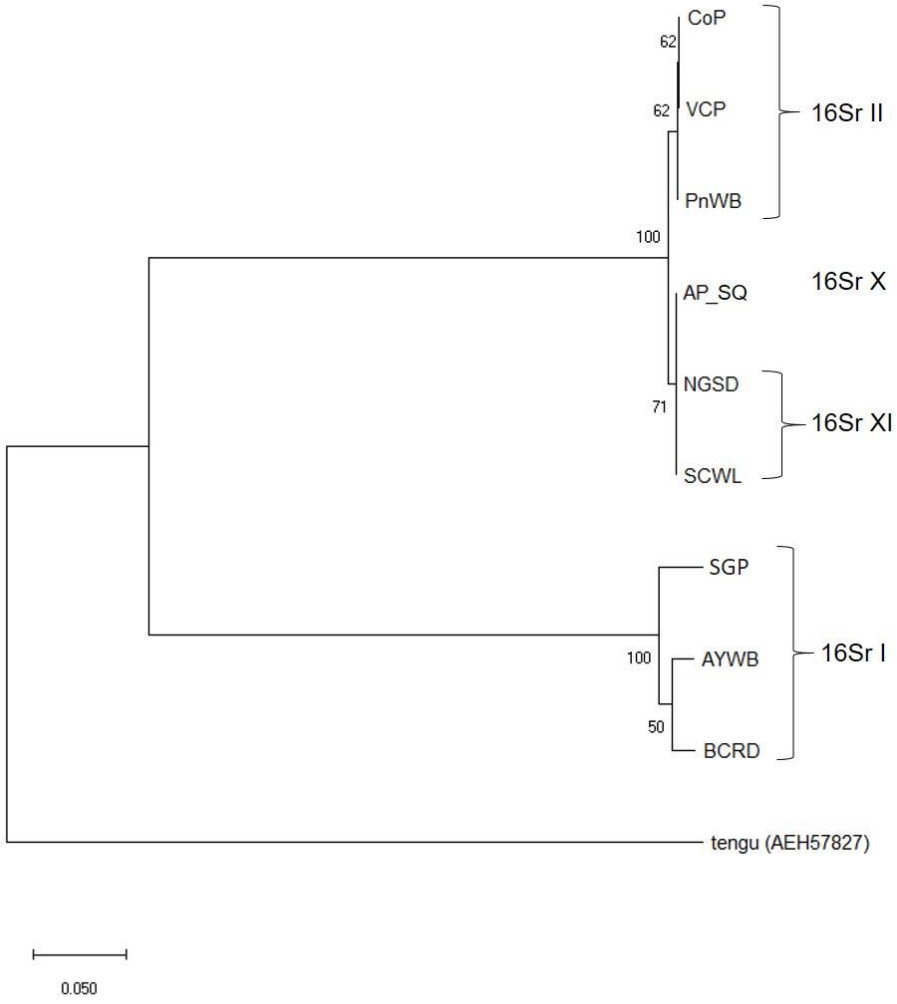


Figure 4.23 The phylogenetic tree was constructed from SAP11 proteins and candidate hypothetical proteins using neighbour-joining in MEGA X program used 1000 replicates for bootstrap analysis.

All of the candidate effectors were integrated into pDestination vector pGWB5 and pBRACT214 for transformation into *Arabidopsis* and *Brachypodium*, respectively. This step was done with LR clonase Gateway before introducing into *Agrobacterium*; GV3101 and AGL1.

The T_1 *Arabidopsis* seeds were selected on ½ MS containing 50 μg/ml of hygromycin and Figure 4.24 shows that the resistant transformed *Arabidopsis* could grow on the selective medium within two-three weeks. The resistant plants were then moved into soil and PCR was done for effector gene insertion (Figure 4.25).

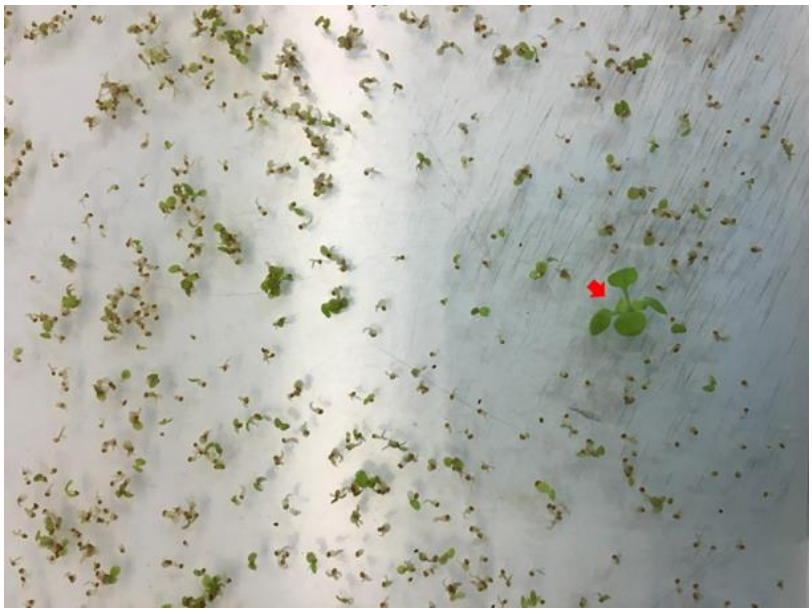


Figure 4.24 T_1 transformed Arabidopsis screening on 0.8% of ½ MS agar with 50 μg/ml hygromycin. The red arrow shows transformed-resistant Arabidopsis.

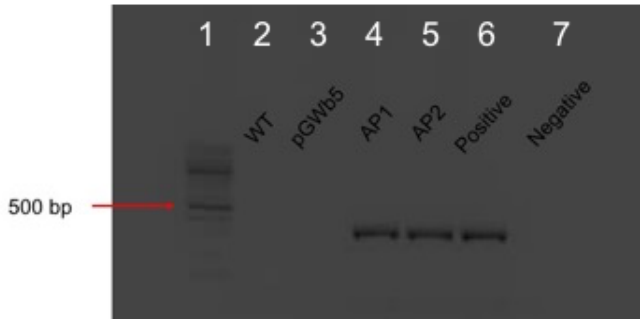


Figure 4. 25 PCR product of $SAP11_{AP_SQ}$ T_1 transformed plants compared with wild type and pGWB5. Lanes (1) 100 bp ladder, (2) Arabidopsis wild type, (3) Arabidopsis transformed with Vector pGWB5 only, (4) Arabidopsis transformed with $SAP11_{AP_SQ}$ line 1, (5) Arabidopsis transformed with $SAP11_{AP_SQ}$ line 2, (6) pGWB5 with $SAP11_{AP_SQ}$ effector gene insert and (7) Non-template control.

For *Brachypodium*, the transformed callus produced two types of regenerating shoot, green shoots and albino shoots, which were grown on selective medium (Figure 4.26) although almost all of the callus could not regenerate shoots. Moreover, some green shoots died within two weeks of shoot regeneration in MSB3 containing selective antibiotics, so green shoots were moved to MS medium containing Timentin without hygromycin. After the green shoots had established, they were moved to soil and a small piece of leaf was cut for PCR with specific primers (Figure 4.27).

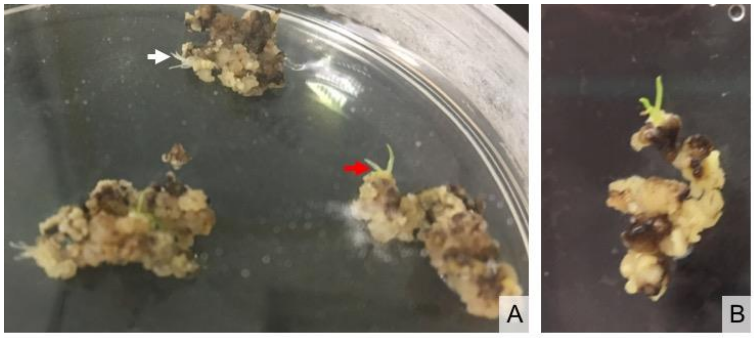


Figure 4.26T_0 transformed Brachypodium screened on MSMO adding 300 mg/L Timentin and 30 µg/ml hygromycin. A. The red arrow shows green resistant transformed Brachypodium and the white arrow shows the albino transformed plant. B. Green shoot of transformed Brachypodium.

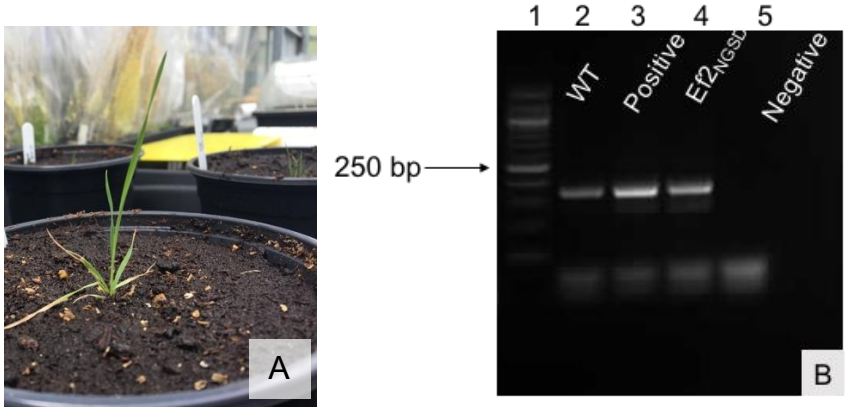


Figure 4.27 A. transformed Brachypodium in glasshouse. B. PCR product of $Ef2_{NGSD}$ T_0 transformed Brachypodium compared with wild type and positive control. Lanes (1) 100 bp ladder, (2) Brachypodium wild type, (3) $Ef2_{NGSD}$-pBRACT214 vector, (4) $Ef2_{NGSD}$ T_0 transformed Brachypodium, (5) Non-template control.

4.4 Discussion

4.4.1 SAP11 conserved sequences

In this chapter, phytoplasma effector proteins were amplified from 16SrI, 16SrII and 16SrX phytoplasmas because they are relatively closely related groups of phytoplasmas based on the 16S rRNA, and the equivalent effectors from AY-WB and OY-M have been shown to induce symptom changes in transformed plants in previous experiments by others, so they could be used as controls for the testing of effectors from the 16SrXI napier grass stunt and sugarcane phytoplasma (Figure 4.28).

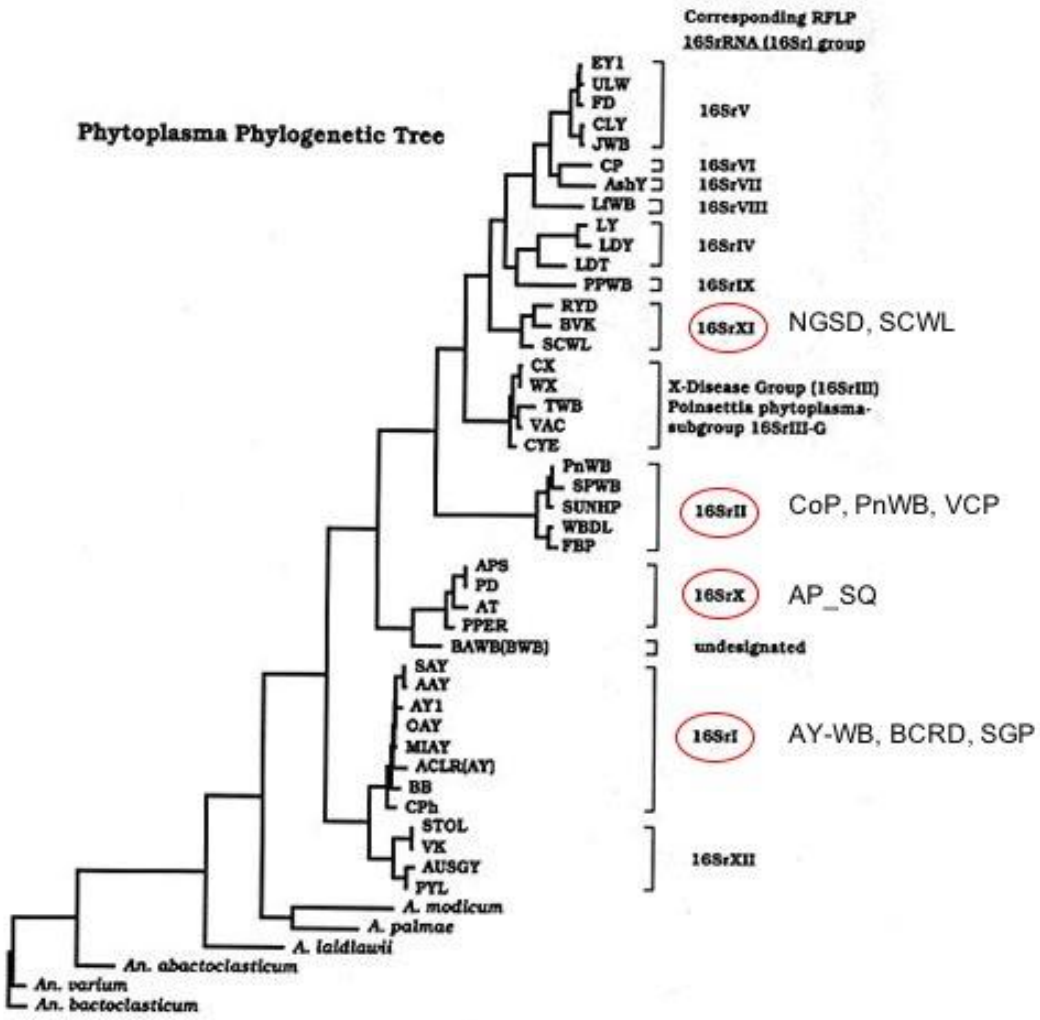


Figure 4.28 The phylogenetic tree showing the relationship between different groups of phytoplasmas (Nicolaisen and Harvath, 2001), noting the ones used in this study and the groups they belong to.

In previous work done by others, phytoplasma effectors have been cloned and analysed from 16SrI group phytoplasma (Sugio *et al.,* 2011; Oshima *et al*., 2013). However, little is known about the effectors from other phylogenetic groups, such as the phytoplasmas of the grasses (sugarcane and napier grass). The aim was therefore to attempt to isolate potential effectors from other phytoplasmas held in our collection at the University of Nottingham,

notably the 16SrII and 16SrX groups (using those from the 16SrI groups as controls), and from the Napier grass stunt and Sugarcane white leaf phytoplasmas (16SrXI)- see Chapter 3 for the details of which isolates were used. To do this, for the 16SrI, II and X groups, primers were used that had been developed by others for amplifying the *SAP11* gene, whilst for the napier grass stunt phytoplasma, the draft genome produced at the University of Nottingham was analysed for potential small secreted protein genes, and primers were then used to amplify these from DNA extracted from infected plants, and also from DNA extracted from the sugarcane plants infected with the closely related Sugarcane white leaf phytoplasma (for which no genome sequence is available).

According to Figure 4.23, the SAP11 effector and candidate effector phylogenetic tree showed that the 16SrX (*SAP11*$_{AP_SQ}$) was closely related to 16SrXI (*SAP11*$_{NGSD}$ and *SAP11*$_{SGWL}$) that are in the same group with 71 bootstrap value and they were separated from 16SrII (*SAP11*$_{PnWB}$ *SAP11*$_{VCP}$ and *SAP11*$_{CoP}$) with 100 bootstrap value. The 16SrI group was an outgroup to 16SrII 16SrX and 16SrXI and this group was separated into two branches, the first clade consisting of *SAP11*$_{AYWB}$ and *SAP11*$_{BCRD}$ and the second clade of *SAP11*$_{SGP}$ because the *SAP11*$_{SGP}$ lacks a part of the protein sequence. Additionally, 16SrII-F (*SAP11*$_{CoP}$ and *SAP11*$_{VCP}$) were similar to *SAP11*$_{PnWB}$ (16SrII-A) (100%) (Table 4.5); moreover, *SAP11*$_{AP_SQ}$ (16SrX) was also 98% similar to *SAP11*$_{PnWB}$ with one amino acid different (T instead of I) (Figure 4.15) even though they are from different groups. Interestingly, the *SAP11*$_{AP_SQ}$ from strain SQ is different from the *SAP11*$_{CaPM}$ (ATP_00189) from strain AT (Figure

4.17), which is the strain that forms the basis of the complete genome sequence of AP and most subsequent publications on this phytoplasma. Nonetheless, these phytoplasma groups were separated from 16SrI group (Figure 4.23). Furthermore, previous studies showed some samples in 16SrII-D from Oman had an amino acid mutation from the *SAP11*$_{PnWB}$ and *SAP11*$_{SPLL}$ protein sequences; however, the proteins were similar to SAP11 protein (100%) because of a silent mutation (Al-Subhi *et al*., 2018).

Interestingly, *SAP11*$_{BCRD}$ and *SAP11*$_{SGP}$ are in the same 16SrI as *SAP11*$_{AY-WB}$ however, the SAP11 proteins were not identical (Table 4.5) and three amino acids were different to *SAP11*$_{AY-WB}$ (Figure 4.13). These results are interesting and may reflect the different subgroups that these phytoplasmas are in, with AY-WB being in subgroup I-A whereas BCRD and SGP are both in subgroup I-C (Padovana *et al.,* 2000; Hodgetts *et al.,* 2008). Even though BCRD and SGP are in the same subgroup the *SAP11*$_{BCRD}$ protein was 99% identical to *SAP11*$_{AY-WB}$ whilst *SAP11*$_{BCRD}$ was only 75% identical to *SAP11*$_{SGP}$ because *SAP11*$_{SGP}$ lacks the SP region. This is similar to the situation with SAP11 homologs from the 16SrI PLY_3690 and OYV_05290 (Cho *et al*., 2019) which also lack a part of the SP region but do have the NLS and TCP-binding regions to interact with plant genes.

Based on Figure 2.11, the *SAP11* gene could not be used to classify SCWLs and NGSD including BGWLs even though the SCGSSLK3 was an outlier. The *SAP11* gene is a well conserved sequence in each phytoplasma group. Moreover, previous studies showed that the samples in 16SrII-B subgroup

from Oman, which were collected at the same areas, showed conserved sequences and the samples were distinct from 16SrI and 16SrX-A groups (Al-Subhi *et al*., 2018). In the same way, the *SAP11* gene from different locations in Oman; semitropical areas, subtropical areas and desert areas showed the samples were in the same cluster and the bootstrap value was strong (100%) to support the phylogenetic tree whilst the alfalfa witches' broom (16SrII-D) from the databases was separated to another cluster (Al-Ghaithi *et al*., 2018) even though it was a closely related strain to the Oman samples. Interestingly, the *SAP11* conserved sequences are essential for phytoplasma effector proteins to interact with plant genes for transmission (MacLean *et al*., 2011; Wei *et al*., 2013; Chang *et al*., 2019). The SAP11 protein requires SP sequences for cleavage via the Sec-A pathway and NLS for SAP11 effector translocation to plant cell nuclei whilst the TCP-binding region is important for interactions with the TCP plant gene family for plant morphological and physiological changes.

4.4.2 Plasmid construction and transformation

For cloning, the Gateway binary vector plasmids (pGWBs and pBRACT) are efficient for cloning because they are constructed for fusing genes by the simple clonase reaction because there are the N- or C-terminal tags that are automatically fused subsequent to the LR reaction. Furthermore, the pGWB vector contains the Cauliflower mosaic virus (CaMV) 35S promoter which provides high-level expression of transgenes in dicot plants whilst the maize ubiquitin1 promoter is more suitable for expression in monocot plants and there are various reporter genes for selection. The pGWB vector had been

used for many purposes such as protein-protein interactions, nuclear localization observation and promoter::reporter analysis (Zhang *et al*., 2017; Jiang *et al*., 2018). Furthermore, the pBRACT214 is also a gateway binary vector to recombine with genes of interest using the LR clonase reaction; however, it has the ubiquitin promoter instead of CaMV35S promoter, so is more suitable for cereals and other monocots (Smedley and Harwood, 2015).

The binary vector system was used for transformation into higher plants. There are two plasmid vectors in the system; Binary vector or T-DNA and Helper Ti plasmid. The binary vector is a shuttle vector that can replicate in multiple hosts such as *E.coli* and *Agrobacterium;* moreover, this vector consists of the left border (LB), right border (RB), selectable marker for two host bacteria, reporter markers and exact multiple cloning sites for the inserted gene. The other vector is the helper Ti plasmid which is important for transferring T-DNA or the binary vector into plant cells. This plasmid consists of active virulence genes (*vir* gene) and there is a selectable marker gene for Agrobacterium selection (Smedley and Harwood, 2015).

In the transformation experiments, there were two types of plant for transformation, a dicot and a monocot, and there were different methods for transformation. For the dicot, *Arabidopsis thaliana,* the floral dip method was used. This method requires surfactants to increase transformation efficiency such as Silwet L-77, Tween20 and Triton X, which are nonionic detergents to promote transformation. In particular, 0.02% Silwet L-77 and Tween-20 have been shown to increase transformation rates to 80% and 53% respectively,

whilst Triton X has been shown to be toxic to plant tissue (Dehestani *et al*., 2010).

In addition, there are other methods for *Arabidopsis* transformation, such as vacuum filtration, which requires a vacuum chamber to introduce *Agrobacterium* into the intercellular space within plant tissue; however, the success rate of transformation between the vacuum filtration and floral dip methods was not significantly different (Clough and Bent, 1998). The other methods are modified from floral dip namely floral drop and floral spray. Both methods reduce cost, time and space for transformation. For floral drop, this method requires 5 µl of *Agrobacterium* cell suspension to drop in flower buds and gave 15-50 transformed plants per pot containing three *A. thaliana* plants (Narusaka *et al*., 2010), whilst for floral spray, the *Agrobacterium* cell suspension is sprayed onto flower buds for one to three times within an 8 hours interval and the transformation rate was 1.33% and 2.41%, respectively (Chung *et al*., 2000).

For *Brachypodium*, *Agrobacterium* transformation is one of a few methods for transformation and the transformation efficiency (TE), which means the percentage of callus to produce transformed plants, has been shown to be dependent on the *B. distachyon* cultivar, such as Bd21, Bd21-3, embryo stage and callus morphology. The immature embryo size (<0.3 mm) is the best to produce embryogenic callus and the TE was 50-70%; furthermore Bd21-3 produced more yellow callus than Bd21 (Vain *et al*., 2008; Vogel and Hill, 2008; Steinwand *et al*., 2013; Bragg *et al*., 2015; Scholthof *et al*., 2018).

Nonetheless, the BD21 transformation efficiency was 3.2% (Vogel *et al*., 2006). Furthermore, the *Agrobacterium* strain, promoter and selective marker used in the binary vector, are factors that affect TE. The *Agrobacterium* strain AGL1 including *Rhizobium rhizogenes* strain 18r12v (Collier *et al*., 2016) are super-virulent strains for transformation, whilst promoters such as the 35S promoter were studied by Vogel and Hill (2008) and their results showed that the TE efficiency into *B. distacyon* line BD21-3 with the 35S promoter was 41% whilst with the rice actin promoter this was 17%. However, Scholthof (2018) found that the CaMV35S promoter had negative effects on growth in *B. distachyon* and that there was another promoter, the Maize ubiquitin promoter, that works better in *B.distachyon* (Scholthof *et al*., 2018).

Additionally, the regeneration step produces two types of shoots; green shoots and albino shoots. Furthermore, the result showed the transformed *Brachypodium* callus produced more albino shoots than green shoots. The albino shoots were regenerated from soft callus and showed small percentages of regeneration. In addition, callus was sub-cultured more than six weeks causing somatic genetic variation and regenerated to albino shoots. (Vogel and Hill, 2008; Vain *et al*., 2008; Collier *et al*., 2016; Behpouri *et al*., 2018). The *Brachypodium* regeneration result in this chapter was in accord with Vogel and Hill's results (2008) who found the immature Bd21 callus was low quality and mainly produced albino shoots whilst Collier and colleagues studied Bd21-3 transformation and their result showed 7% of albino plants, 33% failed to regenerated shoots and 60% of green shoots. Moreover, some of green shoots died in selective medium with hygromycin even though the

hygromycin concentration was reduced to 10 μg/ml so some green shoots were moved to selective medium without hygromycin for regeneration and the transformed plants were screened with the PCR method with specific primers.

Chapter 5: Gene expression analysis

5.1 Introduction

Plant development is under the control of intrinsic and extrinsic factors such as plant growth regulators and light or temperature. In terms of plant growth regulators, these can be divided into two groups; the first group is related to growth promoting activities such as cell division, cell enlargement, pattern formation, flowering, fruiting and seed formation controlled by auxins, gibberellins and cytokinins. The second group play an important role in response to biotic and abiotic stresses, involving abscisic acid and ethylene.

Plants have Shoot Apical Meristems (SAM) which are critical for growth and development of stems and lateral organs to form diverse plant architecture (Bao *et al*., 1973). The plant architecture is controlled by genetics and influenced by environmental conditions such as temperature, light and nutrients. In *Arabidopsis*, SAMs generate leaf primordia to form a basal rosette in a spiral phyllotaxy and form alternatives in other organs such as secondary inflorescence meristems, leaves, flower and silique inflorescences (Teichmann and Muhr, 2015).

5.1.1 The phyllotaxy pattern

Phyllotaxy refers to the divergence angle arrangement of leaves on the stem and how they are positioned (Figure 5.1). Phyllotaxis patterns are controlled by multiple genes such as *BELLRINGER* (*BLR*)/*PENNYWISE* (*PNY*), which is an important gene to control normal shoot development, *PECTINMETHYLTRANSFERASE5* (*PME5*), which is involved in the demethyl-esterification of the pectin polysaccharide homogalacturonan (HG) in plant cell walls and *PECTINMETHYTRANFERASE INHIBITOR* (*PMEI*), which represses *PME* gene function (Peaucelle *et al*., 2011; Etchell *et al*., 2012; Senechal *et al*., 2015). Moreover, the interaction of *PME-PMEI* controls other aspects of plant development including fruit maturation and plant defences to microorganisms (Paynel *et al*., 2014; Senechal *et al*., 2015).

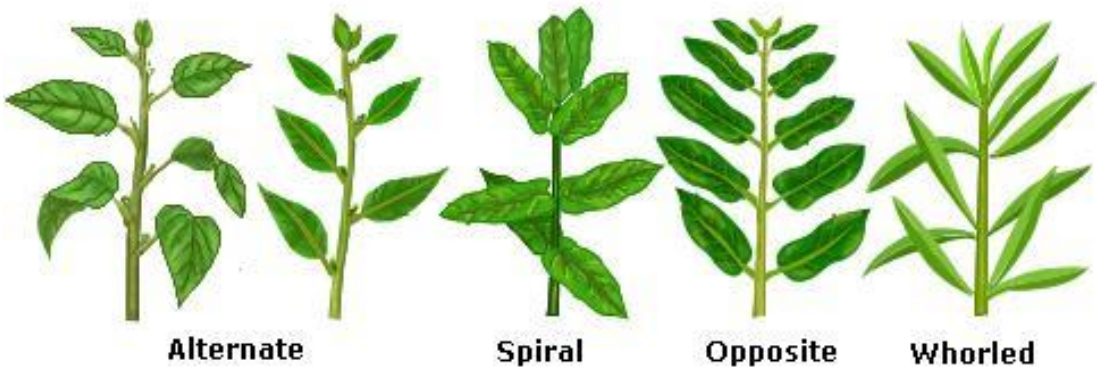


Figure 5.1 A schematic of the common phyllotaxies.

Source:http://www.indiahomeclub.com/botanical_garden/bot_leaf_arrangement.php

In the case of *BLR/PNY*, the gene regulates *PME5* transcription in meristems and internodes (Peaucelle *et al*., 2011); *BLR/PNY* represses *PME5*

expression in the meristem primordia to control phyllotaxy during primordia initiation, whilst *BLR/PNY* promotes *PME5* expression at the internode to maintain the phyllotaxis pattern (Figure 5.2).

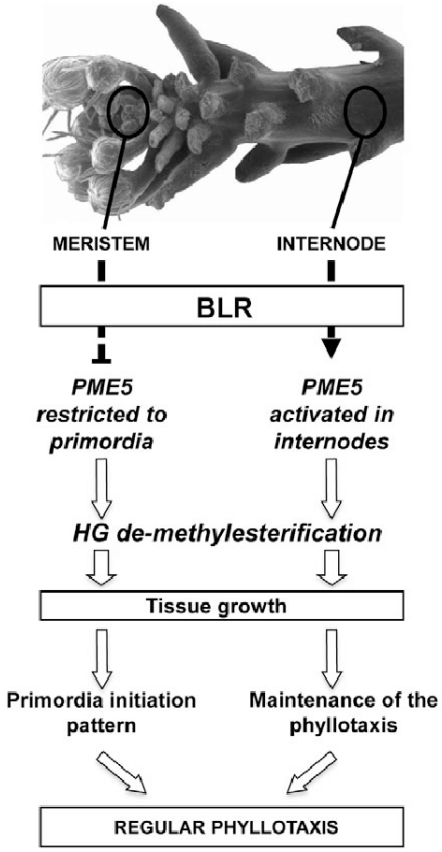


Figure 5.2 A schematic of the role of BLR in PME5 expression in plants at the meristem and internode (Peaucelle *et al*., 2011).

5.1.2 Branching and apical dominance

Branches or lateral shoots or axillary meristems are formed in the axils of the leaves. The axillary meristem development is controlled by a network of genes such as *BRANCH1* (*BRC1*) or *TCP18* and *BLIND* (*BL*) in *Arabidopsis*, or

TEOSINTE BRANCH1 (*TB1*) in maize (Seale *et al*., 2017). The *BRC1* is a major control of shoot branching in axillary buds which is negatively regulated.

Genes that control plant phyllotaxy, branching and development are members of the three-amino-acid-loop-extension (TALE) regulators, which consist of KNOTTED-like (KNOX) and BEL1-like (BLH or BELL) homeodomain proteins (Roth, 2018). In the KNOX family, there are eight genes including *STM* and *BP*/*KNATT1* that play important roles to maintain SAM (undifferentiated cells) and regulate inflorescence structure whilst there are thirteen members in the BLH protein family, including *BLH*$_2$/*SAW1* and *BLH*$_4$/*SAW2* that control leaf margin and *BLH*$_8$/*PNF* and *BLH*$_9$/*BLR/PNY* that maintain inflorescence architecture and floral meristem function (Ung, 2011).

Phytoplasma effectors cause various symptoms in numerous plant species but there are a few common symptoms found in many phytoplasma infected plants. For example, witches' broom symptoms involve loss of apical dominance (Singh *et al*., 2013) and the infected plants produce axillary shoots instead of internode length. In phyllody, leaf-like flower structures are produced and the infected plants are sterile (Hu *et al*., 2015; Yang *et al*., 2015). Moreover, virescence shows green flowers because infected plants lose flower pigment in petal cells, whilst leaf yellowing shows inhibition of photosystem II such that chlorophyll and carotenoid are broken-down (Bermatini *et al*., 2002). These symptoms are believed to be caused by phytoplasma effectors, which destabilise and/or regulate plant developmental pathways. Although, phytoplasmas are restricted to the phloem they release

virulence effectors via Sec-dependent pathways that move to nuclei in plant cells for suppression of plant development (Bai *et al*., 2009; Sugio *et al*., 2011).

One target gene of a phytoplasma effector is the TCP (TEOSINTE-BRANCHED in maize, CYCLOIDEA in snapdragon, PROLIFERATION 1 and 2 in rice) gene family. There are two classes of TCP of which TCP class II is a major target for phytoplasma effectors. The class II TCPs are divided into CIN (CINCINNATA) and TB/CYC subgroups. The CIN subgroups (*TCP2*, *TCP3*, *TCP4*, *TCP5*, *TCP10*, *TCP13*, *TCP17* and *TCP24*) regulate leaf development and flower development, whilst the TB/CYC subgroup (*TCP1*, *TCP12* and *TCP18*) regulate meristem development and axillary bud growth (Antonio *et al*., 2007; Perez-Lopez *et al*., 2016; Chang *et al*., 2019).

As a result of phytoplasma effectors, gene expression during plant development is changed. For example, the $SAP11_{AY\text{-}WB}$ effector protein changes plant morphology to result in crinkly leaves and senescence and involves destabilisation of CIN-TCP, and then the level of the *Lox2* gene is decreased resulting in decreased jasmonic acid (Sugio *et al*., 2011). Similarly, the Tengu virulence effector found in OY-M disrupts auxin pathways and down-regulates jasmonic acid; however, Tengu is localized in the cytoplasm (Hoshi *et al*., 2009) because Tengu has no NLS sequences (Figure 5.3). Additionally, Tengu or PAM765 protein causes severe dwarfism and witches' broom symptoms in infected *Arabidopsis* and in transformed plants more flowers grow from a single point on the main stem (Hoshi *et al*., 2009). The normal phyllotaxy requires correct patterning of cell division, which depends

on cell wall regulation. The cell wall regulation is controlled by genes such as *pectinmethytransferase5* (*PME5*), which controls internode elongation during plant development.

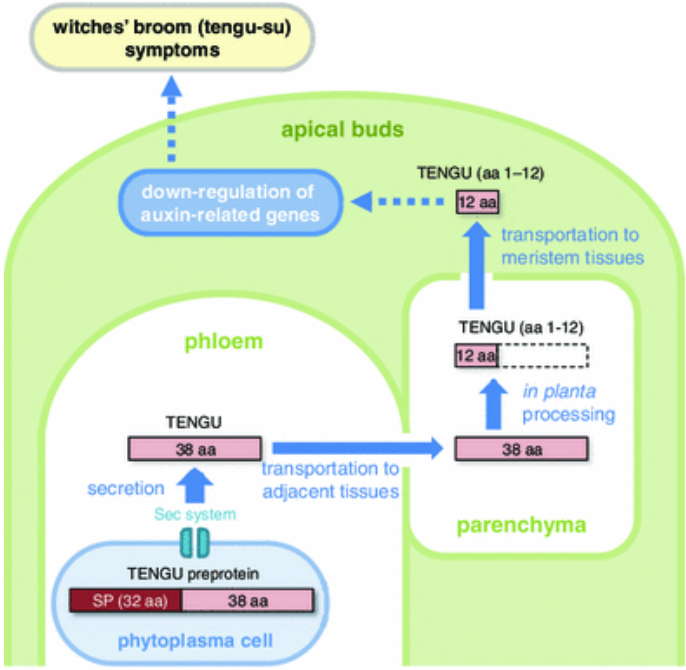


Figure 5.3 A Schematic of witches' broom induced by the Tengu effector protein (Maejama *et al*., 2014).

Conversely, SWP1, which is a SAP11-like effector from the Wheat blue dwarf (WBD) phytoplasma, destabilises CYC-TCP18 (*BRC1*) resulting in branching symptoms and the *BRC1* gene level decreases (Figure 5.4) (Wang and Jiao 2018).

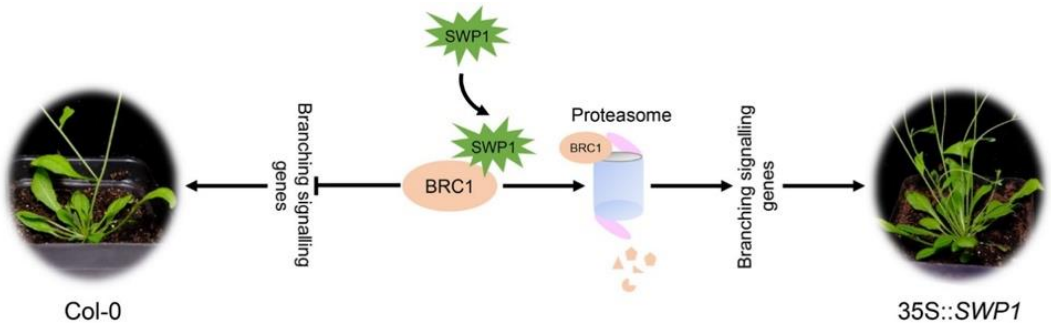


Figure 5.4 Scheme of SWP1 function in inducing witches' broom symptoms by mediating the degradation of BRC1 through a proteasome system (Wang and Jiao 2018).

The symptom of flower malfunction appears to be controlled by *SAP54*, *PHYL1*, which is a *SAP54* ortholog, and Tengu in aster yellows type phytoplasmas. *SAP54* interacts with the MADS-domain transcription factor (MTF) family, especially *RADIATION SENSITIVE23* (*RAD23*) causing flowers to be leaf-like and sterile as shown in Figure 5.5 (MacLean *et al*., 2014).

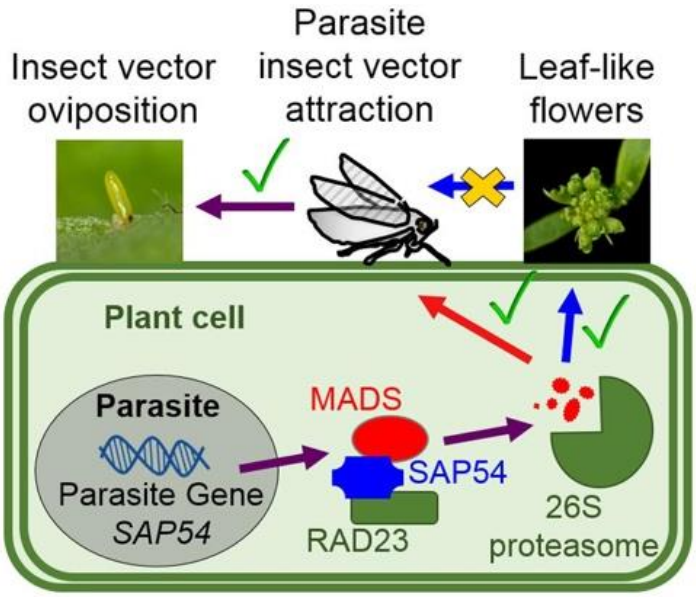


Figure 5.5 The SAP54 effector protein interacted with specific MADS-box transcription factors (MTFs) and degrades via the 26S proteasome, which leads to leaf-like flower structure (MacLean et al., 2011 and 2014).

In the case of *PHYL1* the effector interacts with and degrades *SEPALLATA3* (*SEP3*), *APETALA1* (*AP1*) and *CAULIFLOWER* (Orlovskis *et al*., 2016) to cause phyllody or leaf-like structures (Figure 5.6).

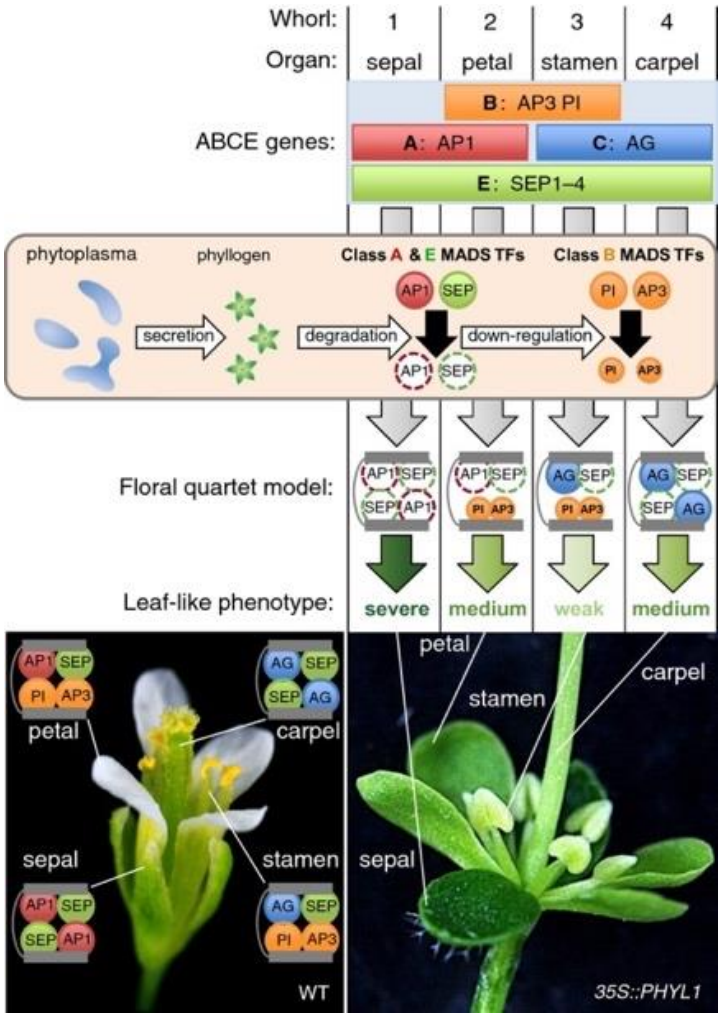


Figure 5.6 Schematic of phyllody-like symptoms induced by the phyllogen effector protein (Maejima *et al*., 2014).

In the case of Tengu, this effector downregulates the *auxin respond factors* (*ARF6*) and *ARF8* which regulate floral development via the phytohormones auxin and jasmonic acid (Figure 5.7).

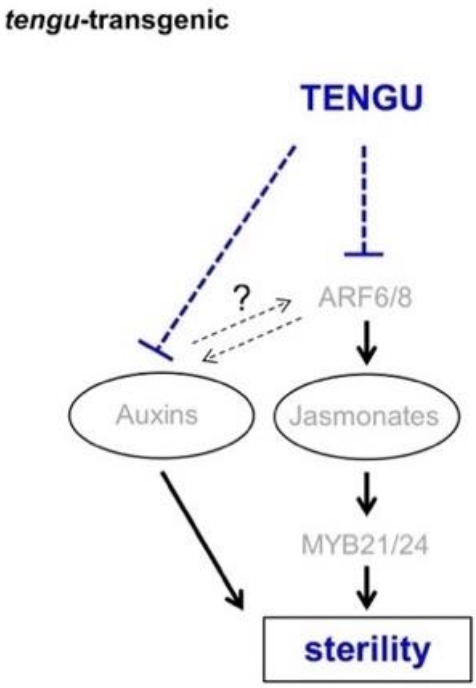


Figure 5.7 Schematic of TENGU-induced reduction of jasmonic acid and auxin levels (Minato *et al*., 2014).

This chapter details the results of gene expression changes caused by transformation of candidate phytoplasma virulence effector genes into *Arabidopsis thaliana* Col-0 and *Brachypodium distachyon* 21.

5.2 Materials and Methods

5.2.1 T_2 transformant detection

5.2.1.1 *Arabidopsis* transformed plants

T_2 seeds were sterilised in 5% bleach solution with 0.5% Tween-20, mixed occasionally for 5 min and the solution was then discarded and the seeds were

rinsed with sterile water 3 times and placed on 0.8% of 0.5x MS (Murashigi and Skoog) (Sigma-Aldrich Co., UK) agar supplemented with 50 μg/ml hygromycin without sugar. The T_2 seed plates were placed at 4°C for 2-3 nights and transferred into the growth room for 10-14 days then put into soil and moved to the glasshouse. A week later, the transformant leaves were placed into 20 µl dilution buffer of Thermo Scientific Phire Plant Direct PCR master Mix (ThermoFisher Scientific, UK) and then the leaf was crushed with a pipette tip by pressing briefly against tube wall. The tubes were spun down and 0.5 µl of supernatant was used as a template in PCR with specific primers for the effector genes. The PCR products were visualised on 1.5% agarose gel added 1 μg/ml of gel red (Biotium, USA.)

5.2.1.2 *Brachypodium* transformed plants

The T_0 mature seeds were surface sterilised in 5% bleach solution with 0.5% tween-20 for 4 mins shaking at room temperature and then washed with sterile water 3 times before the seeds were placed on MS with sucrose supplemented with 50 μg/ml hygromycin. Subsequently, the plates were incubated at 28°C at 20 hours light/ 4 hours dark cycle for germination. After five days, the T_1 resistant seedlings were transferred to soil at 23°C at 20 hours light/ 4 hours dark cycle for 2 weeks and then the leaves of seedlings were collected for PCR analysis with specific primers as describe above.

5.2.2 RNA extraction and reverse transcription

Three or four weeks after selection, the transformant leaves and stems were collected into tubes and placed into liquid nitrogen until RNA extraction. The transformant leaves were crushed with plastic pastels to a powder and 500 µl of lysis solution with β-mercaptoethanol from Spectrum™ Plant Total RNA kit (Sigma-Aldrich Co., UK), was added and RNA extracted following the manufacturer's instruction. The RNA concentration was measured by NanoDrop2000 Spectrophotometer (Thermo Fisher Scientific Inc.). For the next step, cDNA was synthesized using the SensiFast™ cDNA synthesis kit (Bioline, UK) 1x cDNA reaction consists of 4 µl of 5x TransAmp buffer, 1 µl of Reverse Transcriptase, x µl of RNA product and total volume of 10 µl. The cDNA synthesis cycle was 25°C for 10 min and then cDNA was synthesized at 42°C for 60 mins and the reaction was stopped at 85°C for 5 min.

5.2.3 Relative quantitative PCR

The 1x qPCR reactions were performed using 5 µl of 2x SensiFast Buffer (Bioline, UK), 2 µl of 5 ng cDNA, 0.5 µl of 10 mM of each primer and the total volume was 10 µl. The qPCR amplification cycle was denaturation at 98°C for 30 min for 1 cycle and then denaturation at 98°C for 30 sec, annealing at X°C for 30 sec, extension at 72°C for 1 min for 45 cycles and melt curve at 55°C to 95°C in 0.5 °C increments for 39 sec. Each reaction was triplicated and average threshold cycle (Ct/Cq) was used to determine the fold change of gene expression by comparing to the reference *PP2A* gene with the Pffaffl

equation (Pfaffl, 2001), and then the wild type gene level was set at one before comparing with the other transformed plants.

Pffaffl equation used to calculate the fold change:

$$\text{Ratio} = 2^{-[Ct_{(\text{target,test})} - Ct_{(\text{target,calibrator})}] - [Ct_{(\text{reference ,test})} - Ct_{(\text{reference, calibrator})}]}$$

Test = transformed plant, Calibrator = wild type, Reference = reference gene, Target = gene of interest

The student *t*-test analysis was performed to compare expression level for transformed plants, vector only and wild type ($p<0.05$).

Table 5.1 List of qPCR primers used for relative quantitative PCR

Primer name	Primer sequences (5′-3′)
16SrI_qPCR_F	AAATTTTAGAAAACCCTGAATT
16SrI_qPCR_R	TTAGAATCATCAGGTTGTTTT
16SrII_qPCR_F, EF7_F and Standard qPCR_F	CTCTTGAAAATTATTCTGAAGAAGATCG
16SrII_qPCR_R, EF7_R and Standard qPCR_R	ATCATCAGGTTTTTAGAAGAAGA
EF1_F	ACAAAAAGCAGGCTGGGGGGATATCCCATTTCTTCTAATTCTG
EF1_R	ACAAGAAAGCTGGGTGGCAATATCTTTGAATATGAT C
EF2_F	TCAACAAGCAGAAATTAAACA
EF2_R	GTTCCTTCGATTTTAACTTCTAAA
EF3_F	TCTCCCAATTTCATTATTCAA
EF3_R	AAATTAACAAGTAGTCTCCAA
EF4_F	ACAAAAAGCAGGCTGGGGAGTCATTCCTAAAATAATAGTT
EF4_R	ACAAGAAAGCTGGGTAACTGGAGAAAATGAACCAATAGAAAAA
EF5_F	ACAAAAAGCAGGCTGGGCTCCTTTACTGATTACTTTTGTA
EF5_R	ACAAGAAAGCTGGGTATTTAGGTACTATGAATTTATTATTT
EF6_F	ACAAAAAGCAGGCTTGTATTTATTATCTAATTTTCGTTC
EF6_R	ACAAGAAAGCTGGGTCCATGAACGTATAAATGAGGCCATTG
BRC1_F	CTTAGTCAACTACAAACCGAACTCAT
BRC1_R	GATCCGTAAACTGATGCTGCT
BLH_F	AACGGTGGCTTGTTCGGGTA
BLH-R	CGTGGTTCCAGTTGCTTGCA
BLR_F	CGTCGAATGTGCCGGTGATG
BLR_R	GCCCTTCATACCCACCACCA
PME5_F	TCCGACCGTTTCCTTTCTCA
PME5_R	ACAAGCTGCAACCAACGAAA
BP_F	GGGAAGAGTGACAATATGGG
BP_R	TATGGACCGAGACGATAAGG
PP2A3F	TCCGTGAAGCTGCTGCAAAC
PP2A3R	CACCAAGCATGGCCGTATCA

5.3 Results

5.3.1 *SAP11* gene expression and plant developmental gene expression

5.3.1.1 *SAP11*$_{AP_SQ}$ transformed plants

Arabidopsis T_2 transformed plants were analysed for *SAP11*$_{AP_SQ}$ gene expression level and the results showed the *SAP11*$_{AP_SQ}$ level in three transformed plant lines were significantly higher than wild type and vector only (p<0.05) (Figure 5.8).

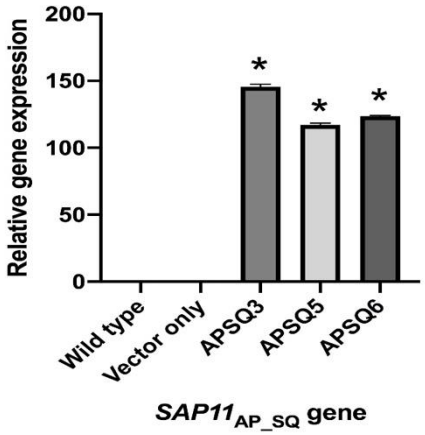


Figure 5.8 Relative gene expression of transgene compared to *PP2A* (actin) gene that were examined by relative quantitative RT-PCR with the gene expression level in wild type set to 1. The columns show gene expression levels of wild type, vector only and three transformed plants and standard errors (SEs) (bars) of relative quantitative RT-PCR from three biological replicates. The * above the columns indicates statistical difference (p<0.05) by student *t*-test.

In terms of plant morphology, the *SAP11*$_{AP_SQ}$ transformed plants produced more leaves than wild type and vector only and there were a lot of clustered cauline leaves (aerial rosettes) on the stems (Figure 5.9B, C); moreover, the transformed leaves were narrower than wild type (Figure 5.9D). Interestingly, the transformed plants did not form any flowers and siliques and the height was smaller than controls (Figure 5.9A, C).

Furthermore, another transformed plant showed only one main stem; however, at a point on the primary main stems, there were secondary inflorescence meristems and each of the secondary inflorescence stems produced axillary stems and lots of clustered cauline leaves on the secondary inflorescence meristems (Figure 5.9E, F and G).



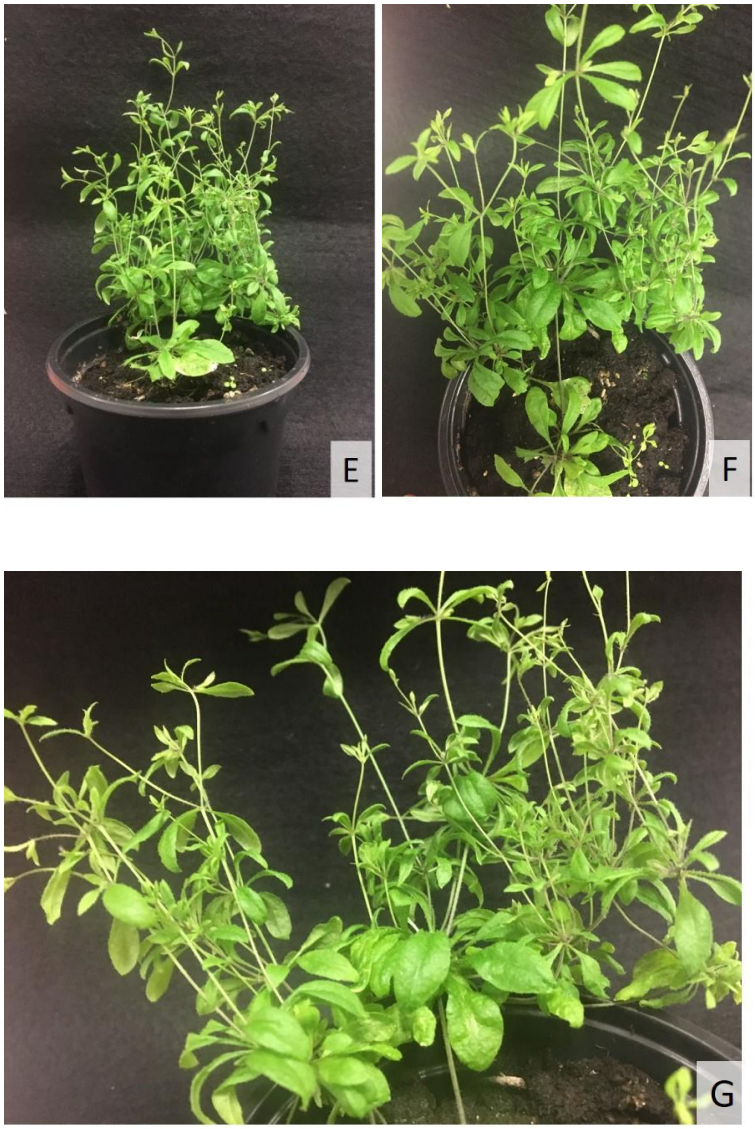


Figure 5.9 Arabidopsis T_2 generation and *SAP11*$_{AP_SQ}$ transformed plants. A. T_2 *SAP11*$_{AP_SQ}$ transformed plant compared to wild type and vector only. B. *SAP11*$_{AP_SQ}$ transformed plant showing the clustered cauline leaves (aerial rosettes). C. Clustered cauline leaves (aerial rosettes) (white arrow) and terminated flower (red arrow) and D. Wild type leaf compared to *SAP11*$_{AP_SQ}$ transformed leaf. E, F, and G. The transformed plant showing secondary stems at the same point on the primary stem.

In the transformed plants, the expression levels of genes that control plant architecture were determined, such as the *BRANCH1* (*BRC1*) gene and the *Pectinmethytrasferase5* (*PME5*) gene. The Bel 1-like homeodomain (*BLH*$_8$) or *POUNDFOOLISH* (*pnf*) and *BLH*$_9$ or *Pennywise* (*BLR/PNY*) are necessary for floral evocation whilst *BREVIPEDICELLUS* (*BP*)/*KNATT1* has a primary role in internode patterning or is a key for inflorescence architecture regulation which involves stem elongation (Venglat *et al*., 2001; Mele *et al*., 2003).

As for the secondary stem, the *SAP11*$_{AP_SQ}$ transformed plants produced more secondary inflorescence meristems and clustered cauline leaves than wild type and vector only as a result of the defective phyllotaxis pattern. The phyllotaxis pattern is controlled by the *BRC1* and *PME5* genes and the gene expression results of *SAP11*$_{AP_SQ}$ transformed plant showed down regulation compared to wild type and vector only, which indicates that the SAP11$_{AP_SQ}$ protein reduced the expression level of the *BRC1* and *PME5* genes (Figure 5.10).

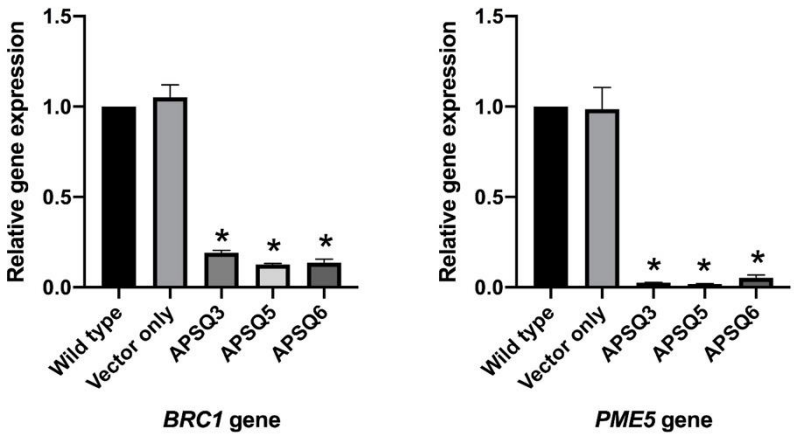


Figure 5.10 Relative gene expression of *BRC1* and *PME5* genes compared to *PP2A* (actin) gene that were examined by relative quantitative RT-PCR with the gene expression level in wild type set to 1. The columns show gene expression levels of wild type, vector only and three transformed plants and standard errors (SEs) (bars) of relative quantitative RT-PCR from three biological replicates. The * above the columns indicates statistical differences ($p<0.05$) by student t-test.

For stem and flower development, Figure 5.11 shows that the *PNF* expression level in three transformed plant lines was highly downregulated compared to wild type; moreover, the *BLR/PNY* expression level was also downregulated compared to wild type, indicating that the gene expression level of *PNF* and *BLR/PNY* genes were reduced by $SAP11_{AP_SQ}$ and as a result the transformed plant lines produced terminated flowers on the pedicel (Figure 5.9C). Furthermore, for the *BP/KNATT1* gene, the expression level was significantly decreased (Figure 5.11) indicating that the *BP/KNATT1* gene was affected from the $SAP11_{AP_SQ}$ to result in the different stem elongation from wild type and vector only.

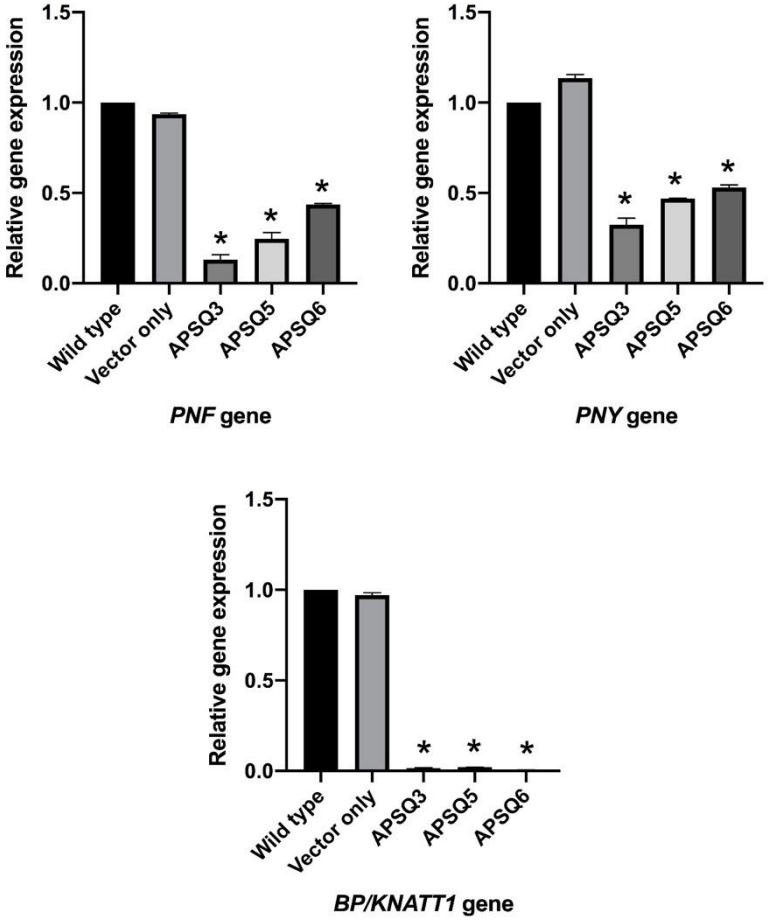


Figure 5.11 Relative gene expression of *PNF, PNY* and *BP/KNATT1* genes compared to *PP2A* (actin) gene that were examined by relative quantitative RT-PCR with the gene expression level in wild type set to 1. The columns show gene expression levels of wild type, vector only and three transformed plants and standard errors (SEs) (bars) of relative quantitative RT-PCR from three biological replicates. The * above the columns indicates statistical differences ($p<0.05$) by student t-test.

5.3.1.2 *SAP11*$_{BCRD}$ transformed plants

SAP11$_{BCRD}$ gene expression was significant greater for all of the three transformed plants compared to wild type and vector only (*p<0.05*) (Figure 5.12).

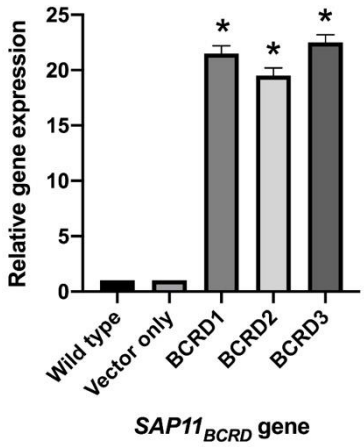


Figure 5.12 Relative gene expression of transgene compared to *PP2A* (actin) gene that were examined by relative quantitative RT-PCR with the gene expression level in wild type set to 1. The columns show gene expression levels of wild type, vector only and three transformed plants and standard errors (SEs) (bars) of relative quantitative RT-PCR from three biological replicates. The * above the columns indicates statistical differences (p<0.05) by student t-test.

The *SAP11*$_{BCRD}$ transformed plants showed organ fusion of the secondary inflorescence meristems with primary inflorescence stems causing phyllotaxis defects, which are two or more secondary inflorescence meristem growing at a single point or means the internode could not be elongated during plant development (Figure 5.13). The cell wall development is controlled by the

pectinmethyltransferase5 (*PME5*) gene. Figure 5.14 shows the *PME5* gene expression levels between transformed plants and wild type and that the *PME5* gene of transformed plants was down-regulated compared to wild type and vector only. As a result, the *SAP11*$_{BCRD}$ could be effect to the *PME5* gene during plant development. However, the *BRC1* gene was at the same level as in wild type and vector only plants, so the *SAP11*$_{BCRD}$ did not affect the *BRC1* gene and they did not produce more axillary stems (Figure 5.14).

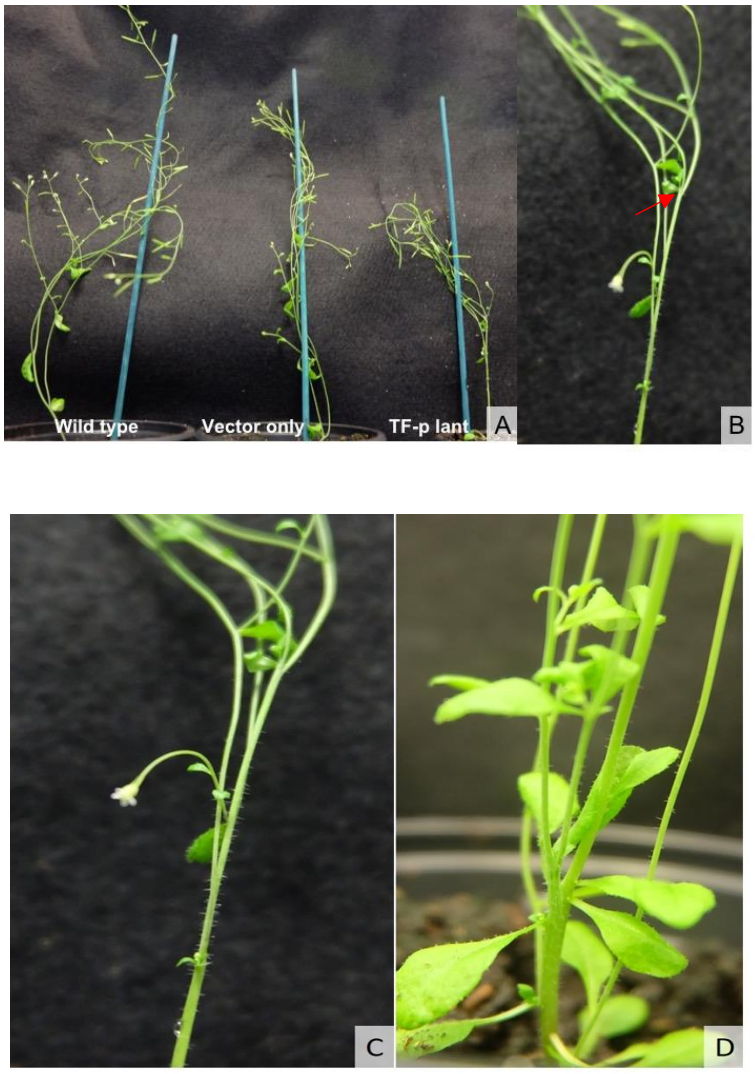


Figure 5.13 Arabidopsis T_2 generation and *SAP11*$_{BCRD}$ transformed plants. A. T_2 *SAP11*$_{BCRD}$ transformed plant compared to wild type and vector only. B. *SAP11*$_{BCRD}$ transformed plant showing phyllotaxis symptom.

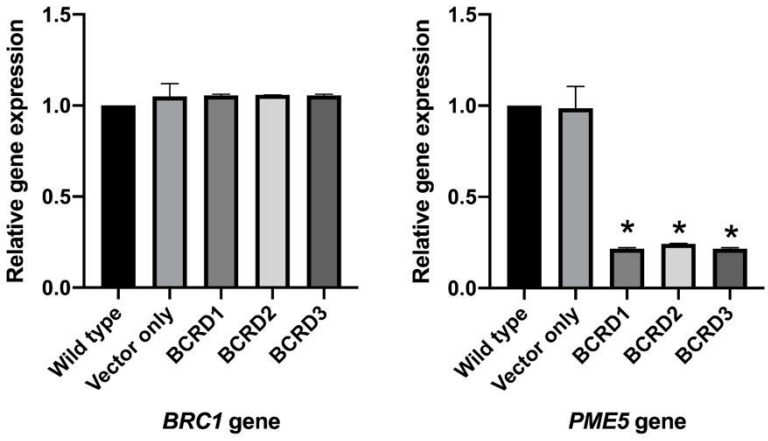


Figure 5.14 Relative gene expression of *BRC1* and *PME5* genes compared to *PP2A* (actin) gene that were examined by relative quantitative RT-PCR with the gene expression level in wild type set to 1. The columns show gene expression levels of wild type, vector only and three transformed plants and standard errors (SEs) (bars) of relative quantitative RT-PCR from three biological replicates. The * above the columns indicates statistical differences ($p<0.05$) by student t-test.

Moreover, The *SAP11*$_{BCRD}$ did not affect the *PNF BLR/PNY* and *BP/KNATT1* genes so the transformed plants could produce flowers and siliques and the stem height was regular (Figure 5.15).

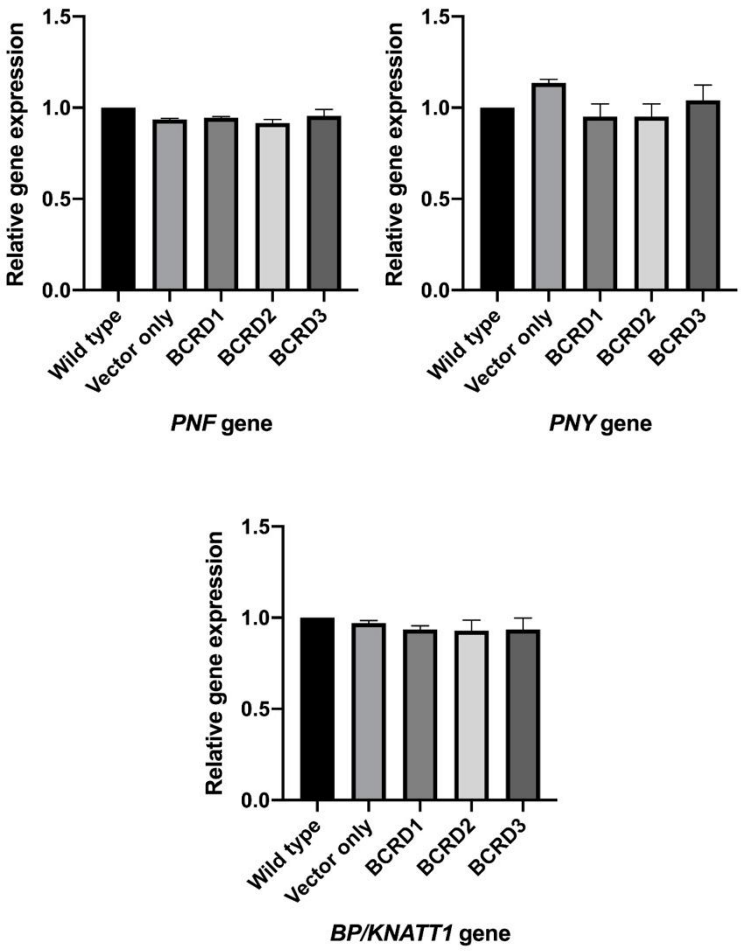


Figure 5.15 Relative gene expression of *PNF, PNY* and *BP/KNATT1* genes compared to *PP2A* (actin) gene that were examined by relative quantitative RT-PCR with the gene expression level in wild type set to 1. The columns show gene expression levels of wild type, vector only and three transformed plants and standard errors (SEs) (bars) of relative quantitative RT-PCR from three biological replicates. The * above the columns indicates statistical differences ($p<0.05$) by student t-test.

In addition, the transformed flowers were normal and the same as on wild type and vector only plants, which consist of carpel, stamen, sepal and petal. So, the *SAP11*$_{BCRD}$ did not affect flower development (Figure 5.16).

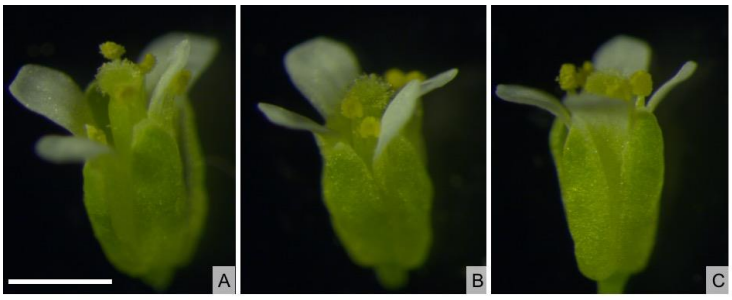


Figure 5.16 Photograph showing the flowers of wild type (A), vector only (B) and *SAP11*$_{BCRD}$ transformed plants (C) bar = 1mm.

5.3.1.3 *SAP11*$_{CoP}$ Transformed plants

For *SAP11*$_{CoP}$ three transformed plants, the *SAP11* gene expression were increased compared to controls and the levels in transformed plants were different and depended on gene copy number inserted into the *Arabidopsis* genome and the insertion position (Figure 5.17).

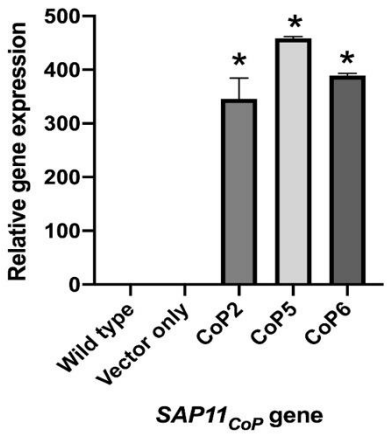


Figure 5.17 Relative gene expression of transgene compared to *PP2A* (actin) gene that were examined by relative quantitative RT-PCR with the gene expression level in wild type set to 1. The columns show gene expression levels of wild type, vector only and three transformed plants and standard errors (SEs) (bars) of relative quantitative RT-PCR from three biological replicates. The * above the columns indicates statistical differences ($p<0.05$) by student t-test.

The *SAP11*$_{CoP}$ transformed plant morphology was the same as for *SAP11*$_{BCRD}$ transformed plants. They showed the organ fusion of secondary inflorescence meristems (Figure 5.18) and then the *PME5* gene expression of transformed plants were reduced compared to wild type and vector only (Figure 5.19). However, the *BRC1* gene expression was reduced compared to wild type and vector only causing the transformed plants to produce more axillary stems than wild type and vector only (Figure 5.18A).

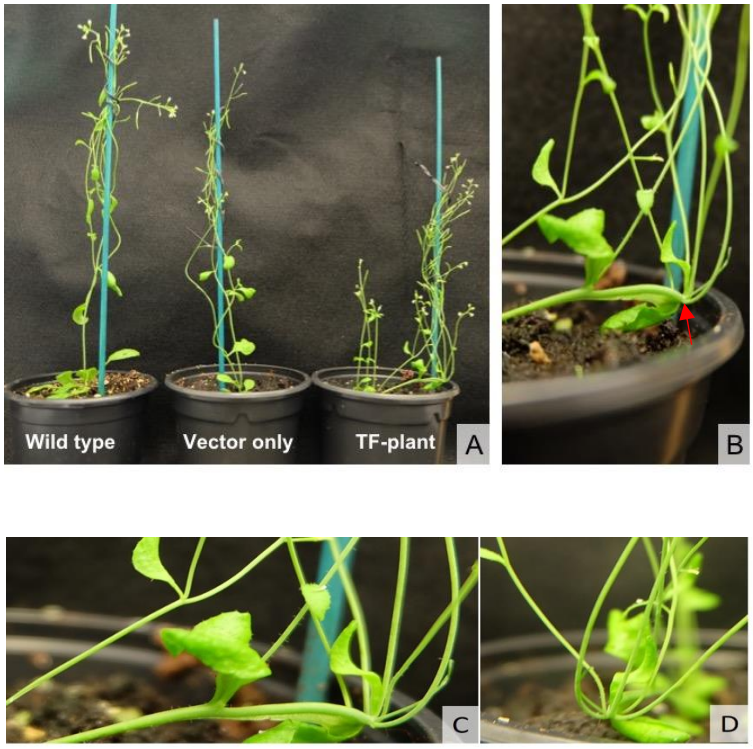


Figure 5.18 Arabidopsis T_2 generation and *SAP11*$_{CoP}$ transformed plants. A. T_2 *SAP11*$_{CoP}$ transformed plant compared to wild type and vector only. B. *SAP11*$_{CoP}$ transformed plant showing phyllotaxis symptom.

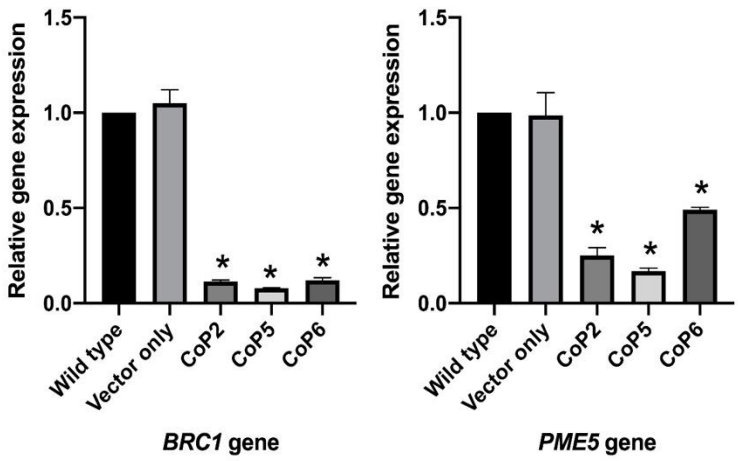


Figure 5.19 Relative gene expression of *BRC1* and *PME5* genes compared to *PP2A* (actin) gene that were examined by relative quantitative RT-PCR with the gene expression level in wild type set to 1. The columns show gene expression levels of wild type, vector only and three transformed plants and standard errors (SEs) (bars) of relative quantitative RT-PCR from three biological replicates. The * above the columns indicates statistical differences ($p<0.05$) by student t-test.

Furthermore, the $SAP11_{CoP}$ gene did not affect flower development and main stem elongation and the *PNF BLR/PNY* and *BP/KNATT1* gene expression levels were the same as wild type and vector only (Figure 5.20).

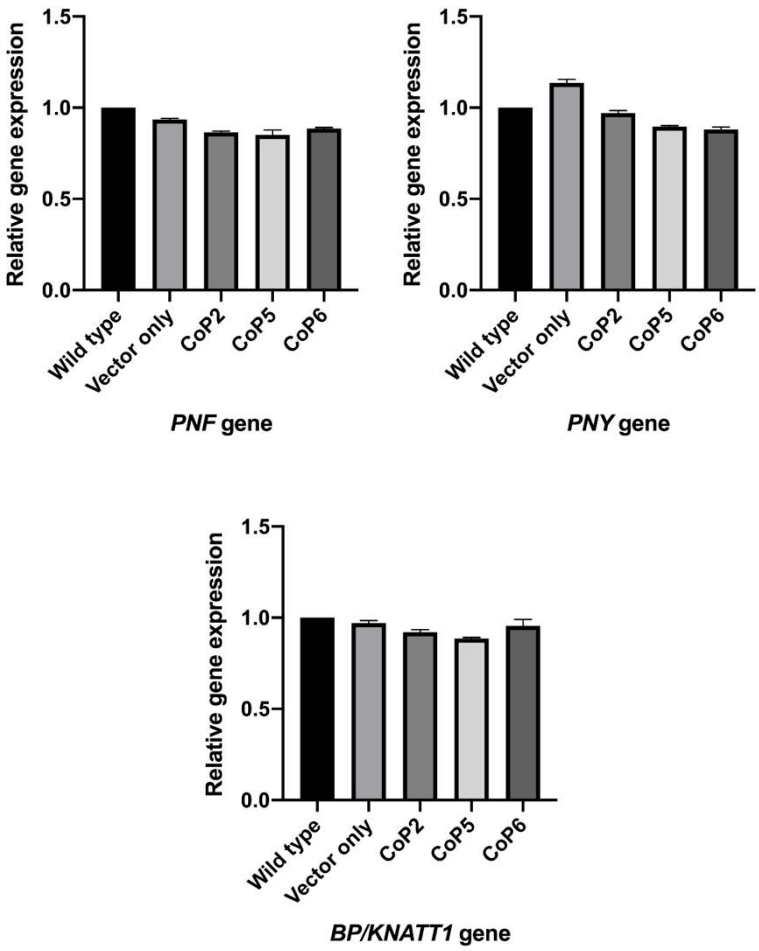


Figure 5.20 Relative gene expression of *PNF, PNY* and *BP/KNATT1* genes compared to *PP2A* (actin) gene that were examined by relative quantitative RT-PCR with the gene expression level in wild type set to 1. The columns show gene expression levels of wild type, vector only and three transformed plants and standard errors (SEs) (bars) of relative quantitative RT-PCR from three biological replicates. The * above the columns indicates statistical differences ($p<0.05$) by student t-test.

Figure 5.21 shows that the transformed flowers were normal when compared to wild type and vector only and they could form siliques for reproduction.

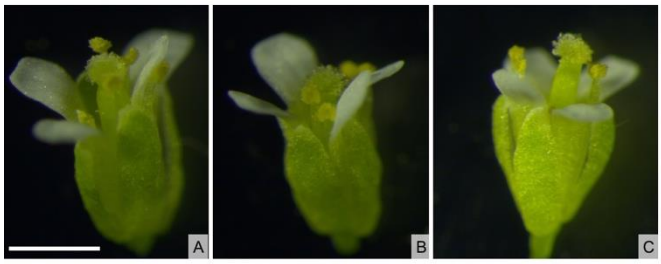


Figure 5.21. Photograph showing the flowers of wild type (A), vector only (B) and *SAP11*$_{CoP}$ transformed plants (C) bar = 1mm.

5.3.1.4 *SAP11*$_{SGP}$ Transformed plants

The *SAP11*$_{SGP}$ gene expression level in three transformed plants were higher than in wild type and vector only and the level varied within the transformed plants depending on copy number and insert position (Figure 5.22).

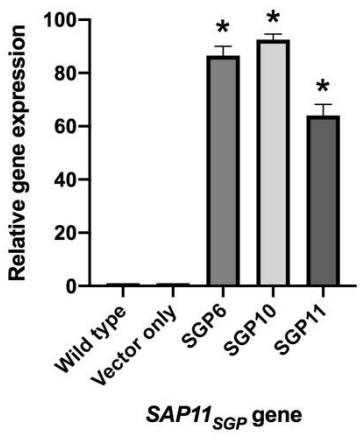


Figure 5.22. Relative gene expression of transgene compared to *PP2A* (actin) gene that were examined by relative quantitative RT-PCR with the gene expression level in wild type set to 1. The columns show gene expression levels of wild type, vector only and three transformed plants and standard errors (SEs) (bars) of relative quantitative RT-PCR from three biological replicates. The * above the columns indicates statistical differences (p<0.05) by student *t*-test.

Morphologically, transformed plants produced more axillary stems than wild type and vector only (Figure 5.23); however, the transformed plants did not show short internodes and sterility. The branching of stems is controlled by the *BRC1* gene and real time PCR results showed that the *BRC1* level in transformed plants was down regulated compared to wild type and vector only (Figure 5.24) whilst the *PME5* gene expression level was the same as in wild type and vector only plants (Figure 5.24).

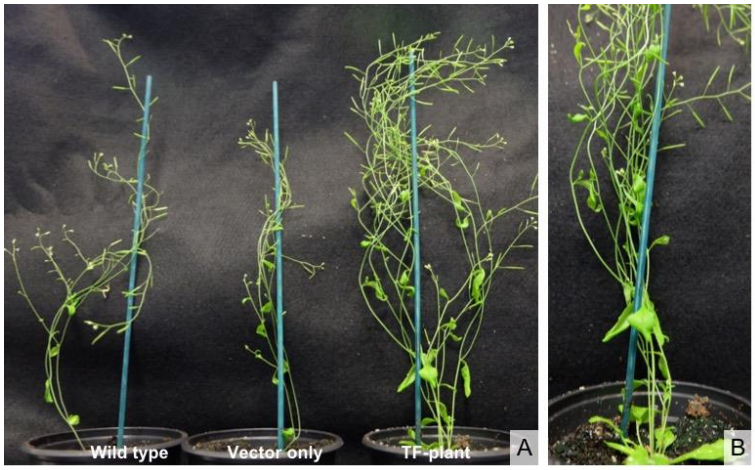


Figure 5.23 Arabidopsis T_2 generation and *SAP11*$_{SGP}$ transformed plants. A. T_2 *SAP11*$_{SGP}$ transformed plant compared to wild type and vector only. B. *SAP11*$_{SGP}$ transformed plant showing more branching stem.

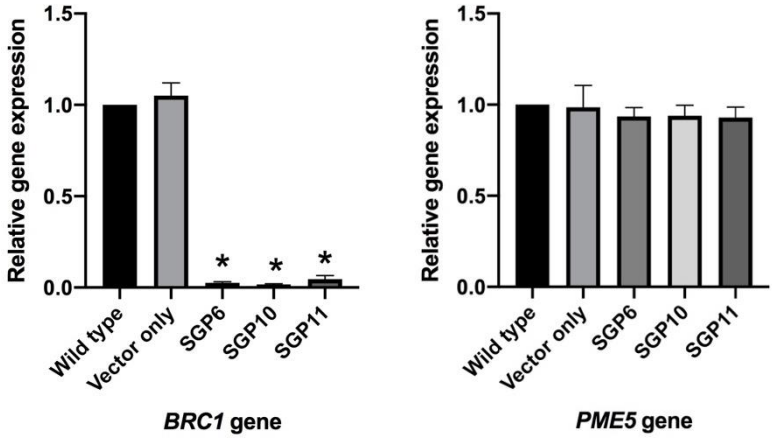


Figure 5.24 Relative gene expression of *BRC1* and *PME5* genes compared to *PP2A* (actin) gene that were examined by relative quantitative RT-PCR with the gene expression level in wild type set to 1. The columns show gene expression levels of wild type, vector only and three transformed plants and standard errors (SEs) (bars) of relative quantitative RT-PCR from three biological replicates. The * above the columns indicates statistical differences ($p<0.05$) by student t-test.

SAP11$_{SGP}$ did not affect the floral organs and the main stem elongation with the height of transformed plants being normal, and the *BLR/PNY PNF* and *BP/KNATT1* gene expression levels did not differ from wild type and vector only plants (Figure 5.25).

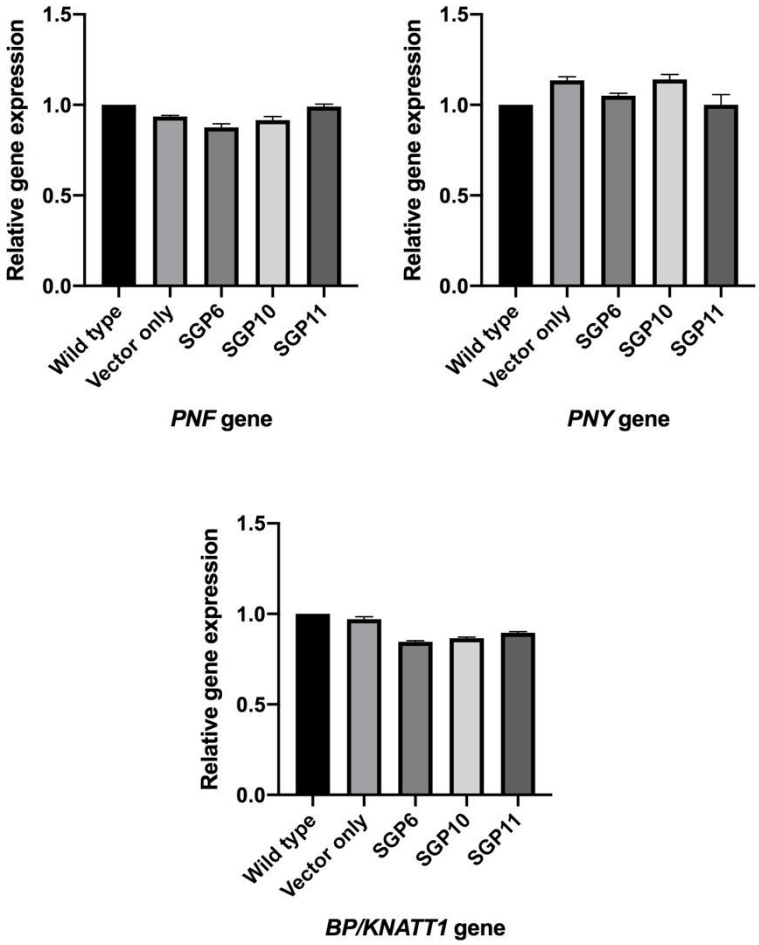


Figure 5.25 Relative gene expression of *PNF, PNY* and *BP/KNATT1* genes compared to *PP2A* (actin) gene that were examined by relative quantitative RT-PCR with the gene expression level in wild type set to 1. The columns show gene expression levels of wild type, vector only and three transformed plants and standard errors (SEs) (bars) of relative quantitative RT-PCR from three biological replicates. The * above the columns indicates statistical differences ($p<0.05$) by student t-test.

Furthermore, the transformed plant produced normal flowers and they were fertile to form siliques for reproduction (Figure 5.26).

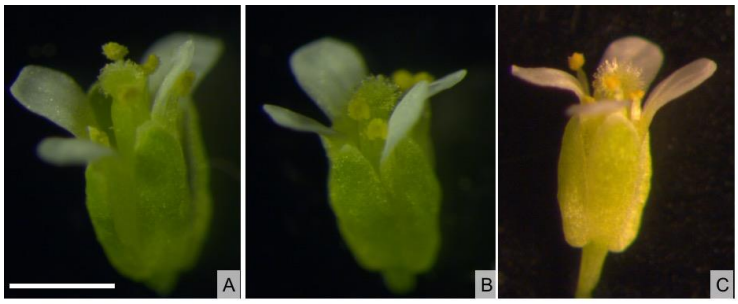


Figure 5.26 Photograph showing the flowers of wild type (A), vector only (B) and *SAP11*$_{SGP}$ transformed plants (C) bar = 1mm.

5.3.1.5 *SAP11*$_{VCP}$ Transformed plants

The *SAP11*$_{VCP}$ gene expression level of three transformed plants were increased compared to the wild type and vector only; however, the level was different in each plant (Figure 5.27).

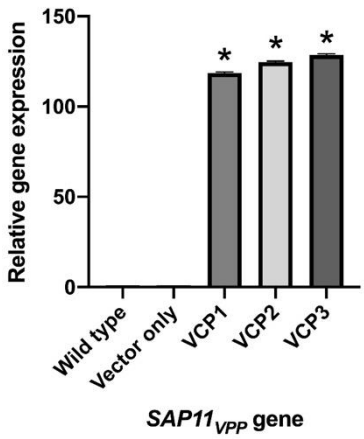


Figure 5.27 Relative gene expression of transgene compared to *PP2A* (actin) gene that were examined by relative quantitative RT-PCR with the gene expression level in wild type set to 1. The columns show gene expression levels of wild type, vector only and three transformed plants and standard errors (SEs) (bars) of relative quantitative RT-PCR from three biological replicates. The * above the columns indicates statistical differences ($p<0.05$) by student t-test.

Morphologically, the *SAP11*$_{VCP}$ transformed plants were significantly shorter than wild type and vector only and the flowers and siliques were also smaller than wild type (Figure 5.28A, B). Moreover, the flower inflorescences were compact compared to normal and the flower stalk (pedicel) was shorter than wild type and vector only (Figure 5.28C and D). In addition, leaves were small and quite curled (Figure 5.28E) whilst wild type leaves were plain (Figure 5.28F) and the siliques showed a phyllotaxis defect in which they produced silique inflorescences at the same point, whilst the control plants showed normal phyllotaxis patterns (Figure 5.28G and H). Furthermore, Figure 5.28I

shows the organ fusion of secondary inflorescence meristems with primary inflorescences.





Figure 5.28 Arabidopsis T_2 generation and *SAP11*$_{VCP}$ transformed plants. A. T_2 *SAP11*$_{VCP}$ transformed plant compared to wild type and vector only. B. *SAP11*$_{VCP}$ transformed plant showed the height of transformed plant and phyllotaxis of secondary inflorescence meristems. C. A representative flower. D. Wild type flower. E. Transformed leaf. F. Wild type leaf G. Phyllotaxis symptom at siliques and H. Normal silique pattern (Wild type). I. Transformed plant showing the organ fusion.

BRC1 gene expression, which controls the axillary pattern, was not different from wild type and vector only plants, whilst the *PME5* gene expression level was down regulated compared to the wild type and vector only (Figure 5.29)

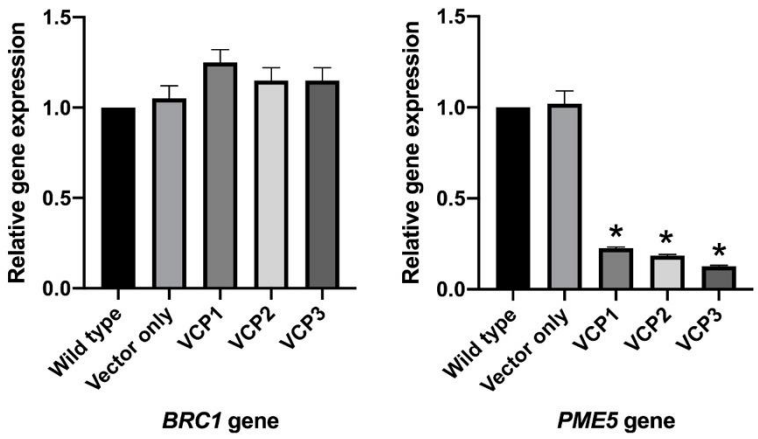


Figure 5.29 Relative gene expression of *BRC1* and *PME5* genes compared to *PP2A* (actin) gene that were examined by relative quantitative RT-PCR with the gene expression level in wild type set to 1. The columns show gene expression levels of wild type, vector only and three transformed plants and standard errors (SEs) (bars) of relative quantitative RT-PCR from three biological replicates. The * above the columns indicates statistical differences ($p<0.05$) by student t-test.

For the *PNF* gene, expression in transformed plants was lower than wild type and vector only plants but it was not significant whilst the *BP/KNATT1* and *BLR/PNY* gene expression levels in transformed plants, which control primary stem elongation, were significantly decreased compared to wild type and vector only (Figure 5.30).

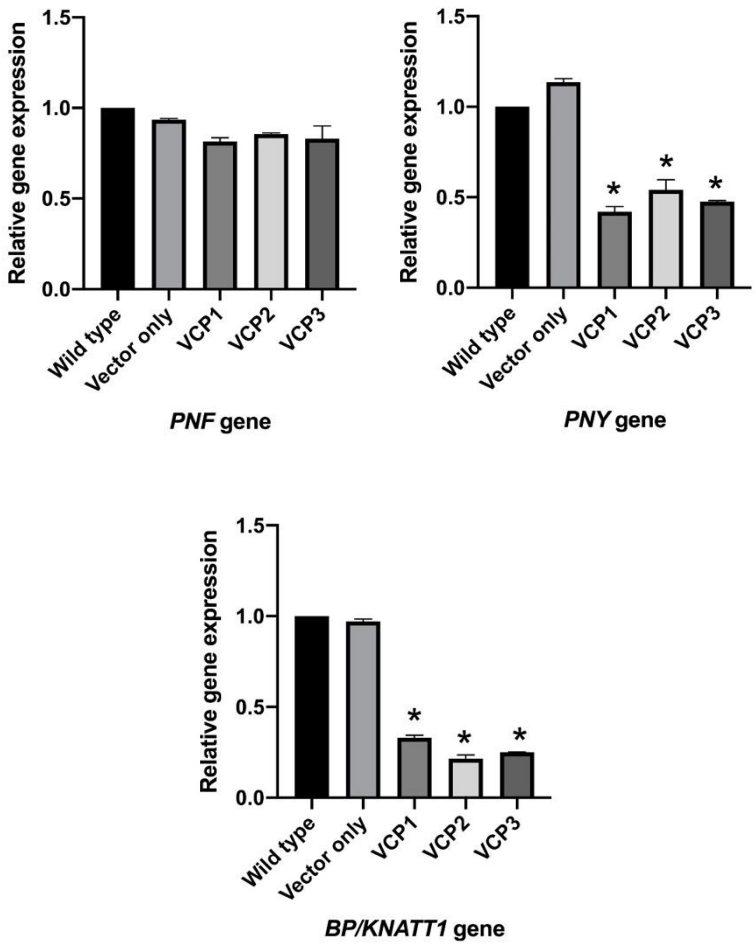


Figure 5.30 Relative gene expression of *PNF, PNY* and *BP/KNATT1* genes compared to *PP2A* (actin) gene that were examined by relative quantitative RT-PCR with the gene expression level in wild type set to 1. The columns show gene expression levels of wild type, vector only and three transformed plants and standard errors (SEs) (bars) of relative quantitative RT-PCR from three biological replicates. The * above the columns indicates statistical differences ($p<0.05$) by student t-test.

The flowers of the *SAP11*$_{VCP}$ transformed plants were smaller than in wild type and vector only plants although they appeared normal and were completely fertile (Figure 5.31).

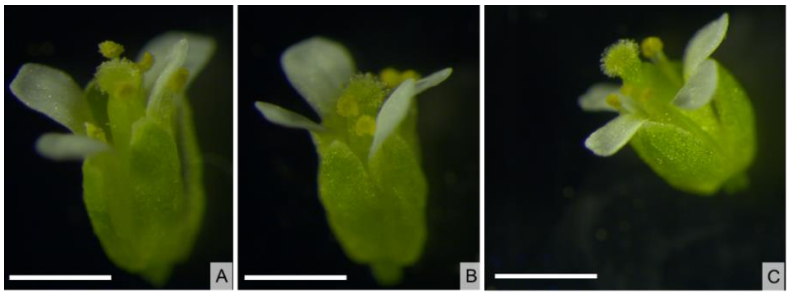


Figure 5.31 Photograph showing the flowers of wild type (A), vector only (B) and *SAP11*$_{VCP}$ transformed plants (C) bar = 1mm.

5.3.1.6 *EF1*$_{NGSD}$ Transformed plants

For *EF1*$_{NGSD}$ transformed plants transgene expression was significantly higher than in wild type and vector plants (Figure 5.32).

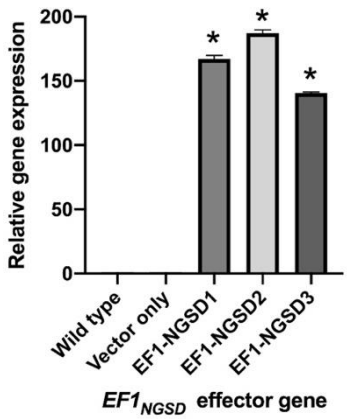


Figure 5.32 Relative gene expression of transgene compared to *PP2A* (actin) gene that were examined by relative quantitative RT-PCR with the gene expression level in wild type set to 1. The columns show gene expression levels of wild type, vector only and three transformed plants and standard errors (SEs) (bars) of relative quantitative RT-PCR from three biological replicates. The * above the columns indicates statistical differences ($p<0.05$) by student t-test.

The transformed plants did not show any altered phenotype and were the same height as wild type and vector only and they had only one primary stem. Moreover, secondary inflorescence meristems and flower inflorescences including siliques were the same as wild type (Figure 5.33) and the flowers of transformed plants were normal (Figure 5.34).

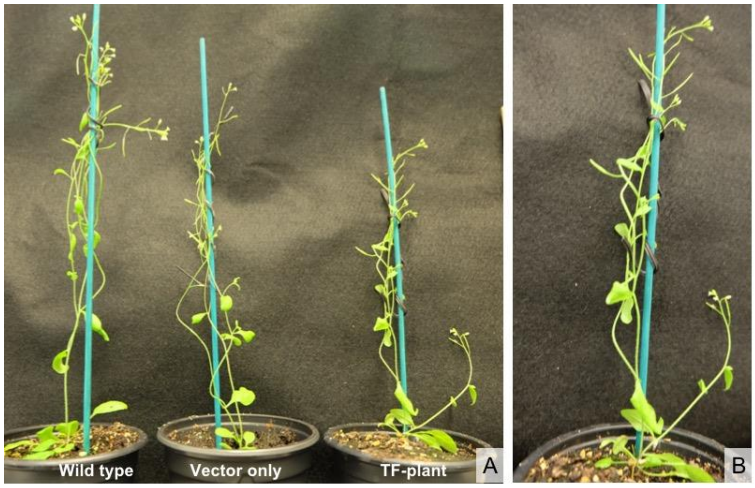


Figure 5.33 Arabidopsis T_2 generation and *EF1*$_{NGSD}$ transformed plants. A. T_2 *EF1*$_{NGSD}$ transformed plant compared to wild type and vector only. B. *EF1*$_{NGSD}$ transformed plant showing the normal morphology.

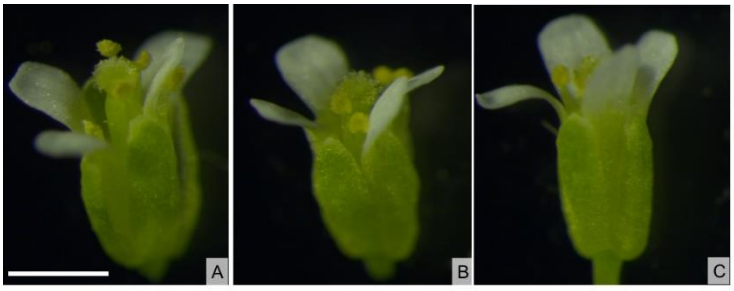


Figure 5.34 Photograph showing the flowers of wild type (A), vector only (B) and *EF1*$_{NGSD}$ transformed plants (C) bar = 1mm.

5.3.1.7 *EF2*$_{NGSD}$ Transformed plants

In the three transformed plants the transgene expression was significantly increased compared to the wild type and vector only (Figure 5.35).

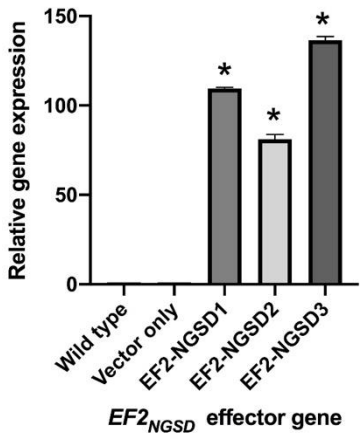


Figure 5.35 Relative gene expression of transgene compared to *PP2A* (actin) gene that were examined by relative quantitative RT-PCR with the gene expression level in wild type set to 1. The columns show gene expression levels of wild type, vector only and three transformed plants and standard errors (SEs) (bars) of relative quantitative RT-PCR from three biological replicates. The * above the columns indicates statistical differences ($p<0.05$) by student t-test.

As shown in chapter 3, this effector gene is similar to the SAP67-like protein of Chrysanthemum yellows phytoplasma, and the transformed *Arabidopsis* phenotype produced more axillary stems than wild type and vector only but there was no dwarfism (Figure 5.36). Branching is controlled by the *BRC1* gene, so *BRC1* gene expression was analysed by quantitative PCR. The result showed that the *BRC1* gene in transformed plants was significantly decreased compared to wild type and vector only as shown in Figure 5.37. However, the effector did not affect expression of the *PME5* gene, which was the same as in normal plants.



Figure 5.36 Arabidopsis T_2 generation and *EF2*$_{NGSD}$ transformed plants. A. T_2 *EF2*$_{NGSD}$ transformed plant compared to wild type and vector only. B. *EF2*$_{NGSD}$ transformed plant showing the more branching stem.

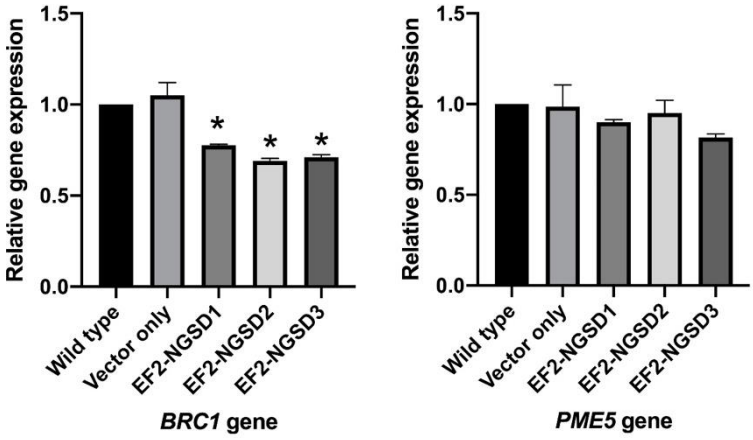


Figure 5.37. Relative gene expression of *BRC1* and *PME5* genes compared to *PP2A* (actin) gene that were examined by relative quantitative RT-PCR with the gene expression level in wild type set to 1. The columns show gene expression levels of wild type, vector only and three transformed plants and standard errors (SEs) (bars) of relative quantitative RT-PCR from three biological replicates. The * above the columns indicates statistical differences ($p<0.05$) by student t-test.

Even though the transformed plants produced more axillary stems than wild type and vector only main stem elongation and floral organ function were normal and the *PNF*, *BLR/PNY* and *BP/KNATT1* gene expression levels were the same as wild type and vector only plants (Figure 5.38).

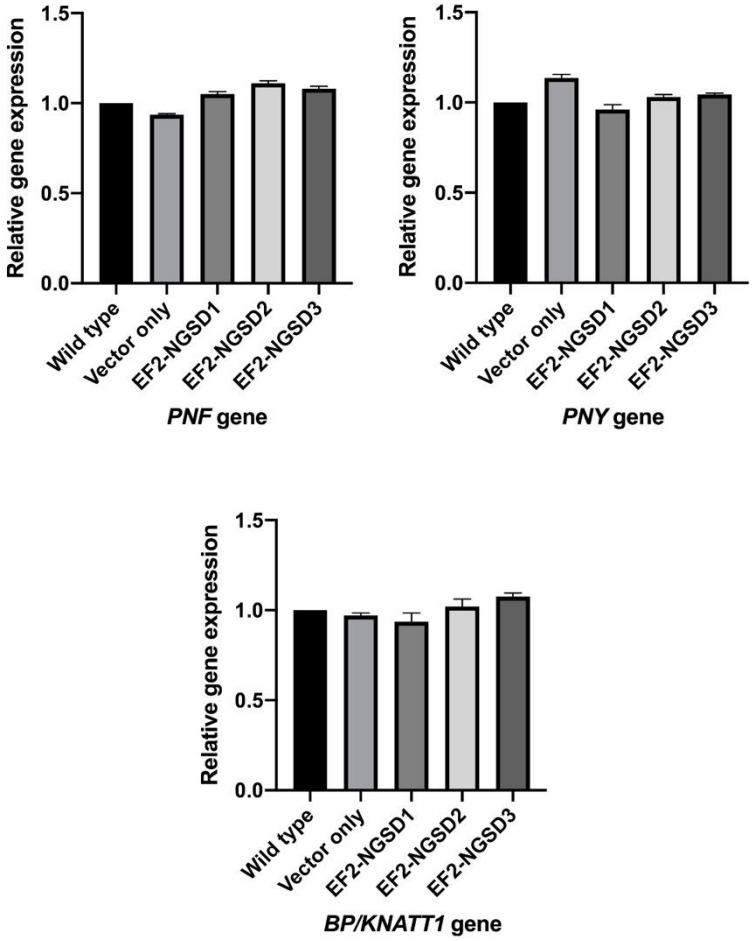


Figure 5.38. Relative gene expression of *PNF, PNY* and *BP/KNATT1* genes compared to *PP2A* (actin) gene that were examined by relative quantitative RT-PCR with the gene expression level in wild type set to 1. The columns show gene expression levels of wild type, vector only and three transformed plants and standard errors (SEs) (bars) of relative quantitative RT-PCR from

three biological replicates. The * above the columns indicates statistical differences ($p<0.05$) by student t-test.

In addition, this effector gene did not affect flower development because the transformed flowers were normal and fertility was the same as in wild type and vector only plants (Figure 5.39).

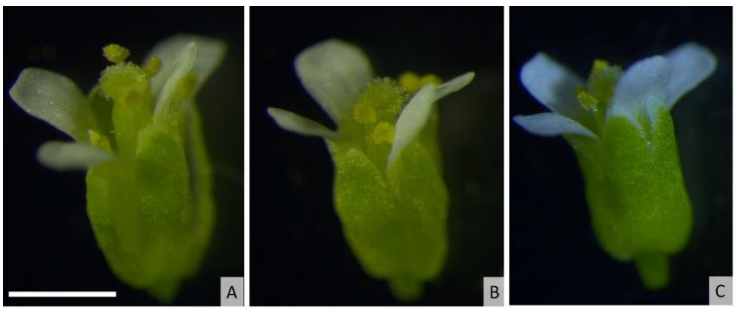


Figure 5.39.Photograph showing the flowers of wild type (A), vector only (B) and *EF2*$_{NGSD}$ transformed plants (C) bar = 1mm.

5.3.1.8 *EF3*$_{NGSD}$ Transformed plants

For the *EF3*$_{NGSD}$ gene expression levels were higher in three transformed plants than wild type and vector only (Figure 5.40). However, the phenotype of the transformed plants was normal with the transformed plants producing only one main stem and the main stem height was normal with regular secondary inflorescence meristems and flower inflorescences and a regular phyllotaxis pattern (Figure 5.41).

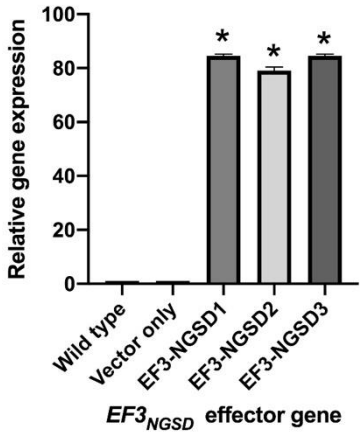


Figure 5.40. Relative gene expression of transgene compared to *PP2A* (actin) gene that were examined by relative quantitative RT-PCR with the gene expression level in wild type set to 1. The columns show gene expression levels of wild type, vector only and three transformed plants and standard errors (SEs) (bars) of relative quantitative RT-PCR from three biological replicates. The * above the columns indicates statistical differences ($p<0.05$) by student t-test.



Figure 5. 41.Arabidopsis T_2 generation and *EF3*$_{NGSD}$ transformed plants. A. T_2 *EF3*$_{NGSD}$ transformed plant compared to wild type and vector only. B. *EF3*$_{NGSD}$ transformed plant showing the normal morphology.

The transformed plants produced normal flowers which were the same as in wild type and vector only plants (Figure 5.42).

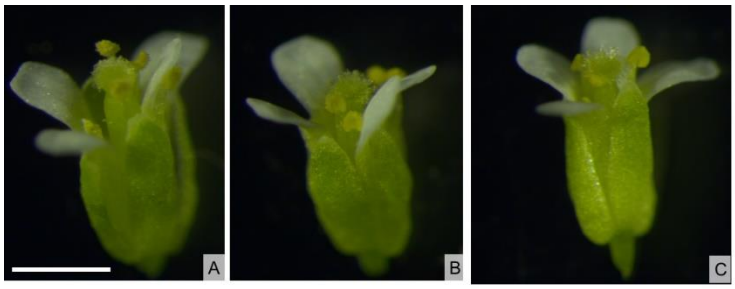


Figure 5.42. Photograph showing the flowers of wild type (A), vector only (B) and *EF3*$_{NGSD}$ transformed plants (C) bar = 1mm.

5.3.1.9 *EF4*$_{NGSD}$ Transformed plants

The *EF4*$_{NGSD}$ gene expression level of three transformed plants was higher than wild type and vector only (Figure 5.43). Nevertheless, the transformed plant morphology was similar to wild type and vector only. The transformed plant height was equal to wild type and vector only and there was only one main stem (Figure 5.44) and the phyllotaxis pattern of secondary inflorescence meristems including flower inflorescences was normal.

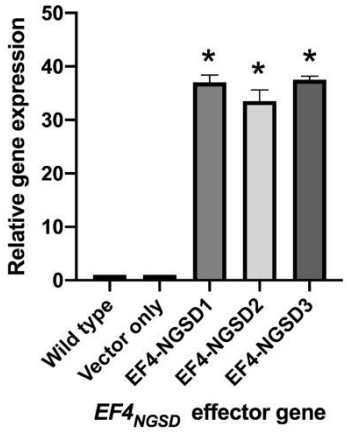


Figure 5.43. Relative gene expression of transgene compared to *PP2A* (actin) gene that were examined by relative quantitative RT-PCR with the gene expression level in wild type set to 1. The columns show gene expression levels of wild type, vector only and three transformed plants and standard errors (SEs) (bars) of relative quantitative RT-PCR from three biological replicates. The * above the columns indicates statistical differences ($p<0.05$) by student t-test.

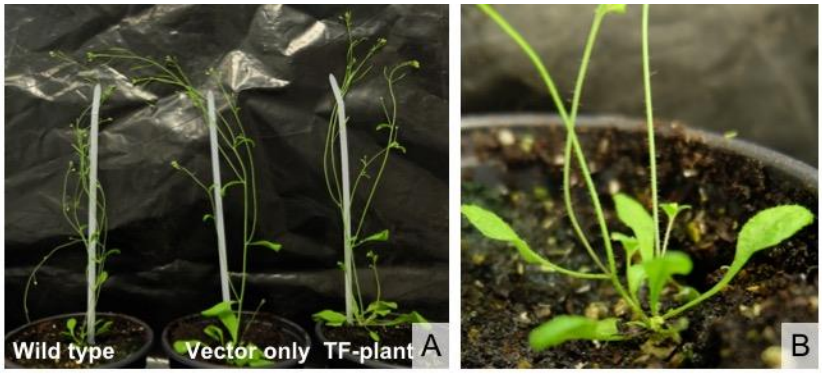


Figure 5.44. Arabidopsis T_2 generation and *EF4*$_{NGSD}$ transformed plants. A. T_2 *EF4*$_{NGSD}$ transformed plant compared to wild type and vector only. B. *EF4*$_{NGSD}$ transformed plant showing the normal morphology.

The transformed plants produced normal flowers which were the same as wild type and vector only (Figure 5.45).

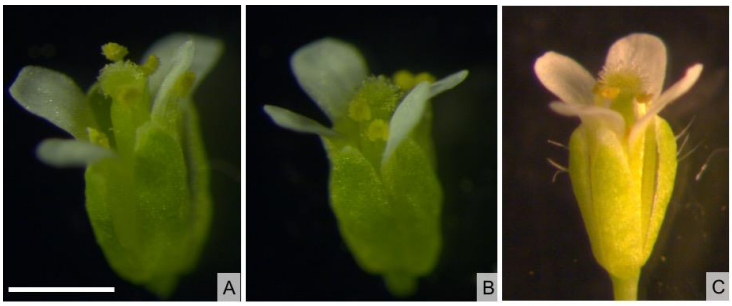


Figure 5.45. Photograph showing the flowers of wild type (A), vector only (B) and *EF4*$_{NGSD}$ transformed plants (C) bar = 1mm.

5.3.1.10 *EF5*$_{NGSD}$ Transformed plants

The *EF5*$_{NGSD}$ gene expression level of three transformed plants were higher than wild type (Figure 5.46). Transformed plants were the same height as wild type and there was also a primary stem (Figure 5.47) and the phyllotaxis form of secondary inflorescence meristems was the same as wild type and vector only.

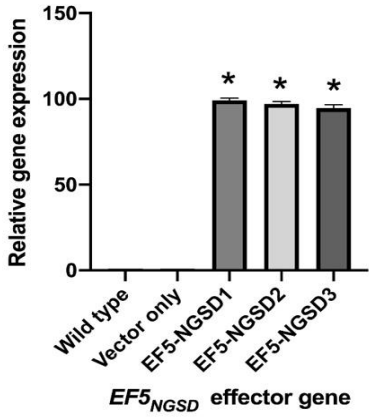


Figure 5.46.Relative gene expression of transgene compared to *PP2A* (actin) gene that were examined by relative quantitative RT-PCR with the gene expression level in wild type set to 1. The columns show gene expression levels of wild type, vector only and three transformed plants and standard errors (SEs) (bars) of relative quantitative RT-PCR from three biological replicates. The * above the columns indicates statistical differences ($p<0.05$) by student t-test.



Figure 5.47. Arabidopsis T_2 generation and *EF5*$_{NGSD}$ transformed plants. A. T_2 *EF5*$_{NGSD}$ transformed plant compared to wild type and vector only. B. *EF5*$_{NGSD}$ transformed plant showing the normal morphology.

Transformed plants produced normal flowers which were the same as wild type and vector only (Figure 5.48).

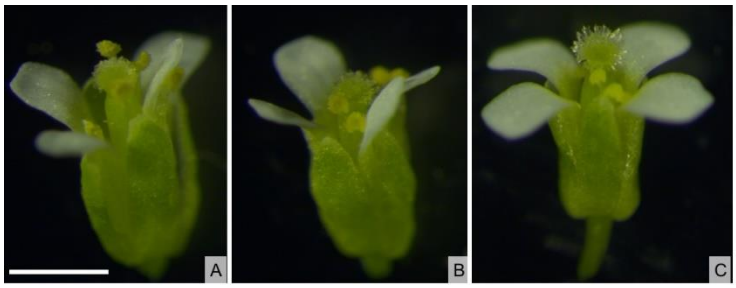


Figure 5.48. Photograph showing the flowers of wild type (A), vector only (B) and *EF5*$_{NGSD}$ transformed plants (C) bar = 1mm.

5.3.1.11 *EF6*$_{NGSD}$ Transformed plants

The *EF6*$_{NGSD}$ gene expression level of three transformed plants were higher than wild type (Figure 5.49). transformed plants had a primary main stem

similar to wild type and the secondary inflorescence meristems and flower inflorescences had the regular phyllotaxis pattern and were the same as wild type and vector only (Figure 5.50).

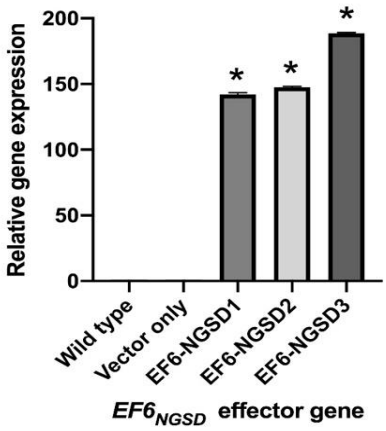


Figure 5.49. Relative gene expression of transgene compared to *PP2A* (actin) gene that were examined by relative quantitative RT-PCR with the gene expression level in wild type set to 1. The columns show gene expression levels of wild type, vector only and transformed plants and standard errors (SEs) (bars) of relative quantitative RT-PCR from three biological replicates. The * above the columns indicates statistical differences ($p<0.05$) by student t-test.

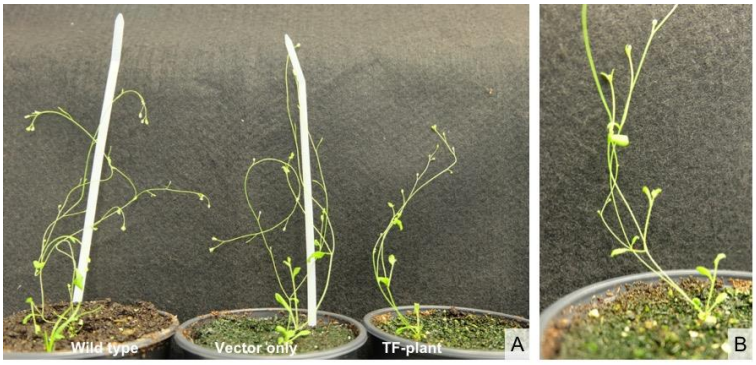


Figure 5.50.Arabidopsis T_2 generation and *EF6*$_{NGSD}$ transformed plants. A. T_2 *EF6*$_{NGSD}$ transformed plant compared to wild type and vector only. B. *EF6*$_{NGSD}$ transformed plant showing the normal morphology.

Ttransformed plants produced normal flowers which were the same as wild type and vector only (Figure 5.51).

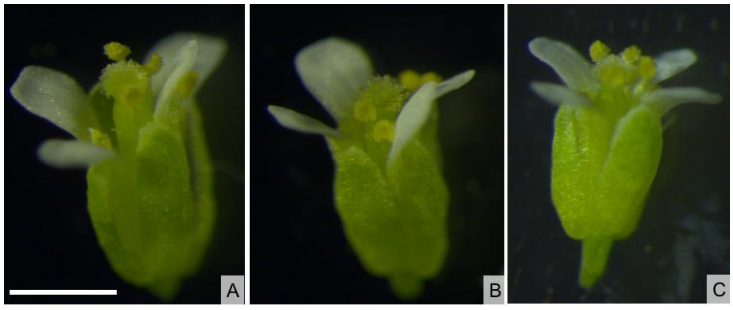


Figure 5.51. Photograph showing the flowers of wild type (A), vector only (B) and *EF6*$_{NGSD}$ transformed plants (C) bar = 1mm.

5.3.1.12 *EF7*$_{NGSD}$ Transformed plants

The *EF7*$_{NGSD}$ gene encodes a SAP11 like protein and the *EF7*$_{NGSD}$ gene expression was significant increased in three transformed plants compared to wild type and vector only (Figure 5.52).

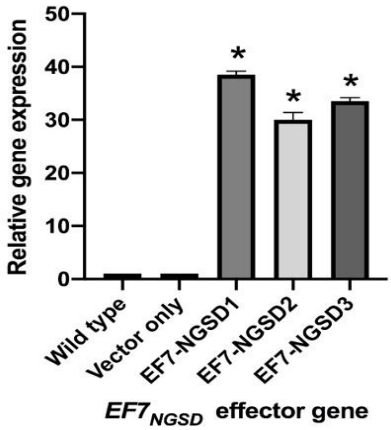


Figure 5.52 Relative gene expression of transgene compared to *PP2A* (actin) gene that were examined by relative quantitative RT-PCR with the gene expression level in wild type set to 1. The columns show gene expression levels of wild type, vector only and three transformed plants and standard errors (SEs) (bars) of relative quantitative RT-PCR from three biological replicates. The * above the columns indicates statistical differences (p<0.05) by student *t*-test.

Transformed plants produced more axillary inflorescences than wild type and vector only; however, the transformed plant height was the same as wild type and vector only (Figure 5.53).

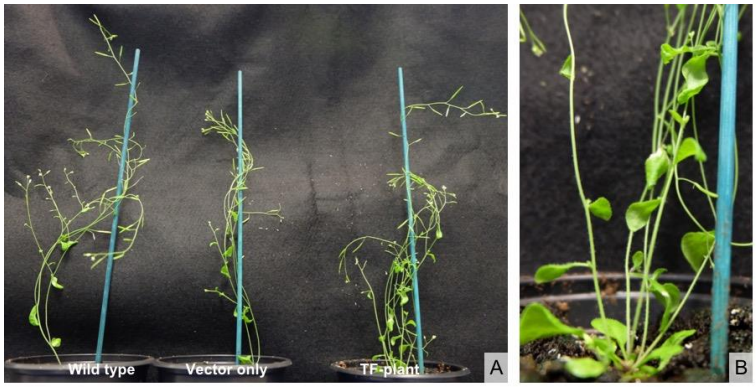


Figure 5.53. Arabidopsis T_2 generation and *EF7*$_{NGSD}$ transformed plants. A. T_2 *EF7*$_{NGSD}$ transformed plant compared to wild type and vector only. B. *EF7*$_{NGSD}$ transformed plant showing a more branched stem.

The *BRC1* gene expression level of transformed plants was significantly decreased compared to wild type (Figure 5.54). However, even though the *BRC1* gene was less expressed it did not affect the phyllotaxis pattern of secondary inflorescence meristems and the *PME5* gene expression levels were the same as wild type and vector only (Figure 5.54).

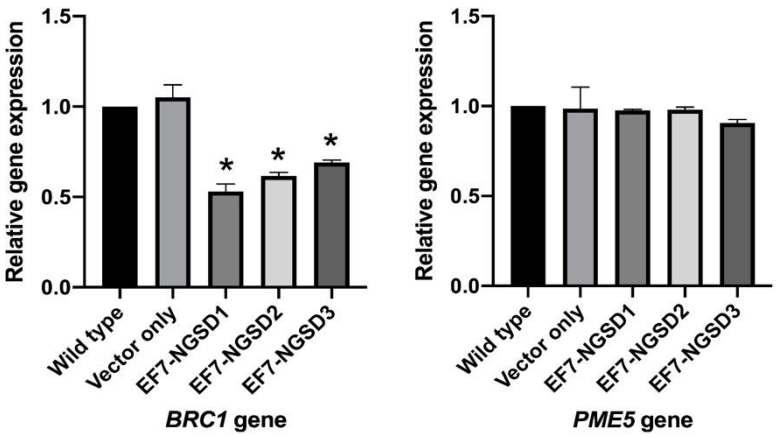


Figure 5.54. Relative gene expression of *BRC1* and *PME5* genes compared to *PP2A* (actin) gene that were examined by relative quantitative RT-PCR with the gene expression level in wild type set to 1. The columns show gene expression levels of wild type, vector only and three transformed plants and standard errors (SEs) (bars) of relative quantitative RT-PCR from three biological replicates. The * above the columns indicates statistical differences ($p<0.05$) by student t-test.

Furthermore, the *EF7*$_{NGSD}$ effector gene did not affect floral organ formation and the primary main stem elongation and the *PNF BLR/PNY* and *BP/KNATT1* gene expression levels were not different to wild type and vector only (Figure 5.55).

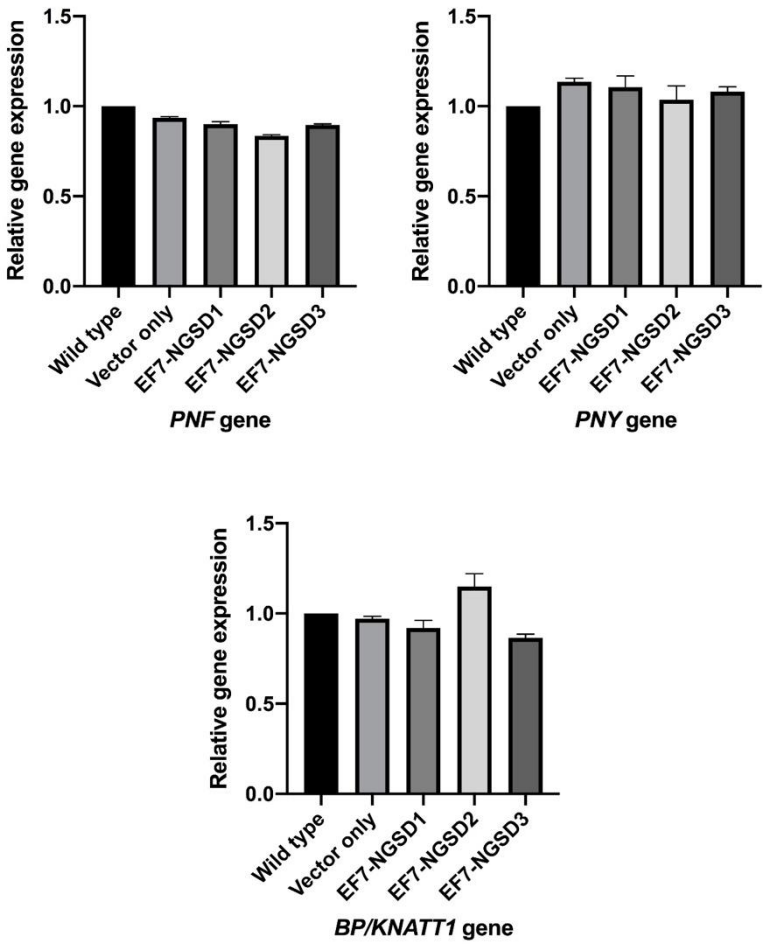


Figure 5.55 Relative gene expression of *PNF, PNY* and *BP/KNATT1* genes compared to *PP2A* (actin) gene that were examined by relative quantitative RT-PCR the gene expression level in wild type set to 1. The columns show gene expression levels of wild type, vector only and three transformed plants and standard errors (SEs) (bars) of relative quantitative RT-PCR from three biological replicates. The * above the columns indicates statistical differences ($p<0.05$) by student t-test.

Flowers were normal and they produced siliques (Figure 5.56).

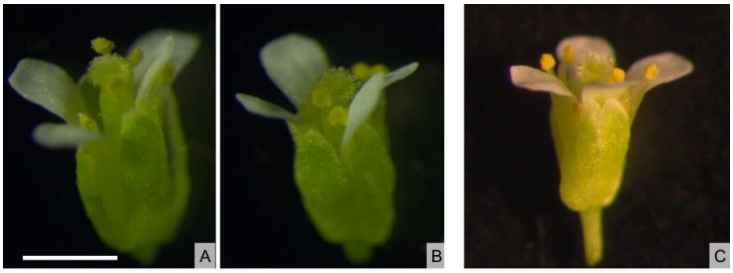


Figure 5.56. Photograph showing the flowers of wild type (A), vector only (B) and *EF7*$_{NGSD}$ transformed plants (C) bar = 1mm.

5.3.1.13 *EF2*$_{SCWL}$ Transformed plants

The *EF2*$_{SCWL}$ gene, was similar to the *EF2*$_{NGSD}$ gene, encoding a SAP67-like protein and the *EF2*$_{SCWL}$ gene expression levels were significantly higher in three transformed plants than wild type and vector only (Figure 5.57).

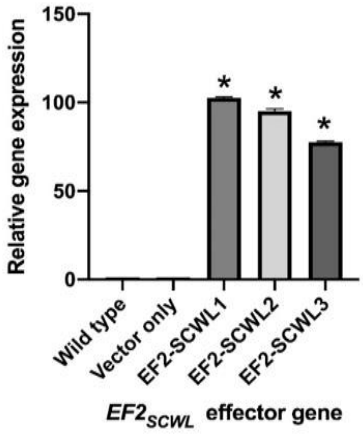


Figure 5.57. Relative gene expression of transgene compared to *PP2A* (actin) gene that were examined by relative quantitative RT-PCR with the gene expression level in wild type set to 1. The columns show gene expression levels of wild type, vector only and three transformed plants and standard errors (SEs) (bars) of relative quantitative RT-PCR from three biological

replicates. The * above the columns indicates statistical differences ($p<0.05$) by student t-test.

EF2$_{NGSD}$ transformed plants produced more axillary stems than wild type and vector only, similar to the *EF2*$_{SCWL}$ transformed plants which also produced more axillary stems than wild type and vector only (Figure 5.58). *BRC1* gene expression level of transformed plants were significantly decreased compared to wild type and vector only whilst the *PME5* gene expression level was the same as wild type and vector only (Figure 5.59).



Figure 5.58 Arabidopsis T_2 generation and *EF2*$_{SCWL}$ transformed plants. A. T_2 *EF2*$_{SCWL}$ transformed plant compared to wild type and vector only. B. *EF2*$_{SCWL}$ transformed plant showing a more branched stem.

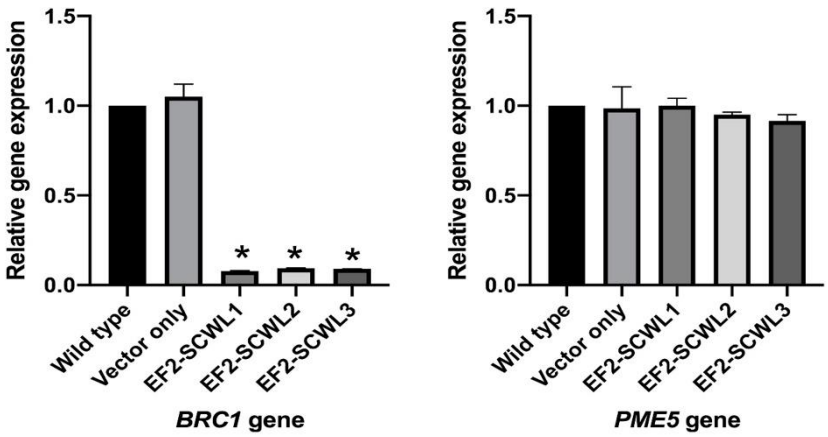


Figure 5.59 Relative gene expression of *BRC1* and *PME5* genes compared to *PP2A* (actin) gene that were examined by relative quantitative RT-PCR with the gene expression level in wild type set to 1. The columns show gene expression levels of wild type, vector only and three transformed plants and standard errors (SEs) (bars) of relative quantitative RT-PCR from three biological replicates. The * above the columns indicates statistical differences ($p<0.05$) by student t-test.

The phyllotaxis pattern of transformed plants in secondary inflorescence meristems was normal and the *PME5* gene expression level was not different from wild type and vector only (Figure 5.59). Three transformed plants were of normal height and floral organ function was the same as wild type and vector only, and the *PNF BLR/PNY* and *BP/KNATT1* gene expression levels were the same as wild type and vector only (Figure 5.60).

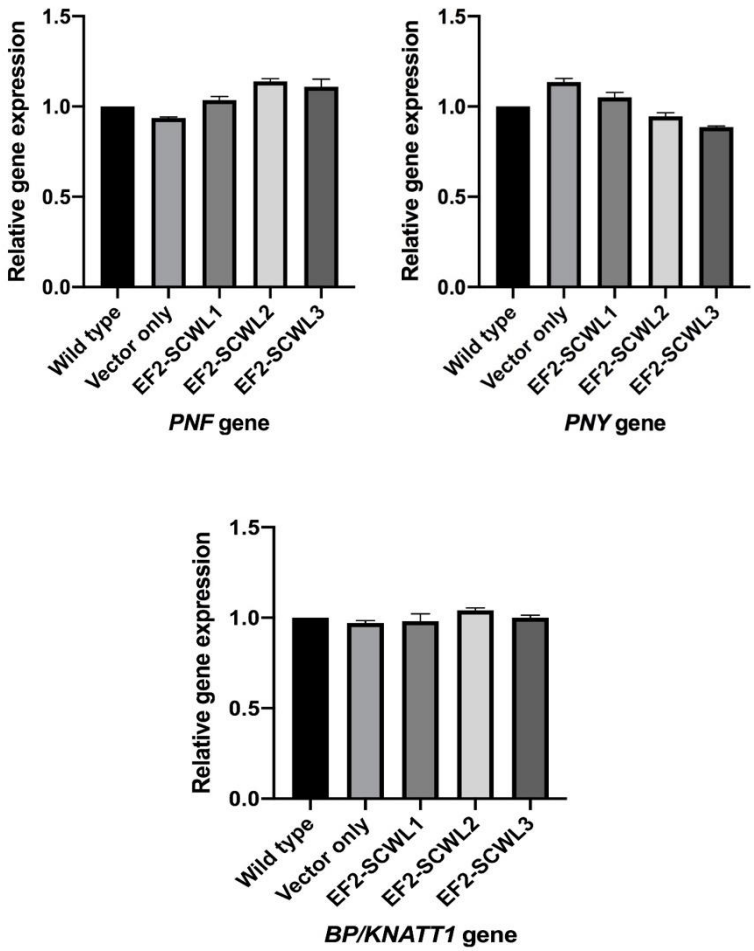


Figure 5.60. Relative gene expression of *PNF, PNY* and *BP/KNATT1* genes compared to *PP2A* (actin) gene that were examined by relative quantitative RT-PCR with the gene expression level in wild type set to 1. The columns show gene expression levels of wild type, vector only and three transformed plants and standard errors (SEs) (bars) of relative quantitative RT-PCR from three biological replicates. The * above the columns indicates statistical differences ($p<0.05$) by student t-test.

Even though the *BRC1* gene was down-regulated, flower morphology was unaffected (Figure 5.61) and the plants could produce the next generation.

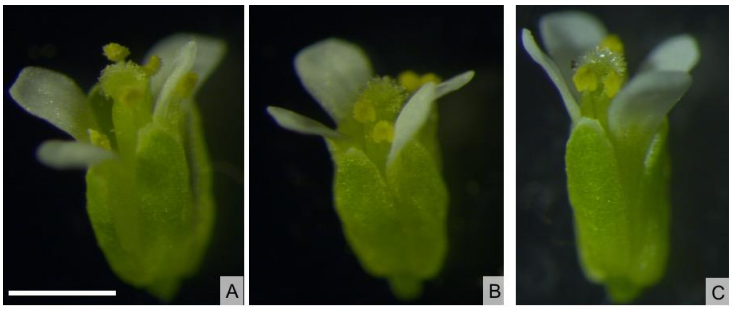


Figure 5.61 Photograph showing the flowers of wild type (A), vector only (B) and *EF2*$_{SCWL}$ transformed plants (C) bar = 1mm.

5.3.1.15 *EF7*$_{SCWL}$ Transformed plants

The *EF7*$_{SCWL}$ gene was similar to the SAP11 like gene of the PnWB phytoplasma and the *EF7*$_{NGSD}$ gene and *EF7*$_{SCWL}$ gene expression levels were significantly up-regulated in three transformed plants compared to wild type and vector only (Figure 5.62).

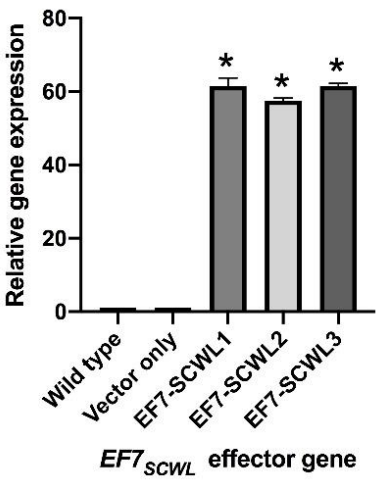


Figure 5.62. Relative gene expression of transgene compared to *PP2A* (actin) gene that were examined by relative quantitative RT-PCR with the gene expression level in wild type set to 1. The columns show gene expression levels of wild type, vector only and three transformed plants and standard errors (SEs) (bars) of relative quantitative RT-PCR from three biological replicates. The * above the columns indicates statistical differences ($p<0.05$) by student t-test.

Transformed plants produced more axillary inflorescence stems than wild type although the height of transformed plants was normal (Figure 5.63).

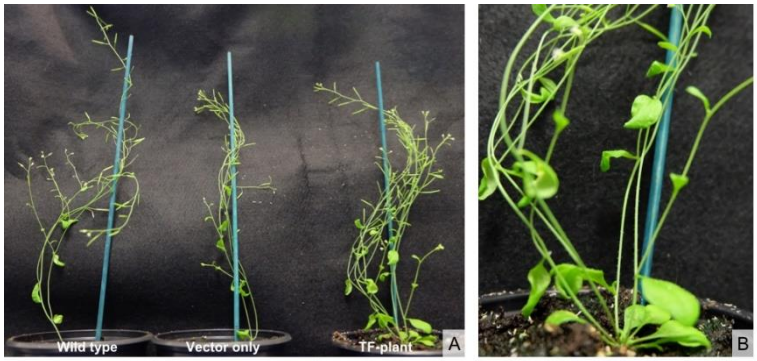


Figure 5.63 Arabidopsis T_2 generation and *EF7*$_{SCWL}$ transformed plants. A. T_2 *EF7*$_{SCWL}$ transformed plant compared to wild type and vector only. B. *EF7*$_{SCWL}$ transformed plants showing more branched stems.

The *BRC1* gene expression levels were significantly down regulated compared to wild type and vector, but the *EF7*$_{SCWL}$ effector gene did not affect flower and siliques inflorescences including secondary inflorescence meristems and the *PME5* gene expression level was the same as wild type and vector only (Figure 5.64).

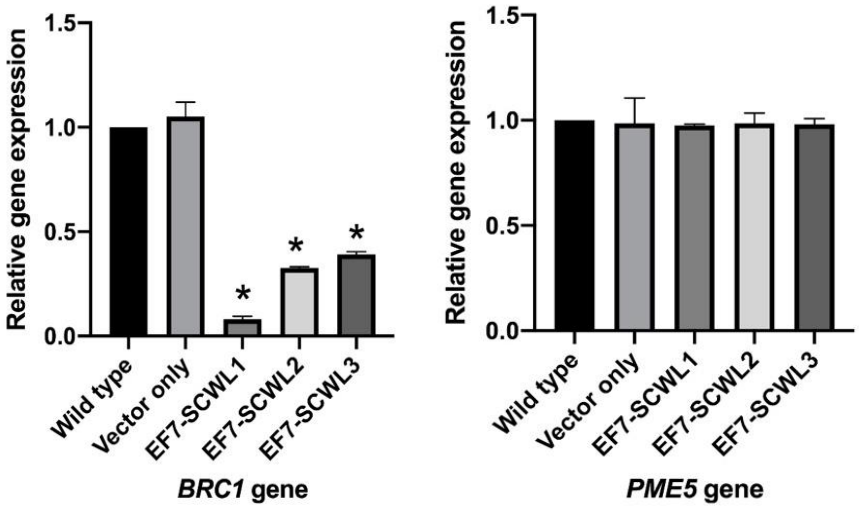


Figure 5.64. Relative gene expression of *BRC1* and *PME5* genes compared to *PP2A* (actin) gene that were examined by relative quantitative RT-PCR with the gene expression level in wild type set to 1. The columns show gene expression levels of wild type, vector only and three transformed plants and standard errors (SEs) (bars) of relative quantitative RT-PCR from three biological replicates. The * above the columns indicates statistical differences ($p<0.05$) by student t-test.

Furthermore, the *EF7*$_{SCWL}$ did not affect primary main stem elongation and floral organ function and the *PNF BLR/PNY* and *BP/KNATT1* gene expression levels were normal (Figure 5.65).

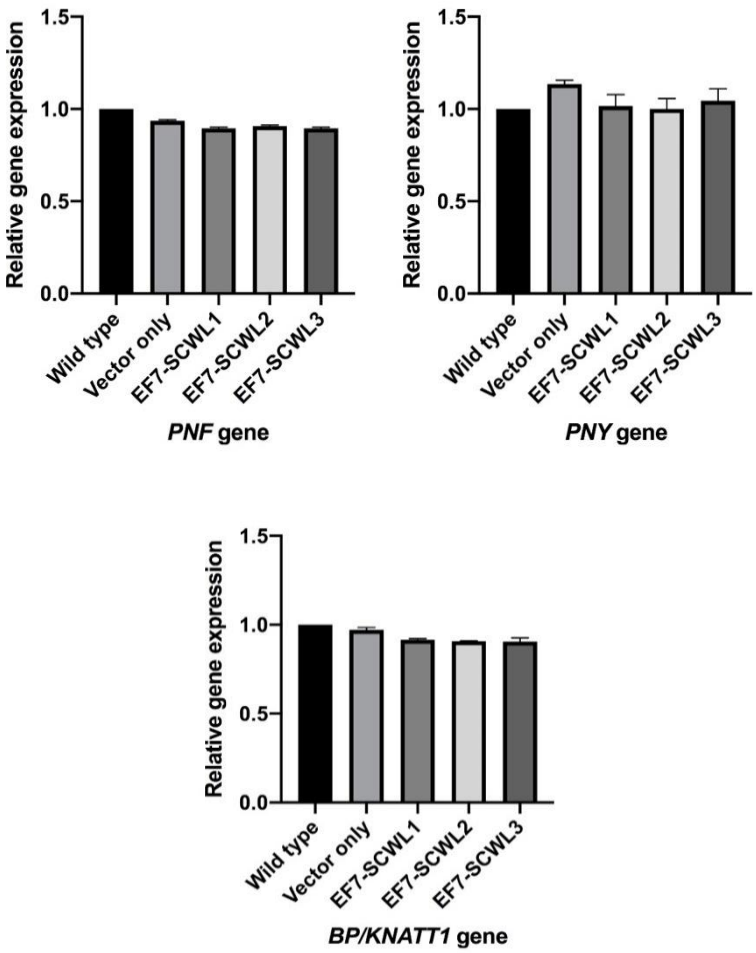


Figure 5.65 Relative gene expression of *PNF, PNY* and *BP/KNATT1* genes compared to *PP2A* (actin) gene that were examined by relative quantitative RT-PCR with the gene expression level in wild type set to 1. The columns show gene expression levels of wild type, vector only and three transformed plants and standard errors (SEs) (bars) of relative quantitative RT-PCR from three biological replicates. The * above the columns indicates statistical differences ($p<0.05$) by student t-test.

Transformed plants produced normal flowers and siliques for reproduction (Figure 5.66).

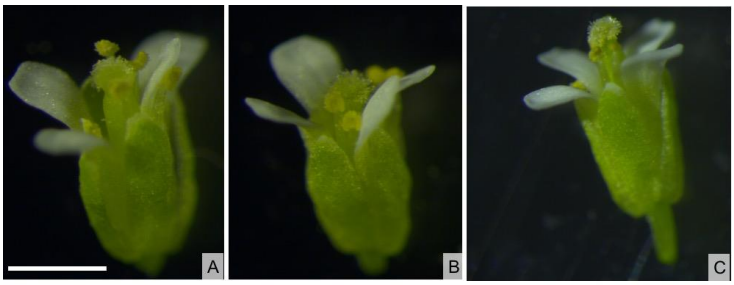


Figure 5.66. Photograph showing the flowers of wild type (A), vector only (B) and *EF7*$_{SCWL}$ transformed plants (C) bar = 1mm.

Table 5.2 shows the summary of the effect of each *SAP11* candidate effector protein on plant gene development.

Table 5.2 Summary of the effect of the effector proteins on plant gene expression

Transformed plants	BRC1 gene	PME5 gene	*PNY* gene	*PNF* gene	*BP* gene
$SAP11_{AP_SQ}$	√	√	√	√	√
$SAP11_{BCRD}$	√	√	X	X	X
$SAP11_{CoP}$	√	√	X	X	X
$SAP11_{SGP}$	√	X	X	X	X
$SAP11_{VCP}$	√	√	√	X	√
$EF1_{NGSD}$	na	na	na	na	na
$EF2_{NGSD}$	√	X	X	X	X
$EF3_{NGSD}$	na	na	na	na	na
$EF4_{NGSD}$	na	na	na	na	na
$EF5_{NGSD}$	na	na	na	na	na
$EF6_{NGSD}$	na	na	na	na	na
$EF7_{NGSD}$	√	X	X	X	X
$EF2_{SCWL}$	√	X	X	X	X
$EF7_{SCWL}$	√	X	X	X	X

√: plant gene affected by the effector protein

X: gene expression at the same level as wild type

na: the phenotype of transformed plants did not show any symptoms and qPCR was not done

For the *Brachypodium* transformation, the transformation efficiency was low because of the *B.distacyon* cultivar (described in chapter 4) and moreover, the regeneration stage from callus to plantlet until form spikelets formed and mature seed was produced for the next generation took more than 6 months, Since the gene expression experiments require the 2nd generation to observe the symptoms and analyse gene expression level the *Brachypodium distachyon* transformation experiments could not be finished within the PhD period and due to COVID-19.

5.4 Discussion

Plant development is controlled by gene regulatory networks (GRNs), which are important for organisms to control cell and tissue specification via transcriptional programming in early development of SAM (Scofield *et al*., 2018). SAM is controlled by TALEs, which are in two families, KNOX and BEL and TCP family. There are various publications that have examined the effect of phytoplasma effectors on plant architecture, such as *SWP1* which is a kind of *SAP11* effector protein that destabilises the *BRC1* gene (Wang and Jiao, 2018) such that the plants show more branched stems than wild type. In this chapter different phytoplasma effectors were examined for their effect on symptoms and plant gene expression.

5.4.1 Plant Branching

The phenotypic results classified transformed plants into three groups based on plant morphology; branching, phyllotaxis defects and normal plants. The branching group consists of *SAP11*$_{AP_SQ}$ *SAP11*$_{CoP}$ *SAP11*$_{SGP}$ *EF2*$_{NGSD}$ *EF2*$_{SCWL}$ *EF7*$_{NGSD}$ and *EF7*$_{SCWL}$ transformed plants. These plants produced more axillary inflorescences than wild type and vector only; however, the height of the plants was normal except *SAP11*$_{AP_SQ}$ which was shorter than wild type.

Shoot branching is controlled by the *BRANCH1* (*BRC1/TCP18*) gene to regulate axillary bud growth. The real-time PCR results showed that the *BRC1* gene expression level was down-regulated in these plants, which was the same as found for the *SWP1* (*SAP11* like) effector from wheat blue dwarf phytoplasma, which destabilised transcription factor TCP (TEOSINTE-BRANCHED, CYCLOIDEA) and transcription factor *BRANCHED1* (*BRC1*) via the proteasome system (Wang and Jiao, 2018). This previous study also found that SWP1 had an NLS and coiled coil domain which were important for inducing witches' broom. Moreover, the previous study examined the *BRC1* function by reverse genetics and the result described the *BRC1* mutant plants as having more axillary branches, indicating that the *BRC1* gene arrests bud development (Antonio *et al*., 2007; Seale *et al*., 2016). Similarly, Chang *et al*. (2018) transformed *SAP11*$_{AY\text{-}WB}$ *SAP11*$_{CaPM}$ *SAP11*$_{PnWB}$ and *SAP11*$_{OYM}$ into *Arabidopsis* and their results showed the *TB/CYC (TEOSINTE-BRABCHED/CYCLODEA)-TCP* was destabilised and the transformed plants produced more axillary meristems.

On the other hand, the *SAP11*$_{AY\text{-}WB}$ did not affect to *BRC1* gene which is in the *TB/CYC* subclass; however, *SAP11*$_{AY\text{-}WB}$ destabilised *CIN-TCP* which regulates various plant developmental functions especially leaf development and the result showed the transformed plants produced crinkled leaves (Palatnik *et al*., 2003; Lu *et al*., 2014; Sugio *et al*., 2014; Chang *et al.,* 2018). Moreover, *SAP11*$_{CaPM}$ (cause of apple proliferation symptoms, ATP_00189) transformed plants also showed crinkled leaves (Tan *et al*., 2016) even though these studies were in *Nicotiana benthamiana* (Tan *et al*., 2016) so these results were different to the ones presented in Figure 5.9. In this study, the *SAP11*$_{AP_SQ}$ did not produced crinkled leaves and the *SAP11*$_{AP_SQ}$ transformed plants produced more secondary stems and leaves including aerial clustered cauline leaves (aerial rosettes) and these symptoms were the same as apple proliferation symptoms.

It is interesting to note that Sugio *et al*. (2011) studied the phytoplasma infection to *Arabidopsis thaliana* Col-0 by *M. quadrilineatus,* which was inoculated with AY-WB phytoplasma, and their results found the infected plants showed witches' broom with short internodes, and flowers become leafy. However, when they amplified the *SAP11* gene from the AY-WB phytoplasma and transformed it into *A. thaliana*, the results were different and the transformed plants produced crinkled leaves and siliques, produced more stems and smaller rosettes than wild type, and the transformed plants had impaired *CIN-TCP* function. Meanwhile, the *Teugu* (*PAM765*) effector from OY-M showed the same results between infected plants and transformed

plants (Hoshi *et al*., 2009) and they examined the plant phytohormones and the results showed that *Tengu* inhibited auxin related pathways to change plant morphology and that *Tengu* is localized in the cytoplasm and did not affect the TCP family. It is possible that the *SAP11* effectors have broad-spectrum activities to change plant morphology and physiology in different plant hosts.

5.4.2 Plant phyllotaxis patterns

The SAP11 effector proteins including hypothetical and candidate effector proteins affected other parts of plant development. In the case of phyllotaxis patterns, the transformed plants with phyllotaxis defects were *SAP11*$_{AP_SQ}$ *SAP11*$_{BCRD}$ *SAP11*$_{CoP}$ and *SAP11*$_{VCP}$. Additionally, previous studies showed the phyllotaxis defect in Tengu transformed plants (Hoshi *et al*., 2009). The transformed plants produced secondary inflorescence meristems, although they did not form at regular positions or show normal phyllotaxis patterns. There are some factors known to control the phyllotaxis pattern at the internode, including *BLR/PNY* and *PECTINMETHYLTRANSFERASE5* (*PME5*) genes which are controlled by the *BLR/PNY* gene (Peaucelle *et al*., 2011; Etchell *et al*., 2012).

The *BLR/PNY* gene expression results in *SAP11*$_{BCRD}$ and *SAP11*$_{CoP}$ showed the same level as in wild type and vector only, whilst *PME5* was down regulated in *SAP11*$_{AP_SQ}$ *SAP11*$_{BCRD}$ *SAP11*$_{CoP}$ and *SAP11*$_{VCP}$ causing the transformed plants to show fused stems at the secondary inflorescence

meristems and the phyllotaxy defect. The *PME5* gene regulates the spacing of lateral organs by demethyl-esterification during the primordial development and there is another gene, *PECTINMETHYLTRANSFERASE INHIBITOR3* (*PMEI3*) that inhibits PME5 activity during primordial formation so *PME* is controlled by *PMEI* to control plant development (Peaucelle *et al*., 2008, 2011; Senechal *et al*., 2015). In this chapter, the $SAP11_{BCRD}$ $SAP11_{CoP}$ and $SAP11_{VCP}$ transformed plants exhibited fused stems of secondary inflorescence and primary inflorescence. Furthermore, the phyllotaxis pattern is related to *PME5* and *PMEI5* levels in the cell wall (Muller *et al*., 2013), and in this study the *PME5* gene was affected by the effector protein since the *PME5* level was down-regulated (Figures 5.10, 5.14, 5.19, 5.29). As a result, the *PMEI5* level was higher than the *PME5* level so that the secondary inflorescence failed to separate from the primary inflorescence (Muller *et al*., 2013) and the plants showed the phyllotaxy defect.

It is interesting to note $SAP11_{AP_SQ}$ and $SAP11_{VCP}$ transformed plants not only showed the phyllotaxis defect but were also shorter than wild type and vector only plants, which correlated with *BLR/PNY* and *BREVIPEDCELLUS* (*BP*) gene expression levels. Previous studies showed the interaction between *BLR/PNY* and *BP* to control internode elongation and regulate inflorescence stem growth in *Arabidopsis* (Smith and Hake, 2003; Bhatt *et al*., 2004) Interestingly, previous studies using single mutants of *bp* and *pny* showed that the *bp* mutant exhibited pedicel and style development defects and the flowers had compact inflorescence architecture, whilst the *pny* mutant caused a dwarf phenotype (Venglat *et al*., 2002; Bhatt *et al*., 2004).

For the *SAP11*$_{AP_SQ}$ and *SAP11*$_{VCP}$ phenotypes in this study, the *BLR/PNY* and *BP* gene expression was determined and the result showed *BLR/PNY* and *BP* genes were down regulated. That correlated with the height of transformed plants and flower inflorescences in *SAP11*$_{AP_SQ}$ and *SAP11*$_{VCP}$. Previous studies using a *pny bp* double mutant showed unelongated internodes, siliques formed at the same position, and clustered cauline leaves appeared on the primary inflorescence including vascular patterning disruption (Smith and Hake, 2003). Moreover, the phenotypes of the single mutants of *pny* or *bp* were less severe than the double mutant because the *BLR/PNY* can interact with another KNOX protein and vice versa. Furthermore, the *SAP11*$_{VCP}$ flowers were compact and the flower inflorescences were shorter than wild type and this result was also observed in *bp-1* mutant plants (Venglat *et al*., 2002; Roth *et al*., 2018). Even though the *SAP11*$_{VCP}$ flowers were compact, they were fertile. However, the *SAP11*$_{AP_SQ}$ plants were shorter than wild type and produced more leaves including more clustered cauline leaves on the secondary mainstems, and it is interesting to note that the transformed plants were non-flowering plants so it is possible that the *SAP11*$_{AP_SQ}$ not only affected the *BP* and *BLR/PNY* genes but also affected other genes that control flower development.

Previous studies showed the relationship between *BLR/PNY* and *BLH*$_8$*/PNF* to maintain flower specification involving flower development, floral inflorescences and aerial inflorescence architecture (Bhatt *et al*., 2004; Kumar *et al*., 2007; Kanrar *et al*., 2006, 2008). Loss of the *BLR/PNY* gene in *pny*

mutant plants (single mutant) caused the dwarf phenotype, produced extra cauline leaves and produced clusters of floral primordia (Bhatt *et al*., 2004; Kanrar *et al*., 2006) whilst loss of the *BLR/PNY* and *BLH8/PNF* genes in *pny pnf* double mutant resulted in leafy shoots and sterile flowers (Kanrar *et al*., 2006, 2008). Therefore, the $SAP11_{AP_SQ}$ and $SAP11_{VCP}$ effector proteins appear to affect the *BP* and *BLR/PNY* genes and the $SAP11_{AP_SQ}$ was the only effector protein affecting the *PNF* gene.

Figure 5.67 shows the conclusions for the interactions between each *SAP11* candidate effector protein and other proteins involved in plant development.

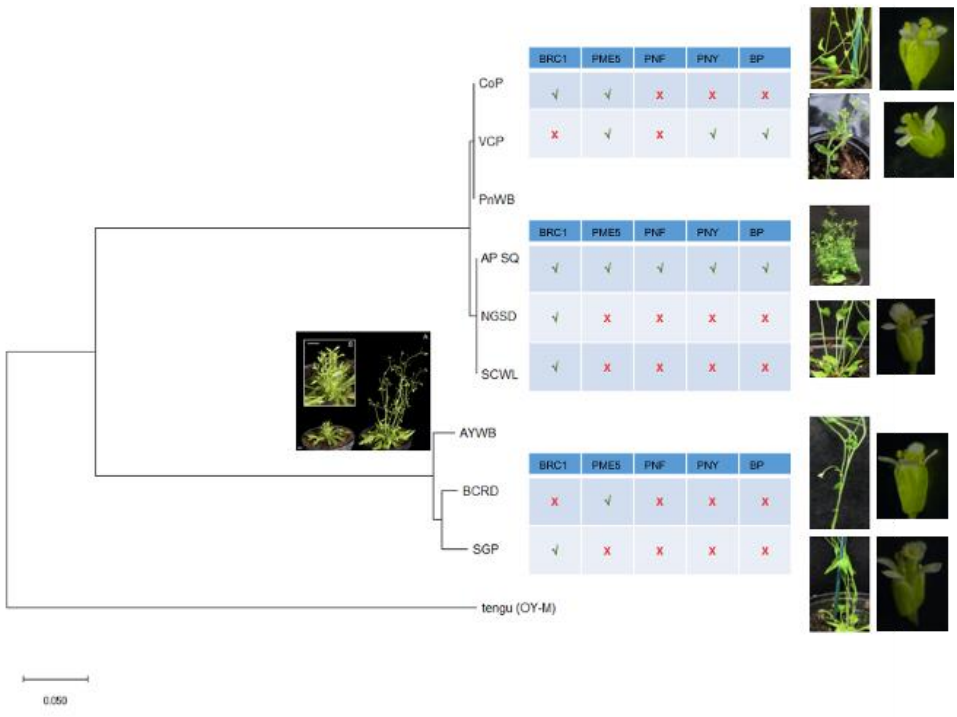


Figure 5.67. SAP11 protein homologs interacted with different plant genes and showed various phenotypes and flowers and √ represents plant gene was affected by effect from effector proteins and X represents plant gene was not affected by effector proteins.

Some effector proteins did not show any phenotypes in *Arabidopsis*, including *EF1*$_{NGSD}$ *EF3*$_{NGSD}$ *EF4*$_{NGSD}$ *EF5*$_{NGSD}$ and *EF6*$_{NGSD}$. These effector proteins were similar to two hypothetical proteins, two ATPase protein and another one could not be identified. In the case of the ATPase transformation, the ATPase gene overexpression did not affect plant morphology; however, this gene has been shown to increase the number of stomata opening and transformed plants had increased viability under environmental stress (Folta *et al*., 2014; Farhanah *et al*., 2017).

Chapter 6 General discussion and conclusions

The aim of this study was to revise the classification of the 16SrXI group of phytoplasmas, especially SCWL and SCGS from different regions of the World, using the MLST technique and then identify phytoplasma effectors, particularly from the 16SrXI group, and observe their effect on plant development and gene expression through amplification and transformation into model plants.

6.1 Geographic phytoplasma distribution and diversity

Phytoplasmas are impacting on agriculture worldwide and their invasion of plant hosts is dependent on insect vector types and feeding behaviours. As insect vectors adapt and spread to new environments or geographic locations, phytoplasma distribution is spreading. Furthermore, human activities are helping to spread phytoplasmas to new lands particularly through the distribution of infected planting material (Cordova *et al*., 2003; Pierro *et al*., 2019). As the phytoplasma distribution alters, so also does the genetic variation in the phytoplasmas as they potentially have to adapt and change some of their effector genes to adapt to new plant hosts and environmental conditions (Oshima *et al.*, 2002; Kube *et al*., 2012; Foissac and Maixner, 2013). The effector genes often lie on PMUs and previous studies have shown that the PMU sizes are different in different phytoplasmas (Bai *et al.*, 2013; Hogenhout and Loria, 2008). Studies on the variation in effector and housekeeping genes are important to classify the phytoplasmas and are often

combined into the technique called MLST (Abeysinghe *et al.,* 2016; Shaoshuai *et al.,* 2016; Plavec *et al.,* 2019; Pilet *et al.,* 2019).

6.2 Classification of phytoplasmas of gramineous plants

Phytoplasma infections of sugarcane (*Saccharum officinarum*) can cause sugarcane white leaf (SCWL), sugarcane grassy shoot (SCGS) and sugarcane yellow leaf (SCYL) (Nasare *et al.*, 2007). These phytoplasmas are reported to be in the 16SrXI group based on 16S rRNA analysis, and this group also comprises Rice dwarf yellow (RYD) and Napier grass stunt disease (NGSD). However, whilst some studies have indicated that SCWL and SCGS are caused by different phytoplasmas, others suggest they are caused by the same phytoplasma (Nasare and Yadav, 2007, Li *et al*., 2014; Wang *et al*., 2014). Therefore, the aim of chapter 2 was to classify SCWL and SCGS using the MLST technique. The results showed that the genes used classified SCWL and SCGS based on their geographic origin and not based on the symptoms they cause. Interestingly, the NGSD was classified as being in a 16SrXI outgroup supporting the results of Abeysinghe *et al.* (2016) who proposed that NGSD should be classified into a new group. However, when effector genes were used for the classification, the sequences were identical in the sugarcane and napier grass stunt phytoplasmas, indicating that the phytoplasmas may be using conserved effectors to attack their host plants (Rümpler *et al.,* 2015).

6.3 SAP11 gene diversity

When the *SAP11* gene was compared between different 16SrXI and 16SrXIV phytoplasmas using the EF7 primers (chapter 2) all the sequences were very similar as shown in Figure 6.1A. Furthermore, when *SAP11* sequences were cloned and sequenced from other phytoplasmas (Chapter 4), other 16Sr groups were shown to align to the 16SrXI and XIV (Figure 6.1B). In particular, the 16SrII and 16SrX phytoplasmas grouped with 16SrXI, whilst the 16SrI phytoplasmas formed a separate group. Whilst there are conserved protein sequences between the SAP11 effectors from certain groups, these do not appear to be directly correlated to specific symptoms in plant hosts suggesting that the symptoms depend on host types and environments.

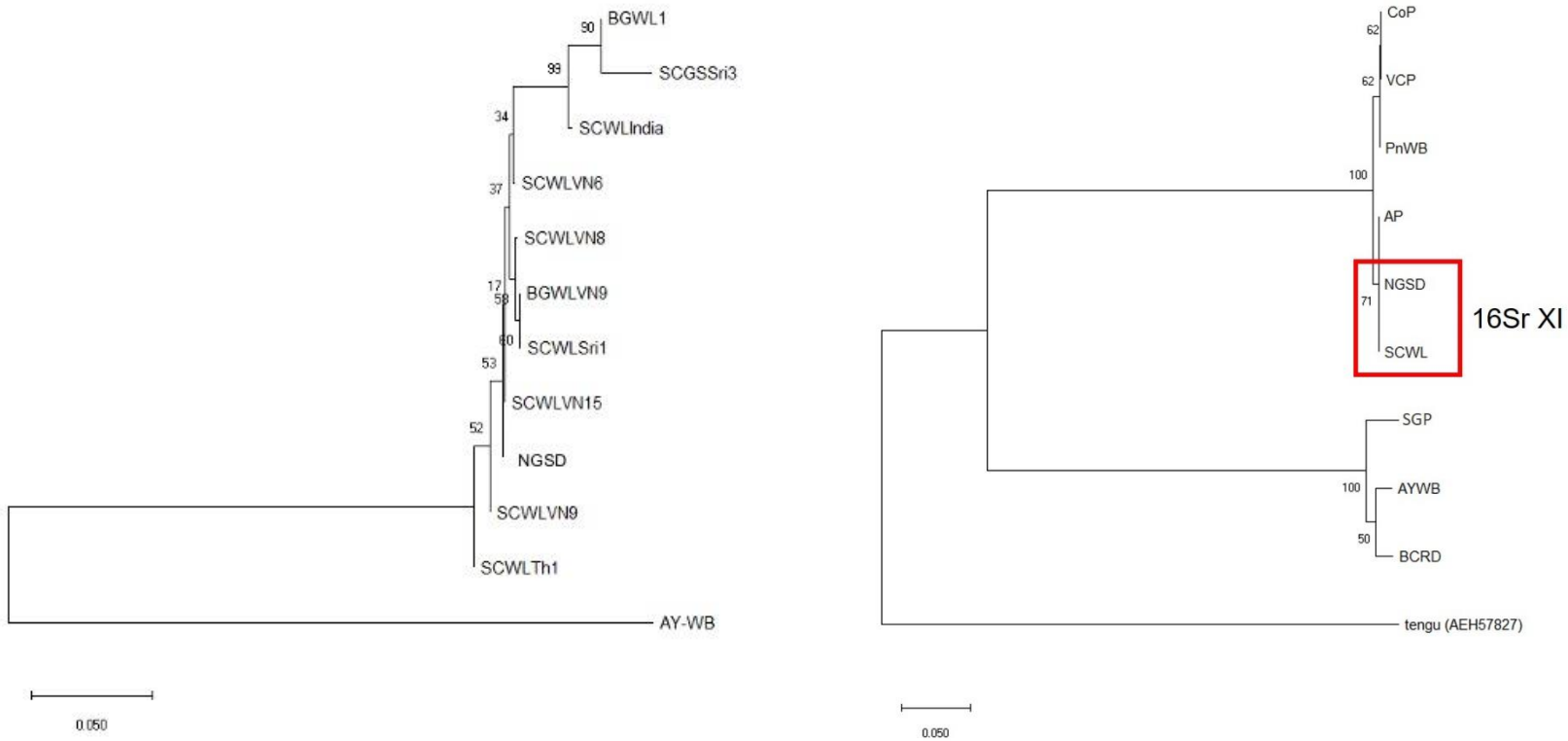


Figure 6.1The phylogenetic tree was constructed from SAP11 sequences obtained in this thesis. A. The SAP11 phylogenetic tree between 16SrX, 16SrXI and 16SrXIV. B. The phylogenetic tree between 16SrI, 16SrII, 16SrX and 16SrXI.

6.4 The effect of phytoplasma effectors on plant development

6.4.1 Transformation efficiency

There are numerous factors that affect transformation efficiency such as the plasmid vectors used for construction and transformation into the model plants, which are different between monocot and dicot plants. The suitable plasmids use different promoters with the CaMV 35S promoter used for dicot plants whilst the Ubiquitin promoter is more suitable for monocot plants (Smedley and Harwood, 2005). However, *Agrobacterium* strains can be used for both plants with the *A. tumefaciens* strain GV3310 suitable for the floral dip method in *Arabidopsis*, whilst *A. tumefaciens* strain AGL1 is suitable for *Brachypodium* callus (Collier *et al*., 2016). Furthermore, the selective markers used, surfactants and techniques can affect the transformation efficiency in *Arabidopsis* (Davey *et al*., 1999; Chung *et al*., 2000; Dehestani *et al*., 2010; Rashid *et al*., 2018). In terms of *Brachypodium*, the transformation efficiency is generally much lower and depends on *Brachypodium* cultivar, and in the regeneration stage, the transformed callus produce two types of plantlet, normal plantlets and albino plants depending on cultivar, for example BD21-3 produced more green shoots than Bd21 (Vogel and Hill, 2008; Vain *et al*., 2008; Collier *et al*., 2016; Behpouri *et al*., 2018).

6.4.2 Interaction of phytoplasma effectors with plant genes and development

Previous studies found that the SAP11 effector interacted with class II CIN-TCP transcription factors causing the transformed plants to produce crinkled leaves and excessive branching (Palatnik *et al*., 2003; Lu *et al*., 2014; Sugio *et al*., 2014; Chang *et al.,* 2018). However, in this study the transformed plants did not produce crinkled leaves although some of the effectors produced more axillary stems which is in line with previous studies where Wang and Jiao (2018) found the *BRC1* gene controlling the branching system was destablised by the SAP11 effector protein via proteasome pathway and as a result plants produced more axillary shoots (Figure 6.2).

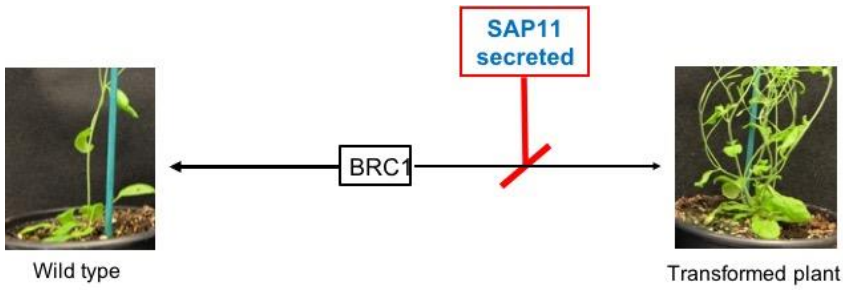


Figure 6.2 The effect of the BRC1 gene by the SAP11 effector protein causing branching (Wang and Jiao, 2018).

Moreover, the SAP11 proteins also affected other plant genes, causing changes in plant morphology such as fusion of stems, phyllotaxis pattern defects, short internodes and non-production of flowers. The *BLR* gene is one of the genes that controls phyllotaxis pattern (Figure 6.3), inhibiting the

transcription process at the internode to result in the phyllotaxis defects. Moreover, the *PME5* gene is the downstream gene of the *BLR* gene, that regulates cell wall spacing by homogalacturonan demethylesterification (Peaucelle *et al*., 2008, 2011; Senechal *et al*., 2015) (Figure 6.3). In addition, there is the *PMEI5* gene that also controls the *PME5* expression level.

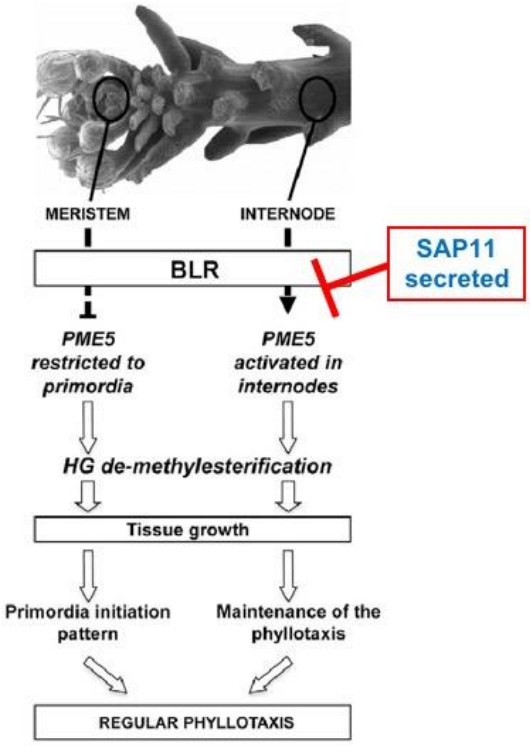


Figure 6.3 Inhibition of the BLR and PME5 genes in plant development by SAP11 (Peaucelle *et al*., 2011).

The *PME5* and *PMEI5* expression level is another factor to control phyllotaxis pattern that is related to the down regulation of *PME5* with the result that homogalacturonan cannot be demethylated and the *PMEI5* level is higher than

PME5 such that the plant shows stem fusion and phyllotaxis defects (Muller *et al*., 2013) (Figure 6.4).

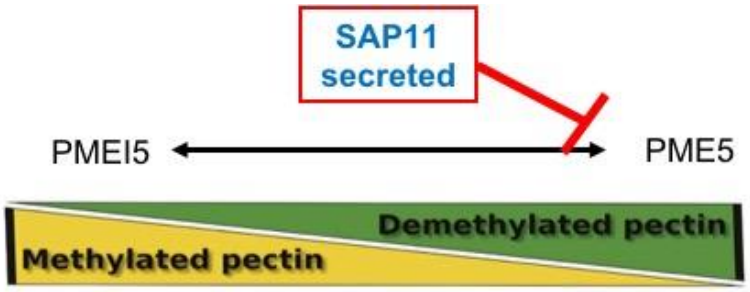


Figure 6.4 Effect of inhibiting the PME5 level to cause organ fusion (Andres-Robin *et al*., 2018)

Additionally, the effector proteins did not directly affect the MADS-box transcription factor. However, the effector proteins reduced *PNF* and *PNY* genes expression that controls flower specification (Bhatt *et al*., 2004; Kumar *et al*., 2007; Kanrar *et al*., 2006, 2008) (Figure 6.5). The reduction of *PNF/PNY* gene expression caused the flowers to be smaller than wild type and produced terminated flowers that were found in $SAP11_{VCP}$ and $SAP11_{AP_SQ}$ transformed plants, respectively.

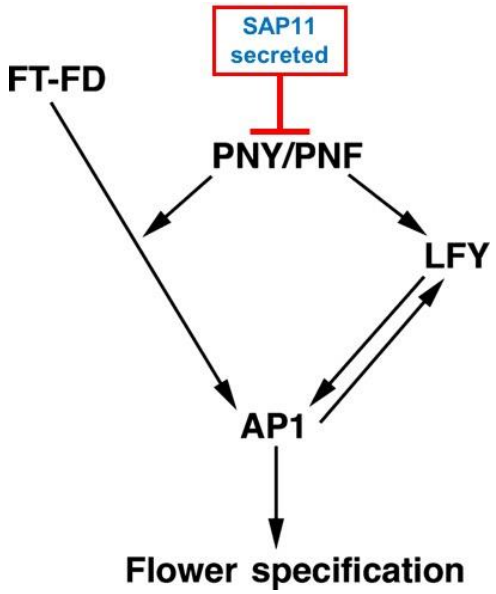


Figure 6.5 Inhibition of the PNF/PNY gene for flower development by SAP11 (Kanrar *et al*., 2008).

6.5 Suggestions for future studies

To achieve a further understanding on the roles of phytoplasma effectors in eliciting disease symptoms, studies on effectors from phytoplasmas that infect monocot plants need to be continued in monocots such as *Brachypodium*, maize, barley and rice. This is especially true since the effector genes from napier grass stunt and sugarcane white leaf did not show any symptoms that related to stunt or white leaf in transformed *Arabidopsis* plants. Pecher *et al*. (2019) studied *SAP11*$_{\text{AY-WB}}$ (16SrI-A) and *SAP11*$_{\text{MBSP}}$(16SrI-B) in *Arabidopsis* and the results showed crinkled leaf in *SAP11*$_{\text{AY-WB}}$ whilst *SAP11*$_{\text{MBSP}}$ did not show any symptoms, presumably because the effector is restricted to only destabilise TB1/CYC TCPs in maize, so the *SAP11*$_{\text{MBSP}}$ showed axillary branching. In maize, *SAP11*$_{\text{AY-WB}}$ caused male sterility and feminization of

tassels whilst *SAP11*$_{MBSP}$ caused female sterility but the plants produced pollen; moreover, the transformed maize produced small ears similar to those in the *Z. mays tb1* mutant. From their results, it might be possible that the phytoplasma effectors cause various symptoms depending on host range (Tan *et al*., 2016) and the effectors are specific to plant hosts especially in their *SAP11*-TCP interactions (Pecher *et al*., 2019). Moreover, the infection technique might have an effect on the symptoms that appear, as was shown in the results of Sugio (2011). Therefore, it is important to do further studies on the phytoplasma symptoms especially those caused by NGSD and SCWL effectors in monocot plants, and such a study might also show whether the phytoplasma effectors are restricted to specific or broad plant hosts for specific symptoms.

According to the MLST analysis, the effector genes are an important intrinsic factor to develop plant morphology, and previous studies showed that effector genes are reflected by various plant morphological changes. For example, *SAP11*$_{AY\text{-}WB}$ (16SrI-A) (Sugio *et al*., 2011; Hoshi *et al*, 2009) produces witches' broom which is different from *SAP11*$_{SGP}$ and *SAP11*$_{BCRD}$ (16srI-C) that produce green petal leaves and big buds, respectively (Jones, 2000; Perez-Lopez, 2019) even though they are in the same group and the protein sequences of *SAP11*$_{BCRD}$ and *SAP11*$_{SGP}$ are similar to *SAP11*$_{AY\text{-}WB}$ 100% and 75%, respectively (Figure 4.21). Moreover, environmental factors such as soil and nutrients appear to be additional extrinsic factor that affect symptoms, for example to account for the differences between white leaf and grassy shoot symptoms in sugarcane caused by the same phytoplasma. Therefore, the

effectors should be examined from sugarcane samples showing the same and different symptoms in different regions and included alongside an analysis of different environmental factors within and between countries, to try and ascertain how genetic and environmental factors interact to result in symptom expression.

Bibliography

Abesysinghe , S., Abesinghe, P. D., Kanatiwela-De Silva, C., Udagama, P., Waraeichanee, K., Al-Jelfar, N., Kawicha, P. and Dickinson, M. 2016. Refinement of the Taxonomic Structure of 16SrXI and 16SrXIV Phytoplasmas of Gramineous Plants using Multilocus Sequence Typing. *Plant Dis,* 100**,** 2001-2010.

Al-Saady, N. A., Khan, A.J., CalariA, A., Al-Ssubhi, A.M. and Bertaccini A. 2008. 'Candidatus Phytoplasma omanense', a phytoplasma associated with witches' broom of Cassia italica (Mill.) Lam. in Oman. *Int. J. Syst. Evol Microbiol,* 58**,** 461-466.

Al-Ghaithi, A. G., Al-Subhi, Ali M., Al-Mahmooli, Issa, H., and Al-Sadi A.M. 2018. Genetic analysis of 'Candidatus Phytoplasma aurantifolia' associated with witches' broom on acid lime trees. *PeerJ,* 6.

Al-Subhi, A., Hogenhout, S. A., Al-Yahyai, R. A. and Al-Sadi, A. M. 2017. Classification of a new phytoplasmas subgroup 16SrII-W associated with Crotalaria witches' broom diseases in Oman based on multigene sequence analysis. *BMC Microbiol,* 17**,** 221.

Al-Subhi, A. M., Hogenhout, S.A., Al-Yahyai, R. and Al-Sadi, A. M. 2018. Detection, Identification, and Molecular Characterization of the 16SrII-D Phytoplasmas Infecting Vegetable and Field Crops in Oman. *Ali M. Al-Subhi, Saskia A. Hogenhout, Rashid A. Al-Yahyai, and Abdullah M. Al-Sadi,* 102**,** 576-588.

Alves, S. C., Worland, B., Thole, V., Snape, J. W., Bevan, M. W., and Vain, P. 2009. A protocol for Agrobacterium-mediated transformation of

Brachypodium distachyon community standard line Bd21. *Nat Protoc,* 4**,** 638-49.

Anebestania, A., Izadpanahb, K., Abbaa, S., Galettoa, L., Ghorbanib, A., Plamnoa, S., Siampourc, M., Verattia, F. and Marzachi, C. 2017. Identification of putative effector genes and their transcripts in three strains related to 'Candidatus Phytoplasma aurantifolia'. *Microbiol Res,* 199**,** 57-66.

Andres-Robin, A., Reymond, M. C., Dupire, A., Battu, V., Dunrulle, N., Mouille, G., Lefebvre, V., Pelloux, J., Boudaoud, A., Traas, J., Scutt, C. P. and Moneger, F. 2018. Evidence for the Regulation of Gynoecium Morphogenesis by ETTIN via Cell Wall Dynamics. *Plant Physiol,* 178**,** 1222-1232.

Antonio , J., Martinez, A., , Poza-Carrio´ C. and Cubas, P. 2007. Arabidopsis BRANCHED1 Acts as an Integrator of Branching Signals within Axillary Buds. *The Plant Cell,* 19**,** 458-472.

Arnaud, G., Malembic-Maher, S., Salar, P., Bonnet, P., Maizner, M., Marcone, C., Boudon-Padieu, E. and Foissac, X. 2007. Multilocus sequence typing confirms the close genetic interrelatedness of three distinct flavescence doree phytoplasma strain clusters and group 16SrV phytoplasmas infecting grapevine and alder in Europe. *Appl Environ Microbiol,* 73**,** 4001-10.

Arocha, Y., Lopez, M., PinolL, B., Fernandez, M., PicornellI, B., Almeida, R., Palenzuela, I., Wilson, M. R. and Jones, P. 2005. 'Candidatus Phytoplasma graminis' and 'Candidatus Phytoplasma caricae', two

novel phytoplasmas associated with diseases of sugarcane, weeds and papaya in Cuba. *Int J Syst Evol Microbiol,* 55**,** 2451-63.

Asudi, G. O., Van Den Berg, J., Midega, C. A. O., Pittchar, J., Pickett, J. A. and Khan, Z.R. 2015. Napier grass stunt disease in East Africa: Farmers' perspectives on disease management. *Crop Prot,* 71**,** 116-124.

Bai, X., Ammar, E. D. and Hogenhout, S. A. 2007. Accumulates in nuclei and alters gene expression of host plant cells, and is detected in various tissues of the leafhopper Macrosteles quadrilineatus. *Bull Insectol,* 60**,** 217-218.

Bai, X., Correa, V. R., Toruno, T. Y., Ammar, E. D., Kamoun, S. and Hogenhout, S. A. 2009a. AY-WB Phytoplasma Secretes a Protein That Targets Plant Cell Nuclei. *MPMI,* 22**,** 18-30.

Bai, X., Zhang, J., Ewing, A., Miller, S. A., Radex, A. J., Shevchenko, D. V., Tsukerman, K., Walunas T., Lapidus A., Campbell, J. W. and Hogenout, S. A. 2006. Living withgenome instability: the adaptationof phytoplasmas to diverse environ-ments of their insect and plant hosts. *J Bacteriol,* 188**,** 3682-3696.

Bao, D**.** 1973. *Control of Plant Architecture by Distinctive TALE Homeobox Gene Interactions*, Optima Grafische Communicatie.

Barros, T. S. L., Davis, R.E., Resende, R.O. and Dally, E.L. 2002. Erigeron witches' broom phytoplasma in Brazil represents new subgroup VII-B in 16S rRNA gene group VII, the ash yellows phyto- plasma group. *Plant Disease,* 86**,** 1142–1148.

Behpouri, A., Perpchon, A., Doohan, F. M. and Ng, C. K. Y. 2018. Optimizing callus induction and proliferation for Agrobacterium-mediated transformation of Brachypodium distachyon. *Cereal Res Comm,* 46**,** 221-231.

Bekele, B., Abeysinghe, B., Hoat, S., Hodgetts, J. and Dickinson, M. 2011. Development of specific secA-based diagnostics for the 16SrXI and 16SrXIV phytoplasmas of the Gramineae. *Bull Insectol,* 64**,** S15-S16.

Bekeli, B., Hodgetts, J., Jomlinson, T., Boonham, N., Nikolic´C, P.,Swarbrick, P. and Dickinson, M. 2011. Use of a real-time LAMP isothermal assay for detecting 16SrII and XII phytoplasmas in fruit and weeds of the Ethiopian Rift Valley. *Plant Pathol,* 60**,** 345-355.

Bertaccini, A. 2007. Phytoplasmas: diversity, taxonomy, and epidemiology. *Fronts Biosci,* 12**,** 673-689.

Bertaccini, M., Grando, M. S., Muthuchelian, K., and Nedunchezhian, N. 2002. Effect of phytoplasmal infection on photosystem II efficiency and thylakoid membrane protein changes in field grown apple (Malus pumila) leaves. *Phys Mol Plant Pathol,* 61**,** 349-356.

Betekhtin, A., Rojek, M., Milewska-Hendel, A., Gawecki, R., Karcz, J., Kurcznska, E. and Hasterok, R. 2016. Spatial Distribution of Selected Chemical Cell Wall Components in the Embryogenic Callus of Brachypodium distachyon. *PLoS One,* 11**,** e0167426.

Bhatt, A. H., Etchells, J.P., Canles, C., Lagodienko, A. and Dickinson, H. 2004. VAAMANA--a BEL1-like homeodomain protein, interacts with KNOX proteins BP and STM and regulates inflorescence stem growth in Arabidopsis. *Gene,* 328**,** 103-111.

Blanche, K. R., Tran-Nguyen, L.T.T. and Gibb, K.S. 2003. Detection, identification and significance of phytoplasmas in grasses in northern Australia. *Plant Pathology,* 52**,** 505-512.

Bragg, J. N., Anderton, A., Nieu, R. and Vogel, J. P. 2015. Brachypodium distachyon. *Methods Mol Biol,* 1223**,** 17-33.

Chang, L., Mei, G., Hu, Y., Deng, J. and Zhang, T. 2019. LMI1-like and KNOX1 genes coordinately regulate plant leaf development in dicotyledons. *Plant Mol Biol,* 99**,** 449-460.

Chang, S. H., Tan, C. M., Wu, C. T., Lin, T. H., Jiang, S. Y., Li, R. C., Tsai, M., C., Su, L.W. and Yang, J. Y. 2018a. Alterations of plant architecture and phase transition by the phytoplasma virulence factor SAP11. *J Exp Bot,* 69**,** 5389-5401.

Chen, W., Li, Y., Wang, Q., Wang, N. and Wu, Y. 2014. Comparative genome analysis of wheat blue dwarf phytoplasma, an obligate pathogen that causes wheat blue dwarf disease in China. *PLoS One,* 9**,** e96436.

Chen, W. Y., Huang, Y.C., Tsai, M. and Lin, C. 2011. Detection and identification of a new phytoplasma associated with periwinkle leaf yellowing disease in Taiwan. *Aus Plant Path,* 40**,** 476-483.

Constable, F. E., Gibb, K. S., Moran, J. R. and Wilson, Y. M. 1998. Incidence of phytoplasma associated with yellows, restricted spring growth and late season leaf curl symptoms in grapevines. *Aust. Grapegr. Winem.,* 490**,** 19-20.

Czechchowski, T., Stitt, M., Altmann, T., Udvardi, M.K. and Scheible, W.G. 2005. Genome-Wide Identification and Testing of Superior Reference

Genes for Transcript Normalization in Arabidopsis. *Plant Physiology,* 137**,** 5-17.

Cho, S. T., Lin, C. P. and Kuo, C. H. 2019. Genomic Characterization of the Periwinkle Leaf Yellowing (PLY) Phytoplasmas in Taiwan. *Front Microbiol,* 10**,** 2194.

Christensen, N. M., Axelsen, K. B., Nicolaisen, M. and Schulz, A. 2005. Phytoplasmas and their interactions with hosts. *Trends Plant Sci,* 10**,** 526-35.

Chung, M. S., Chen, M. K. and Pan, S. M. 2000a. Floral spray transformation can efficiently generate Arabidopsis transgenic plants. *Transgen Res,* 9**,** 471-476.

Chung, W. C., Chen, L. L., Lo, W. S., Lin, C. P. and Kuo, C. H. 2013. Comparative Analysis of the Peanut Witches'-Broom Phytoplasma Genome Reveals Horizontal Transfer of Potential Mobile Units and Effectors. *PLOS ONE,* 8**,** e62770.

Cieslinska, M. and Morgas, H. 2011. Detection and Identification of 'Candidatus Phytoplasma prunorum', 'Candidatus Phytoplasma mali' and 'Candidatus phytoplasma pyri' in stone fruit tree in Poland. *J Phytopathol,* 159**,** 217-222.

Clough, S. J. and Bent, A.F. 1998. Floral dip: a simplified method for Agrobacterium-mediated transformation of Arabidopsis thaliana. *The Plant J,* 16**,** 735-743.

Collier, R., Bragg, J., Hernandez, B. T., Vogel, J. P. and Thilmony, R. 2016. Use of Agrobacterium rhizogenes Strain 18r12v and Paromomycin

Selection for Transformation of Brachypodium distachyon and Brachypodium sylvaticum. *Front Plant Sci,* 7**,** 716.

Cordova, I., Jones, P., Harrison, N. A. and Oropez, C. 2003. In situ PCR detection of phytoplasma DNA in embryos from coconut palms with lethal yellowing disease. *Mol Plant Pathol,* 4**,** 99-108.

Daire, X., Boudon-Padieu, E., Berville´, A., Schneider, B. and Caudwell, A. 1992. Cloned DNA probes for detection of grapevine flavescence dore´e mycoplasma-like organism (MLO). *Ann Appl Biol,* 121**,** 95-103.

Dalbey, R. D. and Kuhn, A. 2000. Evolutionarily related insertion pathways of bacterial, mitochondrial, and thylakoid membrane proteins. *Annu. Rev. Cell Dev. Biol,* 16.

Davey, M. W., Gilot, C., Persiau, G., Ostergaard, J., Han, Y., Bauw, G. C. and Van Montagu, M. C. 1999. Ascorbate Biosynthesis in Arabidopsis Cell Suspension Culture. *Plant Phys,* 121**,** 535–543.

Davis, R. E., Dally, E. L. and Converse, R.H. 2001a. Molecular Identification of a Phytoplasma Associated with Witches'Broom Disease of Black Raspberry in Oregon and Its Classification in Group 16SrIII, New Subgroup Q. *Plant Disease,* 85**,** 1121-1121.

Davis, R. E., Dally, E. L., Gundersen, D. E., Lee, I.M. and Habili, N. 1997. ‘‘Candidatus Phytoplasma australiense,’’ a new phytoplasma taxon associated with Australian grapevine yellows. *Int J Syst Bacteriol,* 47**,** 262-269.

Davis, R. E., Harrison,N.A., Zhao,Y., Wei,W. and Dally, E.L. 2016. Mexican periwinkle virescence phytoplasma 16S ribosomal RNA gene, complete sequence; tRNA-Ile gene, complete sequence; and 23S

ribosomal RNA gene, partial sequence. *Int. J. Syst. Evol. Microbiol,* 66**,** 3463-3467.

Dehestain A., A. G., Ssalmanian A. H., Jelodar N. B. and Kazemitabar, K. 2010. Transformation efficiency enhancement of Arabidopsis vacuum infiltration by application and apicla inflorescence removal *Trakia J Sci,* 8**,** 19-26.

Deng, S., and Hiruki. D. 1991. Amplification of 16S rRNA genes from culturable and nonculturable mollicutes. *J. Microbiol. Method,* 14**,** 53-61.

Devulder, G., Pe´Rouse De Montclos, M. and Flandrois, J. P. 2005. A multigene approach to phylogenetic analysis using the genus Mycobacterium as a model. *International J. Sys. and Evol. Microl.,* 55**,** 293–302.

Dickinson, M. 2010. Mobile units of DNA in phytoplasma genomes. *Mol Microbiol,* 77**,** 1351-3.

Doi, Y., Teranaka, M., Yora, K. and Asuyama, H. 1997. Mycoplasma- or PLT group-like microorganismsfound in the phloem elements of plants infected withmulberry dwarf, potato witches' broom, aster yellows,or paulownia witches' broom. *Annals Phytopathol Soc Japan,* 33**,** 259–266.

Drapper, J., Mur L. A. J., Jenkins, G., Ghosh-Biswas, G. C., Bablak P., Hasterok, R. and Routledge, A. P. M. 2001. Brachypodium distachyon. A New Model System for Functional Genomics in Grasses. *Plant Physiol,* 127**,** 1539-1555.

Duduk., B., Mejia, J.F., Calari, A. and Bertaccini, A. 2008. Identification of 16SrIX group phytoplas- mas infecting Colombian periwinkles and molecular characterization on several genes. *17th Congress Intaernational Organization for Mycoplasmology, Tienjin, China,,* 112**,** 83.

Duduk, B. and Bertaccini, A. 2011. Phytoplasma classification: Taxonomy based on 16S ribosomal gene, is it enough? *Phytopath Moll,* 1**,** 3-13.

Etchells, J. P., Moore, L., Jiang, W. Z., Prescott, H., CapperA, R., Saunders\, N. J., Bhatt, A.J. and Dickinson, H.G. 2012. A role for BELLRINGER in cell wall development is supported by loss-of-function phenotypes. *Plant Biol,* 12**,** 1-12.

Farhanah, A., Suharsono, Wattimena,G. A. and WidyastutiI, U. 2017. Genetic engineering of potato plant (Solanum tuberosum L.) cv. Jala Ipam with MmPMA gene encoding plasma membrane H+-ATPASE. *Pak. J. Biotechnol,* 14**,** 37-42.

Foissac, X. and Maixner, M. 2013. Spread of grapevine phytoplasma diseases in Europe. *Phytopath Moll,* 3.

Folta, A., Severing, E. I., Krauskops, J., Geest, H., Verver, J., Nap, J. and Mlymarova, L. 2014. Over-expression of Arabidopsis AtCHR23 chromatin remodeling ATPase results in increased variability of growth and gene expression. *BMC Plant Biol,* 14**,** 1-18.

Freudl, R. 2018. Signal peptides for recombinant protein secretion in bacterial expression systems. *Freudl Microb Cell Fact***,** 17-52.

Gadagkar, U. R., Rosenberg, M. S. and Kumar, S. 2005. Inferring Species Phylogenies From Multiple Genes:Concatenated Sequence Tree

Versus ConsensusGene Tree. *JOURNAL OF EXPERIMENTAL ZOOLOGY* 304B**,** 64–74.

Gaura, R. K., Raizadab , R. and Rao, G. P. 2008. Sugarcane yellow leaf phytoplasma associated for the first time with sugarcane yellow leaf syndrome in India. *Plant Pathol,* 57**,** 772-772.

Ghedira, R., De Buck, S., Nolf, J. and Depicker, A. 2013. The efficiency of Arabidopsis thaliana floral dip transformation is determined not only by the Agrobacterium strain used but also by the physiology and the ecotype of the dipped plant. *Mol Plant Microbe Interact,* 26**,** 823-32.

Gibb, K. S., Padovan, A.C. and Mogen B.D. 1995. Studies on Sweet Potato Little-Leaf Phytoplasma Detected in Sweet Potato and Other Plant Species Growing in Northern Australia. *Phytopathology* 85**,** 169-174.

Griffiths, H. M., Sinclair, W. A., Smart, C. D. and Davis, R. E. 1999. The phytoplasma associated with ash yellows and lilac witches'- broom: 'Candidatus Phytoplasma fraxini'. *Int J Syst Bacteriol,* 49**,** 1605-1614.

Gundersen, D. E., Lee, I.-M., Rehner, S. A., Davis, R. E. and Kingsbury, D. T. 1994. Phylogeny of mycoplasmalike organisms (phytoplasmas): a basis for their classification. *J Bacteriol,* 176**,** 5244-5254.

Gundersen, D. E. and Lee., I-M. 1996. Ultrasensitive detection of phytoplasmas by nested-PCR assays using two universal primer pair. *Phytopathologia Mediterrranea,* 35**,** 144-151.

Harrison, N. A., Richarson, P.A., Kramer, J.B. and Tsai, J.H. 1994. Detection of the mycoplasma-like organ- ism associated with lethal yellowing disease of palms in Florida by polymerase chain reaction. *Plant Pathology,* 43**,** 998–1008.

Harrison, N. A., Womack, M. and Carpio, M.L. 2002. Detection and characterization of a lethal yellowing (16SrIV) group phytoplasma in Canary Island date palms affected by lethal decline in Texas. *Plant Disease,* 86**,** 676–681.

Hiller, K., Grote, A., Scheer, M., Munch, R. and Jahn, D. 2004. PrediSi: prediction of signal peptides and their cleavage positions. *Nucl Acids Res,* 32**,** W375-379.

Hiruki, C. and Wang, K. 2004. Clover proliferation phytoplasma: 'Candidatus Phytoplasma trifolii'. *Int J Syst Evol Microbiol* 54**,** 1349-1353.

Ho, K., Tsai, C. and Chung, T. 2001. Organization of ribosomal RNA genes from a loofah witches' broom phytoplasma. *DNA and Cell Biology,* 20**,** 115–122.

Hodgetts, J., Boonhnam, N., Mumford, R., Harrison, N. and Dickinson, M. 2008. Phytoplasma phylogenetics based on analysis of secA and 23S rRNA gene sequences for improved resolution of candidate species of 'Candidatus Phytoplasma'. *Int J Syst Evol Microbiol,* 58**,** 1826-37.

Hogenhouts, S. A., Oshima, K., Ammar El, D., KakizawaA, S., Kingdom, H. N. and Namba, S. 2008a. Phytoplasmas: bacteria that manipulate plants and insects. *Mol Plant Pathol,* 9**,** 403-23.

Hogenhout, S. A. and Boss, J.I. 2011. Effector proteins that modulate plant–insect interactions. *Curr Opin Plant Biol,* 14**,** 422-428.

Hogenhout, S. A. and Loria, L. 2008b. Virulence mechanisms of Gram-positive plant pathogenic bacteria. *Curr Opin Plant Biol* 11**,** 449-456.

Hoshi, A., Oshima, K., Kakizawa, S., Ishii, Y., Ozeki, J., Hahimoto, M., Komatsu, K., Kadiwada, S., Yamaji, Y. and Namba, S. 2009. A unique

virulence factor for proliferation and dwarfism in plants identified from a phytopathogenic bacterium. *Proc Natl Acad Sci U S A,* 106**,** 6416-21.

Hu, S. F., Huang, Y. H., Lin, C. P., Liu, L. Y., Hong, S. F., Yang, C. Y., Lo, H. F., Tseng, T. Y., Chen, W. Y. and Lin, S. S. 2015. Development of a Mild Viral Expression System for Gain-Of-Function Study of Phytoplasma Effector In Planta. *PLoS One,* 10**,** e0130139.

Huang, H., Liu, B., Liu, L. and Song, S. 2017. Jasmonate action in plant growth and development. *J Exp Bot,* 68**,** 1349-1359.

Jacobs, K. A., Lee, I-M., Griffiths, H.M., Miller, F.D. JR. and Bottner, K.D. 2003. A new member of the clo- ver proliferation phytoplasma group (16SrVI) associated with elm yellows in Illinois. *Plant DiseaseA,* 87**,** 241–246.

Janik, K., Mithofer, A., Raffeiner, M., Stellmach, H., Hause, B. and Schlink, K. 2017. An effector of apple proliferation phytoplasma targets TCP transcription factors-a generalized virulence strategy of phytoplasma? *Mol Plant Pathol,* 18**,** 435-442.

Jiang, P., Zhang, K., Ding, Z., He, Q., Li, W., Zhu, S., Cheng, W., Zhang, K. and Li, K. 2018. Characterization of a strong and constitutive promoter from the Arabidopsis serine carboxypeptidase-like gene AtSCPL30 as a potential tool for crop transgenic breeding. *BMC Biotechnol,* 18**,** 59.

Jomatiene, R., Davis, R. E., Valiunas, D., Alminaite, A. and Staniulis, J. 2002a. New group 16SrIII phytoplasma lineages in Lithuania exhibit rRNA interoperon sequence heterogeneity. *Eur J Plant Pathol* 108**,** 507-517.

Jomatiene, R., Davis, R.E., Maas J. and Dally, E.L. 1998. Classification of new phytoplasmas associated with diseases of strawberry in Florida, based on analysis of 16S rRNA and ribosomal protein gene operon sequences. *International Journal of Systematic Bacteriology,* 48**,** 269–277.

Jomatiene, R., Maas, J.L., Takeda, F. and Davis, R.E. 2002. Molecular identification and classification of strawberry phylloid fruit phytoplasma in group 16SrI, new subgroup. *Plant Disease* 86**,** 920.

Jung, H.-Y., Sawayanagi, T. and Kakizawa, S. 2002. 'Candidatus Phytoplasma castaneae', a novel phytoplasma taxon associated with chestnut witches' broom disease. *Int J Syst Evol Microbiol* 52**,** 1543-1549.

Jung, H. J. S., T., Wongkaew, P., KakizawaA, S., Nishigawa, H., Wei, W., Oshima, K., Miyata, S., Ugaki, M., Hibi, T. and Namba, S. 2003. Candidatus Phytoplasma oryzae', a novel phytoplasma taxon associated with rice yellow dwarf disease. *Int. J. Syst. Evol Microbiol,,* 53**,** 1925-1929.

Jung, H. Y., Sawayanagi, T., and Wongkaew, P. 2003b. 'Candidatus Phytoplasma oryzae', a novel phytoplasma taxon associated with rice yellow dwarf disease. *Int J Syst Evol Microbiol,* 53**,** 1037-1041.

Kakizawa, S., Oshima, K., Nishigawa, H., Jung, H. Y., Wei, W., Suzuki, S., Tanaka, M., Miyata, S., Ugaki, M. and Namba, S. 2004. Secretion of immunodominant membrane protein from onion yellows phytoplasma through the Sec protein-translocation system in Escherichia coli. *Microbiol,* 150**,** 135-42.

Kakizawa, S., Oshima, K., Sawayahangi, T., Kuboyama, T., Miyata, S., Jung, H. Y., Nishigawa H., Tsuchizaki, T., Miyata, S., UgakiI, M. and Namba, S. 2001. Cloning and Expression Analysis of Phytoplasma Protein Translocation Genes. *MPMI,* 14**,** 1043–1050.

Kanrar, S., Bhattacharya, M., Arthur, B., Courtier, J. and Smith, H. M. 2008. Regulatory networks that function to specify flower meristems require the function of homeobox genes PENNYWISE and POUND-FOOLISH in Arabidopsis. *Plant J,* 54**,** 924-37.

Kanrar, S., Onguka, O. and Smith, H. M. 2006. Arabidopsis inflorescence architecture requires the activities of KNOX-BELL homeodomain heterodimers. *Planta,* 224**,** 1163-73.

Kawicha, P. 2014. Phytoplasma: comparative genomics and evidence of competition. Ph.D Thesis.

Kitazawa, Y., Iwabuchi, N., Himeno, M., Sasano, M., Koinuma, H., Nijo, T., Tomonitsu, T., Yoshida, T., Okano, Y., Yoshikawa,N., Maejima, K., Oshima, K. and Namba, S. 2017. Phytoplasma-conserved phyllogen proteins induce phyllody across the Plantae by degrading floral MADS domain proteins. *J Exp Bot,* 68**,** 2799-2811.

Kogovsek, P., Hodgetts, J., Hall, J., Prezelj N., Nikolic, P. and Mehle, N. 2015. LAMP assay and rapid sample preparation method for on-site detection of flavescence doree phytoplasma in grapevine. . *Plant Pathology,* 64**,** 286–296.

Ku, C., Lo, W. S. and Kuo, C. H. 2013. Horizontal transfer of potential mobile units in phytoplasmas. *Mob Genet Elements,* 3**,** e26145.

Kube, M., Mitrovic, J., Duduk, B., Rabus, R. and Seemuller, E. 2012. Current view on phytoplasma genomes and encoded metabolism. *ScientificWorldJournal,* 2012**,** 185942.

Kube, M., Duduk, B and Oshima, K. 2020. Genome Sequencing. *Phytoplasmas: Plant Pathogenic Bacteria - III,* 3**,** 1-16.

Kumar, R., Kushalappa, K., Godt, D., Pidkowich, M. S., Pastorelli, S., Hepworth, S. R. and Haughn, G. W. 2007. The Arabidopsis BEL1-LIKE HOMEODOMAIN proteins SAW1 and SAW2 act redundantly to regulate KNOX expression spatially in leaf margins. *Plant Cell,* 19**,** 2719-35.

Labroussaa, F., Lebaudy, A., Baby, V., Gourgues, G., MatteauA, D., VasheeA, S., Sirand-Pugnet, P., Rodrigue, S. and Lartigue, C. 2016. Impact of donor–recipient phylogenetic distance on bacterial genome transplantation. *Nucl Acids Res,* 17**,** 8501-8511.

Lee, I.-M., Davis, R. E., Chen, T.-A., Chiykowski, L. N., Fletcher, J., HIiruki, C. and Schaff, D. A. 1992. A genotype-based system for identification and classification of mycoplasmalike organisms (MLOs) in the aster yellows MLO strain cluster. *Phytopathology* 82**,** 997-986.

Lee I.-M., Gundersen-Rindal, D. E., Davis, R. E. and Bartoszyk, I. M. 1998. Revised classification scheme of phytoplasmas based on RFLP analyses of 16S rRNA and ribosomal protein gene sequences. *Int J Syst Bacteriol* 48**,** 1153-1169.

Lee, I.-M., Hammond, R., W., Davis, R.E. and Gundersen., D.E. 1993. Universal amplification and analysis of pathogen 16S rDNA for

classification and identification of mycoplasmalike organisms. *Phytopathology,* 83**,** 834–842.

Lee, I.-M., Martini, M., Marcone, C. and Zhu, S. F. 2004. Classification of phytoplasma strains in the elm yellows group (16SrV) and proposal of 'Candidatus Phytoplasma ulmi' for the phytoplasma associated with elm yellows. *Int J Syst Evol Microbiol,* 54**,** 337-347.

Lee I-M, M. M., Bottner K.D., Dand, R.A., Black, M.C. and TroxclairR, N. 2003. Ecological implications from a molecular analysis of phytoplasmas involved in an aster yellows epidemic in vari- ous crops in Texas. *Phytopathology,* 93**,** 1368–1377.

Lee I-M, M. M., Bottner, K.D., SecorE, G. and Rivera-Varas, V. 2006. 'Candidatus Phytoplasma americanum', a phytoplasma associated with a potato purple top wilt disease complex. *International Journal of Systematic and Evolutionary Microbiology,* 56**,** 1593-1597.

Lee, C., Kim, J., Shin, S. G. and Hwanf, S. 2006. Absolute and relative QPCR quantification of plasmid copy number in Escherichia coli. *J Biotechnol,* 123**,** 273-80.Li, Y., Chen, W., Ma, D. and Wu, Y. 2013. cDNA-AFLP analysis revealed genes potentially implicated in Catharanthus roseus flowers during wheat blue dwarf phytoplasma infection. *Physiological and Molecular Plant Pathol,* 84**,** 1-9.

Li Y., Piao, C. G., Tian, G. Z., Liu, Z. X., Guo, M. W., Lin, C. L. and Wang, X. Z. 2014. Multilocus sequences confirm the close genetic relationship of four phytoplasmas of peanut witches'-broom group 16SrII-A. *J Basic Microbiol,* 54**,** 818-27.

Liefting, L. W., Andersen, M. T., Beever, R. E., Gardner, R. C. and Foster, R. L. S. 1996. Sequence heterogeneity in the two 16S rRNA genes of Phormium yellow leaf phytoplasma. *Appl Environ Microbiol***,** 3133-3139.

Liu, C. T., Huang, H. M., Hong, S. F., Kuo-Huang, L. L., Yang, C. Y., Lin, Y. Y., Lin, C. P. and Lin, S. S. 2015. Peanut witches' broom (PnWB) phytoplasma-mediated leafy flower symptoms and abnormal vascular bundles development. *Plant Sign Behav,* 10**,** e1107690.

Lu, Y. T., Li, M. Y., Cheng, K. T., Tan, C. M., Su, L. W., Lin, W. Y., Shih, H. T., Chiou, T. J. and Yang, J. Y. 2014. Transgenic plants that express the phytoplasma effector SAP11 show altered phosphate starvation and defense responses. *Plant Physiol,* 164**,** 1456-69.

Ma, K. W. and Ma, W. 2016. Phytohormone pathways as targets of pathogens to facilitate infection. *Plant Mol Biol,* 91**,** 713-25.

Maclean, A. M., Orlovskis, Z., Kowitwanich, K., Zdziarska, A. M., Angenen, G. C., Immink, R. G. and Hogenhout, S. A. 2014. Phytoplasma effector SAP54 hijacks plant reproduction by degrading MADS-box proteins and promotes insect colonization in a RAD23-dependent manner. *PLoS Biol,* 12**,** e1001835.

MacLean, A. M., Sugio, A., Makarova, O. V., Findlay, K. C., Grieve, V. M., Toth, R., Nicolaisen, M. and Hogenhout, S. A. 2011. Phytoplasma effector SAP54 induces indeterminate leaf-like flower development in Arabidopsis plants. *Plant Physiol,* 157**,** 831-41.

Maejima, K., Kitazawa, Y., Tomomitsu, T., Yusa, A., Neriya, Y., Himeno, M.,Yamaji, Y., Oshima, K. and Namba, S. 2015. Degradation of class

E MADS-domain transcription factors in Arabidopsis by a phytoplasmal effector, phyllogen. *Plant Sig Beh,* 10**,** 1-3.

Maejima, K., Oshima, K. and Namba, S. 2014. Exploring the phytoplasmas, plant pathogenic bacteria. *J Gen Plant Pathol,* 80**,** 210-221.

Manassero, N. G. U., Viola, I. L., Welchen, E. and Gonzalez, D. H. 2013. TCP transcription factors: architectures of plant form. *BioMol Concepts***,** 1-18.

Mannan, S., Ibrahim, M., Chohan, S. N. and Holford, P. 2010. Detection of Phytoplasma in Citrus Orchards of Pakistan. *J Phytol,* 2010**,** 49-54.

Marcone, C., Schneide B. and Seemu¨ller, E. 2004. 'Candidatus Phytoplasma cynodontis', the phytoplasma associated with Bermuda grass white leaf disease. *Int. J. Syst. Evol Microbiol,,* 54**,** 1077-1082.

Martini, M., Lee, I-M., Bottner, K.D., Zhao, Y., Botti, S., Bertaccini, A., Harrison, N.A., Carraro, L., Marcone, C. and Osler, R. 2007. Ribosomal protein gene-based phylogeny for finer differentiation and classification of phytoplasmas. *Int. J. Syst. Evol Microbiol,,* 57**,** 2037–2051.

Meinke, D. W., Cherry, J. M., Dean, C., Rounsley, S.D. and Koornneef, M. 1998. Arabidopsis thaliana: a model plant for genome analysis. *Science,* 282**,** 662-682.

Minato, N., Himeno, M., Hoshi, A., Maejima, K., Komatsu, K., Takebayashi, Y., Kasahara, H., Yusa, A., Yamaji, Y., Oshima, K., Kamiya, Y. and Namba, S. 2014. The phytoplasmal virulence factor TENGU causes plant sterility by downregulating of the jasmonic acid and auxin pathways. *Sci Rep,* 4**,** 7399.

Montano, H. G., Davis, R. E., Dally, E. L., Hogenhout, S., Pimentel, J. P. and Brioso, P. S. T. 2001. 'Candidatus Phytoplasma brasiliense', a new phytoplasma taxon associated with hibiscus witches'-broom disease. *Int J Syst Evol Microbiol* 51**,** 1109-1118.

Muller, K., Levesque-Tremblay, G., Fernandes, A., Wormit, A., Bartels, S., Usudel, B. and Kermode, A. 2013. Overexpression of a pectin methylesterase inhibitor in Arabidopsis thaliana leads to altered growth morphology of the stem and defective organ separation. *Plant Signal Behav,* 8**,** e26464.

Namba, S. 2019. Molecular and biological properties of phytoplasmas. *Proc Jpn Acad Ser B Phys Biol Sci,* 95**,** 401-418.

Narusaka, M., Shiraishi, T., Iwabuchi, M. and Narusaka,Y. 2010. The floral inoculating protocol: A simplified Arabidopsis thaliana transformation method modified from floral dipping. *Plant Biotech,* 27**,** 349-351.

Nasare, K., Yadav, A., Singh, A. K., Shivasharranappa, K. B., Nerkar, Y. S. and Reddy, V. S. 2007. Molecular and Symptom Analysis Reveal the Presence of New Phytoplasmas Associated with Sugarcane Grassy Shoot Disease in India. *Plant Dis,* 91**,** 1413-1418.

Neriya, Y., Sugawara, K., Maejima, K., Hashimoto, M., Komatsu, K., Minato, N., Miura, C., Kakizawa, S., Yamaji, Y., Oshima, K. and Namba, S. 2011. Cloning, expression analysis, and sequence diversity of genes encoding two different immunodominant membrane proteins in poinsettia branch-inducing phytoplasma (PoiBI). *FEMS Microbiol Lett,* 324**,** 38-47.

Nicolaisen, M. and Horvath, D. P. 2008. A Branch-inducing Phytoplasma in Euphorbia pulcherrima is Associated with Changes in Expression of Host Genes. *J. Phytopathol,* 156**,** 403-407.

Orlovskis, Z. and Hogenhout, S. A. 2016. A bacterial parasite effector mediates insect vector attraction in host plants independently of developmental changes.

Oshima, K., Maejima, K. and Namba, S. 2013. Genomic and evolutionary aspects of phytoplasmas. *Front Microbiol,* 4**,** 1-8.

Oshima, K., Smiyata, S., Sawayanagi, T., Kakizawai, S., , Niahigawa, H., Jung, H. Y., Furuki, K., Yanazakv, M., Suzuki, S., Wei, W., Kyboyama, T., Ugakp, M. and Namba, S. 2002. Minimal set of metabolic pathways sug-gested from the genome of onionyellows phytoplasma. *J. Gen. Plant Patho,* 68**,** 225-236.

Oshima, K., Skakizawa, S., Nishigawa, H., Jung, H. Y., Wei, W., Suzuki, S., Arahida, R., Nakata, D., Miyata, S., Ugami, M. and Namba, S. 2004. Reductive evolution suggested from the complete genome sequence of a plant-pathogenic phytoplasma. *NATURE GENETICS,* 35**,** 27-29.

Padovana , A., Gibba, K. and Persley, D. 2000. Association of `Candidatus Phytoplasma australiense' with green petal and lethal yellows diseases in strawberry. *Plant Pathol,* 49**,** 362-369.

Palatnik, J. F., Allen, E., Wu, X., Schommer, C., Schwab, R., Carrington, J. C. and Weigel, D. 2003. Control of leaf morphogenesis by microRNAs. *Nature,* 425**,** 257-263.

Paynel, F., Leroux, C., Surcouf, O., Schaumann, A., Pelloux, J., Driouich, A., Mollet, J.C., Lerouge, P., Lehner, A. and Mareck, A. 2014. Kiwi fruit

PMEI inhibits PME activity, modulates root elongation and induces pollen tube burst in Arabidopsis thaliana. *Plant Growth Reg,* 74**,** 285-297.

Peaucelle, A., Louvet, R., Johansen, J. N., Hofte, H., Laufs, P. and Pelloux, J. 2008. Arabidopsis phyllotaxis is controlled by the methyl-esterification status of cell-wall pectins. *Curr Biol,* 18**,** 1943-1948.

Peaucelle, A., Louvet, R., Johansen, J. N., Salsac, F., Morin, H., Fournet, F., Belcram, K., Gillet, F., Hofte, H., Laufs, P., Mouille, G. and Pelloux, J. 2011. The transcription factor BELLRINGER modulates phyllotaxis by regulating the expression of a pectin methylesterase in Arabidopsis. *Development,* 138**,** 4733-4741.

Pecher, P., Moro, G., Canale, M. C., Capdevielle, S., Singh, A., Maclean, A., Sugio, A., Kuo, C. H., Lopes, J. R. S. and Hogenhout, S. A. 2019. Phytoplasma SAP11 effector destabilization of TCP transcription factors differentially impact development and defence of Arabidopsis versus maize. *Pathogen***,** 1-27.

Perez-Lopez, E., Olivier, C. Y. , Luna-Rodriguez, M. and Dumonceaux, T. J. 2016. Phytoplasma classification and phylogeny based on in silico and in vitro RFLP analysis of cpn60 universal target sequences. *Int J Syst Evol Microbiol,* 66**,** 5600-5613.

Pfaffl, M. W. 2001. A new mathematical model for relative quantification in real-time RT–PCR. *Nucleic Acids Research,* 29**,** 2002-2007.

Pierrol, R., Semeraro, T., Luvisi, A., Garg, H., Vergine, M., De Bellis, L. and Gill, H. K. 2019. The Distribution of Phytoplasmas in South and East

Asia: An Emerging Threat to Grapevine Cultivation. *Front Plant Sci,* 10**,** 1108.

Pilet, F., Quaicoe, R. N., Osagie, I. J., Freire, M. and Foissac, X. 2019. Multilocus Sequence Analysis Reveals Three Distinct Populations of "Candidatus Phytoplasma palmicola" with a Specific Geographical Distribution on the African Continent. *Appl Environ Microbiol,* 85.

Plaveca, J., Budinscaka, X., Krizanaca, I., Skori, D., Foissacc, X. and Seruga Musi, M. 2019. Multilocus sequence typing reveals the presence of three distinct flavescence dor!ee phytoplasma genetic clusters in Croatian vineyards. *Plant Pathol,* 68**,** 18-30.

Plewczynski, D., Slabinski, L., Ginalski, K. and Rychlewski, L. 2008. Prediction of signal peptides in protein sequences by neural networks. *Acta Biochim Pol..* 55**,** 261-267.

Quaglino, F., Kube, M., Jawhari, M., Abou-Jawdah, Y., Siewert, C., Choueiri, E., Sobh, H., Casati, P., Tedeschi, R., Lova, M. M., Alma, A. and Bianco, P. A. 2015. 'Candidatus Phytoplasma phoenicium' associated with almond witches'-broom disease: from draft genome to genetic diversity among strain populations. *BMC Microbiol,* 15**,** 148.

Rao, G. P., Srivastava, S., Gupta, P.S., Sharma, S. R., Singh, A., Singh, S., Singh, M. and Marcone, C. 2008. Detection of sugarcane grassy shoot phytoplasma infecting sugarcane in India and its phylogenetic relationships to closely related phytoplasmas. *Sugar Tech,* 10.

Rashid, U., Bilal, S., Bhat, K. A., Shah, T. A., Wani, T. A., Bhat, F. A., Mughal, M. N. and Nazir, N. 2018. Phytoplasma Effectors and their

Role in Plant-Insect Interaction. *Int J Curr Microbiol Appl Sci,* 7**,** 1136-1148.

Razin, S., Yogev, D. and Naot, Y. 1998. Molecular Biology and Pathogenicity of Mycoplasmas. *Microbiol Mol Biol Rev***,** 1394-1156.

Richardson, J. E., Fay, M. F., Cronk, Q., C., B., Bowman, D. and Chase, M. W. 2000. A Phylogenetic analysis of Phamnaceae using rbcl and trnl-f plastid DNA sequences *American Journal of Botany* 87**,** 1309–1324.

Roth, O., Alvarez, J. P., Levy, M., Bowman, J. L., Ori, N. and Shani, E. 2018. The KNOXI Transcription Factor SHOOT MERISTEMLESS Regulates Floral Fate in Arabidopsis. *Plant Cell,* 30**,** 1309-1321.

Rumpler, F., Gramzow, L., Theissen, G. and Melzer, R. 2015. Did Convergent Protein Evolution Enable Phytoplasmas to Generate 'Zombie Plants'? *Trends Plant Sci,* 20**,** 798-806.

Sarvepalli, K. and Nath., U. 2018. CIN-TCP transcription factors: Transiting cell proliferation in plants. *IUBMB Life,* 70**,** 718-731.

Shaoshuai, Y., Yong L., Zhengguang, R., Chuansheng, S., Caili, L., Chungen, P. and Guozhong, T. 2017. Multilocus Sequence Analysis for Revealing Finer Genetic Variation and Phylogenetic Interrelatedness of Phytoplasma Strains in 16SrI Group in China. *Scientia Silvae Sinicae,* 53**,** 105-118.

Schneider, B., Seemu¨ller, E., Smart, C.D. and KirkpatrickI. B. C. 1995. Phylogenetic classification of plant pathogenic mycoplasma-like organisms or phytoplasmas, p. 369–380. In S. Razin and J. G. Tully (ed.). *Molecular and diagnostic procedures in mycoplasmology,,* 1.

Schneider, B., Torres, E., Martin, M.P., Schroder, M., Behnke, H.D. and Seemuller, E. 2005. 'Candidatus Phytoplasma pini', a novel taxon from Pinus silvestris and Pinus halepensis. *Int. J. Syst. Evol Microbiol,,* 55**,** 303–307.

Scholthof, K. B. G., Irigoyen, S., Catalan, P. and Mandadia, K. K. 2018. Brachypodium: A Monocot Grass Model Genus for Plant Biology. *Plant Cell,* 30**,** 1763-1694.

Scofield, S., Murison, A., Jones, A., Fozard, J., Aida, M., Band, L. R., Bennett, M and Murray, J. A. H. 2018. Coordination of meristem and boundary functions by transcription factors in the SHOOT MERISTEMLESS regulatory network. *Development* 145**,** 1-14.

Seale, M., Bennett, T. and Leyser, O. 2017. BRC1 expression regulates bud activation potential but is not necessary or sufficient for bud growth inhibition in Arabidopsis. *Development,* 144**,** 1661-1673.

Seemu¨ller, E., Marcone, C., Lauer, U., Ragozzino, A. and Goschl, M 1998. Current status of molecular classification of the phytoplasmas. *J Plant Pathol,* 80**,** 3-26.

Seemu¨ller, E. and Schneider, B. 2004. 'Candidatus Phytoplasma mali', 'Candidatus Phytoplasma pyri' and 'Candidatus Phytoplasma prunorum', the causal agents of apple proliferation, pear decline and European stone fruit yellows, respectively. *Int J Syst Evol Microbiol,* 80**,** 3-26.

Senechal, F., Mareck, A., Marcelo, P., Lerouge, P. and Pelloux, J. 2015. Arabidopsis PME17 Activity can be Controlled by Pectin Methylesterase Inhibitor4. *Plant Signal Behav,* 10**,** e983351.

Serek, J., Bauer-Manz, G., Struhalla, G., Berg, L. V. D., Kieffer, D., Dalbey, R. and Kuhn, A. 2004. Escherichia coli YidC is a membrane insertase for Sec-independent proteins. *The EMBO J,* 23**,** 294-301.

ŠerugaM, S. Bottis, K. D., Paltrinieris, S., Jureric, N. and Bertaccini, A. 2003. Molecular characteriza- tion of a phytoplasma from the aster yellows (16SrI) group naturally infecting Populus nigra L. “Italica” trees in Croatia. . *Forest Pathology,* 33**,** 113–125.

Shaoshuai, Y., Yong, L., Zhengguang, R., Chuansheng, S., Caili, L., Chungen, P. and Guozhong, T. 2017. Multilocus Sequence Analysis for Revealing Finer Genetic Variation and Phylogenetic Interrelatedness of Phytoplasma Strains in 16SrI Group in China. *Scientia Silvae Sinicae,* 53**,** 105-118.

Siller, W., Kuhbandner, B., Marwitz, R., Petzold, H. and SeeMuller, E. 1987. Occurrence of Mycoplasma-like Organisms in Parenchyma Cells of Cuscuta odorata (Ruiz et Pav.). *J Phytopathol,* 119**,** 147-159.

Singh, A. K., Bhatt, B.P. and Manibhushan. 2013. Occurrence of phytoplasma phyllody and witches' broom disease of faba bean in Bihar. *J Environ Biol. ,* 34**,** 837-840.

Smedley, M. A. and Harwood, W. A. 2015. Gateway(R)-compatible plant transformation vectors. *Methods Mol Biol,* 1223**,** 3-16.

Smith, H. M. and Hake, S. 2003. The interaction of two homeobox genes, BREVIPEDICELLUS and PENNYWISE, regulates internode patterning in the Arabidopsis inflorescence. *Plant Cell,* 15**,** 1717-27.

Steinwand, M. A., Young, H. A., Bragg, J. N., Tobias, C. M. and Vogel, J. P. 2013. Brachypodium sylvaticum, a model for perennial grasses: transformation and inbred line development. *PLoS One,* 8**,** e75180.

Sugawara, K., Honma, Y., Komatsu, K., Himeno, M., Oshima, K. and Namba, S. 2013. The alteration of plant morphology by small peptides released from the proteolytic processing of the bacterial peptide TENGU. *Plant Physiol,* 162**,** 2005-14.

Sugio, A., Kingdom, H. N., MacLean, A. M., Grieve, V. M. and Hogenhout ,S. A. 2011a. Phytoplasma protein effector SAP11 enhances insect vector reproduction by manipulating plant development and defense hormone biosynthesis. *Proc Natl Acad Sci U S A,* 108**,** 254-63.

Sugio, A., MacLean, A. M. and Hogenhout, S. A. 2014. The small phytoplasma virulence effector SAP11 contains distinct domains required for nuclear targeting and CIN-TCP binding and destabilization. *New Phytol,* 202**,** 838-48.

Sugio, A., MacLean, A. M., Kingdom, H. N., Grieve, V. M., Manimekalai, R. and Hogenhout, S. A. 2011b. Diverse targets of phytoplasma effectors: from plant development to defense against insects. *Annu Rev Phytopathol,* 49**,** 175-95.

Sugio, A. and. Hoghenout, S. A. 2012. The genome biology of phytoplasma: modulators of plants and insects. *Curr Opin Microbiol,* 15**,** 247-54.

Tan, C. M., Li, C. H., Tsao, N. W., Su, L. W., Lu, Y. T.,Chang, S. H., Lin, Y. Y., Liou, J. C., Hsieh, L. C., Yu, J. Z., Sheue, C. R., Wang, S. Y., Lee, C. and Yang, J. Y. 2016. Phytoplasma SAP11 alters 3-isobutyl-2-

methoxypyrazine biosynthesis in Nicotiana benthamiana by suppressing NbOMT1. *J Exp Bot,* 67**,** 4415-4425.

Tanno, K., Maejima, K., Miyazaki, A., Koinuma, H., Iwabuchi, N., Kitazawa, Y,. Nijo, T., Hashimoto, M., Yamaji, Y. and Namba, S 2018. Comprehensive screening of antimicrobials to control phytoplasma diseases using an in vitro plant–phytoplasma co-culture system. *Microbiol,* 164**,** 1048-1058.

Taylor, N. J. and. Fauquet, C.M. 2002. Microparticle Bombardment as a Tool in Plant Science and Agricultural Biotechnology. *DNA Cell Biol,* 21**,** 963-977.

Teichamann, T. and. Muhr, M. 2015. Shaping plant architecture. *Front Plant Sci,* 6**,** 233.

Thiergart, T., Landan, G. and Martin, W. F. 2014. Concatenated alignments and the case of the disappearing tree. *BMC Evolutionary Biology,* 14**,** 266.

Thole, V. and Vain, P. 2012. Agrobacterium-mediated transformation of Brachypodium distachyon. *Methods Mol Biol,* 847**,** 137-49.

Tomlinson, J. A., Ostoja-Starzewska, S., Adams, I. P., Miano, D. W., Abidrabo, P., Kinyua, Z., Alicai, T., Dickinson, M. J., Peters, D., Boonham, N. and Smith, J. 2013. Loop-mediated isothermal amplification for rapid detection of the causal agents of cassava brown streak disease. *J Virol Methods,* 191**,** 148-54.

Torres, E., Bertolini, E., Cambra, M., Monton, C. and Martin, M.P. 2005. Real-time PCR for simultaneous and quantitative detection of

quarantine phytoplasmas from apple proliferation (16SrX) group. *Molecular and Cellular Probes,* 19**,** 334–340.

Toruna, T. Y., Music, M. S., Simi, S., Nicolaisen, M. and Hogenhout, S. A. 2010. Phytoplasma PMU1 exists as linear chromosomal and circular extrachromosomal elements and has enhanced expression in insect vectors compared with plant hosts. *Mol Microbiol,* 77**,** 1406-15.

Tran-Nguyena, L., Blanchea, K. R., Eganb, B. and Gibb, K. S. 2000. Diversity of phytoplasmas in northern Australian sugarcane and other grasses. *Plant Pathol,* 49**,** 666-679.

Tsirigotaki, A., De Geyter, J., Šostaric, N., Economou, A. and Karamanou, S. 2017. Protein export through the bacterial Sec pathway. *Nat Rev Microbiol.,* 15**,** 21-36.

Tymon, A. M., Jones, P. and Harrison, N. A. 1998. Phylogenetic relationships of coconut phytoplasmas and the development of specific oligonucleotide PCR primers. *Ann Appl Biol* 132**,** 437-452.

Ung, N., Lal, S. and Smith, H. M. 2011. The role of PENNYWISE and POUND-FOOLISH in the maintenance of the shoot apical meristem in Arabidopsis. *Plant Physiol,* 156**,** 605-14.

Vain, P., Worland, B., Thole, V., Mckenzie, N., Alves, S. C., Opanowicz, M., Fish, L. J., Bevan, M. W. and Snape, J. W. 2008. Agrobacterium-mediated transformation of the temperate grass Brachypodium distachyon (genotype Bd21) for T-DNA insertional mutagenesis. *Plant Biotechnol J,* 6**,** 236-45.

Valiunas, D., Jomantiene, R., Ivanauskas, A., Abraitis, R., Staniene, G., Zhao, Y. and Davis, R.E. 2009. First report of a new phytoplasma

subgroup, 16SrIII-T, associated with decline disease affecting sweet and sour cherry trees in Lithuania. *Plant Disease,* 93**,** 50.

Valiunas D., S., J. and Davis, R.E. 2006. ‘Candidatus Phytoplasma fragariae’, a novel phyto- plasma taxon discovered in yellows diseased strawberry, Fragaria x ananassa. *Int. J. Syst. Evol Microbiol,i,* 56**,** 277–281.

Venglat, S. P., Dumonceaux, T., Rozwadowski, K., Parnell, K., Babic, V., Keller, W., Martienssen, R., Selvaraj, G. and Dalta, R. 2002. The homeobox gene BREVIPEDICELLUS is a key regulator of inflorescence architecture in Arabidopsis. *PNAS,* 99**,** 4730-4735.

Verdin, E., Salar, P., Danet, J. L., Chouiri, E., Jreijiri, F., El Zammar, S., Gelie, B., Bove, J. M. and Garnier, M. 2003. 'Candidatus phytoplasma phoenicium' sp. nov., a novel phytoplasma associated with an emerging lethal disease of almond trees in Lebanon and Iran. *Int J Syst Evol Microbiol,* 53**,** 833-8.

Viktorava, J., Klcova, B., Rehorova, K., Vlcko, T., Stankova, L., Jelenova, N., Cejnar, P., Kundu, J. K. Ohnoutkova, L. and Macek, T. 2019. Recombinant expression of osmotin in barley improves stress resistance and food safety during adverse growing conditions. *PLoS One,* 14**,** e0212718.

Viswanathan, R., Chinnaraja, C., Karuppaiah, R., Ganesh K. V., Jenshi R., J. and Malathi, P. 2011. Genetic Diversity of Sugarcane Grassy Shoot (SCGS)-Phytoplasmas Causing Grassy Shoot Disease in India. *Sugar Tech,* 13**,** 220-228.

Vogel, J. and Hill, T. 2008. High-efficiency Agrobacterium-mediated transformation of Brachypodium distachyon inbred line Bd21-3. *Plant Cell Rep,* 27**,** 471-8.

Vogel, J. P., Garvin, D. F., Leong, O. M. and Hayden, D. M. 2006. Agrobacterium-mediated transformation and inbred line development in the model grass Brachypodium distachyon. *Plant Cell Tiss Organ Cult,* 84**,** 199-211.

Wang, X. Y., Li, W. F., Huang, Y. K., Zhang, R. Y., Luo, Z. M., Shan H., L., Yin, J., Shen, K., Jia, Y. M. and Bai, Z. G. 2014. Analyses of the 16S-23S intergenic region of the phytoplasma causing the sugarcane white leaf disease in Yunnan Province, China. *Trop Plant Pathol,* 39**,** 184-188.

Wang, Y. and Jiao, Y. 2018. Axillary meristem initiation-a way to branch out. *Curr Opin Plant Biol,* 41**,** 61-66.

Wei, W., Davis, R. E., Lee, I. M. and Zhao, Y. 2007. Computer-simulated RFLP analysis of 16S rRNA genes: identification of ten new phytoplasma groups. *Int J Syst Evol Microbiol,* 57**,** 1855-67.

Wei, W., Davis, R. E., Nuss, D. L. and Zhao, Y. 2013. Phytoplasmal infection derails genetically preprogrammed meristem fate and alters plant architecture. *Proc Natl Acad Sci U S A,* 110**,** 19149-54.

Weintraub, P. G. and Beanland, L. 2006. Insect vectors of phytoplasmas. *Annu Rev Entomol,* 51**,** 91-111.

Wongkaew, P., Hanboonsong, Y., Sirithorn, P., Choosia, C., Boonkrong, TinnangwattanaI, S., Kitchareonpanya, R. and Damak, S. 1997. Differentiation of phytoplasmas associated with sugarcane and

gramineous weed white leaf disease and sugarcane grassy shoot disease by RFLP and sequencing. *Theor Appl Gen,* 95**,** 660–663.

Yadav, A., Thorat, V., Deokule, S., Shouche, Y. and Prasad, D.T. 2016. New subgroup 16SrXI-F phytoplasma strain associated with sugarcane grassy shoot (SCGS) disease in India. *Int J Syst Evol Microbiol,* 67**,** 374-378.

Yang, C. Y., Huang, Y. H., Lin, C. P., Lin, Y. Y., Hsu, H. C., Wang, C. N., Liu, L. Y., Shen, B. N. and Lin, S. S. 2015. Insect Molecular Biology. *Plant Physiol,* 168**,** 1702-16.

Yusuf, A. J., Dakhil, H., El-Mehtar, S. and Lee, I. M. 2003. Almond witches'-broom phytoplasma: a potential threat to almond, peach, and nectarine. *Can. J. Plant Pathol,* 25**,** 28-32.

Zhang, L., Zhang, F., Melotto, M., Yao, J. and He, S. Y. 2017. Jasmonate signaling and manipulation by pathogens and insects. *J Exp Bot,* 68**,** 1371-1385.

Zhang, R. Y. Li, W. F., Huang, Y. K., Wang, X. Y., Shan, H. L., Luo, Z. M. and Yin, J. 2016. Group 16SrXI phytoplasma strains, including subgroup 16SrXI-B and a new subgroup, 16SrXI-D,are associated with sugar cane white leaf. *Int J System Evol Microbiol,* 66**,** 487-491.

Zhao, Y. and Davis, R.E. 2016. Criteria for phytoplasma 16Sr group/subgroup delineation and the need of a platform for proper registration of new groups and subgroups. *Int J System Evol Microbiol,* 66**,** 2121-2123.

Zhussupova, A. I., Omirbekova, N. Z.H., Malik, A. and Almaganbetov, Z.H. 2013. Perspectives for study of Brachypodium distachyon as a model

object for genetic and biochemical study in Kazakhstan. *Int J Biol Chem,* 6**,** 17.

Zreik, L., Carel, P., Bove´ , J. M. and Garnier, M. 1995. Characterization of the mycoplasmalike organism associated with witches'-broom disease of lime and proposition of a ''Candidatus'' taxon for the organism, ''Candidatus Phytoplasma aurantifolia''. *Int J Syst Bacteriol.,* 45**,** 449-453.

Appendices

Chapter 2

```
Domain: Data
NGS        I KTG* RRSI GS* CRRFCSNCQKRR* I CCFKFTFRRN* KSI KRV* SNYRNYR* * I I * I NKTWKSRKKTLFI FSS
SCWLTH1    . . . RWWW* . S . Q . . YI S . DY* . . . K . . RY . . . . G . . . . . F . CL . . . . . CC . . . . L . V . . K . * . W* N . . . . Y . .
SCWLTH2    . . . RWWW* . S . Q . . YI S . DY* . . . K . . RY . . . . G . . . . . F . CL . . . . . CC . . . . L . V . . K . * . W* N . . . . Y . .
SCWLSri1   . . . RWWW* . S . Q . . YI S . DY* . . . K . . RY . . . . G . . . . . F . CL . . . . . CC . . . . L . V . . K . * . W* N . . . . Y . .
SCWLSri3   . . . RWWW* . S . Q . . YI S . DY* . . . K . . RY . . . . G . . . . . F . CL . . . . . CC . . . . L . V . . K . * . W* N . . . . Y . .
SCWLVN15   . . . RWWW* . S . Q . . YI S . DY* . . . K . . RY . . . . G . . . . . F . CL . . . . . CC . . . . L . V . . K . * . W* N . . . . Y . .
SCGSSri1   . * . RWWW* . S . Q . . YI S . DY* . . . K . . RY . . . . G . . . . . F . CL . . . . . CC . . . . L . V . . K . * . W* N . . . . Y . .
SCGSSri2   . . . RWWW* . S . Q . . YI S . DY* . . . K . . RY . . . . G . . . . . F . CL . . . . . CC . . . . L . V . . K . * . W* N . . . . Y . .
SCGSSri3   . . . RWWW* . S . Q . . YI S . DY* . . . K . . RY . . . . G . . . . . F . CL . . . . . CC . . . . L . V . . K . * . W* N . . . . Y . .
SCGSVN1    . . . RWWW* . S . Q . . YI S . DY* . . . K . . RY . . . . G . . . . . F . CL . . . . . CC . . . . L . V . . K . * . W* N . . . . Y . .
SCGSVN2    . . . RWWW* . S . Q . . YI S . DY* . . . K . . RY . . . . G . . . . . F . CL . . . . . CC . . . . L . V . . K . * . W* N . . . . Y . .
BGWL1      . . . RK . WP . ST . RGNI S . DY* . . . . . . . YW . A . . . . . . NFRSL . . . . . SC . KR . L . . . QKR . . . . N . . . V . . .
BGWL2      . . . RK . WP . ST . RGNI S . DY* . . . . . . . YW . A . . . . . . NFRSL . . . . . SC . KR . L . . . QKR . . . . N . . . V . . .
SCWLVN9    T . . RWWW* . S . Q . . YI S . DY* . . . K . . RY . . . . G . . . . . F . CL . . . . . CC . . . . L . V . . K . * . W* N . . . . YT .
SCWLVN2    T . . RWWW* . S . Q . . YI S . DY* . . . K . . RY . . . . G . . . . . F . CL . . . . . CC . . . . L . V . . K . * . W* N . . . . Y . .
BGWLVN9    . . . RK . WP . ST . RGNI S . DY* . . . . . . . YW . A . . . . . . NFRSL . . . . . SC . KR . L . . . QKR . . . . N . . . V . . .
SCWLVN21   T . . RWWW* . S . Q . . YI S . DY* . . . K . . RY . . . . G . . . . . F . CL . . . . . CC . . . . L . V . . K . * . W* N . . . . Y . .
AY-WB      . . . RQ . . TNC . . . WF . L . . Y* * . . Q . RTI TSSI . . SSQ . ACNLSCY . . RD . . R . LQT . *LRQ . . Q . . FLRNKT
Sequence 1 - - - - - - - - - - - - - - - - - - - - - - - - - - - - - - - - - - - - - - - - - - - - - - - - - - - - - - - - - - - - - - - - - - - -
```

Figure A2.1 50S protein alignment between samples and Aster Yellow Witches’ Broom (AY-WB). The sequences were align using CLUSTAL W and dots represent amino acid identical to NGSD consensus sequences; dash represents amino acid deletion in the gene.

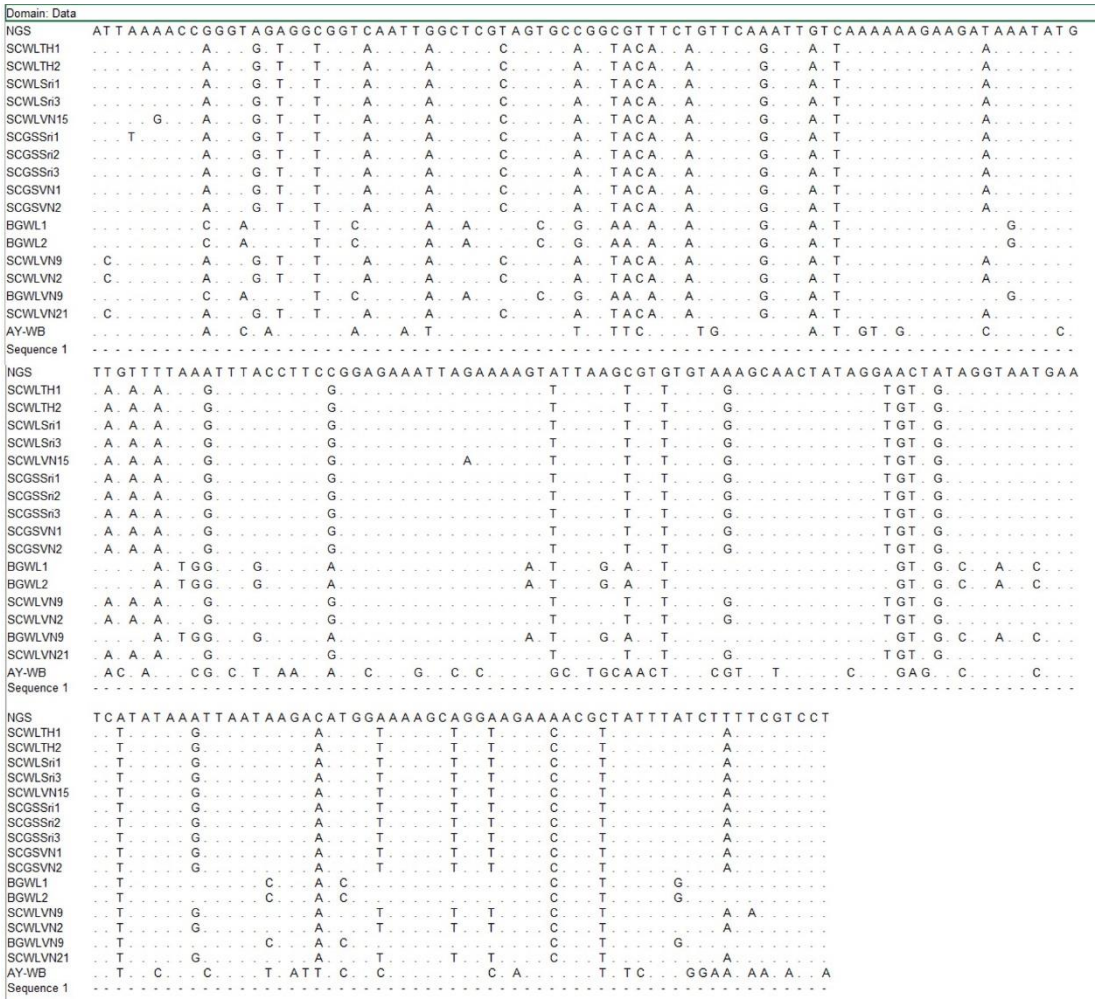


Figure A2.2 *50S* nucleotide alignment between samples and Aster Yellow Witches' Broom (AY-WB). The sequences showed nucleotide transition and transversion.

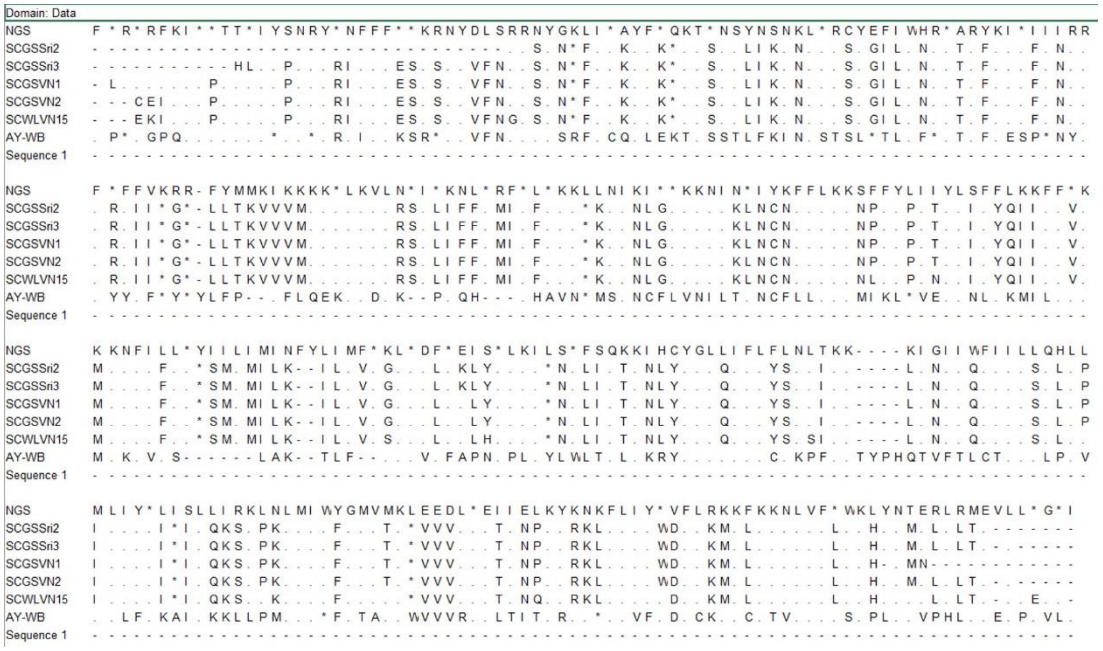


Figure A2.3 Asp protein alignment between samples and Aster Yellow Witches' Broom (AY-WB). The sequences were align using CLUSTAL W and dots represent amino acid identical to NGSD consensus sequences; dash represents amino acid deletion in the gene.

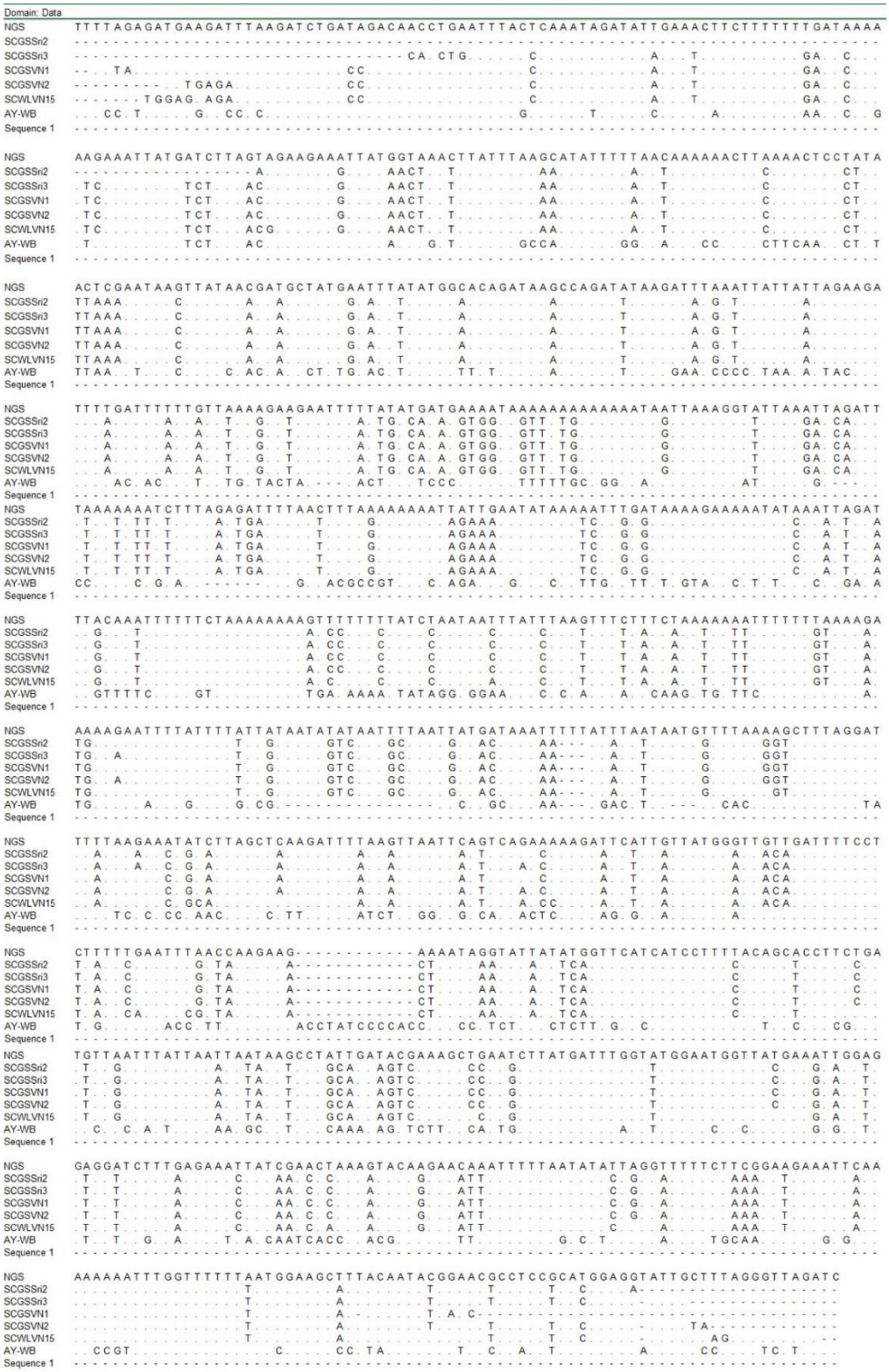


Figure A2.4 *Asp* nucleotide alignment between samples and Aster Yellow Witches' Broom (AY-WB). The sequences showed nucleotide transition and transversion.

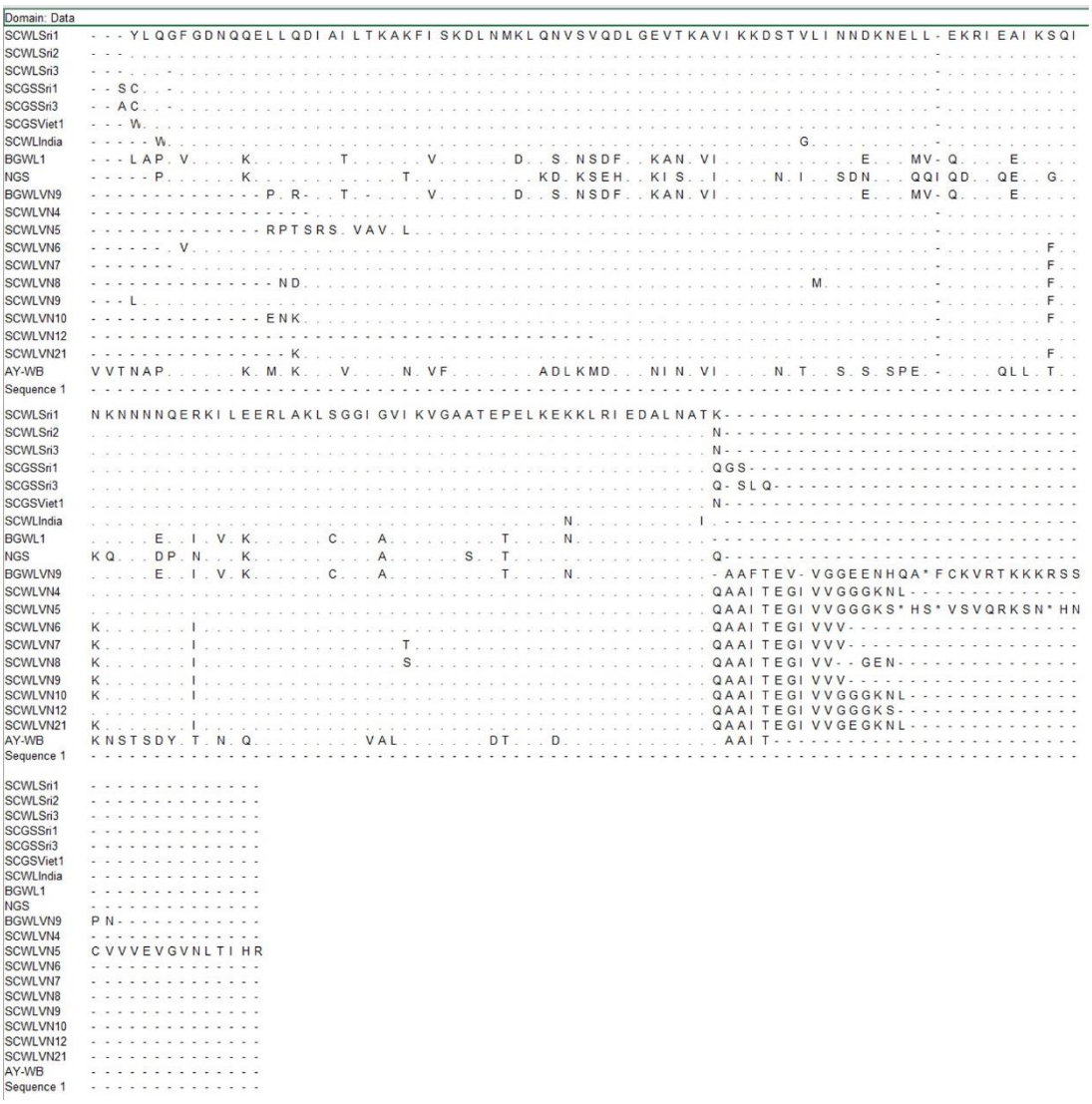


Figure A2.5 Gro protein alignment between samples and Aster Yellow Witches' Broom (AY-WB). The sequences were align using CLUSTAL W and dots represent amino acid identical to SCWLSri1 consensus sequences; dash represents amino acid deletion in the gene.

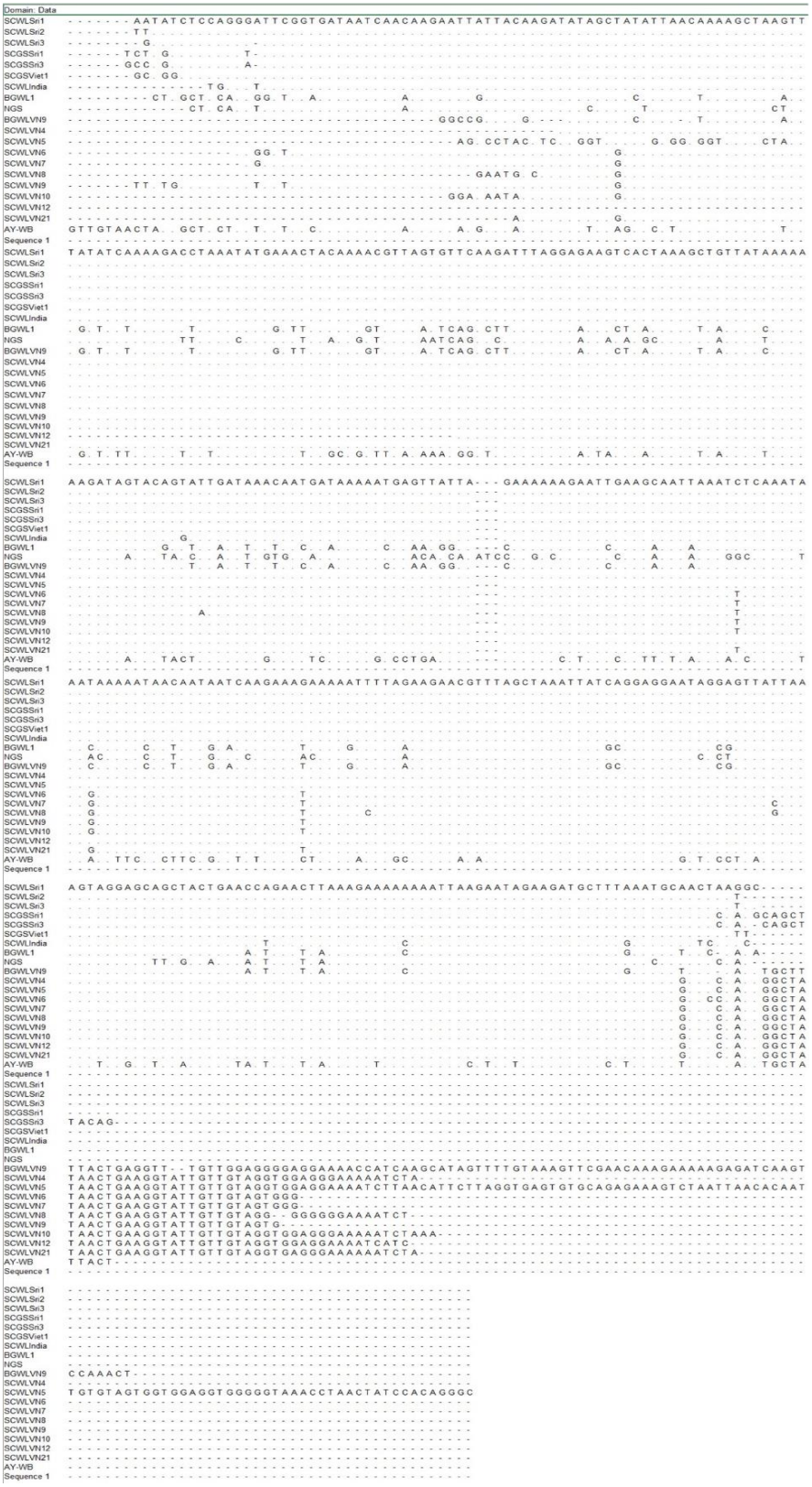


Figure A2.6 *Gro* nucleotide alignment between samples and Aster Yellow Witches' Broom (AY-WB). The sequences showed nucleotide transition and transversion.

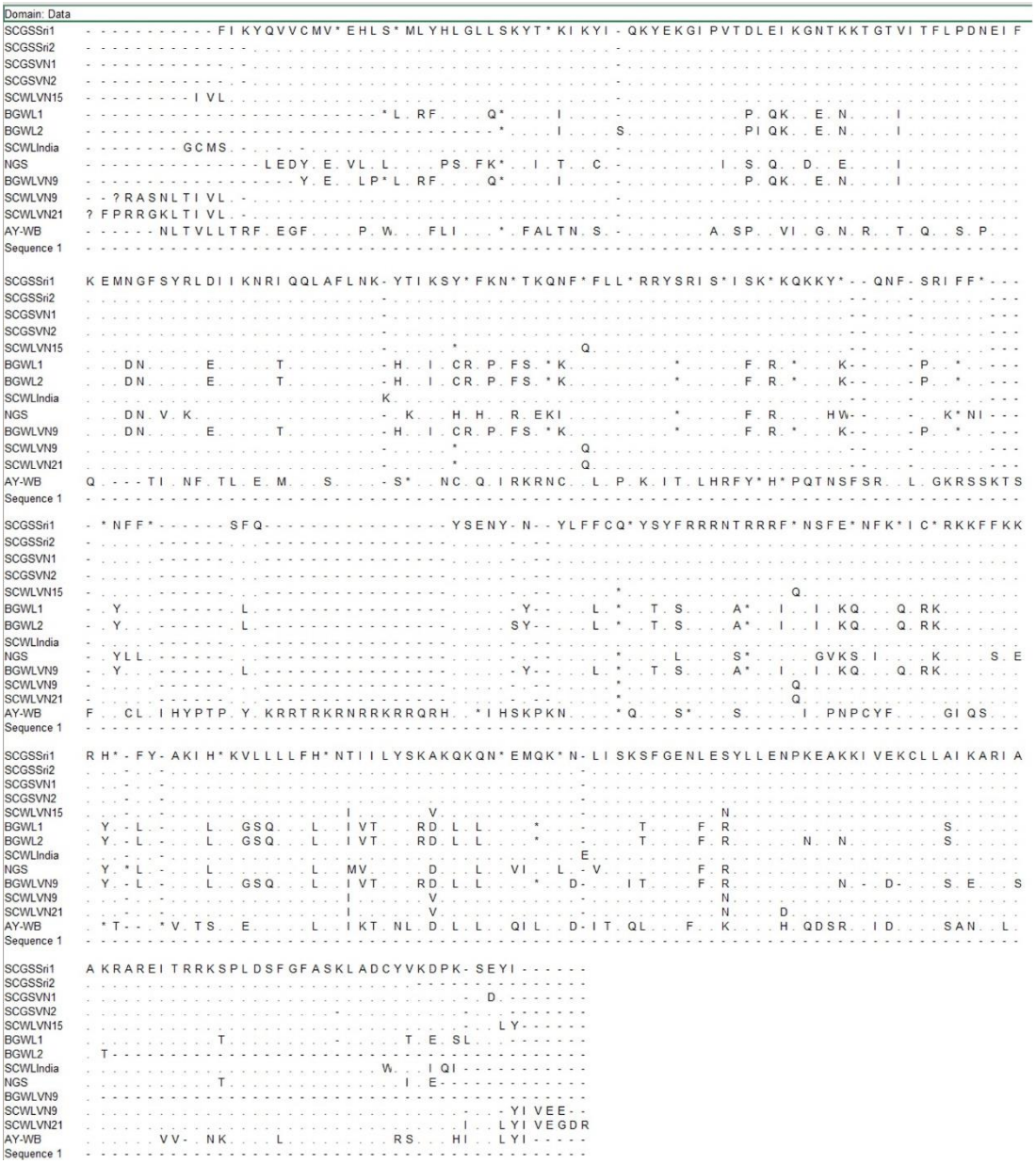


Figure A2.7 GryB protein alignment between samples and Aster Yellow Witches' Broom (AY-WB). The sequences were align using CLUSTAL W and dots represent amino acid identical to SCGSSri1 consensus sequences; dash represents amino acid deletion in the gene.

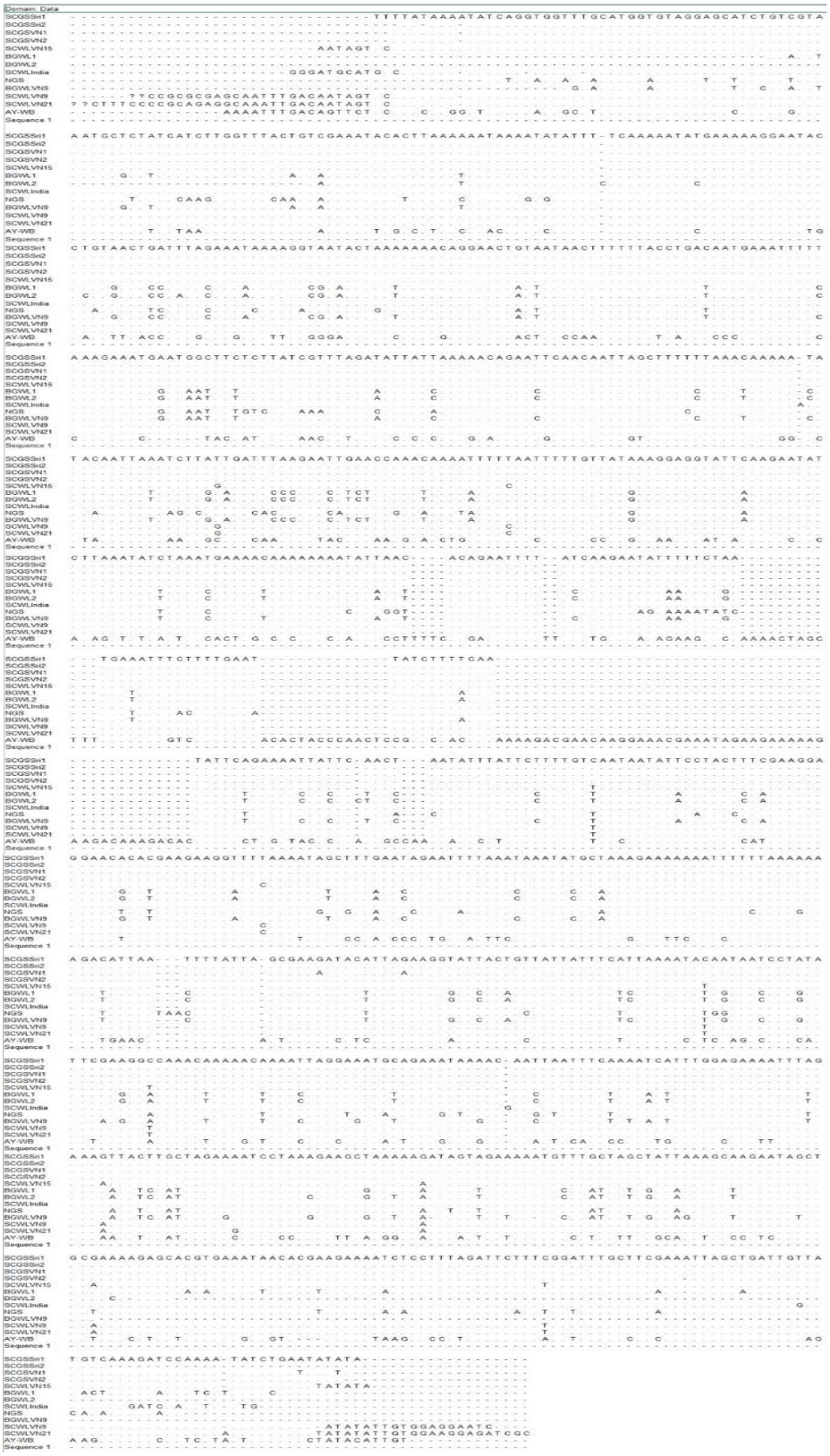


Figure A2.8 *GryB* nucleotide alignment between samples and Aster Yellow Witches' Broom (AY-WB). The sequences showed nucleotide transition and transversion.

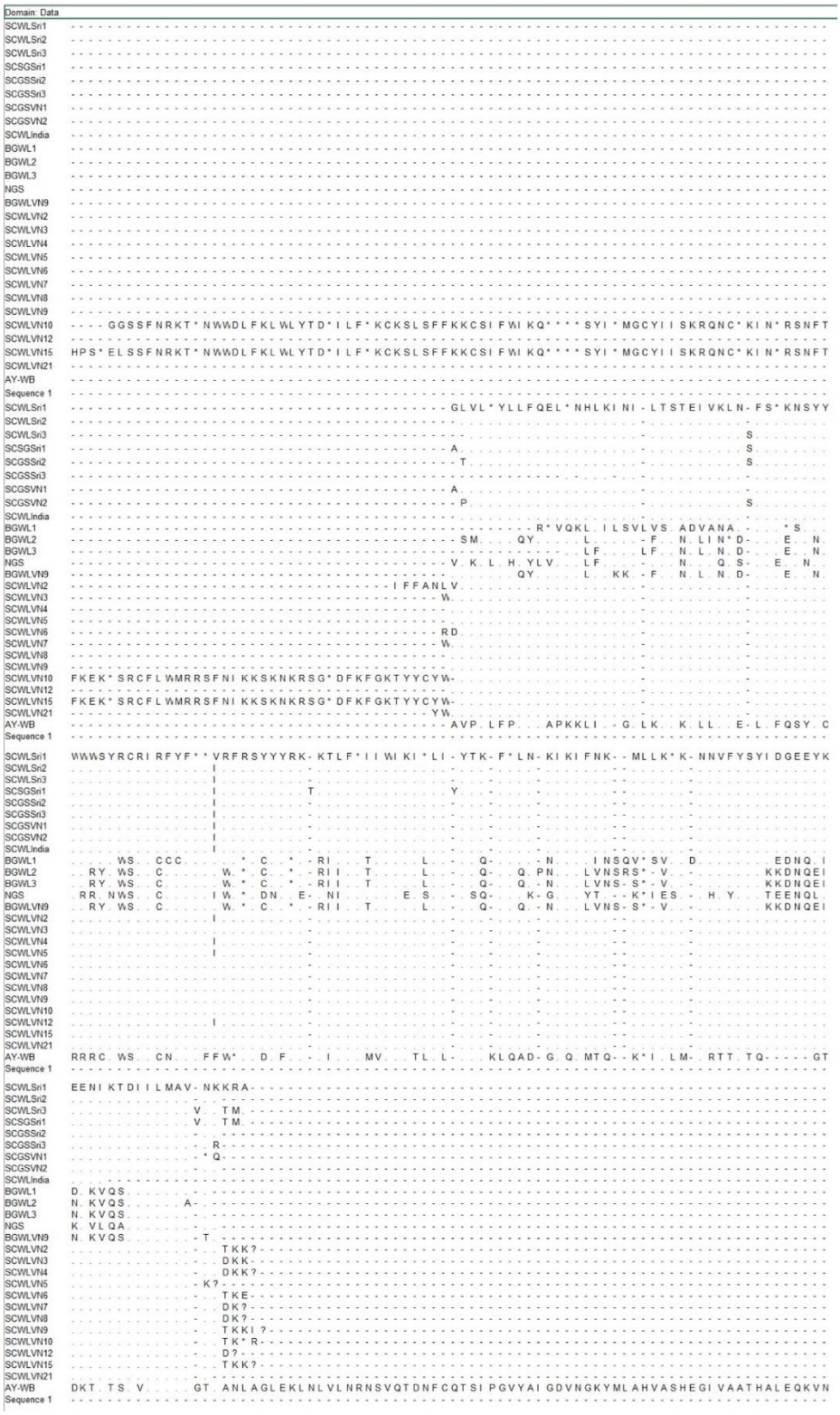


Figure A2.9 Lpd protein alignment between samples and Aster Yellow Witches' Broom (AY-WB). The sequences were align using CLUSTAL W and dots represent amino acid identical to SCWLSri1 consensus sequences; dash represents amino acid deletion in the gene.

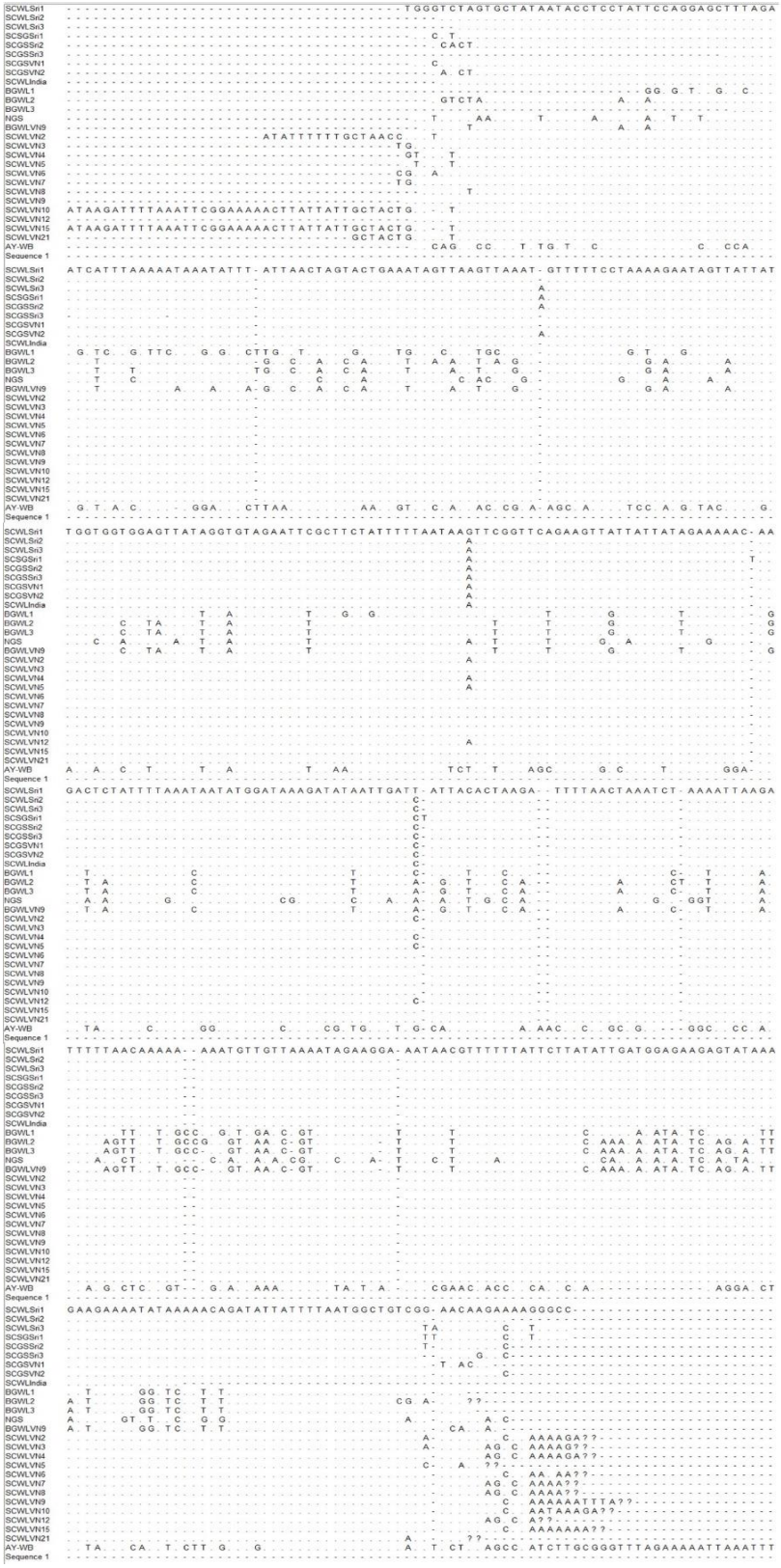


Figure A2.10 *Lpd* nucleotide alignment between samples and Aster Yellow Witches' Broom (AY-WB). The sequences showed nucleotide transition and transversion.

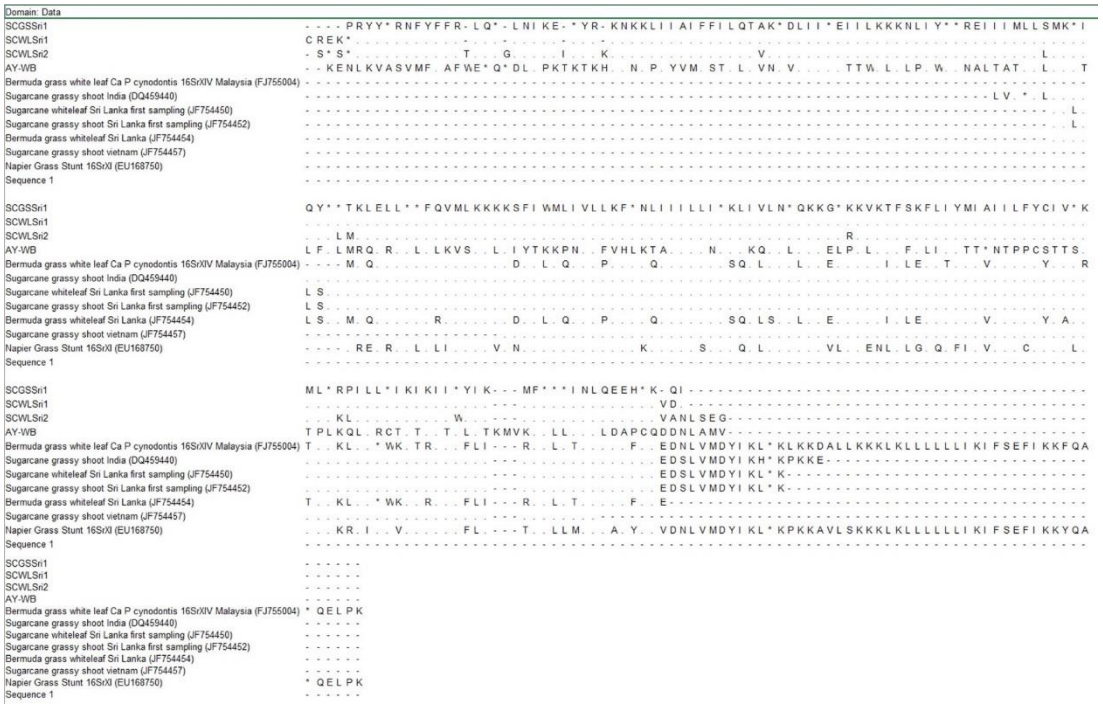


Figure A2.11 Sec protein alignment between samples and Aster Yellow Witches' Broom (AY-WB). The sequences were align using CLUSTAL W and dots represent amino acid identical to SCGSSri1 consensus sequences; dash represents amino acid deletion in the gene.

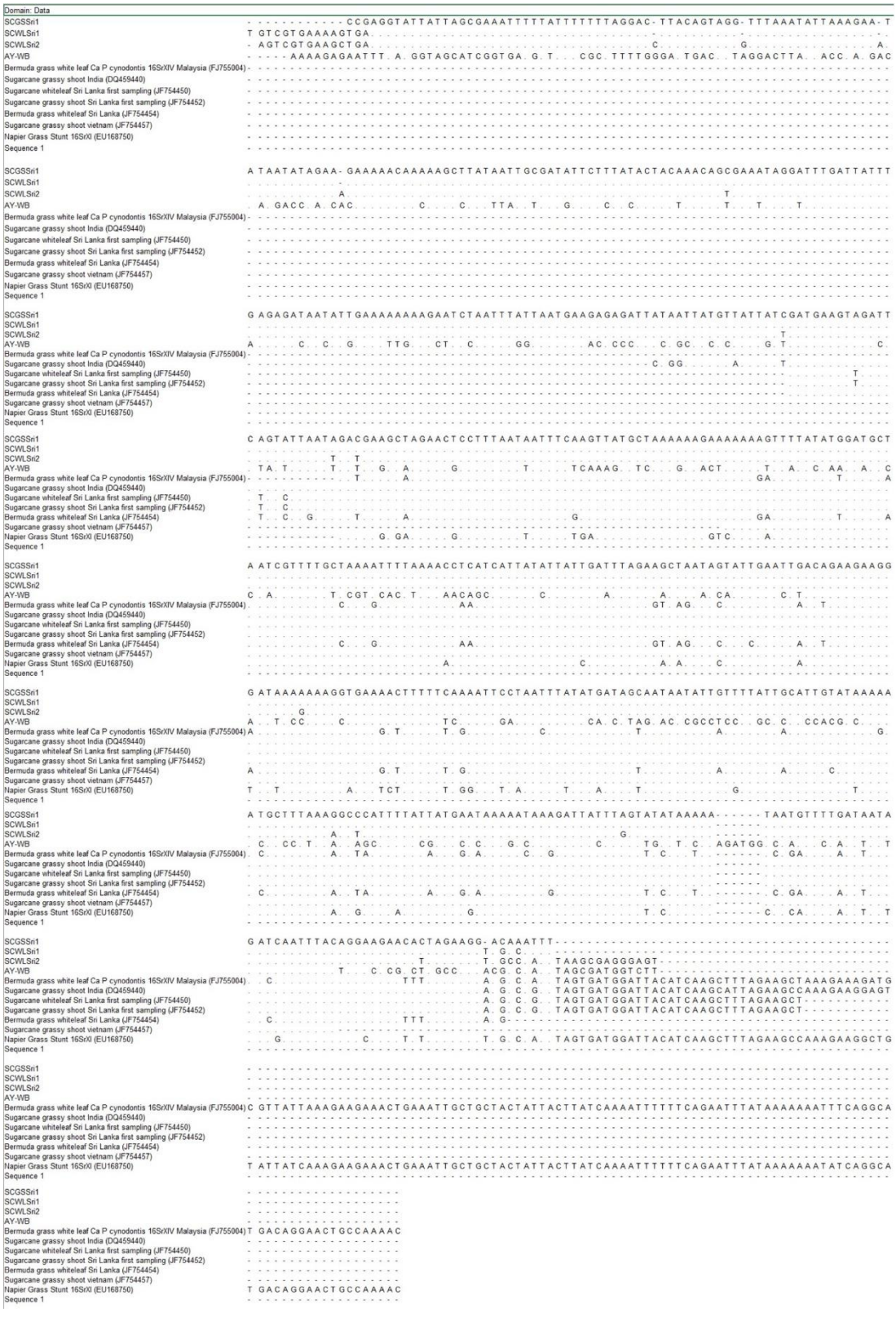


Figure A2.12 *Sec* nucleotide alignment between samples and Aster Yellow Witches' Broom (AY-WB). The sequences showed nucleotide transition and transversion.

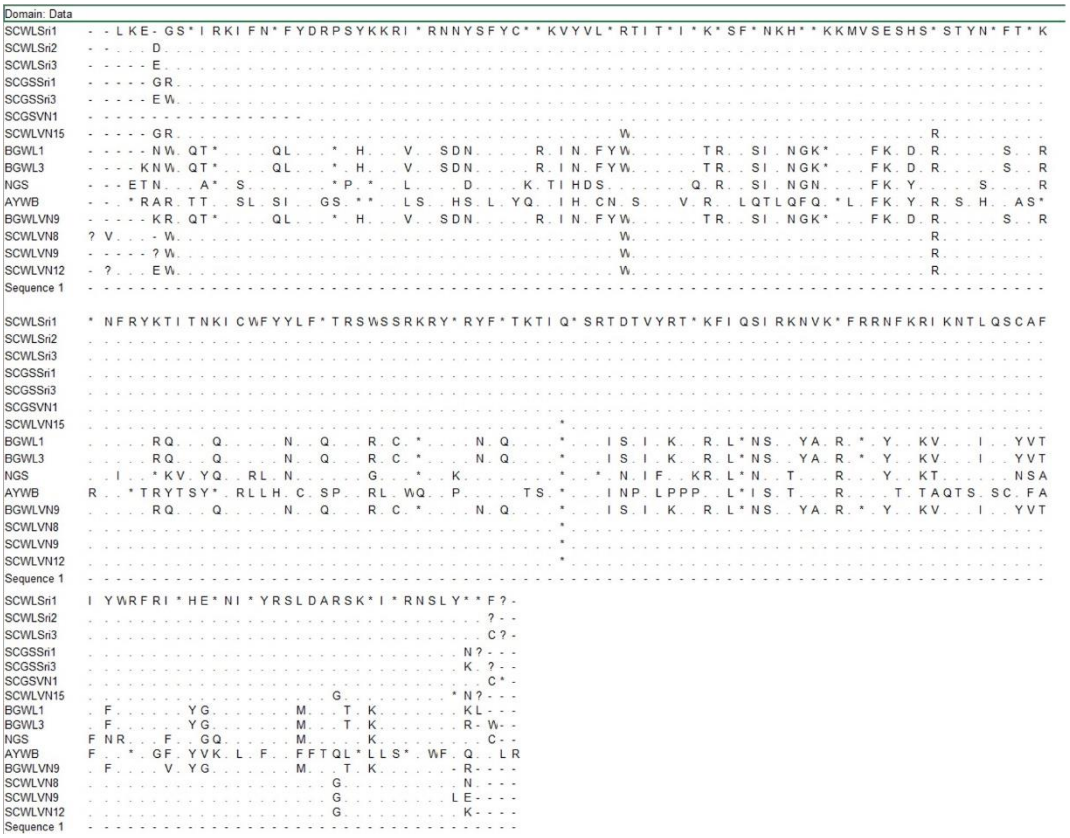


Figure A2.13 Ser protein alignment between samples and Aster Yellow Witches' Broom (AY-WB). The sequences were align using CLUSTAL W and dots represent amino acid identical to SCWLSri1 consensus sequences; dash represents amino acid deletion in the gene.

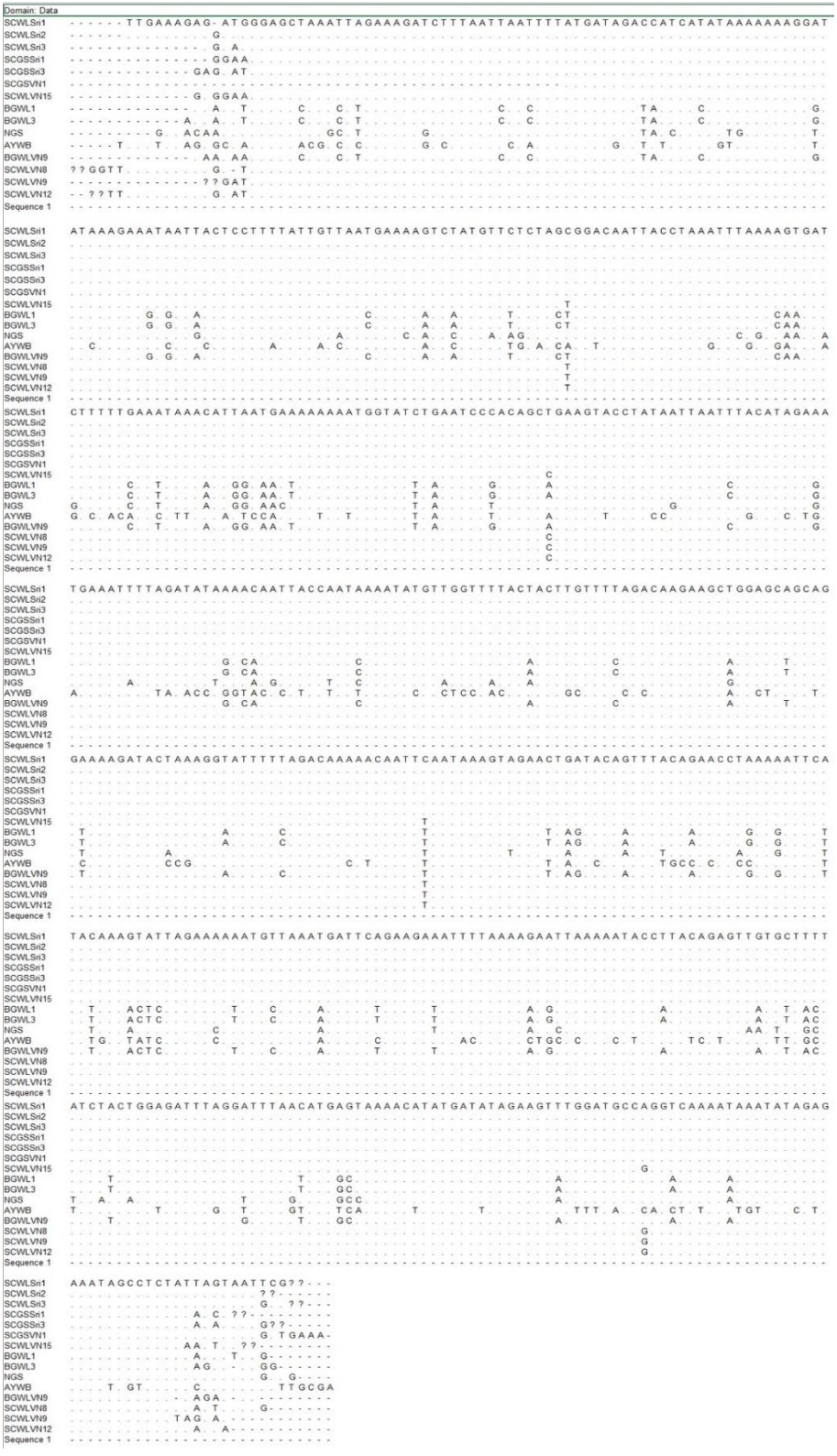


Figure A2.14 *Ser* nucleotide alignment between samples and Aster Yellow Witches' Broom (AY-WB). The sequences showed nucleotide transition and transversion.

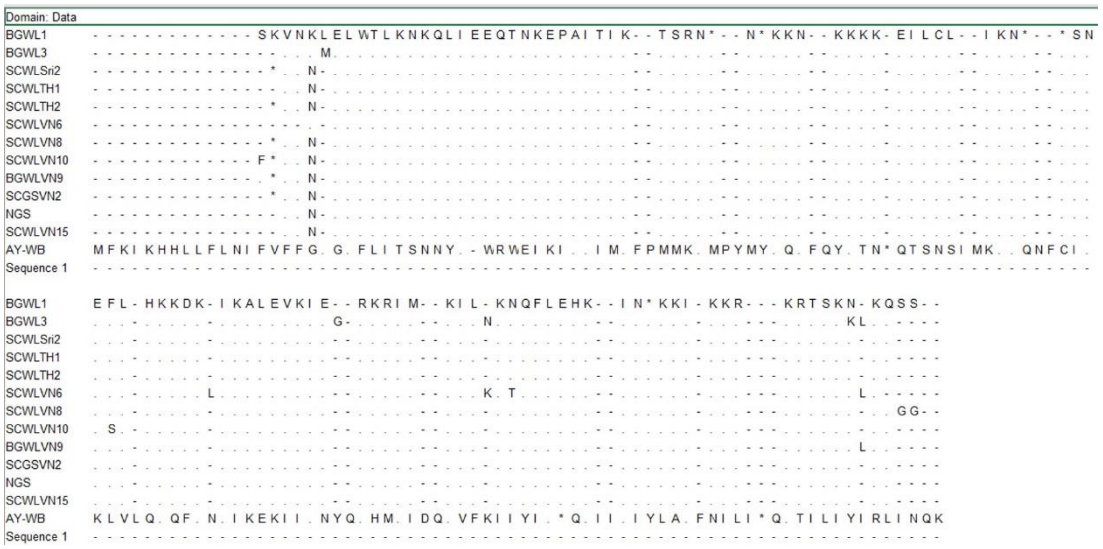


Figure A2.15 EF2 protein alignment between samples and Aster Yellow Witches' Broom (AY-WB). The sequences were align using CLUSTAL W and dots represent amino acid identical to BGWL1 consensus sequences; dash represents amino acid deletion in the gene.

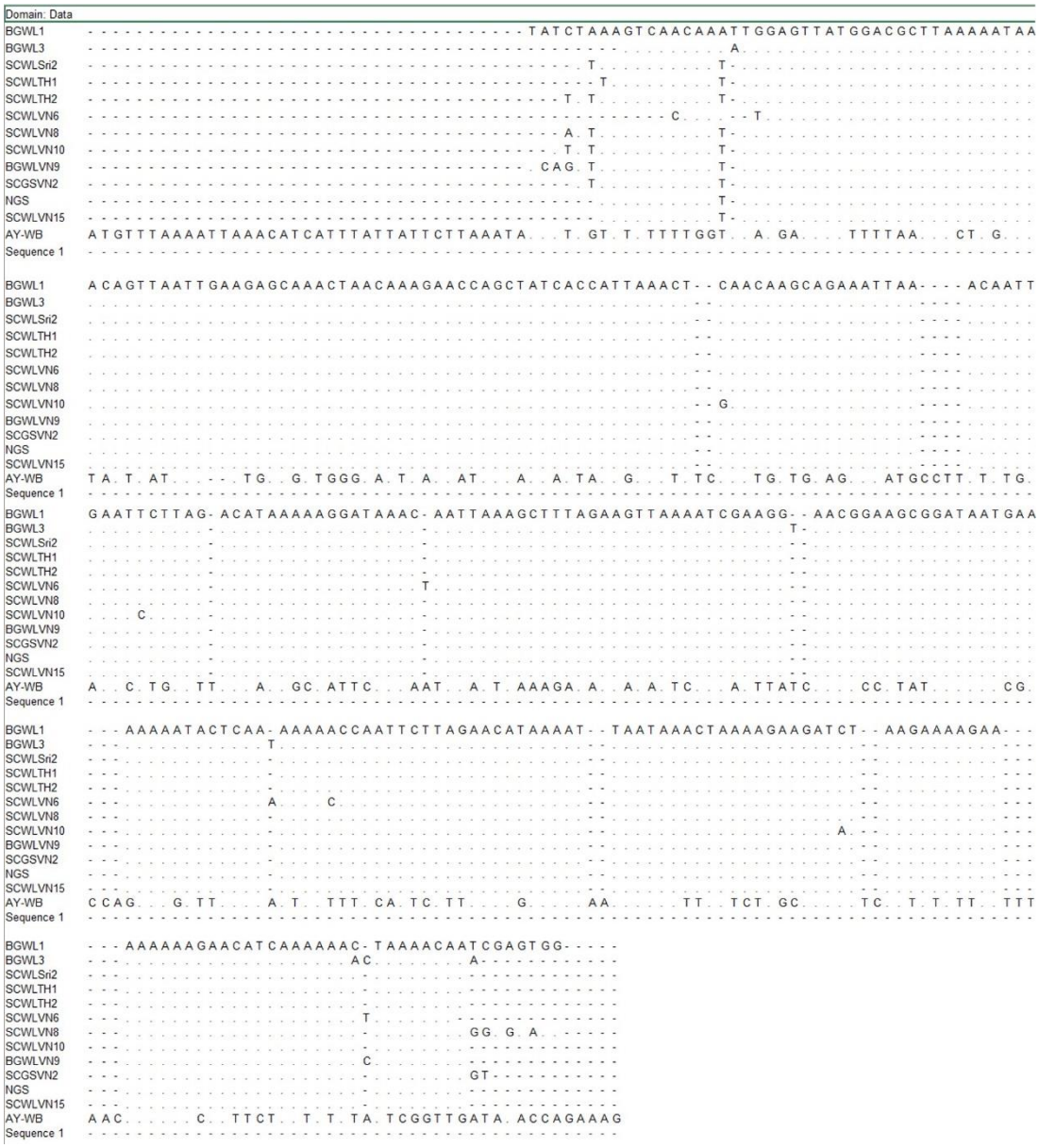


Figure A2.16 *EF2* nucleotide alignment between samples and Aster Yellow Witches' Broom (AY-WB). The sequences showed nucleotide transition and transversion.

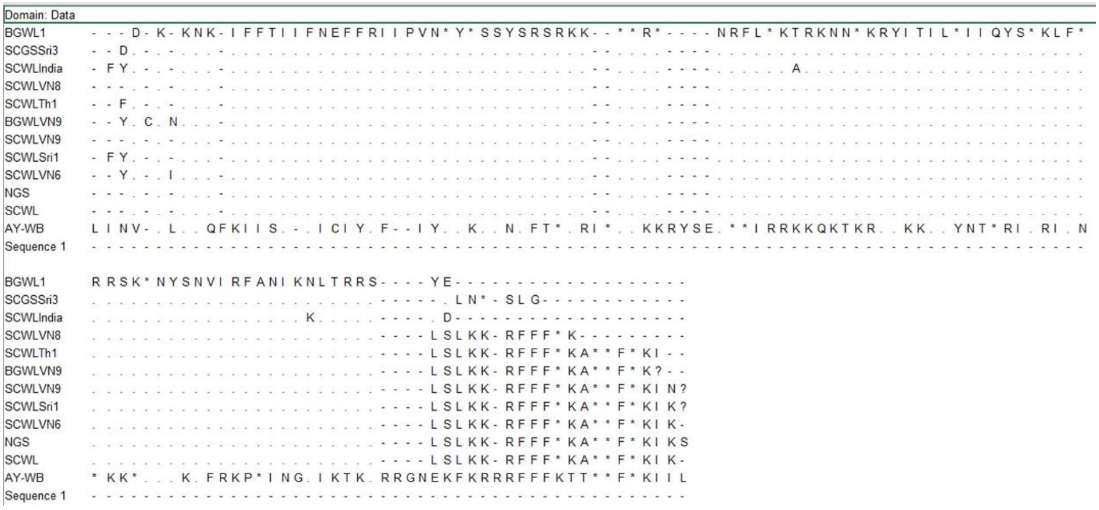


Figure A2.17 EF7 protein alignment between samples and Aster Yellow Witches' Broom (AY-WB). The sequences were align using CLUSTAL W and dots represent amino acid identical to BGWL1 consensus sequences; dash represents amino acid deletion in the gene.

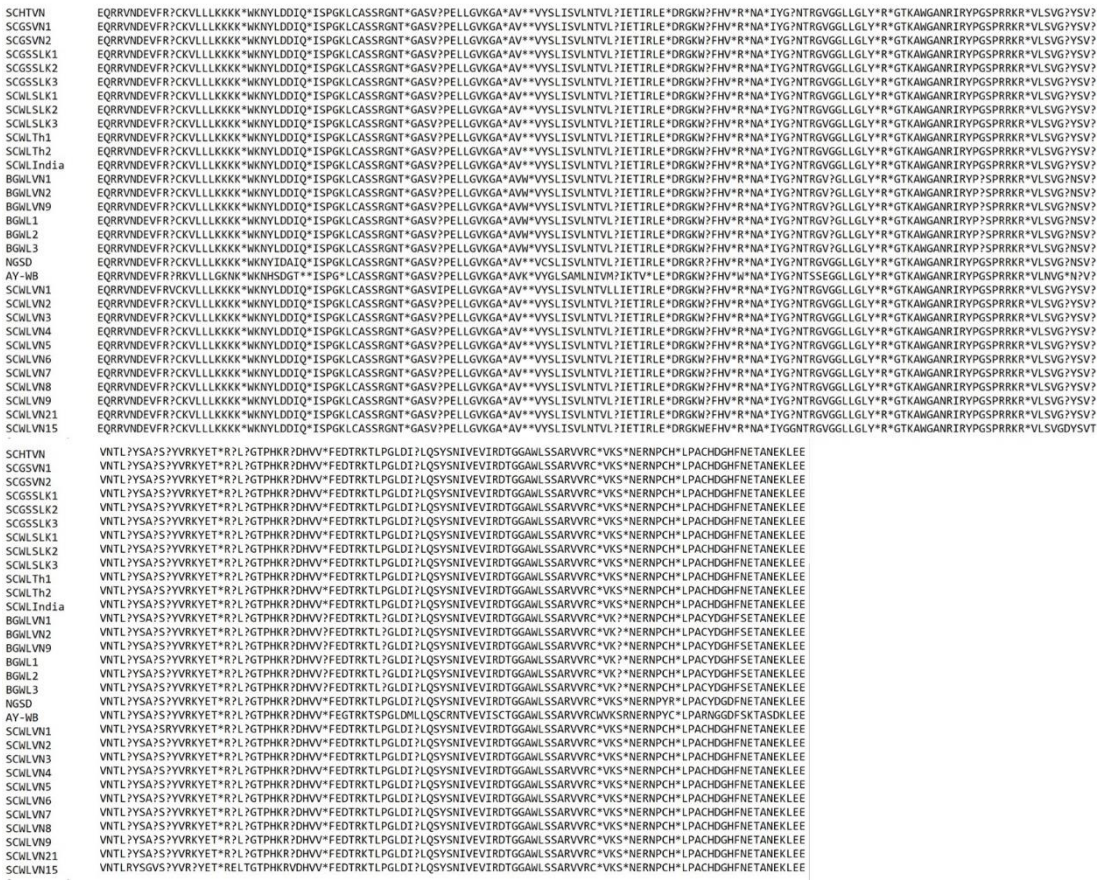


Figure A2.18 *Ef7* nucleotide alignment between samples and Aster Yellow Witches' Broom (AY-WB). The sequences showed nucleotide transition and transversion.